

**Interspecific interactions between saprotrophic basidiomycetes:  
effect on volatile production and gene expression of mycelia**

**A thesis submitted for the degree of  
Doctor of Philosophy  
at the University of Wales, Cardiff.**

**Catherine Eyre**

**2007**

UMI Number: U585027

All rights reserved

INFORMATION TO ALL USERS

The quality of this reproduction is dependent upon the quality of the copy submitted.

In the unlikely event that the author did not send a complete manuscript and there are missing pages, these will be noted. Also, if material had to be removed, a note will indicate the deletion.



UMI U585027

Published by ProQuest LLC 2013. Copyright in the Dissertation held by the Author.  
Microform Edition © ProQuest LLC.

All rights reserved. This work is protected against  
unauthorized copying under Title 17, United States Code.



ProQuest LLC  
789 East Eisenhower Parkway  
P.O. Box 1346  
Ann Arbor, MI 48106-1346

**DECLARATION**

This work has not previously been accepted in substance for any degree and is not concurrently submitted in candidature for any degree.

Signed *Catherine Gye* ..... Date *1/4/08* .....

**STATEMENT 1**

This thesis is being submitted in partial fulfillment of the requirements for the degree of PhD.

Signed *Catherine Gye* ..... Date *1/4/08* .....

**STATEMENT 2**

This thesis is the result of my own independent work/investigation, except where otherwise stated.  
Other sources are acknowledged by explicit references.

Signed *Catherine Gye* ..... Date *1/4/08* .....

**STATEMENT 3**

I hereby give consent for my thesis, if accepted, to be available for photocopying and for inter-library loan, and for the title and summary to be made available to outside organisations.

Signed *Catherine Gye* ..... Date *1/4/08* .....

**STATEMENT 4: PREVIOUSLY APPROVED BAR ON ACCESS**

I hereby give consent for my thesis, if accepted, to be available for photocopying and for inter-library loans **after expiry of a bar on access previously approved by the Graduate Development Committee.**

Signed *Catherine Gye* ..... Date *1/4/08* .....

## Table of Contents

Abstract.....	i
Acknowledgements.....	ii
Figures.....	iii
Tables.....	vii
Abbreviations.....	ix
<b>1. Introduction.....</b>	<b>1</b>
1.1 Fungi in the environment.....	1
1.2 Decomposition.....	2
1.3 Competition.....	4
1.4 Fungal competition.....	4
1.5 Mechanisms of combat.....	6
1.6 Outcomes of interactions.....	7
1.7 Studying interactions.....	9
1.8 Extracellular enzyme activity.....	10
1.9 Chemicals as the effectors of interactions.....	12
1.10 The molecular basis of interactions.....	14
1.11 Methods for the study of gene expression.....	15
1.12 Functional genomics.....	20
1.13 Project objectives.....	21
<b>2. General Materials and Methods.....</b>	<b>24</b>
2.1 Routine culture conditions.....	24
2.2 Growth of mycelium for RNA extraction.....	24
2.3 RNA extraction.....	25
2.4 Polymerase chain reaction (PCR).....	26
2.5 Purification of PCR reactions using QIAquick PCR purification columns (Qiagen).....	26
2.6 Gel electrophoresis of nucleic acids.....	27
2.7 Nucleic acid quantification.....	28
2.7.1 Spectrophotometer quantification.....	28
2.7.2 Ethidium bromide spot assay.....	28
2.7.3 Hyperladder quantification.....	29
2.8 Purification of RNA.....	29
2.9 Purification of <i>Taq</i> polymerase from overexpressing recombinant <i>Escherichia coli</i> .....	30
2.9.1 Culturing of <i>E. coli</i> .....	30
2.9.2 Purification of <i>Taq</i> polymerase.....	30
2.9.3 Analysis of <i>Taq</i> efficiency.....	32
2.10 SDS-PAGE analysis.....	32
2.10.1 Gel preparation.....	32
2.10.2 Sample loading.....	33
2.10.3 Gel staining.....	33
2.10.4 Gel imaging.....	33
2.11 Preparation of media for cloning.....	34
2.11.1 NZY broth.....	34
2.11.2 LB medium.....	34
2.11.3 SOC medium.....	34

---

<b>3. Agar Interactions.....</b>	<b>35</b>
3.1 Introduction.....	35
3.2 Materials and methods.....	36
3.2.1 Fungal isolates.....	36
3.2.2 Outcome of interactions.....	37
3.2.3 Extension rate measurement.....	37
3.2.3.1 Single species.....	37
3.2.3.2 Paired interactions.....	38
3.2.4 Statistical analysis.....	39
3.2.4.1 Comparison of mycelial extension rate of single species....	39
3.2.4.2 Comparison of mycelial extension rate between single and paired inocula.....	39
3.2.4.3 Comparison of mycelial extension rate within self paired inocula.....	40
3.2.4.4 Comparison of mycelial extension rate of <i>T. versicolor</i> with different treatments.....	40
3.3 Results.....	41
3.3.1 Outcomes of interactions.....	41
3.3.1.1 Self pairings.....	41
3.3.1.2 Interspecific interactions.....	41
3.3.2 Extension rates.....	48
3.3.2.1 Single species inocula.....	48
3.3.2.2 Self pairings.....	49
3.3.2.3 Interspecific interactions.....	50
3.4 Discussion.....	51
3.4.1 Outcomes of interactions.....	51
3.4.2 Morphological changes.....	53
3.4.3 Extension rates.....	54
3.4.4 Effect of interspecific interactions on extension of <i>T. versicolor</i> ....	55
3.4.5 Experimental design.....	56
3.4.6 Data analysis.....	57
3.4.7 Selection of <i>T. versicolor</i> for continued study.....	58
<b>4. Volatile production during interactions.....</b>	<b>59</b>
4.1 Introduction.....	59
4.1.1 The effects of volatile compounds on fungi.....	61
4.1.2 VOC profiles.....	62
4.1.3 Bioactivity of volatiles.....	64
4.1.4 Sampling of volatiles.....	65
4.1.5 Objectives.....	67
4.2 Materials and Methods.....	68
4.2.1 Growth conditions.....	68
4.2.2 Interactions in Reacsyn™ vessel microcosm.....	68
4.2.3 Volatile sampling.....	70
4.2.4 Fibre conditioning.....	71
4.2.5 Headspace sampling.....	71
4.2.6 Volatile compound separation and detection.....	71
4.2.6.1 Fungal volatiles.....	71
4.2.6.2 Calibration and performance checks.....	72

---

4.2.6.3	External standard.....	72
4.2.7	Data analysis.....	73
4.2.7.1	Peak assignment.....	73
4.2.7.2	Production of mass spectra for individual peaks.....	74
4.2.7.3	Peak Identification.....	74
4.2.7.4	Quantification.....	74
4.3	Results.....	75
4.3.1	Mycelial growth.....	75
4.3.2	Fibre Blank.....	76
4.3.3	Polar Test mix.....	76
4.3.4	Terpene Standard Mix.....	77
4.3.5	Malt broth blank.....	78
4.3.6	VOCs produced during mycelial interactions - Day 1.....	82
4.3.7	VOCs produced during mycelial interactions - Day 6.....	84
4.3.7.1	Treatments involving <i>S. gausapatum</i> .....	86
4.3.7.2	Interspecific interaction.....	86
4.3.8	Normalisation.....	89
4.3.9	Quantification.....	89
4.4	Discussion.....	92
4.4.1	Quantification.....	95
4.4.2	Plasticiser volatiles.....	96
4.4.3	Quantification and normalisation method.....	97
4.4.4	Volatile sampling method.....	99
4.4.5	Experimental platform.....	100
4.4.6	Future work.....	100
<b>5.</b>	<b>Suppression Subtractive Hybridisation (SSH).....</b>	<b>102</b>
5.1	Introduction.....	102
5.1.1	SMART cDNA synthesis.....	104
5.1.2	PCR-select cDNA subtraction.....	106
5.1.3	Subtraction verification.....	109
5.1.4	Objectives.....	111
5.2	Materials and Methods.....	112
5.2.1	Growth of mycelium for RNA extraction.....	112
5.2.2	RNA extraction.....	112
5.2.3	SMART cDNA synthesis.....	112
5.2.3.1	First Strand cDNA synthesis.....	112
5.2.3.2	cDNA Amplification by LD-PCR.....	113
5.2.3.3	Purification of LD-PCR reactions.....	115
5.2.4	RsaI Digestion and purification.....	115
5.2.5	Adaptor ligation.....	116
5.2.5.1	Adaptor ligation method.....	116
5.2.6	Ligation efficiency analysis.....	118
5.2.6.1	Design of primers to a constitutively expressed gene.....	119
5.2.6.2	Ligation efficiency analysis method.....	120
5.2.7	First Hybridisation.....	120
5.2.8	Second Hybridisation.....	121
5.2.9	PCR amplification.....	123
5.2.9.1	Primary PCR.....	123
5.2.9.2	Secondary PCR.....	124

---

5.2.9.3	Purification of PCR products .....	124
5.2.10	Vector Ligation.....	125
5.2.11	Transformation of ligation reactions.....	126
5.2.11.1	Transformation of Forward and Reverse subtraction vector ligation reactions.....	126
5.2.11.2	Transformation of control vector ligation reactions.....	127
5.2.12	Screening of transformants.....	127
5.2.13	Miniprepping for Sequencing.....	128
5.2.14	Sequencing.....	129
5.2.15	Sequence Analysis.....	130
5.2.16	Database Similarity searching.....	130
5.2.17	Storage of clones.....	130
5.2.17.1	Temporary storage on patch plates.....	130
5.2.17.2	Long term storage in glycerol stocks.....	131
5.3	Results and Discussion.....	132
5.3.1	SMART cDNA synthesis.....	132
5.3.2	RsaI digestion.....	133
5.3.3	Ligation efficiency analysis.....	134
5.3.3.1	Design of primers to a constitutively expressed gene.....	134
5.3.3.2	Testing $\beta$ -tubulin primers.....	136
5.3.3.3	Adaptor ligation.....	136
5.3.4	Hybridisation .....	138
5.3.5	PCR amplification.....	138
5.3.5.1	Primary PCR.....	139
5.3.5.2	Secondary PCR.....	139
5.3.6	Transformation and cloning.....	140
5.3.6.1	Control vector ligation reactions.....	140
5.3.6.2	Forward and reverse vector ligation reactions.....	141
5.3.7	Screening of transformants.....	141
5.3.8	Sequencing of clones.....	142
5.4	Conclusion.....	143
<b>6. Sequencing of SSH library.....</b>		<b>144</b>
6.1	Introduction.....	144
6.1.1	Objectives.....	149
6.2	Materials and Methods.....	150
6.2.1	PCR with clones from glycerol stocks.....	150
6.2.2	Purification of colony PCR products .....	150
6.2.3	Sequencing.....	151
6.2.4	Partigene.....	151
6.2.4.1	Cross_match.....	151
6.2.4.2	CLOBB.....	151
6.2.4.3	Phrap.....	152
6.2.5	BLAST similarity searches.....	152
6.2.6	Blast2GO.....	152
6.3	Results.....	153
6.3.1	Sequencing.....	153
6.3.2	Clustering analysis with Partigene.....	154
6.3.3	Analysis of clustering of <i>T. versicolor</i> SSH clone sequences.....	155
6.3.4	BLAST search results.....	157

---

6.3.5	Gene Ontology.....	163
6.3.5.1	Biological process.....	163
6.3.5.2	Molecular function.....	164
6.3.5.3	Cellular component.....	166
6.3.5.4	Forward and Reverse SSH libraries.....	167
6.4	Discussion.....	169
6.4.1	Sequence analysis.....	169
6.4.2	Functional annotation.....	172
6.5	Conclusion.....	179
<b>7</b>	<b>Microarrays.....</b>	<b>180</b>
7.1	Introduction.....	180
7.1.1	Array Fabrication.....	181
7.1.2	Probe preparation.....	183
7.1.3	Hybridisation.....	184
7.1.4	Data collection, normalisation and analysis.....	185
7.1.5	Replication.....	186
7.1.6	Microarray standards.....	187
7.1.7	Objectives.....	188
7.2	Materials and Methods.....	189
7.2.1	Array Fabrication.....	189
7.2.1.1	Colony PCR and screening.....	189
7.2.1.2	Transfer to 384 well plates.....	189
7.2.1.3	Invariant Genes.....	190
7.2.1.4	Printing the array.....	190
7.2.2	Making probes for microarray.....	192
7.2.2.1	Growth of mycelium for RNA extraction.....	192
7.2.2.2	RNA extraction.....	192
7.2.2.3	Screening of RNA extracts for contamination with competitor species.....	192
7.2.2.4	Probe making.....	197
7.2.2.5	Hybridisation.....	202
7.2.2.6	Image analysis.....	203
7.2.2.7	Analysis of data with GeneSpring.....	205
7.3	Results.....	208
7.3.1	Clone PCR screening.....	208
7.3.2	RNA extraction.....	209
7.3.3	DNA extraction for sequencing of opposing species.....	209
7.3.4	PCR on species DNA with ITS1F/4.....	210
7.3.5	ITS sequence alignments.....	210
7.3.6	Testing of species specific primers.....	212
7.3.7	Analysis of cDNA with species specific primers.....	213
7.3.8	Probe label assessment.....	214
7.3.9	Microarray image scanning and spot finding.....	216
7.3.10	Assessment and normalisation of array data.....	217
7.3.11	Filtering of data on expression and confidence.....	226
7.3.11.1	<i>T. versicolor</i> vs <i>S. gausapatum</i> .....	226
7.3.11.2	<i>T. versicolor</i> vs <i>H. fasciculare</i> .....	232
7.3.11.3	<i>T. versicolor</i> vs <i>B. adusta</i> .....	234
7.3.11.4	Comparison of experimental pairings.....	238



---

7.4	Discussion.....	242
7.4.1	Technical aspects of microarray analysis.....	242
7.4.2	Gene lists.....	245
<b>8.</b>	<b>Synthesis.....</b>	<b>250</b>
<b>9.</b>	<b>References.....</b>	<b>256</b>
<b>Appendix 1.....</b>	<b>.....</b>	<b>288</b>
A1.1	The basis of Gas Chromatography-Mass Spectrometry.....	288
A1.1.1	Analysis of volatiles.....	288
A1.1.2	Ionisation with MS.....	288
A1.1.3	Detection with MS.....	289
A1.1.4	Analysis of mass spectra.....	290
A1.2	Chromatograms.....	291

## Abstract

Saprotrophic basidiomycetes play key roles in decomposition and nutrient cycling within woodland ecosystems. Species compete for space and resources, resulting in interactions with a range of outcomes, ranging from deadlock to replacement. *Trametes versicolor* was chosen to study these interactions in more detail and at a molecular level. During interactions *T. versicolor* produced barrages of aerial mycelium at the interaction front, and hyphal growth was inhibited in the presence of an opponent prior to contact. Volatile sesquiterpenes and aromatic hydrocarbons were produced when *T. versicolor* interacted with *Stereum gausapatum*, which may have inhibitory effects and cause DNA and protein damage. Suppression subtractive hybridisation libraries were constructed for the interaction of *T. versicolor* vs *S. gausapatum*. This is one of the first studies to examine interspecific interactions of saprotrophic basidiomycetes from a molecular perspective. Expressed sequence tag analysis coupled with cDNA microarray technology was used to study the molecular basis of interactions of *T. versicolor* with *S. gausapatum*, *Bjerkandera adusta* and *Hypholoma fasciculare*, which are replaced, deadlock and replace *T. versicolor*, respectively. Analysis revealed up-regulation of peroxidases, catalase, chaperone proteins and fungal cell wall enzymes, common to interactions. These genes may be employed to deal with an oxidative environment and intracellular damage generated during interactions and responsible for changes in morphology. More genes were common to interactions in which *T. versicolor* deadlocked with, or replaced its competitor, than when it was replaced itself. Different mechanisms may be employed against different species resulting in the range of outcomes observed.

## **Acknowledgements**

I would like to thank the Natural Environment Research Council and Cardiff University for providing the funding for this project and my supervisors Professor Lynne Boddy and Dr. Hilary Rogers for all their time, support and advice over the last few years. Thanks also go to Dr. Pete Kille, Christine Sambles, Steffan Adams, James Osborne and Steve Turner for help and advice with Bioinformatics and microarrays, and Dr. Carsten Müller and Mike O'Reilly for chemistry advice.

I would also like to thank the members of the fungi and plant labs and the BEPG, past and present, for moral support, help, advice, many happy hours in the grad bar, tea, cake, silly chats and fruit wizening. Thanks especially to Martha, Juliet, George, Tim, Jen, Anne, Liz, Esther, Daire and Paul, but also to everyone else, too numerous to mention, who has helped along the way and made my time in Cardiff lots of fun. Finally, I would like to thank my friends and family for supporting me and keeping me entertained, both in Cardiff and from a distance. In particular Emma, David, Kenneth and the Chus, the Parkstone contingent, and Mycobunny.

Figures

Figure	Page
<b>Figure 2.1</b> Zones from which mycelium was harvested for RNA extraction.	25
<b>Figure 3.1</b> Positions where extension measurements were made on single colonies.	38
<b>Figure 3.2</b> Positions where extension measurements were made during paired interaction experiments.	38
<b>Figure 3.3</b> Self-paired interactions	43
<b>Figure 3.4</b> Interaction between <i>T. versicolor</i> and <i>S. hirsutum</i> over time.	44
<b>Figure 3.5</b> Interactions resulting in partial replacement or total replacement of one species by another.	45
<b>Figure 3.6</b> Interactions resulting in deadlock	46
<b>Figure 3.7</b> Interactions between <i>T. versicolor</i> (D2) and competitor species resulting in a range of outcomes.	47
<b>Figure 3.8</b> Comparison of mycelial extension rate ( $\text{mm d}^{-1}$ ) of singly inoculated isolates of four species.	48
<b>Figure 3.9</b> Comparison of mycelial extension rate ( $\text{mm d}^{-1}$ ) of single and self paired inoculations of isolates of four species.	49
<b>Figure 3.10</b> Comparison of extension rates within self paired interactions.	50
<b>Figure 3.11</b> Comparison of extension rate of <i>T. versicolor</i> after different treatments.	51
<b>Figure 4.1</b> Diagram of Reacsyn <sup>TM</sup> vessels used for culturing fungi to enable sampling of volatiles during growth.	68
<b>Figure 4.2</b> Gantt chart showing the timespan of experiment.	70
<b>Figure 4.3</b> Chromatogram for PDMS 100 $\mu\text{m}$ fibre blank run.	76
<b>Figure 4.4</b> Chromatogram of Polar test mix.	77
<b>Figure 4.5</b> Representative chromatogram for terpene test mix.	78
<b>Figure 4.6</b> Representative chromatogram for malt bottle blank day 6.	82
<b>Figure 4.7</b> Representative chromatograms for day 1 samples for all treatments.	83
<b>Figure 4.8</b> Representative chromatograms for day 6 samples for all 5 treatments.	85
<b>Figure 4.9</b> Mass spectra for Peak 1 from both TvSg and TvTv treatments.	86
<b>Figure 4.10</b> Chromatograms showing the distribution of (a) 204 and (b) 136 fragments and (c) the chromatogram for TvSg day 6.	87
<b>Figure 4.11</b> Comparison of the amounts of volatiles detected for each peak on day 1 where peaks were observed in more than one treatment.	90
<b>Figure 4.12</b> Comparison of the amounts of volatile detected for each peak on day 6 where peaks are observed in more than one treatment.	91
<b>Figure 5.1</b> Simplified summary of Suppression subtractive hybridisation (SSH).	103
<b>Figure 5.2</b> The basis of SMART <sup>TM</sup> cDNA synthesis.	105
<b>Figure 5.3</b> Molecular basis of PCR-Select cDNA subtraction.	107

<b>Figure 5.4</b> Summary of the preparation of adaptor-ligated tester cDNAs for hybridisation and PCR, for forward and reverse subtractions.	117
<b>Figure 5.5</b> Sequences of the PCR-Select cDNA adaptors and PCR primers.	123
<b>Figure 5.6</b> Layout of patch plate for temporary storage of clones.	131
<b>Figure 5.7</b> Optimisation of LD-PCR.	132
<b>Figure 5.8</b> Optimised LD-PCR reactions.	133
<b>Figure 5.9</b> Comparison of undigested tester cDNA with <i>RsaI</i> -digested tester cDNA.	133
<b>Figure 5.10</b> Alignment of $\beta$ -tubulin gene amino acid sequences for basidiomycetes <i>T. versicolor</i> , <i>C. cinerea</i> , <i>P. sajor-caju</i> , <i>P. involutus</i> , <i>M. lini</i> , <i>M. violaceum</i>	135
<b>Figure 5.11</b> Testing of $\beta$ -tubulin primers.	136
<b>Figure 5.12</b> Analysis of adaptor ligation efficiency.	137
<b>Figure 5.13</b> $\beta$ -tubulin gene sequence from <i>T. versicolor</i> .	138
<b>Figure 5.14</b> Primary PCR	139
<b>Figure 5.15</b> Secondary PCR	140
<b>Figure 5.16</b> Clone PCR	141
<b>Figure 5.17</b> Examples of the forward subtraction clone sequences from clones screened.	143
<b>Figure 6.1</b> Summary of the basic steps involved in EST analysis.	147
<b>Figure 6.2</b> Example of a high quality sequence chromatogram.	153
<b>Figure 6.3</b> Frequency distribution for SSH clone sequence length (base pairs - bp) after vector and primer sequence removal.	153
<b>Figure 6.4</b> Representation of forward and reverse subtracted SSH clone sequences within the singletons and clusters identified using partigene clustering of all <i>T. versicolor</i> SSH clone sequences.	155
<b>Figure 6.5</b> Frequency distribution of cluster size for clusters produced from partigene clustering analysis with <i>T. versicolor</i> SSH clone sequences only (TVC).	156
<b>Figure 6.6</b> Frequency distribution of cluster size for clusters containing only containing forward subtracted SSH clones, reverse subtracted SSH clones only and mixed clusters.	156
<b>Figure 6.7</b> Distribution of forward and reverse SSH clone sequences within mixed clusters.	156
<b>Figure 6.8</b> Frequency distribution for Contig clone sequence length (base pairs - bp) after vector and primer sequence removal.	157
<b>Figure 6.9</b> Biological process gene ontologies	164
<b>Figure 6.10</b> Molecular function gene ontologies	165
<b>Figure 6.11</b> Cellular component gene ontologies	166
<b>Figure 6.12</b> Graphs showing the relative proportion of each function class in forward and reverse subtracted libraries for each level of level 2 gene ontologies.	168
<b>Figure 7.1</b> Summary of the main stages in microarray analysis.	181
<b>Figure 7.2</b> Layout of subgrids on each microarray slide.	190
<b>Figure 7.3</b> Screening of clone PCR products.	208
<b>Figure 7.4</b> RNA extracted from two sets of biological replicates.	209

<b>Figure 7.5</b> DNA extracted from <i>Bjerkandera adusta</i> .	209
<b>Figure 7.6</b> <i>S. gausapatum</i> DNA amplified with ITS 1F/4 primers.	210
<b>Figure 7.7</b> Alignment of ITS sequences for <i>T. versicolor</i> (TvD2), <i>B. adusta</i> (Bk1), <i>H. fasciculare</i> (HfGTWV2).	211
<b>Figure 7.8</b> Test of <i>S. gausapatum</i> specific primers.	212
<b>Figure 7.9</b> Test of <i>B. adusta</i> specific primers.	212
<b>Figure 7.10</b> Test of <i>H. fasciculare</i> specific primers.	213
<b>Figure 7.11</b> An example of the PCR products from testing Reference and Tester cDNAs with ITS1F/4 primers to ensure cDNA sythesis was successful.	213
<b>Figure 7.12</b> PCR products from testing Reference and Tester cDNAs with <i>S. gausapatum</i> specific primers to test for contamination with <i>S. gausapatum</i> in extracted RNA from <i>T. versicolor</i> .	214
<b>Figure 7.13</b> PCR products from testing Reference and Tester cDNAs with <i>B. adusta</i> specific primers to test for contamination with <i>B. adusta</i> in extracted RNA from <i>T. versicolor</i> .	214
<b>Figure 7.14</b> PCR products from testing Reference and Tester cDNAs with <i>H. fasciculare</i> specific primers to test for contamination with <i>H. fasciculare</i> in extracted RNA from <i>T. versicolor</i> .	215
<b>Figure 7.15</b> Scanned image of John gel for probe labelling assessment.	215
<b>Figure 7.16</b> Composite scanned image of a microarray slide.	217
<b>Figure 7.17</b> Box plots of raw data for all replicate slides of all experiments.	218
<b>Figure 7.18</b> MA plots for microarray slides probed with RNA from <i>T. versicolor</i> interacting with <i>S. gausapatum</i> . Raw data, slides 1 and 15.	219
<b>Figure 7.19</b> MA plots for microarray slides probed with RNA from <i>T. versicolor</i> interacting with <i>S. gausapatum</i> . Raw and normalised data, slides 12, 9, 10.	220
<b>Figure 7.20</b> MA plots for microarray slides probed with RNA from <i>B. adustar</i> interacting with <i>S. gausapatum</i> . Raw and normalised data, slides 14, 8, 9.	221
<b>Figure 7.21</b> MA plots for microarray slides probed with RNA from <i>T. versicolor</i> interacting with <i>H. fasciculare</i> . Raw and normalised data, slides 13, 6, 11.	222
<b>Figure 7.22</b> Scorecard calibration curve.	223
<b>Figure 7.23</b> Boxplots for data normalised with print-tip lowess.	224
<b>Figure 7.24</b> Box plot of normalised data for all three experiments.	225
<b>Figure 7.25</b> PCA plot of normalised data for replicate slides for all experiments.	225
<b>Figure 7.26</b> Expression profile for a $\beta$ -tubulin invariant gene control spot after normalisation.	226
<b>Figure 7.27</b> Line graph showing the normalised expression profile of all <i>T. versicolor</i> spots for hybridisations with test probes for <i>T. versicolor</i> vs <i>S. gausapatum</i> across the three biological replicates.	227
<b>Figure 7.28</b> Line graph showing the normalised expression profile of all Tv spots for hybridisations with test probes for <i>T. versicolor</i> vs <i>H. fasciculare</i> across the three biological replicates.	232

<b>Figure 7.29</b> Line graph showing the normalised expression profile of all Tv spots for hybridisations with test probes for <i>T. versicolor</i> vs <i>B. adusta</i> across biological replicates.	234
<b>Figure 7.30</b> Venn diagrams showing up-regulated genes for all three experiments.	239
<b>Figure 7.31</b> Venn diagrams showing down-regulated genes for all three experiments.	240
<b>Figure A1.1</b> Schematic of a quadrupole mass filter.	290
<b>Figure A1.2</b> Chromatogram for TvSg day 1	291
<b>Figure A1.3</b> Chromatogram for SgSg, day 1.	291
<b>Figure A1.4</b> Chromatogram for TvTv.	292
<b>Figure A1.5</b> Chromatogram for Sg alone.	292
<b>Figure A1.6</b> Chromatogram for Tv alone.	293
<b>Figure A1.7</b> Spectra for peak 1 and 1-3-bis(1,1-dimethylethyl)benzene.	293
<b>Figure A1.8</b> Spectra for peak 2 and 2,6-dimethylbenzaldehyde.	294
<b>Figure A1.9</b> Spectra for peak 3 and Z-3-dodecene.	294
<b>Figure A1.10</b> Spectra for peak 4 and 3,5-bis(1,1-dimethylethyl) phenol.	294
<b>Figure A1.11</b> Spectrum for peak 5.	295
<b>Figure A1.12</b> Spectra for peak 6 and 1,3-diisocyanatomethyl-benzene.	295
<b>Figure A1.13</b> Spectrum for peak 7. Note the decreasing size of peaks, which indicates the fragmentation of a hydrocarbon chain.	295
<b>Figure A1.14</b> Spectrum for peak 8.	296
<b>Figure A1.15</b> Spectra for peak 9 and S-trizolo 4,3-apyridine,3-amino-6-methyl.	296
<b>Figure A1.16</b> Spectrum for peak 10.	296
<b>Figure A1.17</b> Spectra for peak 11 and $\alpha$ -4-dimethyl-3-cylcohexene-1-acetaldehyde.	297
<b>Figure A1.18</b> Spectra for peak 12 and germacrene D.	297
<b>Figure A1.19</b> Spectra for peak 13 and benzoic acid, methyl ester.	297
<b>Figure A1.20</b> Spectrum for peak 14.	298
<b>Figure A1.21</b> Spectrum for peak 15.	298
<b>Figure A1.22</b> Spectra for peak 15 and D-limonene.	298
<b>Figure A1.23</b> Spectra for peak 16 and germacrene D.	299
<b>Figure A1.24</b> Spectra for peak 16 and $\zeta$ -cadineine.	299
<b>Figure A1.25</b> Spectra for peak 16 and 1H-cyclopenta-1,3-cyclopropa-1,2-benzene,octahydro-7-methyl-3- .	299
<b>Figure A1.26</b> Spectrum for peak 17.	300
<b>Figure A1.27</b> Spectra for peak 18 and methyl 3,5-dimethyl benzoate.	300
<b>Figure A1.28</b> Spectrum for peak 19.	300
<b>Figure A1.29</b> Spectrum for peak 20.	301
<b>Figure A1.30</b> Spectra for peak 20 and 2,5-cyclohexadiene-1,4-dione,2,3,5-trimethyl-6-(3-methyl-2-butenyl).	301
<b>Figure A1.31</b> Spectra for peak 21 and benzoic acid, 3-methoxy,-methyl ester (syn. m-anisic acid methyl ester).	301

## Tables

Table	Page
<b>Table 3.1</b> Isolates used for preliminary agar growth rates and interaction experiments.	36
<b>Table 3.2</b> Summary of the outcomes of interactions.	42
<b>Table 4.1</b> Allocation of replicates for each combination to experimental sets 1 and 2	70
<b>Table 4.2</b> Summary of peak analysis for all treatments on days 1 and 6	79
<b>Table 5.1</b> Experimental set up for first strand synthesis for tester and driver samples	113
<b>Table 5.2</b> Reagents added to tester and driver samples for first strand synthesis.	113
<b>Table 5.3</b> Adaptor Ligation experimental set up	117
<b>Table 5.4</b> Ligation efficiency analysis PCR set up	120
<b>Table 5.5</b> Subtraction reaction mixture for forward subtraction	121
<b>Table 5.6</b> Subtraction reaction mixture for reverse subtraction	121
<b>Table 5.7</b> Second Hybridisation reaction mixtures	122
<b>Table 5.8</b> Plasmid ligation reactions set up	125
<b>Table 6.1</b> Results of clustering analysis of <i>T. versicolor</i> SSH clone sequences with partigene	154
<b>Table 6.2</b> Summary of significant results returned from BLAST searches of 882 submitted contig sequences vs different databases	158
<b>Table 6.3</b> Blast results for contigs with ten or more sequences within them	159
<b>Table 6.4</b> Summary of the significant BLAST results for the Forward library with informative annotation	160
<b>Table 6.5</b> Summary of the significant BLAST results for the reverse subtracted library with informative annotation	161
<b>Table 7.1</b> Control samples in Lucidea Universal Scorecard	191
<b>Table 7.2</b> Species specific primers used to test extracted <i>T. versicolor</i> RNA for contamination by opposing species	197
<b>Table 7.3</b> Species specific primers used to test extracted <i>T. versicolor</i> RNA for contamination by opposing species	210
<b>Table 7.4</b> Typical values from assessment of probe labelling	216
<b>Table 7.5</b> Summary of the numbers of genes identified for each experimental pairing when filtered on expression level	227
<b>Table 7.6</b> List of genes up-regulated, filtered on expression level, with significant annotation for <i>T. versicolor</i> vs <i>S. gausapatum</i>	229
<b>Table 7.7</b> List of genes down-regulated, filtered on expression level, with significant annotation from <i>T. versicolor</i> vs <i>S. gausapatum</i>	231
<b>Table 7.8</b> List of genes up-regulated, filtered on expression level, with annotation for <i>T. versicolor</i> vs <i>H. fasciculare</i>	233
<b>Table 7.9</b> List of genes down-regulated, filtered on expression level, with annotation, for <i>T. versicolor</i> vs <i>H. fasciculare</i>	233
<b>Table 7.10</b> List of genes up-regulated, filtered on expression level, with annotation for <i>T.</i>	236



---

<i>versicolor</i> vs <i>B. adusta</i>	
<b>Table 7.11</b> List of genes down-regulated, filtered on expression level, with annotation, for <i>T. versicolor</i> vs <i>B. adusta</i>	237
<b>Table 7.12</b> List of all genes 1.4 fold up-regulated in all pairings	239
<b>Table 7.13</b> List of genes down-regulated in all three pairings in at least 2 out of 3 arrays for each experiment	241

**Abbreviations**

5'-RACE	Rapid amplification of 5' complementary DNA ends
A	Adenine
AAD	Aryl alcohol dehydrogenase
aa-dUTP	Aminoallyl- 2'-deoxyuridine 5'-triphosphate
Amp50	Ampicillin (50 ng ml <sup>-1</sup> )
ANOVA	Analysis of variance
ATP	Adenosine triphosphate
Bk1	<i>Bjerkandera adusta</i> isolate Bk1
BLAST	Basic local alignment search tool
C	Cytosine
C6	6 carbon molecule
C8	8 carbon molecule
cDNA	Complementary DNA
CI	Chemical ionisation
CLOBB	Clustering on the basis of BLAST
Cy3	Cyanine3
Cy5	Cyanine5
dC	Deoxycytidine
DD	Differential display
DDBJ	DNA Database of Japan
DDHF3	<i>Hypholoma fasciculare</i> isolate DDHF3
DDHF4	<i>Hypholoma fasciculare</i> isolate DDHF3
DMSO	Dimethyl sulfoxide
DNA	Deoxyribonucleic acid
dNTP	Deoxyribonucleotide triphosphate
ds cDNA	Double stranded cDNA
DTT	Dithio-1,4-threitol
EDTA	Ethylenediamine tetraacetic acid
EGTDC	Environmental genomics thematic programme data centre
EI	Electron ionisation
EMBL	European Molecular Biology Laboratory
ESI	Electrospray
EST	Expressed sequence tag
EtBr	Ethidium bromide
FAB	Fast atom bombardment
FGI	Fungal genome initiative
G	Guanine
G3PDH	Glyceraldehydes 3-phosphate dehydrogenase
GC	Gas chromatograph
GC-MS	Gas chromatography-Mass spectrometry
GO	Gene ontology
GTWV1	<i>Hypholoma fasciculare</i> isolate GTWV1
GTWV2	<i>Hypholoma fasciculare</i> isolate GTWV2
HEPES	4-(2-hydroxyethyl)-1-piperazineethanesulfonic acid
HR	Hypersensitive response
HSSE	Headspace sorptive extraction
ICR	Ion cyclotron resonance
IPTG	Isopropyl-1-thio-β-D-galactopyranoside

IPTG	Isopropyl-beta-D-thiogalactopyranoside
LD-PCR	Long distance polymerase chain reaction
LLE	Liquid-liquid extraction
LOWESS	Locally weighted scatterplot smoothing
MA	Malt extract agar
MA313	<i>Bjerdandera adusta</i> isolate MA313
MALDI	Matrix assisted laser desorption
MGED	Microarray Gene Expression Data
MIAME	Minimum information about a microarray experiment
MMLV RT	Moloney murine leukaemia virus reverse transcriptase
MPSS	Massive parallel signature sequencing
mRNA	Messenger RNA
MS	Mass spectrometer
NADPH	Reduced form of Nicotinamide adenine dinucleotide phosphate
NCBI	National Centre for Biotechnology Information
NERC	Natural environment research council
NIST	National institute of standards and technology
P:C:I	Phenol:chloroform;isoamyl alcohol
PA	Polyacrylate
PCA	Principal component analysis
PCR	Polymerase chain reaction
PDMS	Polydimethylsiloxane
PEI	Polyethylenimine
PIR	Protein information resource
PMSF	Phenylmethylsulfonylfluoride
polyA	polyadenylated
Pr175	<i>Phlebia radiata</i> isolate 175
PrCop	<i>Phlebia radiata</i> Cop isolate
RDA	Representational differences analysis
RNA	Ribonucleic acid
RNAi	RNA interference
RT	Retention time
RT	Reverse transcriptase
RT-PCR	Reverse transcriptase PCR
SAGE	Serial analysis of gene expression
SDS	Sodium docecyl sulphate
SDS-PAGE	Sodium dodecyl sulfatate polyacrylamide gel electrophoresis
SE	Standard error
SEM	Standard error of mean
Sg1	<i>Stereum gausapatum</i> isolate 1
Sg2	<i>Stereum gausapatum</i> isolate 2
SgSg	<i>S. gausapatum</i> vs <i>S. gausapatum</i>
SH	Subtractive hybridisation
Sh1	<i>Stereum hirsutum</i> isolate 1
Sh2	<i>Stereum hirsutum</i> isolate 2
Sh3	<i>Stereum hirsutum</i> isolate 3
SMART	Switching Mechanism at 5' End of RNA Template
SPE	Solid phase extraction
SPME	Solid phase microextraction
ss cDNA	Single stranded cDNA

SSH	Suppression subtractive hybridisation
SSI	Solid sample injection
Stu	Standard terpene units
Swiss-Prot	Swiss Institute of Bioinformatics protein database
T	Thymine
TAE	Tri-Acetate-EDTA
TCTP	Translationally controlled tumour protein
TEMED	N,N,N',N'-Tetramethylethylenediamine
TOF	Time of flight
TrEMBL	Translated sequences from the EMBL database
TTC	<i>T. versicolor</i> EST and other <i>T. versicolor</i> ESTs from Genbank partigene clustering ID
TVC	<i>T. versicolor</i> EST partigene clustering ID
TvD1	<i>Trametes versicolor</i> isolate D1
TvD2	<i>Trametes versicolor</i> isolate D2
TvD3	<i>Trametes versicolor</i> isolate D3
TvD4	<i>Trametes versicolor</i> isolate D4
TvBk	<i>T. versicolor</i> vs <i>B. adusta</i> interaction
TvHf	<i>T. versicolor</i> vs <i>H. fasciculare</i> interaction
TvSg	<i>T. versicolor</i> vs <i>S. gausapatum</i> interaction
TvTv	<i>T. versicolor</i> vs <i>T. versicolor</i> self pairing
TYC	<i>T. versicolor</i> EST and <i>S. cerevisiae</i> EST partigene clustering ID
U	Uracil
Uniprot	Universal protein resource
VOC	Volatile organic compounds
X-gal	5-bromo-4-chloro-3-indolyl- $\beta$ -D-galactopyranoside

## 1. Introduction

The woodland ecosystem comprises a complex network of organisms that interact with each other and the abiotic environment to produce a dynamic community. Nutrient cycling, decomposition, pathogenesis, mutualistic symbiosis, succession and biodiversity are all driven and maintained by the communities within this environment and are constantly in a state of flux. Each process is regulated by an array of factors that can vary over space and time.

### 1.1 Fungi in the environment

Fungi play a major role in these woodland ecosystems and, together with bacteria and invertebrates, are amongst the most abundant groups of organisms, accounting for the majority of biomass. Estimates of the number of species of fungi worldwide exceed 1.5 million (Hawksworth, 1995; 2001). Currently only a fraction of these species have been detected, described and classified - approximately 72 000 species (Bridge & Spooner, 2001) spread across seven phyla (Hibbett *et al.*, 2007). However, the number of species described is ever increasing as new techniques are developed for detecting and profiling fungal diversity (Kennedy & Clipson, 2003; Allmér *et al.*, 2006; Mitchell & Zuccaro, 2006). Furthermore, molecular phylogenetic analysis has added a new dimension to species delimitation and many traditional classifications based on morphological characteristics are being revisited and revised (Hibbett *et al.*, 2007).

The greatest fungal diversity can be found in the soil environment and in woodland ecosystems. It is estimated that only 17% of described species can be successfully grown in culture (Bridge & Spooner, 2001) thus many known species are not readily studied. Furthermore, much of the diversity in woods and soil is cryptic and present in resting stages such as conidia, spores and inactive mycelium (Hättenschwiler *et al.*, 2006). Clearly ecological studies to date can only provide a partial picture of the organisms and their functions and interrelationships within ecosystems.

The woodland ecosystem is heterogeneous (White *et al.*, 1998; Boddy, 1999) with respect to the biotic and abiotic environment, both spatially and temporally. Fungi have evolved and adapted to this variable environment, and niche specialisation has resulted in a diverse range of morphologies, ecological strategies and habitats. It is this niche differentiation that shapes and maintains community structure and the spatiotemporal nutritional and structural heterogeneities influence events at all levels, from hyphae to communities (Boswell *et al.*, 2007). Climate change may have implications for changing community structures as changing temperatures may have concomitant effects on many factors in the environment.

### 1.2 Decomposition

Decomposition is a vital process that facilitates nutrient recycling by making nutrient resources in plant and animal material available to a wide range of organisms to utilise. Many organic sources of carbon can be readily used for nutrition, however the more complex polymers such as cellulose and lignin from plant cells, and chitin from invertebrate exoskeletons, are less easily decomposed and are only utilised by specialists. In woodlands the predominant carbon resource is wood litter (Wells & Boddy, 2002), which is resistant to decomposition and many organisms are unable to access and utilise this resource. Thus, many are reliant on the specialist saprotrophic basidiomycetes to initiate decomposition of woody debris, and break down the more refractory compounds into simpler forms, which can then be broken down further and utilised by other organisms. As such, fungi are the main agents of wood decomposition in terrestrial ecosystems (Boddy, 2001). The most common group are the 'white-rot fungi', which are able to penetrate the tissues of wood, digest lignin and cellulose enzymatically and leave wood stringy, bleached and soft. Less common are the 'brown-rot fungi', which are only able to digest cellulose, while lignin is left intact or slightly modified, leaving wood brown and crumbly.

Fungal decomposition is facilitated by a suite of enzymes that act on different wood constituents and can be loosely classified into three groups: (i) enzymes that attack constituents directly e.g. phenoloxidases; (ii) enzymes that do not attack wood directly e.g. superoxide dismutase and glyoxal oxidase; (iii) feedback enzymes which have a

key role in coordinating metabolic pathways during decomposition (Leonowicz *et al.*, 1999). Low molecular weight compounds and free radicals may also act as mobile factors that can permeate wood and initiate decay where high molecular weight enzymes are not able to penetrate completely as they are too large (Evans *et al.*, 1994).

The environment within wood itself is heterogeneous as the water potential, gaseous regime and pH can all vary with the status of wood (Boddy, 1999). Heartwood has very low nitrogen concentrations relative to attached branches, and CO<sub>2</sub> concentration is generally high within wood, and associated with this are low O<sub>2</sub> concentrations. Moreover, there are numerous other compounds within wood such as tannins, gums and resins. Throughout the transition from living to fallen dead wood these conditions change. Dead standing wood dries rapidly, compounds within the wood leach out or break down and thus the conditions and the composition of the wood changes as decomposition progresses (Griffith & Boddy, 1991*a,b*). As conditions change so too does the fungal community because the space and resources available as decomposition progresses will favour a different set of species specialised to a particular niche. Community diversity can also influence decomposition rates with complex communities often resulting in greater decomposition than simple ones, but this also depends on which species are involved (Hättenschwiler *et al.*, 2005).

The abundance and diversity of fungi within woodland ecosystems means that contact, or at least proximity between individuals and other organisms is inevitable and where this occurs there will be interactions. These interactions can take the form of competition, neutralism and mutualism (Rayner & Webber, 1986). Truly neutralistic and mutualistic interactions, however, are thought to be rare as most interactions appear to involve some form of competition for both physical space to colonise and for the resources within that space. Competition is also a major driver of community change.

### 1.3 Competition

Keddy (1989) defines competition as “the negative effects which one organism has upon another by consuming or controlling access to a resource that is limited in availability”. This definition of competition may be applied to fungal systems, however, competition has been alternatively defined as two distinct phenomena, exploitation and interference (Lockwood, 1992). Exploitation is the depletion of a resource by an organism or population, which does not necessarily prevent or limit the access to the same resource by other organisms. Interference is when access to a resource is influenced by the presence of another competitor, either through its behaviour or some sort of chemical mechanism. These definitions, however, are not suitable for fungal systems as the nature of mycelial systems is that a fungus will occupy an area, whether it is soil, litter or wood, and use the resources within that area. Thus, competition for space and resources cannot be uncoupled into separate entities and Keddy’s definition is insufficient to fully describe the interactions that can take place between fungi.

### 1.4 Fungal competition

Boddy (2000) defined fungal competition in two main categories: primary resource capture and secondary resource capture. Primary resource capture is the process by which pioneer species gain access to previously uncolonised resources for the first time, while secondary resource capture describes how species gain access to already occupied space and resources, usually by combat, and thus effect changes in community structure.

Fungal colonisation of wood can occur via many routes and at various stages during the life of a tree. Pioneer species may gain access to live wood as pathogens, through wounds or via insect vectors, or some species may be present as latent propagules within the wood awaiting suitable conditions for extensive mycelial growth (Boddy, 2001). Since the resource has not previously been colonised there is little need for combat to gain access, except perhaps on the surface, hence these primary colonisers are often poor competitors (Holmer & Stenlid, 1997). Consequently, the main factor



affecting the success of primary resource capture is not combat but the ability of species to reach and exploit resources first. This is determined by efficiency of spore dispersal, spore germination, mycelial extension and whether species possess the correct suite of enzymes required to assimilate the resource (Rayner & Webber, 1986; Boddy, 2001). This will favour R-selected or ruderal species which tend to have a transient existence during which mycelium will use only those resources that are readily accessible and assimilated so that establishment, reproduction and dispersal are rapid.

As wood becomes increasingly colonised the domains of pioneer species will extend and some will come into contact. Simultaneously other species may be attempting to gain access to the resources. Combat then occurs and can take two forms: defence and secondary resource capture (Dowson *et al.*, 1988). Primary colonisers use defence strategies to resist replacement, such as the production of pseudosclerotial plates (Griffith & Boddy, 1991*a*) and production of H<sub>2</sub>O<sub>2</sub> (Glass & Dementhon, 2006). Incoming species use secondary resource capture mechanisms to gain access to already occupied areas. This second wave of species needs to withstand or exploit the presence of other species either by coexisting with those already present or by displacing them. Hence they tend to have a greater competitive ability and once they gain access to a resource they are able to dominate it for longer and exploit the resource fully by utilising the more refractory compounds. Furthermore, the conditions in the wood following primary colonisation and as decomposition progresses, such as a reduction in moisture content, may be more favourable to secondary colonisers (Griffith & Boddy, 1991*a,b,c*). While competition can be metabolically costly it can lead to species exclusion and dominance by highly competitive species and the energy expenditure is justified by the eventual acquisition of resources. These are the K-selected species and are at the opposite end of the spectrum of ecological strategies to R-selection (Rayner & Webber, 1986; Boddy, 2001). It is these interactions that largely drive niche differentiation in a variable environment and maintain species diversity in communities.

### 1.5 Mechanisms of combat

Combative interactions may be effected by a number of different mechanisms either singly or in combination depending on the species and conditions involved. Antagonistic interactions can occur at a distance before species have made physical contact. This may be passive inhibition if the growth environment is made unfavourable by the accumulation of waste products or changes in the pH of the area surrounding a colony. However, many fungi are capable of actively producing volatile and diffusible antibiotic compounds that inhibit their competitors (Boddy, 2000; Wheatley, 2002). Antibiosis during interactions is dependent on the species involved, implying that there is recognition between species that elicits antibiotic production. Moreover, varying sensitivity to antibiotics will affect the outcomes of these interactions.

Combat via contact can occur at the level of single hyphae or the mycelia of colonies interacting on a gross scale or via parasitic associations (Boddy, 2000). Mycoparasitism is relatively rare and is often only a temporary strategy used by a parasitising fungus to gain territory from a host rather than using parasitism as its main strategy for nutrient acquisition. Parasitism has a detrimental affect on the host species and some of the changes associated with it are coagulation and degeneration of cytoplasm of hyphae, coiling and invasion of conidiophores and conidia and the production of hydrolytic enzymes. These changes are seen when *Botrytis cinerea* is parasitised by various species (White & Traquair, 2006). Similarly, *Trichoderma* spp. are known to parasitise a number of species including the plant pathogens *Rhizoctonia solani* (Almeida *et al.*, 2007) and *Fusarium oxysporum* (Dubey & Suresh, 2006) making *Trichoderma* spp. a potential candidate for biocontrol of these pathogens. The parasitism of *Agaricus bisporus* by *Verticillium fungicola* causes similar changes and this interaction has commercial significance as it results in disease of this commercial crop (Calonje *et al.*, 2000; Garcia Mendoza, 2005).

Hyphal interference occurs when individual hyphae meet and make contact. Upon contact between different species there may be non-self recognition and incompatibility systems trigger defence responses such as the production of H<sub>2</sub>O<sub>2</sub>, and lysis and cell death of the contacted hyphae prevent further advances (Glass *et al.*,

2000; Micali & Smith, 2003; Silar, 2005; Glass & Dementhon, 2006). A classic example is the interaction between *Phlebiopsis gigantea* and *Heterobasidion annosum* where any hyphae of *H. annosum* that make contact with *P. gigantea* show rapid localised disruption of the cytoplasm and cell membrane (Ikediugwu, 1976).

Gross mycelial contact occurs when whole colonies are involved in confrontations on a bulk scale. The effects can be seen easily on agar during interactions where the morphology of colonies changes dramatically in response to the presence of a combatant. Amongst the most common changes that may be observed are the production of pigments, mycelial fans, mounds of mycelium, cords and rhizomorphs, redistribution of mycelium and induction of sporulation (Rayner & Turton, 1982; Boddy & Rayner, 1983*b*; Rayner & Webber, 1986; Dowson *et al.*, 1998; Wald *et al.*, 2004*a,b*). The result is a dense area of mycelium at the interaction front and depending on how the interaction progresses, this can remain stationary as a blockade to prevent ingress, or it may become an aggressive front that gradually progresses over the opposing colony. It is thought that the mycelium in this zone is non-assimilative (Boddy, 2000) perhaps because most energy is expended on combat.

### 1.6 Outcomes of interactions

There is a spectrum of potential outcomes of combative interactions. Colonies may intermingle, reach a deadlock or there may be complete replacement of one species by another.

Intermingling generally occurs during mycoparasitism and when the mycelium of an isolate meets itself and there is self recognition. However, intermingling can also occur when the mycelium of opposing colonies is sufficiently sparse that individual hyphae can interdigitate and not actually make contact (Rayner & Webber, 1986). Poor nutrient availability can give rise to this circumstance as fungi can adopt an explorative foraging strategy in response to the low nutrient levels which manifests itself as sparse colonies (Tordoff *et al.*, 2006).

The most common outcomes of interspecific confrontations are deadlock and replacement (Boddy, 2000). Deadlock occurs when neither individual is able to wrest territory from the other. The barrages of mycelium produced by both species prevent invasion by the other. Replacement occurs when one individual destructively invades the domain of another and gains control of the space and the nutrients within it. Partial replacement falls somewhere along the continuum between the two extremes of deadlock and total replacement.

The outcome of an interaction is largely dependent on the relative combative ability of the confronting species and a combative hierarchy results (Holmer *et al.*, 1997). However, the timings of interactions play a major role in determining the outcome of an interaction together with the environmental conditions. Kennedy *et al.* (2007) found that when two ectomycorrhizal fungi were inoculated into the roots of a plant at the same time the more competitive species would always eventually displace the other and dominate, whereas if the weaker species was already established in the roots and the other inoculated later then the two species would coexist. Similarly, size of territory occupied by saprotrophic myelia affects the outcome of interactions (Shearer, 1995; Holmer & Stenlid, 1997, 1993).

The abiotic environment has a significant effect on the outcomes of interactions. A substantial amount of work has observed interactions under a variety of experimental conditions, including different gaseous regimes, pH, temperature, water potentials, the presence of other organisms and nutrient availability (Boddy & Rayner, 1983*b*; Boddy *et al.*, 1985; Griffith & Rayner, 1994; Wald *et al.*, 2004*a,b*). The results have shown that the interaction between the same pair of species can have very different outcomes depending on the conditions, which may influence the ecological strategy that a species adopts. For example, Griffiths and Boddy (1991*c*) found that secondary colonisers were associated with a reduction in moisture content, analogous to drying dead wood, which coincides with the arrival of secondary colonisers. Perhaps then the primary colonisers are those species that favour more moist conditions that are found in freshly fallen wood.

Whatever the outcome of an interaction it is important to note that there is a dynamic equilibrium in operation and over long periods of time resources may become

depleted, conditions may change and thus the status of the interaction changes. Moreover, there are also interactions occurring between fungi and other organisms such as bacteria and invertebrates as well as between themselves. Bacteria may benefit from the presence of fungi but fungi may themselves be inhibited by their presence (Romani *et al.*, 2006; De Boer *et al.*, 2007) which in turn influences their interactions with other species and vice versa. Invertebrate feeding can alter the foraging strategies of certain species of fungi (Tordoff *et al.*, 2006) which may also affect the outcome of their interactions with other fungi.

Clearly, ecosystems are a complex network of inter-relationships between many organisms and the environment on many different levels. It is synergistic interactions between species and the environment that influence the rate of decomposition, drive niche differentiation and act to maintain diversity and function. For example, Toljander *et al.* (2006) found that decomposition was greatest when there was intermediate diversity and temperature fluctuations and also that the temperature fluctuations facilitated the co-existence of species.

### 1.7 Studying interactions

The majority of research to date on interspecific interactions has been qualitative and has involved confronting species using a number of systems such as inoculating onto agar, wood blocks, soil trays, logs, microscope slides, 3-dimensional columns of growth media and gradient plates (Holmer *et al.*, 1997; Donnelly & Boddy, 2001; Tordoff *et al.*, 2006) in a variety of conditions, and assessing the outcome of interactions. Interactions are most easily observed when using agar. This is not the most realistic growth condition for fungi, thus outcomes may not always mirror those of the natural environment. Nevertheless, this system allows controlled manipulation of environmental factors and can offer valuable insight into the mechanisms involved in interactions. Other systems may more closely resemble the natural environment but mycelium is less easily visualised or separated from these media for study. A combination of these methods is necessary for a full understanding of interactions. Although the mechanisms of interactions have been described, very little is known about the chemistry and molecular biology that underpin them.

### 1.8 Extracellular enzyme activity

The decomposition of wood by basidiomycetes involves the biodegradation of lignin and is a multienzymatic process involving many phenoloxidising enzymes (Leonowicz *et al.*, 1999). Phenoloxidising enzymes also appear to be important in the changes that take place in offensive and defensive strategies during interactions (Score *et al.*, 1997). More than 100 different enzymes have been isolated from fungi (Baldrian, 2006) and isozymes vary in number and function between species (Luis *et al.*, 2005). Furthermore different species possess different sets of enzymes. The most common enzymes, however, are manganese-peroxidase, laccase and lignin peroxidase, which are predominantly used for wood decomposition by white rot fungi and are consequently the most studied. Their study may also provide some information about the function and distribution of other less studied enzymes. Brown rot fungi tend to produce a different set of enzymes as they target primarily cellulose for decomposition rather than lignin (Valaskova & Baldrian, 2006). Laccase is one of the most dominant of the enzymes produced by fungi and most ligninolytic species produce at least one laccase isozyme (Baldrian, 2006). Luis *et al.* (2005) found 167 different fungal laccase sequences from a sample of colonised soil. Laccase is capable of oxidising phenolic compounds and is involved in the decomposition of lignocellulose (Leonowicz *et al.*, 1999) making this enzyme and the fungi that produce it very important in the wood pulping industry. Laccase has also been implicated in the production of invasive hyphae or defensive hyphal barrages, detoxification of phenolics and the production of melanins (Rayner *et al.*, 1994). Laccase can be produced in pure culture and during interactions (Score *et al.*, 1997). Studies of laccase have found spatial and temporal changes in its production depending on the species and conditions involved (White & Boddy, 1992*a,b*; Iakovlev & Stenlid, 2000; Savoie *et al.*, 2001; Hatvani *et al.*, 2002; Baldrian, 2006).

Lignin peroxidase does not appear to be required for wood decomposition but its presence does accelerate lignin decomposition in the presence of other enzymes. This may be effected either by enhancing the susceptibility of lignin to decomposition by other enzymes or it may detoxify lower molecular weight lignin-derived phenolics during its decomposition (Sarkanen *et al.*, 1991). Peroxidase is involved in the production of melanin and antifungal toxic compounds (Score *et al.*, 1997) but is also

involved in dealing with hostile environments. Many pathogenic fungi produce anti-oxidative stress enzymes such as peroxidase, superoxide dismutase and catalase in response to the oxidative host environment generated by the plant hypersensitive response in response to attack (Zhang *et al.*, 2004; Karlsson *et al.*, 2005) and perhaps similar enzymes are required during hostile confrontations between fungi.

The production of enzymes is affected by nutrient availability, the abiotic environment and by interactions with other organisms. In *Agaricus bisporus* cellulase is regulated by the carbon source available, its production is induced by cellulose but repressed by glucose (Morales & Thurston, 2003). Similarly in *Pleurotus ostreatus* Mn-peroxidase and laccase activity increased when the fungus was grown on media with different carbon contents (Šnajdr & Baldrian, 2006). The presence of fungi also increases the bacterial communities as the fungal enzyme activity provides growth substrate for bacteria (Romaní *et al.*, 2006). The nitrogen content at the centre of wood tends to be very low, which is sub-optimal for fungal growth, however, wood-decomposing fungi are capable of decomposing their own hyphal cell walls from old mycelium and those of other earlier colonisers using enzymes. This recycling provides a source of nitrogen and may help fungi to colonise new resources in inhospitable environments or to replace existing colonisers via secondary resource capture (Lindahl & Finlay, 2006). Similarly, laccase activity increased in some species at the interaction zone and also increased in late stage fungi (Iakovlev & Stenlid, 2000). Thus increased laccase activity may facilitate secondary resource capture and enzyme activity may help shape the ecological strategies of fungi.

Interactions between fungi and other organisms also affect enzyme activity (Tsujiyama & Minami, 2005). *Trametes versicolor* and *Pleurotus ostreatus* both increase their laccase activity after contact with soil fungi, bacteria and yeast and this increase can be as much as 40 fold when confronted with a *Trichoderma* species (Baldrian, 2004). However, this increase in activity may not be related to a defensive strategy (Savoie *et al.*, 2001) but rather it could be that interactions trigger synergism between species to increase enzyme activity and decomposition. An increase in diversity has been observed to increase decomposition rates in some cases (Hättenschwiler *et al.*, 2005) and perhaps enzyme activity is responsible for this effect. Similarly, the spatial distribution of laccase activity varies with the nature of

an interaction. Iakovlev and Stenlid (2000) observed that laccase activity found in an interaction zone was associated with mycelial overgrowth and replacement, while laccase activity in mycelium but not the interaction zone only occurred in fungal species which were overgrown themselves. Similarly, Lindahl and Finlay (2006) found different enzyme activity during the colonisation of wood and during secondary overgrowth of one fungus by another. However, White and Boddy (1992*a,b*) found no such correlation in the species interactions they studied implying that additional factors must be involved. Thus, enzyme activity may be correlated with the outcome of interactions and ecological strategies but clearly a number of factors are involved and no one rule will fit all circumstances. *Phlebia radiata* is an interesting example because colonies exhibit two modes of mycelial growth. Exploratory coenocytic primary mycelium lacks laccase and peroxidase activity (Griffith & Rayner, 1994; Griffith *et al.*, 1994). This mycelium is adapted to rapid extension, primary resource capture and early establishment. As discussed earlier many primary colonisers utilise the readily available carbon compounds rather than decomposing the more complex lignocellulose. The absence of the lignolytic enzymes implies that lignin decomposition is not occurring and supports the exploratory role of the primary mycelium. However, in the septate secondary mycelium there is laccase activity (White & Boddy, 1992*a*; Griffith & Rayner, 1994; Griffith *et al.*, 1994). Septate secondary mycelium is produced 2 cm from the colony margin (Boddy & Rayner, 1983*b*) and is associated with long term occupation of a resource and lignin degradation.

### 1.9 Chemicals as the effectors of interactions

Interactions are undoubtedly effected by a number of mechanisms working in concert. Chemical signalling is likely to play a major role in fungal recognition systems, which allow discrimination between self and non-self interactions, and also in the changes that result from fungal-fungal interactions and interactions with other organisms. Fungi are known to produce a number of volatile and diffusible chemicals, many of which have antibiotic properties that have been exploited in medicine and industry. Many species produce a unique reproducible profile of chemicals which can be used as a sort of fingerprint for their identification (Scotter *et al.*, 2005). A number of



studies have looked at the effects of chemical extracts taken from interacting species of microorganisms, often bacterial-fungal interactions, on the induction of morphological changes (Wheatley, 2002) and their influence on the growth of other species and the outcome of interactions. *Trichoderma* spp. metabolites inhibit the growth of other species (Schoeman *et al.*, 1996), which together may form part of the basis of its ability to parasitise other fungal species and may have potential applications in biocontrol. Similarly the application of bacterial culture extracts from *Bacillus subtilis* to growing cultures of *Phlebia radiata* induced interaction-like changes in morphology (Griffith *et al.*, 1994). Compounds known to affect mitochondrial metabolism, phenol oxidase activity and 2,4-dinitro phenol also induced the same morphological changes (Griffith *et al.*, 1994) perhaps elucidating some of the pathways involved in these changes.

The production of volatile organics compounds (VOCs) by fungi is also well documented, especially from spoilage of stored plant material (Ramin *et al.*, 2005) and in buildings where 'sick building syndrome' is diagnosed (Wady *et al.*, 2005). The production of volatiles in these circumstances appears to have little function and they may just be byproducts or precursors of various pathways. However, the production of particular chemicals can aid the detection and identification of fungi present and allows timely treatments if necessary. For example, toxigenic strains of *Fusarium* spp. produce tricodiene, which is a precursor to the mycotoxin tricothecene (Demyttenaere *et al.*, 2004). Thus, detection of tricodiene within stored crops indicates contamination with a toxigenic strain of *Fusarium*. In addition, fungal volatiles have many ecological functions which include acting as 'pollinator' attractants (Schiestl *et al.*, 2006), chemical cues that aid invertebrates with foraging (Belmain, 1996) and habitat establishment (Martinez *et al.*, 2006; Steiner *et al.*, 2007). They are implicated in the modulation of fungal development (Mendgen *et al.*, 2006) and also known to induce defence responses in plants (Splivallo *et al.*, 2007). During interactions between fungi different profiles of volatiles have been detected compared to those produced by individual species grown alone (Hynes *et al.*, 2007). The nature of the interactions of volatile compounds with fungi and their impact on fungal growth at the molecular level is largely unknown. However, the presence of volatile compounds may change the profile of proteins produced (Humphris *et al.*, 2002;

Myung *et al.*, 2007) and thus the implication is that volatile compounds may have effects at the transcriptional gene expression level.

### 1.10 The molecular basis of interactions

Currently very little is known about the molecular basis of fungal interspecific interactions despite the significant amount of literature on interactions in general. Changes in morphology, enzyme activity and the production of volatile and diffusible compounds are a clear indication that there are physiological changes occurring within mycelia during interactions. A combination of alterations in gene expression and enzyme activity in different conditions are likely to be responsible for these changes, and these in turn will be affected by the genotype of species and how it interacts with its environment.

Fungal gene expression has been mostly studied in model organisms such as *Aspergillus niger* and the yeast *Saccharomyces cerevisiae*. Relatively little is known about basidiomycete gene expression and the majority of research has focussed on development of fruiting structures (Wessels, 1992) and different modes of hyphal growth (Nugent *et al.*, 2004). Where interactions have been studied it has been the interactions between mycorrhizal and pathogenic fungi and their plant hosts (Skinner *et al.*, 2001; Cramer & Lawrence, 2003; Küster *et al.*, 2007), or between fungi and bacteria (Schrey *et al.*, 2005). Few studies have investigated fungal interspecific interactions from a molecular perspective. Where it has been studied it has mostly been with respect to mycoparasitic species with the potential for exploitation for biocontrol. Differentially expressed genes have been identified during mycoparasitism of *Heterbasidion annosum* by *Physisporinus sanguinolentus* (Iakovlev *et al.*, 2004), *Heterbasidion parviporum* by *Phlebiopsis gigantia* (Adomas *et al.*, 2006) and between the biocontrol agent *Trichoderma hamatum* and the phytopathogen *Sclerotinia sclerotiorum* (Carpenter *et al.*, 2005). Similarly, genes involved in the pathogenic interaction between *Verticillium fungicola* and *Agaricus bisporus* (Amey *et al.*, 2003) have been identified.

### 1.11 Methods for the study of gene expression

There are a number of techniques that can be used for gene expression profiling such as differential display (Liang & Pardee, 1992), suppression subtractive hybridisation (SSH) (Diatchenko *et al.*, 1996), representational differences analysis (RDA) (Lisitsyn *et al.*, 1993), serial analysis of gene expression (SAGE) (Velculescu *et al.*, 1995), massive parallel signature sequencing (MPSS) (Brenner *et al.*, 2000) and microarray technology. These methods for differential gene expression analysis provide a snapshot of a transcriptome at a particular time and under certain conditions and provide a set of genes that are differentially expressed. Each method has different capabilities, constraints and limitations which must be considered when choosing which approach to use.

Differential display, SSH and RDA do not require prior sequence knowledge and are relatively simple methods that involve the isolation of RNA from the tissue or cells to be compared, followed by synthesis of cDNA libraries and screening of clones, to confirm differential expression.

Differential display (Liang & Pardee, 1992) involves amplification of selected fragments by PCR using targeted or random primers, followed by electrophoresis of cDNA fragments on polyacrylamide gels to produce a fingerprint of bands for a particular cDNA population. Banding patterns are compared between cDNA populations and the differentially expressed genes identified. Candidate bands are excised from gels, reamplified, cloned, sequenced and compared to sequence databases. Differential display is limited by labour-intensive cloning and screening, can be biased towards higher abundance transcripts and requires significant amounts of RNA (Stein & Liang, 2002; Nagaraj *et al.*, 2007).

Subtractive hybridisation (SH) is a method by which cDNA libraries can be generated that comprise only differentially expressed genes. Briefly, two populations of cDNA, generated from samples that are to be compared are mixed and the transcripts common to both samples hybridise and are removed. The remaining transcripts are differentially expressed and are amplified by PCR. The advantage of SH is that the number of clones required for screening to identify differentially expressed genes is

greatly reduced compared to screening of conventional cDNA libraries, and low and medium abundance mRNA transcripts can be detected. Basic SH involves the physical separation of cDNAs which can result in loss of transcripts, however, a modified version of the method, suppression subtractive hybridisation (SSH) (Diatchenko *et al.*, 1996) removes this step. Instead non-target DNA is suppressed during PCR amplification resulting in enriched target cDNA and improved detection. A similar modification is representational difference analysis (RDA), which is also a PCR-based subtraction technique (Lisitsyn *et al.*, 1993; Hubank & Schatz, 1994). Messenger RNAs present in one condition and not in the other are selectively amplified by PCR, followed by subtractive hybridisation to analyse the differences. The final product of both RDA and SSH is an amplified pool of cDNAs, enriched for transcripts that are specific for the tester sample, however, in SSH the abundance of cDNAs is equalised. Verification of differentially expressed genes is performed using Northern blot analysis, quantitative real time PCR or *in situ* hybridisation

SSH has been used to identify genes differentially expressed during fungal development, such as appressorium maturation in *Magnaporthe grisea* (Lu *et al.*, 2005), between the mycelial and yeast phases of *Ophiostoma piceae* (Dogra & Breuil, 2004) and the different growth forms of the dimorphic fungal pathogen *Coccidioides posadasii* (Delgado *et al.*, 2004), and when studying responses to different growth media (Cappellazzo *et al.*, 2007; Morales & Thurston, 2003). Fungal interaction studies using SSH have mainly focussed on the interactions between mycorrhizal (Frenzel *et al.*, 2005; Küster *et al.*, 2007) and plant pathogenic fungi (Beyer *et al.*, 2002; Sellam *et al.*, 2007) and their plant hosts, but also with bacteria (Schrey *et al.*, 2005) and with other fungi during mycoparasitism (Carpenter *et al.*, 2005; Mukherjee, 2007).

Other techniques require more sequence information to be useful for differential gene expression analysis and include SAGE, massive parallel signature sequencing (MPSS) and microarrays. These are also more appropriate for global analysis of gene expression when large samples are involved.

SAGE is a sequencing based gene expression profiling technique and requires no *a priori* knowledge of the genes to be identified and monitored. It is based on the

principle that a short oligonucleotide defined by a restriction enzyme at a fixed distance from the poly(A) tail can uniquely identify mRNA transcripts. Unique sequence tags are concatenated into long serial molecules that are cloned and sequenced. The sequences produced are entered into a database, which identifies each tag and quantifies its abundance. Tags from highly expressed genes will have high copy number, while low abundance transcripts produce fewer tags. Individual tags are used as queries to search sequence databases using BLAST (Altschul *et al.*, 1990) to facilitate their annotation. Basic SAGE identifies 10 bp sequence tags which gives  $4^{10}$  (1 048 576) different sequence combinations. Modifications such as LongSAGE (Saha *et al.*, 2002) and SuperSAGE (Matsumura *et al.*, 2005) isolate longer SAGE tags, 21 bp and 26 bp respectively, providing more possible unique combinations making duplication less likely. Longer sequences are also more likely to produce matches with sequence databases, otherwise short tags must be extended using 3'/5'-RACE (rapid amplification of 5' ends of cDNA). SAGE requires a relatively large amount of starting material making it unsuitable for analysis of single cells or microdissected tissues. However, modifications to the basic method such as PCR-SAGE (Neilson *et al.*, 2000), SAGElite (Peters *et al.*, 1999) and MicroSAGE (Virlon *et al.*, 1999) use PCR amplification to decrease the amount of starting material required, although this may introduce representational bias with some transcripts preferentially amplified. Small amplified RNA-SAGE (Vilain *et al.*, 2003) counters this bias by omitting the PCR steps and using a loop of linear RNA amplification. This method has been used successfully in fungi but to date mostly when studying plant pathogen development such as *Magnaporthe grisea* (Irie *et al.*, 2003) and *Blumeria graminis* (Thomas *et al.*, 2002).

Massively parallel signature sequencing (MPSS) (Brenner *et al.*, 2000) is similar to SAGE, however, it involves the cloning of a cDNA library on beads and the acquisition of 17-20 base signature sequence tags from these cDNAs by a different method than with SAGE. The abundance of the signature tags reflects gene expression levels in the sampled cells or tissue. This method can generate more than 1 million signatures per library, thus is sensitive to low abundance transcripts. However, the procedure requires specialist facilities and access to a high quality genome sequence and annotation to fully exploit the data generated.

Microarray technology is popular for global analysis of gene expression as it enables the study of the expression of thousands of genes simultaneously. This technology is based on the reassociation properties of DNA that cause hybridisation of homologous sequences. There are two main platforms for microarrays: cDNA arrays and oligonucleotide arrays or “genechips”. cDNA microarrays are produced by robotically spotting arrays of cDNA clones (usually 500-1000 bases) onto a solid surface, usually in the form of PCR products, and does not require knowledge of the spot sequences. This approach allows researchers to construct arrays with their own gene sets for organisms that do not have commercially available genechips. Comparisons can be made between two samples on the same array, such as different treatments of the same cells, different phenotypes or samples taken from different timepoints. Typically, the two different cDNA populations (test or experimental and reference or control probe, respectively) are labelled with fluorescent dyes, such as Cy3 and Cy5, and both labelled samples are hybridised to a single array. Arrays are scanned with different wavelength lasers which excite and fluoresce the two fluorophores. The relative intensity for each spot measures the degree of hybridisation of the cDNA population to each spot. The expression of a gene is expressed as a relative ratio with respect to the control sample and allows identification of genes which are up or down regulated.

The alternative oligonucleotide arrays typically consist of 25-80mer oligonucleotides, either robotically spotted onto a support or synthesised *in situ* by photolithography, and are generally produced commercially. This DNA array platform employs targeted design of probe sets and requires prior knowledge of the gene sequences, thus, it is only available for organisms with well characterised genome sequences. For each gene or EST, multiple 25mer oligonucleotide probes are designed to hybridise to different regions of the same RNA. Incorporating target redundancy by using multiple detectors for the same RNA improves signal-to-noise ratios and reduces the occurrence of false positives. However, the short complementarity between the probe and the target results in reduced specificity but does allow the differential detection of members of gene families or transcripts not distinguishable with full length cDNAs. Affymetrix oligonucleotide arrays use perfect match/mismatch. For each gene the 25mer oligonucleotide probes are designed in pairs. Each pair includes a perfect match 25mer, which is the exact complement to

the gene sequence, and a mismatch control oligonucleotide, which has a deliberate mutation at the 13<sup>th</sup> base. The mismatch probe measures the degree of cross hybridisation, thus, the reported hybridisation intensity for each gene is a composite of all the match/mismatch pair differences for each gene. This allows discrimination between genuine signals and those resulting from non-specific hybridisation. Oligonucleotide arrays are usually hybridised with a single label and are labelled with biotin and visualised by staining with phycoerythrin.

Oligonucleotide arrays provide high reproducibility and printing at much higher densities than cDNA microarrays, and probes are synthesised with less repetitive sequences which minimises cross-hybridisation. The larger size of spotted probes in cDNA microarrays allows for greater specificity in binding to the labelled test and reference samples, but can increase the risk of cross-hybridisation if there are repetitive or common sequences. Prior knowledge is required for probe design for oligonucleotide microarrays but is not for cDNA microarrays which makes them suitable for studying organisms where full genome sequences are not available. Furthermore, the commercial manufacture of oligonucleotide arrays makes them very expensive, while cDNA microarrays can be printed in-house at a much lower cost.

One of the main challenges with microarray technology is the analysis of the vast amounts of data generated and the normalisation of data to allow comparisons between arrays within experiments, and also between different experiments. Microarrays have been used extensively in many fields for gene expression studies and in over 20 species of filamentous fungi to study differential gene expression during metabolism, pathogenicity, different developmental stages, environmental conditions or genetic backgrounds (Breakspear & Momany, 2007).

Theoretically SAGE can provide information on all transcripts present within a cell or tissue (i.e. an 'open' system), whereas microarrays are limited to finite numbers of known gene sequences that are printed onto the chip (i.e. a 'closed' system). However, if other gene expression analysis techniques such as DD, RDA and SSH are coupled with microarray analysis, then unique focussed arrays can be produced that allow novel gene identification, and reduce the number of non-differentially expressed sequences that are screened needlessly. Microarrays can be used to assess global

transcription patterns quickly in large samples, although comparisons between experiments can be difficult due to the potential for random and systematic errors within each individual experiment. SAGE and MPSS data are digital and based on transcript counting and, therefore, more suitable for comparisons between different data sets. However, SAGE is highly labour intensive, MPSS can only be carried out in specialist facilities and sequencing for both can be very expensive.

The subtraction used to create an SSH library is unlikely to be 100% efficient and clones must be verified by differential screening. The thousands of clones produced in an SSH library can be screened simultaneously using microarrays rather than using laborious and expensive northern blot analysis or RT-PCR which limits the numbers of clones that can be screened. Coupling SSH with cDNA microarray technology has the advantage that the majority of the SSH genes spotted on the microarray will be differentially expressed. Moreover, SAGE identifies all genes active at a particular time or under certain conditions, thus, housekeeping and differentially expressed genes are both present and a substantial level of sequencing is required to identify the differentially expressed genes making it unfeasible for small projects. Furthermore, replicates of the same microarrays can be hybridised with many different cDNA populations, derived from different treatments, and the results compared. SAGE analysis requires the generation of separate SAGE libraries for each treatment for comparisons to be made, making it inappropriate if several conditions are to be compared.

### 1.12 Functional genomics

Functional genomics is the process of assigning functions to genes. Genome sequences are available for increasing numbers of organisms and stored in databases, such as Genbank and EMBL. Gene sequences can be compared to the databases using a basic local alignment search tool (BLAST) (Altschul *et al.*, 1990) and, where significant homology between a queried sequence and an annotated gene within the database exists, an analogous function can be inferred. The annotation of available genomes is ongoing and assignment of functions to genes can be achieved by characterising mutant phenotypes following mutagenesis and gene disruption,



transformations or after gene knockdown using RNAi. Even in organisms whose genomes have been fully sequenced, much of the annotation is done, however, by homology to genes of known functions from other organisms.

Many of the genes identified in gene expression studies may have matches in sequence databases that allow their annotation, and will provide information about the signalling pathways and processes active during an interaction or in response to a treatment. For those organisms where complete genome sequences are not available assigning functions to isolated genes can be more problematic but is vital for gaining meaningful information from global gene expression analyses. Genome sequences of species closely related to the organism of study within the databases greatly improves the chances of annotation by comparative genomics. Currently Genbank contains over 2 million fungal nucleotide records, however, only a quarter of these are derived from basidiomycetes and even less have functions assigned to them. Consequently, many studies that have identified a set of differentially expressed transcripts have found that many do not match anything within the databases. There are full genome sequences available for fungi such as the yeast, *Saccharomyces cerevisiae*, and the ascomycete, *Aspergillus niger*, which can be used in comparative studies. More closely related species would be more appropriate for studying the lifestyles and interactions of basidiomycetes, but at this time they are lacking from the databases. The Fungal Genome Initiative (FGI) (<http://www.broad.mit.edu/annotation/fgi/>) proposes to remedy this situation and there are over 25 fungal species that have been sequenced or are being sequenced in a coordinated effort between the Broad Institute (Cambridge, MA, USA) and the wider fungal community. The majority of species are those important to industry, medicine and agriculture and include the basidiomycetes *Coprinus cinerea*, *Cryptococcus neoformans* Serotype A, *Cryptococcus neoformans* Serotype B, *Puccinia graminis* and *Ustilago maydis*. The addition of these sequences to the databases greatly improves the chances of finding matches to the genes identified by differential gene expression analysis.

### 1.13 Project objectives

Very little is known about the chemical and molecular basis of interspecific interactions between saprotrophic basidiomycetes. These interactions are vital for

driving and maintaining decomposition, nutrient recycling, community structure and diversity. A better understanding of the chemicals and genes involved in interactions and how they are transcriptionally regulated may help lead to a better understanding of the fungi themselves. It may help also to develop strategies to manipulate the outcomes of interactions which could be exploited for biocontrol and bioremediation, help understand how communities will be affected by climate change, as well as contributing to the general body of knowledge about these fungi. This project centres around the hypothesis that changes in gene expression occur during interactions between saprotrophic basidiomycetes. These are different to those that occur during solitary growth, and different sets of genes are differentially expressed depending on the pairing and outcome of the interaction. Volatile compounds are also produced by growing saprotrophic basidiomycetes; some compounds are produced specifically during interactions.

To this end, the objectives of this project are:

- Study interspecific interactions on agar to become familiar with the qualitative morphological changes and outcomes of interactions
- Identify for further study a species that produces different outcomes when interacting with different species and investigate the effects of interactions on mycelial extension rate when paired with different competitors
- Identify the profile of volatile compounds produced by the study fungus and make comparisons between solitary growth, self-pairings and interspecific interactions
- Use suppression subtractive hybridisation (SSH) to produce a subtracted cDNA library, for the study fungus, of transcripts differentially expressed during the interspecific interaction with a competitor species
- Create cDNA microarrays using the SSH library

- EST sequencing of the subtractive library and annotation
- Hybridise cDNA microarrays with RNA from the same pairing that was used to construct the SSH library to verify the efficiency of the subtraction
- Hybridise cDNA microarrays with RNA isolated from the study species when interacting with different competitor species that result in different outcomes of the interaction
- Identify genes that are differentially expressed during different types of interaction

## 2. General Materials and Methods

### 2.1 Routine culture conditions

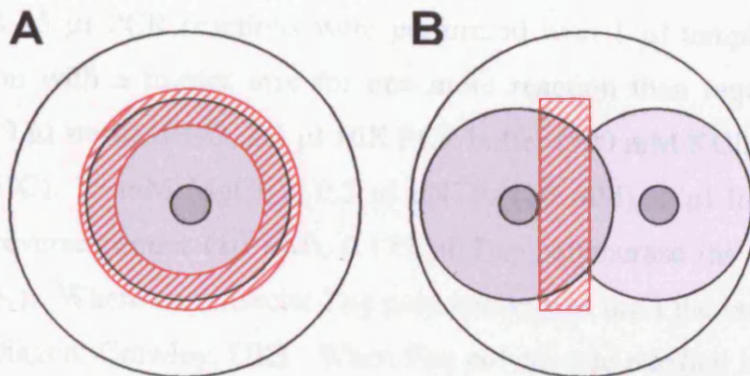
Routine culturing of fungi was carried out in 9 cm non-vented Petri dishes (Greiner Bio-One, Stonehouse, Gloucestershire, UK), on 20 ml 2% w/v malt extract agar (MA), (20 g l<sup>-1</sup> Munton & Fison spray malt, 15 g l<sup>-1</sup> Lab M agar No. 2 [International diagnostics group plc., Bury, Lancashire, UK], made up with distilled water and autoclaved for 20 min at 121°C). Cultures were routinely subcultured by transferring blocks cut from colonised agar to fresh media approximately every 10 d or just before the colony margin reached the edge of the plate. Plates were sealed with Nesco<sup>®</sup> film. Colonies were incubated face downwards in the dark at 20°C in plastic bags to prevent drying out. Stock cultures were maintained on MA slopes at 4°C.

### 2.2 Growth of mycelium for RNA extraction

Plugs of mycelium (6 mm diameter) cut with a no. 3 cork borer from the growing margin of 7 day old growing colonies of *Trametes versicolor* (TvD2), *Stereum gausapatum* (Sg1), *Hypholoma fasciculare* (GTWV2), *Bjerkandera adusta* (MA313) were inoculated mycelium-side-down onto 2 % Thick Malt Extract Agar (20 g l<sup>-1</sup> Munton & Fison spray malt, 20 g l<sup>-1</sup> Lab M agar No. 2 [International diagnostics group plc., Bury, Lancashire, UK]). The amount of agar in the medium was increased compared to MA (see Section 2.1) to make agar plates firmer, which allowed mycelium to be harvested more easily. Plugs of opposing species were placed 3 cm apart at the centre of a 9 cm diameter non-vented Petri dish (Greiner Bio-one, Germany). Plates were stacked in sealed plastic bags and incubated at 20°C for 5 d. Fifty replicates were grown for each pairing and 30 for each singly inoculated reference set.

Colonies were grown for 5 d and mycelium was harvested aseptically from plates using a small spatula to skim the mycelium from the surface of the agar. For those plates inoculated with *T. versicolor* alone, mycelium was harvested from a circular zone 1 cm wide around the growing margin. For interaction plates of *T. versicolor* vs. *S. gausapatum* (or other competitor), mycelium was taken from just behind the *T.*

*versicolor* margin at the interaction zone to ensure no *S. gausapatum* mycelium was collected (Figure 2.1). Mycelium was kept on ice during harvesting in small foil packets, flash frozen by immersion in liquid nitrogen and stored at  $-80^{\circ}\text{C}$  until required for RNA extraction.



**Figure 2.1** Zones (red hatched areas) from which mycelium was harvested for RNA extraction. A – Driver (Reference), *T. versicolor* grown alone; B – Tester, *T. versicolor* (left) grown against a competitor.

### 2.3 RNA extraction

An autoclaved pestle and mortar were cooled to  $-20^{\circ}\text{C}$  and fungal mycelium was ground with liquid nitrogen into a fine dust. TRIreagent (2 ml) was added and mycelium ground into a fine paste. Equal amounts of paste were transferred to two 1.5 ml microcentrifuge tubes, vortexed and allowed to stand at room temperature for 5 min. Samples were centrifuged at 10500 g at  $4^{\circ}\text{C}$  for 10 min using the F2402H rotor in a Beckman Coulter™ Allegra™ 2IR Centrifuge (Beckman Coulter Ltd., High Wycombe, UK). Chloroform (200  $\mu\text{l}$ ) was added to each tube, vortexed for 15 s and left to stand at room temperature for 5 min. Tubes were then centrifuged at 10500 rpm at  $4^{\circ}\text{C}$  for 15 min as above. The aqueous top layer was transferred to new 1.5 ml Eppendorf tubes and 500  $\mu\text{l}$  isopropanol added and left to stand at room temperature for 10 min. Tubes were then centrifuged at 10500 g at  $4^{\circ}\text{C}$  for 10 min as above. The supernatant was removed and 1 ml 75 % v/v ethanol was added and the tubes vortexed for 15 s. Tubes were then centrifuged at 10500 g at  $4^{\circ}\text{C}$  for 10 min as above. The supernatant was removed and the pellet allowed to air dry. Pellets were re-suspended in 50  $\mu\text{l}$  sterile distilled water and the contents of both tubes combined.

RNA was stored at  $-80^{\circ}\text{C}$ . The extracts (10  $\mu\text{l}$ ) were analysed for the presence of RNA by gel electrophoresis on a 1 % agarose/EtBr gel.

## 2.4 Polymerase chain reaction (PCR)

As standard 25  $\mu\text{l}$  PCR reactions were performed with 1  $\mu\text{l}$  template DNA used in each reaction with a master mix for one more reaction than required made up as follows: 18.9  $\mu\text{l}$  sterile  $\text{dH}_2\text{O}$ , 2.5  $\mu\text{l}$  10X PCR buffer (500 mM KCl, 100 mM TrisHCl (pH 9 at  $25^{\circ}\text{C}$ ), 15 mM  $\text{MgCl}_2$ ), 0.5  $\mu\text{l}$  dNTPs (10 mM), 1  $\mu\text{l}$  forward primer (10  $\mu\text{M}$ ), 1  $\mu\text{l}$  reverse primer (10  $\mu\text{M}$ ), 0.125  $\mu\text{l}$  *Taq* polymerase (as supplied, Qiagen, Crawley, UK). Where commercial *Taq* polymerase was used the buffer supplied was also used (Qiagen, Crawley, UK). When *Taq* polymerase purified in-house was used in reactions the following buffer was used: 500 mM KCl, 100 mM Tris-HCl (pH 9), 15 mM  $\text{MgCl}_2$ .

All reagents were kept on ice throughout, followed immediately by thermal cycling according to a basic program:  $95^{\circ}\text{C}$  15 min, [ $94^{\circ}\text{C}$  1 min,  $x^{\circ}\text{C}$  1 min,  $72^{\circ}\text{C}$  1 min] for  $y$  cycles,  $72^{\circ}\text{C}$  7 min,  $4^{\circ}\text{C}$   $\infty$ . Where  $x$  is the annealing temperature for a particular primer pair and  $y$  is the number of cycles desired in each instance. The 15 min hot start at  $95^{\circ}\text{C}$  was only used when commercial hotstart *Taq* (Qiagen, Crawley, UK) was used otherwise it was omitted.

These conditions were altered where necessary and the details are given in the relevant sections.

## 2.5 Purification of PCR reactions using QIAquick PCR purification columns (Qiagen)

Five volumes of Buffer PB were added to 1 volume of PCR product and mixed. This was applied to the QIAquick column resting in a 2 ml collection tube and centrifuged for 1 min at 11500 g in an Eppendorf Minispin microcentrifuge (Eppendorf, Cambridge, UK) and the flow-through discarded. This was repeated until the total volume had been run through the column. Buffer PE (750  $\mu\text{l}$ ) was added to the

column and centrifuged for 1 min at 11500 g as above, and the flow-through discarded. The column was then centrifuged for a further 1 min at 11500 g as above to remove any residual Buffer PE, then transferred from the 2 ml collection tube to a clean 1.5 ml Eppendorf tube. To elute the DNA, 30  $\mu$ l Buffer EB (10 mM Tris-Cl, pH 8.5) was applied to the centre of the column membrane and left to stand for 1 min at room temperature and then centrifuged for 1 min at 11500 g as above. Purified PCR product was stored at -20°C until required.

### 2.6 Gel electrophoresis of nucleic acids

Agarose gels were made by mixing agarose with TAE buffer to the desired concentration of agarose gel, microwaved for 1 min and then cooled slightly before adding ethidium bromide (EtBr) (10  $\mu$ g ml<sup>-1</sup>). Cooled agar was poured into the gel mould and allowed to set. To prevent degradation of RNA samples the gel tank (Mini Sub™ DNA cell, Biorad, Hemel Hempstead, UK) comb and tray were soaked in 0.1 M NaOH for 10 min and rinsed in sterile dH<sub>2</sub>O. Electrophoresis tank, gels and tray were also treated with RNaseZap® RNase Decontamination Solution (Ambion [Europe] Ltd., Huntingdon, Cambs., UK). To run samples, aliquots of DNA or RNA extracts, or PCR products, were mixed with 0.5 volume of loading buffer (16.5 ml 150 mM Tris-HCl pH 7.6, 30 ml glycerol, 3.5 ml H<sub>2</sub>O, bromophenol blue to desired colour) and then pipetted into the wells of agarose gels. For analysis of RNA, a separate dedicated autoclaved loading buffer was used. 1kb DNA ladder (500 ng) (Invitrogen, Paisley, UK) was loaded alongside samples. Samples were run at approximately 110 V for 20 min through agarose gels (various percentages) stained with EtBr in a 1X TAE Buffer (50X TAE: 242 g Tris base, 57.1 ml glacial acetic acid, 100 ml 0.5M EDTA pH 8.0). Gels were viewed under UV light using a GeneGenius Bioimaging System (SynGene, Cambridge, UK) and images captured using Genesnap 4.00.00 software (SynGene, Cambridge, UK).

## 2.7 Nucleic acid quantification

### 2.7.1 Spectrophotometer quantification

Nucleic acid quantification was carried out using an Ultrospec® 2100 pro (Amersham Pharmacia Biotech, Buckinghamshire, UK). For quantification sterile dH<sub>2</sub>O was placed into the bottom well of an Uvette® 220-1600 nm disposable cuvette (Eppendorf) and used as a reference for calibration. Samples to be quantified were diluted into a total volume of 50 µl and then quantified using the spectrophotometer default nucleic acid settings.

### 2.7.2 Ethidium bromide spot assay

To make a quick estimate of the amount of nucleic acids in a particular sample an ethidium bromide spot was used. This test is appropriate as a quick estimate of nucleic acid concentration and when the sample to be tested has gone through a clean-up procedure to remove unincorporated nucleotides.

Dilutions of DNA of known concentration were made to be used as standards for comparison with the samples to be tested. Plasmid DNA of known concentration was diluted with sterile dH<sub>2</sub>O to make a set of standards at 100, 50, 25, 12.5, 6.25 and 3.125 ng µl<sup>-1</sup> with sterile dH<sub>2</sub>O as zero. On the inside of a clean weighing boat, labels were written in reverse and in red pen to be visible under UV light. Sterile dH<sub>2</sub>O (2µl) was dropped next to each label. An ethidium bromide solution 1µg ml<sup>-1</sup> (1 µl) was then added to each drop. The DNA solution or test sample (1 µl) was then added to each drop. This was carried out for each DNA standard and for each sample to be tested. The dots were then visualised under UV light using a GeneGenius Bioimaging System (SynGene, Cambridge, UK) by placing the weighing boat face down onto the gel viewer and images were captured using Genesnap 4.00.00 software (SynGene, Cambridge, UK). An estimate of the amount of DNA, RNA or cDNA was made by comparing the brightness of the sample dots with the standards.



**2.7.3 Hyperladder quantification**

To quantify the amount of RNA or DNA in samples, three lanes of sample were loaded onto 1% agarose/EtBr gel alongside a quantitative Hyperladder I (Bioline, London, UK). The first lane contained 2  $\mu\text{l}$  of pure sample, the second was 2  $\mu\text{l}$  of a 1 in 10 dilution and the third 2  $\mu\text{l}$  of a 1 in 100 dilution, each loaded with 3  $\mu\text{l}$  dedicated RNA loading buffer. Three lanes of Hyperladder I (144  $\text{ng } \mu\text{l}^{-1}$ ) were loaded with different amounts: Lane 1 – 720  $\text{ng}$  (5  $\mu\text{l}$ ), Lane 2 – 288  $\text{ng}$  (2  $\mu\text{l}$ ), Lane 3 – 144  $\text{ng}$  (1  $\mu\text{l}$ ). The concentration of DNA in each band of the ladder is known. Gels were inspected by eye to compare the brightness of RNA bands with those of the Hyperladder I and then the amount of RNA in each band inferred.

**2.8 Purification of RNA**

To remove remnants of protein and cell debris, a clean-up procedure was carried out on each sample. An equal volume of phenol:chloroform:isoamyl alcohol (P:C:I) (25:24:1) was added to the DNA or RNA sample. This was then vortexed and briefly centrifuged. A white band formed at the interface and the top layer was pipetted off and retained. The previous steps were repeated between 1-4 times until the interface became clear. Back-extractions from the bottom layer were also carried out with each successive round of P:C:I treatment to minimise the amount of DNA/RNA lost each time. To back-extract, 50-100  $\mu\text{l}$   $\text{H}_2\text{O}$  was added to the bottom layer of the sample which had previously had the top layer removed. This was then vortexed, centrifuged briefly and the top layer removed and added to the rest of the DNA/RNA sample. This retrieved any DNA/RNA that might have been left in the P:C:I bottom layer. After several rounds of extractions had been carried out the resulting DNA/RNA sample was mixed with an equal volume of chloroform, vortexed, centrifuged briefly and then the top layer removed and retained. To precipitate the DNA/RNA 0.1 volume of 3M sodium acetate pH5.5 and 2 volumes cold 100 % ethanol were added and the tube incubated at  $-20^\circ\text{C}$  for at least 1 hour. The sample was then centrifuged at the highest speed at  $4^\circ\text{C}$  for 15 min. The supernatant was removed and the pellet washed with 70 % ethanol, then the tube centrifuged at the highest speed at  $4^\circ\text{C}$  for 5

min. The supernatant was removed and discarded, the pellet air dried and then resuspended in sterile distilled H<sub>2</sub>O.

### **2.9 Purification of *Taq* polymerase from overexpressing recombinant *Escherichia coli***

Buffers that contained phenylmethylsulfonylfluoride (PMSF) were made up without the PMSF, then autoclaved and the PMSF added afterwards and stirred overnight to dissolve.

#### **2.9.1 Culturing of *E. coli***

A glycerol stock of *Taq* DH5 $\alpha$  was streaked onto an LB (Section 2.11.2) + Ampicillin (50 ng ml<sup>-1</sup>) (Amp50) agar plate and incubated overnight at 37°C. A single colony from this plate was used to inoculate 10 ml LB+Amp50 and then incubated at 37°C overnight, with shaking at 200 rpm in a Gallenkamp Orbital incubator. The overnight culture was centrifuged for 10 min at 2000 rpm in a Beckman Coulter Avanti JE centrifuge and the pellet resuspended in 10 ml fresh LB+Amp50. LB+Amp50 (2 x 500 ml) in conical flasks, was inoculated with 1 ml of the resuspended culture and incubated at 37°C with shaking until an optical density of 0.2 at 600nm was reached (OD<sub>600</sub>=0.2), approximately 4 hours. 1M isopropyl-beta-D-thiogalactopyranoside (IPTG) (0.25 ml) was added to each flask to give a final concentration of 0.5 mM and further incubated at 37°C, with shaking at 200 rpm, for 18-20 hours.

#### **2.9.2 Purification of *Taq* polymerase**

The liquid culture was transferred to sterile centrifuge bottles (4 x 250 ml) and centrifuged at 2500 g for 20 min at 4°C in a pre-chilled rotor in a Beckman Coulter Avanti JE centrifuge. Pellets were resuspended in 50 ml Buffer A (50 mM Tris-HCl pH 7.9, 50 mM dextrose, 1mM EDTA) and centrifuged at 2500 g for 20 min at 4°C as above. Pellets were resuspended in 10 ml Buffer A, lysozyme added to each bottle to give a 0.4% concentration (0.04g added), and incubated at room temperature for 30

min. 10 ml Buffer B (10 mM Tris-HCl pH 7.9, 50 mM KCl, 1mM EDTA, 1mM PMSF, 0.5% Tween-20, 0.5% Igepal CA-630) was added to each bottle and then heated in a water bath at 75°C for 20 min. Bottles were incubated on ice for 30 min and then 300 µl 10% polyethylenimine (PEI) (pH 7.0) added dropwise to give a final concentration of 0.15%. Bottles were incubated on ice for a further 10 min and then the contents transferred to sterile 35 ml centrifuge tubes and centrifuged at 5000 g for 20 min at 4°C as above, to precipitate the *Taq*. Each pellet was resuspended in 10ml Buffer C (20 mM HEPES pH 7.9, 1 mM EDTA, 0.5 mM PMSF, 0.5% Tween-20, 0.5% Igepal CA-630) + 0.025 M KCl and centrifuged at 6500 g for 20 min at 4°C as above, to wash off impurities. The supernatant was discarded and each pellet resuspended in 10 ml Buffer C + 0.15 M KCl and centrifuged at 6500 g for 20 min at 4°C as above, to resolubilise the *Taq*. The supernatant (10 ml) was retained, transferred to new sterile 35 ml tubes and 20 ml Buffer C added, giving a final concentration of 0.05 M KCl, and kept on ice until run through the column.

A 26 mm diameter column containing 17 ml Bio-Rex 70 resin (100-200 mesh) (Bio-Rad, Hemel Hempstead, UK) was prepared by equilibrating the resin with Buffer C by stirring the resin gently with an excess of Buffer C for 1-2 hours. The resin was allowed to settle, the pH recorded, the top liquid discarded and then the resin resuspended in fresh Buffer C with continued stirring. This process was repeated until the pH of the resin was equal to the pH of Buffer C. The equilibrated column was stored in Buffer C at 4°C.

Buffer C was drained from the pre-prepared column and discarded. Samples were loaded onto the column and allowed to run through. The run-through liquid was retained and stored at 4°C until the whole process was finished in case the sample had eluted too early. The column was washed with two columns full of Buffer C + 0.05 M KCl but not allowed to run dry. Again, the run-through was retained temporarily at 4°C in case *Taq* had eluted too early. *Taq* requires high salt to be solubilised and eluted. *Taq* was eluted with 50 ml Buffer C + 0.2M KCl and collected in 5 ml fractions in 5 ml falcon tubes which were stored at 4°C. Each fraction (10 µl) was run on an SDS-PAGE gel and stained with Coomassie blue as described in Section 2.10. Those fractions showing a positive band were pooled and concentrated to 50% with a

Centriprep Concentrator (Millipore) by centrifuging at 3000 g in a bucket rotor for approximately 40 min. Samples were then dialysed overnight in 900 ml Buffer C + glycerol at 4°C.

### 2.9.3 Analysis of *Taq* efficiency

The efficiency of the *Taq*'s activity was assessed by PCR using different dilutions of the *Taq* (undiluted, 1/10, 1/50, 1/100, 1/200, 1/1000) and comparing the products produced with those from an identical PCR reaction but with a commercial non-hotstart *Taq* polymerase (Promega) used instead of the *Taq* purified in house. The PCR reaction mixture for a 50 µl reaction was as follows: 2 µl DNA; 37.8 µl dH<sub>2</sub>O; 5 µl 10X PCR reaction buffer; 1 µl dNTPs (10mM); 2 µl forward primer; 2 µl reverse primer; 0.25 µl *Taq* polymerase. Thermal cycling was performed and cycling parameters were 94°C 1 min; 55°C, 1 min; 72°C 1 min for 35 cycles then 72°C 10 min. Note that there is no hot start when using this *Taq*. Each PCR product (5 µl) was electrophoresed on a 1.2 % Agarose/EtBr gel and the intensity of bands were compared. *Taq* was diluted as appropriate to give a comparable level of activity as that of the commercial *Taq* and aliquotted into pre-chilled eppendorfs to avoid freeze-thaw damage. Small aliquots for immediate use were stored at -20°C and larger aliquots for long term storage were stored at -80°C.

## 2.10 SDS-PAGE analysis

### 2.10.1 Gel preparation

A 10 % resolving gel was prepared by mixing the following reagents together: acrylamide:bis-acrylamide (37.5:1) 1.25 ml, resolving gel buffer (1.5 M Tris-HCl pH 8.8, 0.4 % SDS) 810 µl, sterile dH<sub>2</sub>O 1.61 ml, 10 % w/v ammonium persulphate 37.5 µl, N,N,N',N'-Tetramethylethylenediamine (TEMED) 3.75 µl. TEMED was added just before the gel was ready to be poured as the addition of TEMED initiates polymerisation of the gel. The gel was cast between glass plates clamped together within the gel tank rig (Biorad, CA, USA). Immediately after pouring the gel sterile

dH<sub>2</sub>O was pipetted onto the top of the gel in order to make the top level and prevent the need for degassing of the gel. Once set the water was removed and a 4 % acrylamide Stacking gel was prepared by combining the following reagents: acrylamide:bis-acrylamide (37.5:1) 162.5 µl, resolving gel buffer (1.5 M Tris-HCl, pH 8.8, 0.4 % SDS) 250 µl, sterile dH<sub>2</sub>O water 1 ml, 10 % ammonium persulphate 6.25 µl, TEMED 1.25 µl. Again, TEMED initiates polymerisation of the gel and was therefore only added immediately prior to pouring of the gel. This gel was poured on top of the resolving gel, comb inserted and allowed to set.

### **2.10.2 Sample loading**

10 µl of each fraction taken from the protein column during *Taq* purification was run on the gel. Samples were loaded in a 5:1 ratio with 2X Laemmli sample buffer (20% glycerol, 8 % β-mercaptoethanol, 3.2 % SDS, 0.1 M Tris-HCl, pH 6.8, 0.125 % bromophenol blue) and samples were incubated at 70°C for 10 min, to open up the protein structure, prior to loading on the gel and running in 5X running buffer (1.5 % Tris-base, 7.2 % glycine, 0.5 % SDS) at 150 mV for 1 hour.

### **2.10.3 Gel staining**

Gels were stained by covering with Coomassie blue stain (0.2 % Coomassie Brilliant Blue R-250 in 5:4:1 (v/v) dH<sub>2</sub>O:methanol:acetic acid) and incubated on a gentle rotator for approximately 20 min. The staining solution was removed and replaced with destain solution (5:4:1 (v/v) dH<sub>2</sub>O: methanol: acetic acid) and incubated on a rotator for 20 min. Destain solution was discarded and the wash step was repeated once more. Protein bands on the gel were then visualised.

### **2.10.4 Gel imaging**

Gels were covered in clean destain solution, viewed under white light, and images captured using GeneSnap 4.00.00 software (SynGene, Cambridge, UK)

## 2.11 Preparation of media for cloning

### 2.11.1 NZY broth

The following were combined and made up to 1 litre with dH<sub>2</sub>O: 10 g NZ amine (casein hydrolysate), 5 g yeast extract, 5 g NaCl. The pH was adjusted to pH 7.5 using NaOH and then autoclaved for 20 min at 121°C. The following filter sterilised components were then added: 12.5 ml 1M MgCl<sub>2</sub>, 12.5 ml 1M MgSO<sub>4</sub>, 10 ml 2M glucose. Aliquots of broth were frozen at -20°C for future use.

### 2.11.2 LB medium

The following were combined and made up to 1 litre with dH<sub>2</sub>O: 10 g NaCl, 10 g tryptone, 5 g yeast extract. The pH was adjusted to pH 7.0 with 5M NaOH and then autoclaved for 20 min at 121°C. For LB agar 20 g agar (Sigma, UK) was added. When required ampicillin was added to a concentration of 50 µg ml<sup>-1</sup> after autoclaving and cooling.

### 2.11.3 SOC medium

The following were combined and made up to 1 litre with dH<sub>2</sub>O: 20 g tryptone, 5 g yeast extract, 0.5 g NaCl then autoclaved for 20 min at 121 °C. Aliquots of medium were frozen at -20°C for future use.

### 3. Agar Interactions

#### 3.1 Introduction

Although interactions have been studied extensively in the laboratory and field this has been mostly qualitative and the underlying mechanisms and pathways are poorly understood. The main thrust of this project is to study interactions from a gene expression and chemical production perspective. To fully understand interactions it is, however, necessary to gain an understanding and become familiar with the basics of interactions with respect to the morphological changes that take place, the range of outcomes that are possible and how their outcomes relate to the ecology of fungal species and the woodland ecosystems they reside in. Very little is known about gene expression during interactions and currently there are no model organisms representing the saprotrophic basidiomycetes. Thus, it was necessary to identify a suitable candidate species to use in these studies. As a prelude to studying gene expression in saprotrophic basidiomycetes the objectives were to:

- Set up intra- and interspecific interactions, on agar, between a selection of saprotrophic basidiomycetes species with different ecological strategies
- Observe the qualitative morphological changes that take place during interactions over time and the diversity of outcomes
- Identify a species to study further, which produces a range of outcomes during interspecific interactions with different species, and identify species pairings that result in replacement by, deadlock or replacement of the chosen species of which to study the gene expression profiles.
- Measure and compare mycelial extension rates between isolates of the chosen species
- Measure and compare mycelial extension rates between single and self-pairings of the chosen species

- Study the effect on mycelial extension rate (overall and within the colony) of the chosen study species during interspecific interactions with competitor species that are replaced, deadlock with or are replaced by it

## 3.2 Materials and methods

### 3.2.1 Fungal isolates

Isolates of six different species of saprotrophic basidiomycetes from the Cardiff Mycology Group culture collection were used to carry out preliminary interaction experiments (Table 3.1). Species were chosen to give a sample of fungi representative of different ecological strategies. The overall outcomes of interactions were assessed and the mycelial extension rates measured for each species when grown alone, self-paired and during interspecific interactions. At least two isolates for each species were used to observe variation within species as well as between species.

**Table 3.1** Isolates used for preliminary agar growth rates and interaction experiments. All isolates were from the Cardiff University Mycology Group culture collection.

Ecological role	Species	Isolate code	Isolated by
Primary coloniser, latently present in attached stems and branches <sup>a</sup>	<i>Stereum gausapatum</i>	Sg1	L. Boddy
		Sg2	L. Boddy
Secondary colonisers <sup>a</sup>	<i>Trametes versicolor</i>	D1	L. Boddy
		D2	L. Boddy
		D3	L. Boddy
		D4	L. Boddy
	<i>Phlebia radiata</i>	PrCop	C. Eyre
		Pr175	L. Boddy
<i>Stereum hirsutum</i>	Sh1	L. Boddy	
	Sh2	L. Boddy	
	Sh3	L. Boddy	
Late secondary colonising <sup>a</sup> cord-former	<i>Hypholoma fasciculare</i>	Hfas1	L. Boddy
		DD-HF3	D. Donnelly
		DD-HF4	D. Donnelly
		GTWV1	G. Tordoff
		GTWV2	G. Tordoff
	<i>Bjerkandera adusta</i>	Bk1	L. Boddy
MA313		A.M. Ainsworth	

<sup>a</sup>Rayner & Boddy (1988)



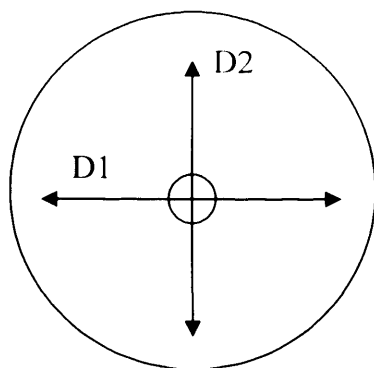
### 3.2.2 Outcome of interactions

Pairings were made by placing two mycelial plugs (6 mm) 3 cm apart on 2% w/v MA (Section 2.1) and were incubated in the dark at 20°C. Both inter- and intra-specific interactions were performed for the species in Table 3.1 in all combinations. Replicates (3-5) were made of each pairing. Any plates that became contaminated during growth were discounted from further analysis. Plates were monitored daily for the first two weeks and then weekly up to 3 months. Images were captured using a Sony Cyber-Shot DSC-P71 digital camera. When the appearance of plates had not changed for 3 weeks the outcomes of interactions were assessed by inspection of plates and categorised as deadlock or replacement. Reisolation was carried out to confirm that the observed outcomes of interactions were correct. Mycelium was subcultured from different areas around the interaction plates and from the underside of the agar and plated onto fresh 2% w/v MA plates. Species that grew out from reisolations were identified by re-pairing with the original isolate cultures. The same species intermingled but different species showed signs of non-self interaction.

### 3.2.3 Extension rate measurement

#### 3.2.3.1 *Single species*

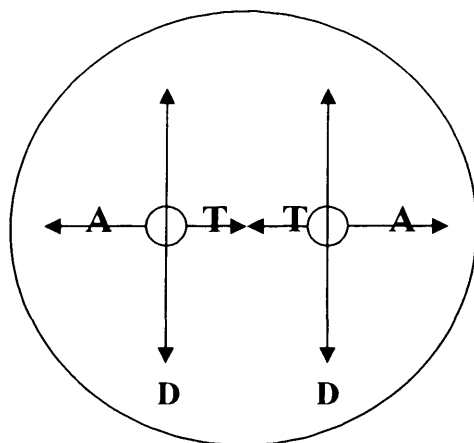
Using a number 3 cork borer, 6 mm plugs of mycelium were taken from the growing margin of colonies and inoculated centrally, mycelium side down onto 2% w/v MA. Plates were sealed with nescofilm and were incubated in the dark at 20°C. Five replicates were grown for each species. Any plates that became contaminated during growth were discounted from further analysis. Each day at approximately the same time, colonies were measured along two perpendicular diameters (Figure 3.1) to the nearest 0.1 mm, using calipers. The diameters measured were scored onto the underside of each plate to ensure the same diameter was measured each time. Plates were measured every day and incubated until the growing mycelium met the edges of the plate



**Figure 3.1** Positions where extension measurements were made on single colonies. Perpendicular diameters, D1 and D2, were measured.

**3.2.3.2 Paired interactions**

Interactions were set up as described in Section 3.2.2 for intraspecific pairings of *T. versicolor* (D2), *S. gausapatum* (Sg1), *B. adusta* (MA313), *H. fasciculare* (GTWV2) and interspecific pairings between *T. versicolor* and opponents, *S. gausapatum* (Sg1), *B. adusta* (MA313) and *H. fasciculare* (GTWV2). The extent of both colonies were measured daily on a line towards (T) and away (A) from each other and along a diameter (D) parallel with the line of interaction (Figure 3.2) for both colonies. Plates were incubated until the growing mycelium reached the edge of the plate. Measurements were taken until mycelia met at the centre (T) or met the edge of the plate (A and D).



**Figure 3.2** Positions where extension measurements were made during paired interaction experiments. T, towards opponent; A, away from opponent; D, diameter along a parallel with zone of interaction.

### 3.2.4 Statistical analysis

Linear regression of radial extents was performed to estimate radial extension rate ( $\text{mm d}^{-1}$ ) as the regression coefficient (slope). Minitab<sup>®</sup> 14.13 (Minitab Inc.) was used for statistical analysis.

#### 3.2.4.1 *Comparison of mycelial extension rate of single species*

A one-way analysis of variance (ANOVA) was used to test for significant differences between the extension rates of singly inoculated species. A Tukey-Kramer *a posteriori* test was used to determine where the significant differences between groups occurred, if the ANOVA concluded that there was a significant difference in extension rates (i.e.  $P < 0.01$ ). Data were tested for normality using Anderson-Darling significance testing and Bartlett's test for equality of variances to ensure that the assumptions of ANOVA were met.  $\text{Log}_{10}$  transformations of data were performed where the assumptions were not met. Where transformation was not sufficient to bring data into line with the assumptions of ANOVA an alternative non-parametric Mann-Whitney test was performed.

#### 3.2.4.2 *Comparison of mycelial extension rate between single and paired inocula*

Two sample t-tests were used to compare the mean mycelial extension rates of each species when inoculated singly and when self-paired for all species and isolates listed in Table 3.1. The mean extension rates in all directions were used for this analysis to assess the overall difference in extension rate regardless of direction. Anderson-Darling and Bartlett's test were used to test normality of data and equality of variances, respectively.  $\text{Log}_{10}$  transformations of the data were performed before analysis if the assumptions of the parametric test were not met. Where transformation was not sufficient to allow parametric analysis an alternative non-parametric Mann-Whitney test was performed.

### 3.2.4.3 *Comparison of mycelial extension rate within self paired inocula*

Paired t-tests were used to compare the mycelial extension rates in different directions in self-pairings of *T. versicolor* (TvD2), *S. gausapatum* (Sg1), *H. fasciculare* (GTWV2) and *B. adusta* (MA313). Individual paired t-tests were performed to compare measurements within the pairing: towards (T) vs away (A), towards (T) vs radius (D/2), away (A) vs radius (D/2). Anderson-Darling Bartlett's tests were used to test for normality of data and equality of variances, respectively. Log<sub>10</sub> transformations were performed on data before analysis if the assumptions of the parametric test were not met. Where transformation of the data was not sufficient non-parametric Wilcoxon tests were performed.

### 3.2.4.4 *Comparison of mycelial extension rate of T. versicolor with different treatments*

A one way ANOVA with a Tukey-Kramer *a posteriori* test was used to test for significant differences between the overall extension rate (mean of T, A and D/2) of *T. versicolor* when grown alone, self-paired and when grown in opposition with *S. gausapatum* (Sg1), *H. fasciculare* (GTWV2) and *B. adusta* (MA313). Data were tested for normality using Anderson-Darling significance testing and Barlett's test for equality of variances to ensure the assumptions of ANOVA were met.

### 3.3 Results

#### 3.3.1 Outcomes of interactions

##### 3.3.1.1 *Self pairings*

During self paired interactions of the same isolate the growing margins of mycelial outgrowth from both inocula plugs met at the centre of the plates and intermingled with no obvious alteration in morphology. Over time mycelial growth covered the entire plate and no distinction could be made between which section of mycelium originated from either plug (Figure 3.3)

##### 3.3.1.2 *Interspecific interactions*

In general, interspecific interactions resulted in changes in morphology of mycelia on both sides of the confrontation. In all pairings, soon after initial contact, there was production of mounds of aerial mycelium in the zone of interaction at the centre of the plate and, in general, mycelium behind the interaction zone tended to be sparse. Figure 3.4 shows the interaction between *T. versicolor* and *S. hirsutum*, and typifies the general morphological changes that were observed over time in the majority of interactions. After initial contact there was production of aerial mycelium and, in some species, pigment production, followed by widening of the interaction zone. The initially sparse mycelium behind the interaction zone became denser over time. An endpoint was reached after approximately 6 weeks when no further changes were observed.

Each species pairing produced slightly different changes during interactions. *S. gausapatum* and *S. hirsutum*, in interactions with all species tested, both produced orange pigments behind the growing edge of mycelium. Over time all the agar on which they were growing became highly pigmented. When challenged by competitors *H. fasciculare* produced cords, which appeared to be a more yellow colour (Figure 3.5 a,b) when compared to solitary growth. In the interactions between *P. radiata* and *Stereum* species a dense line of mycelial thickening developed at the margin between the two species, presumably a strategy to prevent ingress of the competitor (Figure 3.6 f,g and Figure 3.5 f).

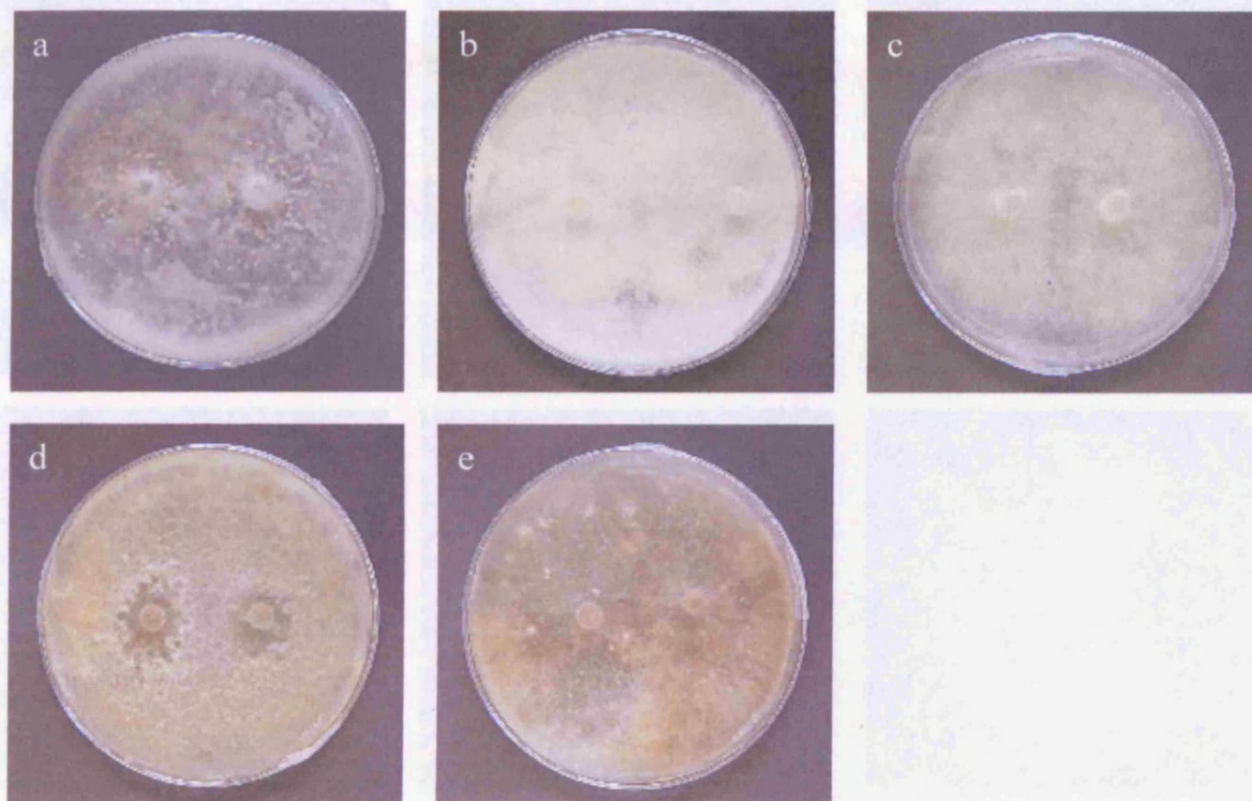
A variety of different overall outcomes were observed for pairings of different species when grown in opposition (Table 3.2) ranging from deadlock (Figure 3.6) to varying degrees of replacement (Figure 3.5). *H. fasciculare* completely replaced *T. versicolor* and *P. radiata* (Figure 3.5 a) but deadlocked when paired with *S. gausapatum* and *S. hirsutum* (Figure 3.5 d,e) and was replaced by *B. adusta* (Figure 3.5 c). *S. gausapatum* and *S. hirsutum* were both partially replaced by *T. versicolor* (Figure 3.5 h,j) and deadlocked with all other species with the exception of *P. radiata* which also partially replaced *S. gausapatum* (Figure 3.5 f). *T. versicolor* partially replaced *S. gausapatum*, *S. hirsutum* and *P. radiata* (Figure 3.7 a-d), but deadlocked with *B. adusta* (Figure 3.7 e) and was replaced by *H. fasciculare* (Figure 3.7 f). *P. radiata* replaced *S. gausapatum*, deadlocked with *S. hirsutum* and was replaced by *T. versicolor* (Figure 3.5 g,i), *H. fasciculare* (Figure 3.5 a,b) and *B. adusta* (Figure 3.5 d,e). These outcomes were confirmed by reisolation and apart from minor variation all replicate pairings produced the same results.

**Table 3.2** Summary of the outcomes of interactions

Species	Outcome of interaction		
	Replaces	Deadlock	Replaced by
<i>H. fasciculare</i> GTWV2	TvD2, Pr 175, PrCop	Sg1, Sh1	Bj MA313
<i>T. versicolor</i> D2	Pr175*, PrCop*, Sh1, Sg1	Bj MA313	Hf GTWV2
<i>B. adusta</i> MA313	PrCop, Hf GTWV2, Pr175	TvD2, Sg1, Sh1	
<i>S. gausapatum</i> Sg1		Sh1, PrCop, Bj MA313, Hf GTWV2	Pr175*, TvD2*
<i>S. hirsutum</i> Sh1		PrCop, Bj MA313, Sg1, Pr175, Hf GTWV2	TvD2*
<i>P. radiata</i> Pr175	Sg1*	Sh1	TvD2*, Hf GTWV2, MA313
<i>P. radiata</i> PrCop		Sg1, Sh1	Hf GTWV2, Bj MA313, TvD2*

\* partial replacement

Abbreviations: Hf GTWV2 – *H. fasciculare* GTWV2; TvD2 – *T. versicolor* D2; Bj MA313 – *B. adusta* MA313; Sg1 – *S. gausapatum* Sg1; Sh1 – *S. hirsutum* Sh1; Pr175 – *P. radiata* Pr175; PrCop – *P. radiata* PrCop.



**Figure 3.3** Self-paired interactions of a) *B. adusta* MA313; b) *T. versicolor* D2; c) *H. fasciculare* GTWV2; d) *S. gausapatum* Sg1; e) *S. hirsutum* Sh1.

**Figure 3.4** Interaction between *T. versicolor* and *S. hirsutum* over time. Interactions were photographed at 7 days (a), 13 days (b), 22 days (c), 29 days (d), 42 days (e), 48 days (f), 95 days (g) post-inoculation.

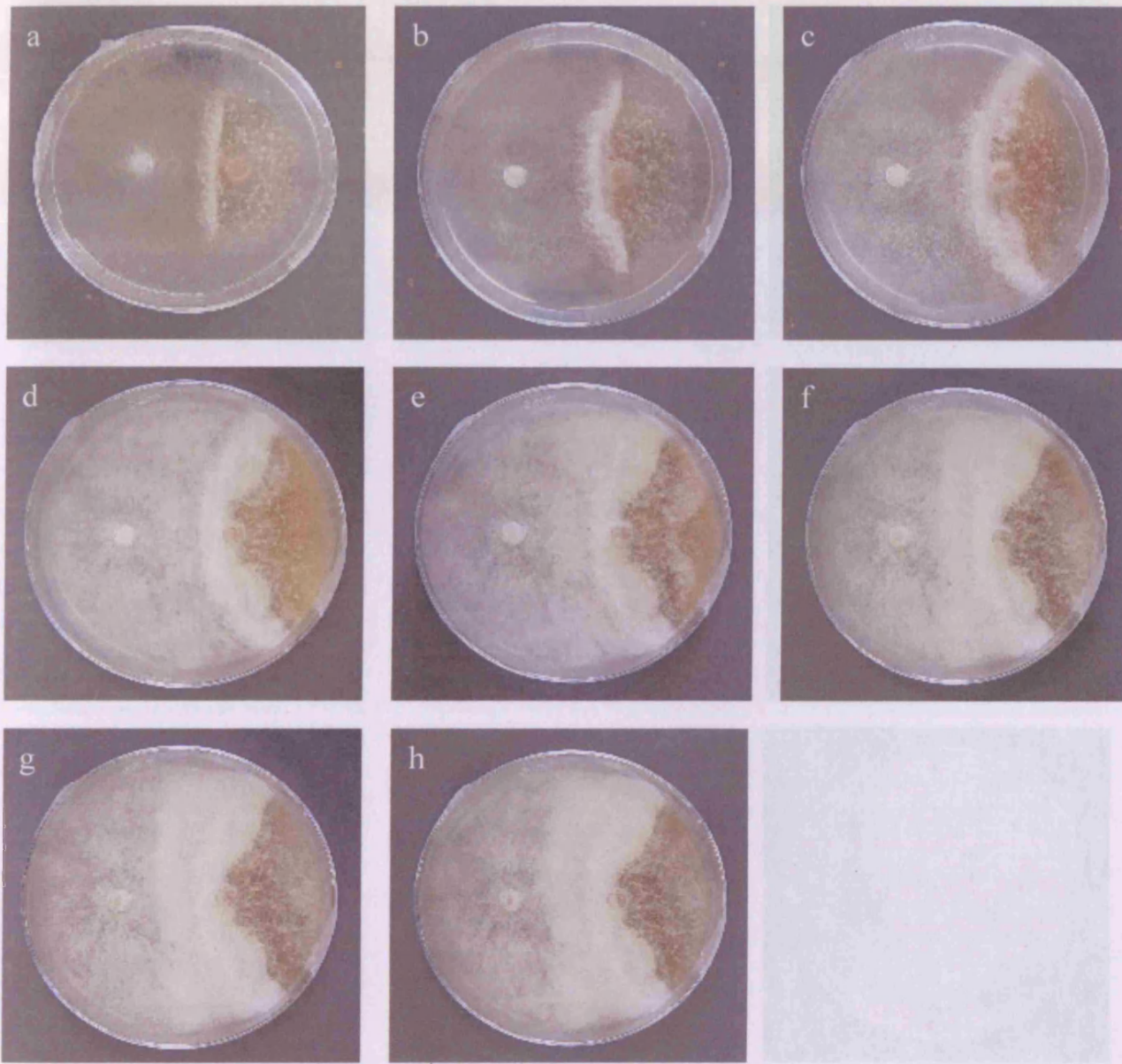


Figure 3.4 Interaction between *T. versicolor* and *S. hirsutum* over time. Interactions were photographed a) 7 days; b) 10 days; c) 13 days; d) 22 days; e) 28 days; f) 36 days; g) 42 days; h) 49 days post inoculation.

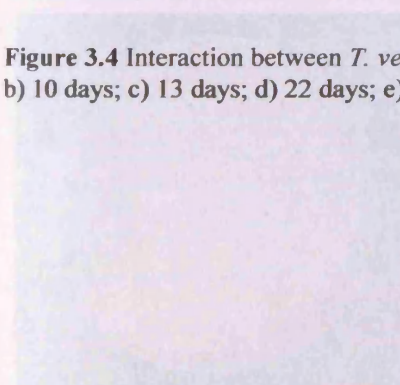


Figure 3.5 Interactions resulting in partial replacement of total replacement of one species by another.

Total replacements: a) *P. radiata* (PrCop) vs *R. ginsengensis* (Sg1)\*, b) *P. radiata* (Pr175)\* vs *R. subinis* (MA311)\*, c) *P. subinis* (MA311)\* vs *R. ginsengensis* (Sg1)\*, d) *P. radiata* (PrCop) vs *R. subinis* (MA311)\*, e) *P. radiata* (Pr175) vs *R. subinis* (MA311)\*.

Partial replacements: f) *P. radiata* (Pr175)\* vs *R. ginsengensis* (Sg1), g) *P. radiata* (Pr175) vs *T. versicolor* (TvD2)\*, h) *S. hirsutum* (Sg1) vs *T. versicolor* (TvD2)\*, i) *P. radiata* (PrCop) vs *T. versicolor* (TvD2)\*, j) *R. ginsengensis* (Sg1) vs *T. versicolor* (TvD2)\*.

\*optimum apparent

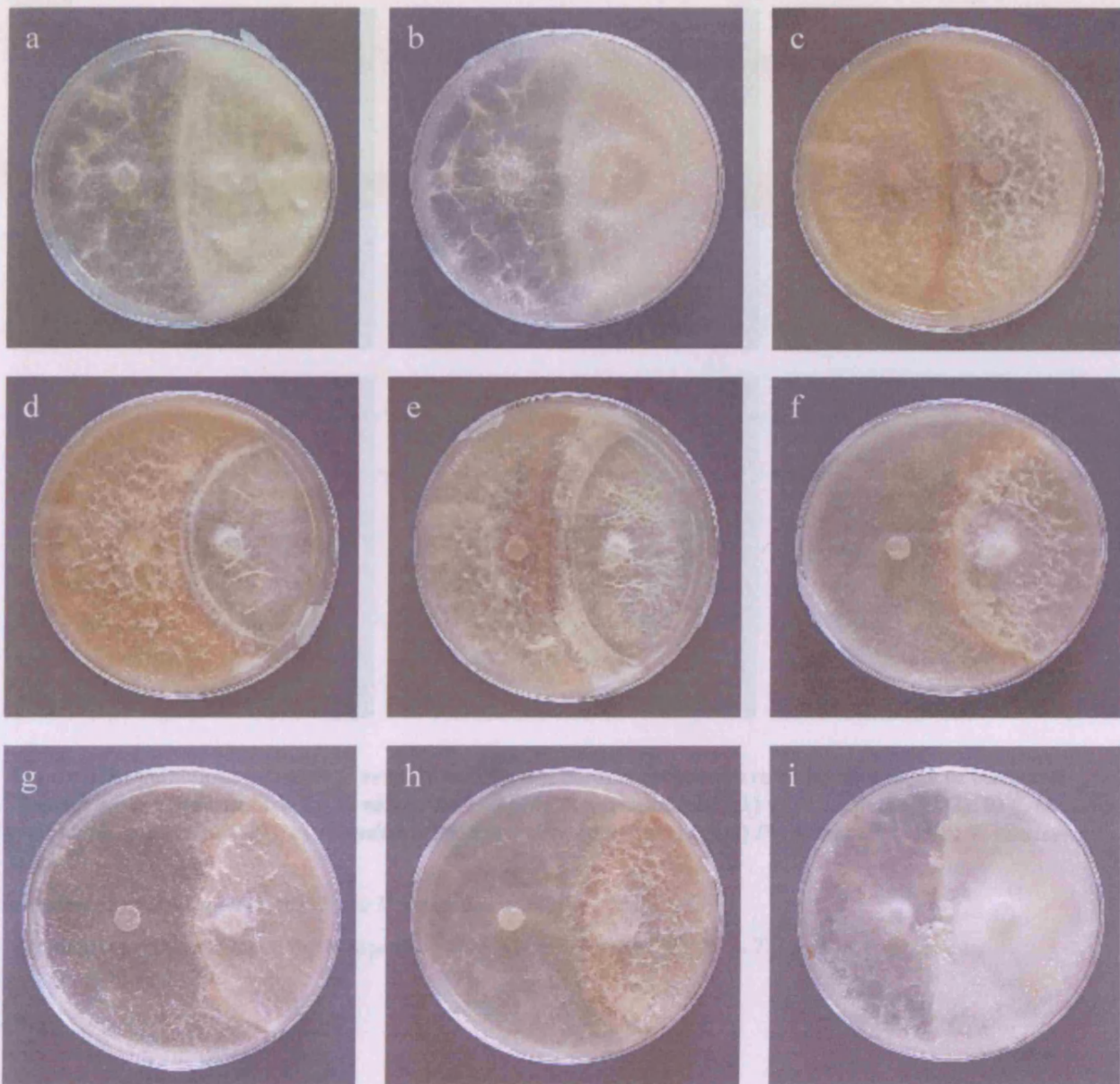




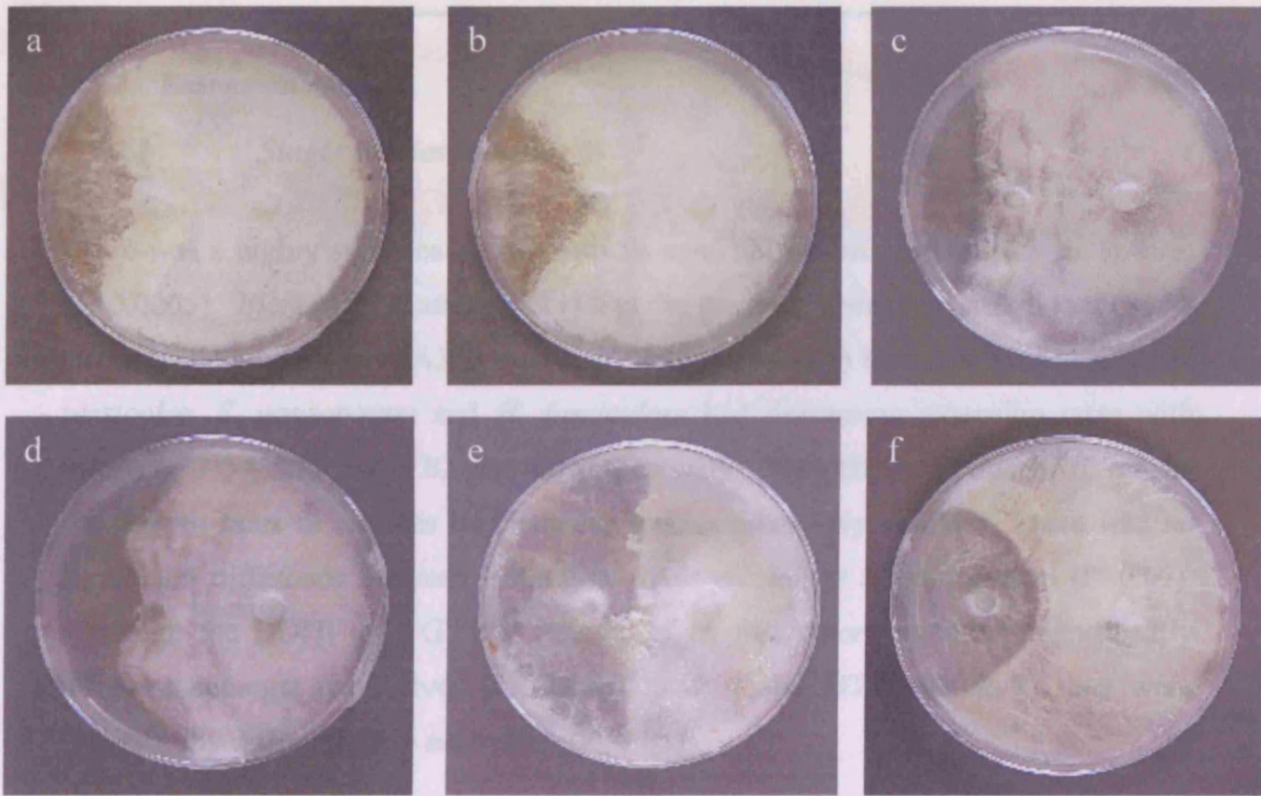
**Figure 3.5** Interactions resulting in partial replacement or total replacement of one species by another. **Total replacement:** a) *P. radiata* (PrCop) vs *H. fasciculare* (GTWV2)\*; b) *P. radiata* (Pr175) vs *H. fasciculare* (GTWV2)\*; c) *B. adusta* (MA313)\* vs *H. fasciculare* (GTWV2); d) *P. radiata* (PrCop) vs *B. adusta* (MA313)\*; e) *P. radiata* (Pr175) vs *B. adusta* (MA313)\*.

**Partial replacement:** f) *P. radiata* (Pr175)\* vs *S. gausapatum* (Sg1); g) *P. radiata* (Pr175) vs *T. versicolor* (D2)\*; h) *S. hirsutum* (Sh1) vs *T. versicolor* (D2)\*; i) *P. radiata* (PrCop) vs *T. versicolor* (TvD2)\*; j) *S. gausapatum* (Sg1) vs *T. versicolor* (D2)\*.

\*replaces opponent



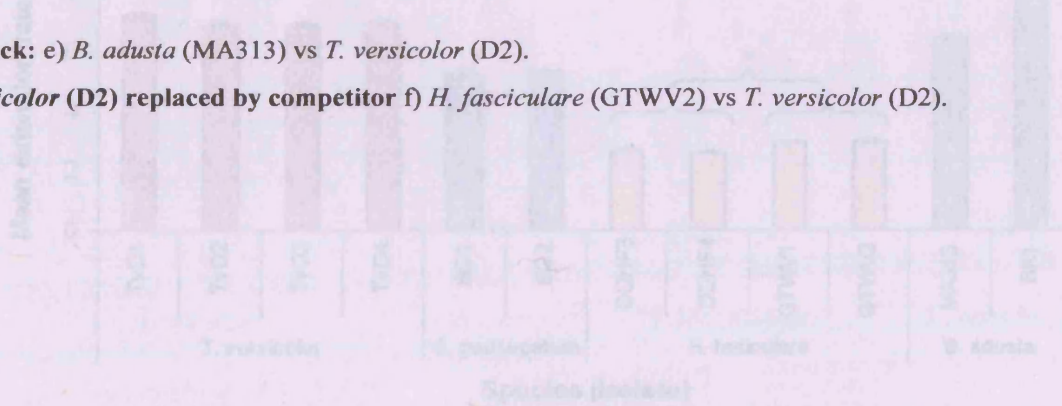
**Figure 3.6** Interactions resulting in deadlock a) *B. adusta* (MA313) vs *S. hirsutum* (Sh1); b) *B. adusta* (MA313) vs *S. gausapatum* (Sg1); c) *S. hirsutum* (Sh1) vs *S. gausapatum* (Sg1); d) *S. hirsutum* (Sh1) vs *H. fasciculare* (GTWV2); e) *S. gausapatum* (Sg1) vs *H. fasciculare* (GTWV2); f) *P. radiata* (PrCop) vs *S. hirsutum* (Sh1); g) *P. radiata* (Pr175) vs *S. hirsutum* (Sh1); h) *P. radiata* (PrCop) vs *S. gausapatum* (Sg1); i) *B. adusta* (MA313) vs *T. versicolor* (D2).



**Figure 3.7** Interactions between *T. versicolor* (D2) and competitor species resulting in a range of outcomes. **Replacement of competitor by *T. versicolor* (D2):** a) *S. gausapatum* (Sg1) vs *T. versicolor* (D2); b) *S. hirsutum* (Sh1) vs *T. versicolor* (D2); c) *P. radiata* (PrCop) vs *T. versicolor* (D2); d) *P. radiata* (Pr175) vs *T. versicolor* (D2).

**Deadlock:** e) *B. adusta* (MA313) vs *T. versicolor* (D2).

***T. versicolor* (D2) replaced by competitor** f) *H. fasciculare* (GTWV2) vs *T. versicolor* (D2).

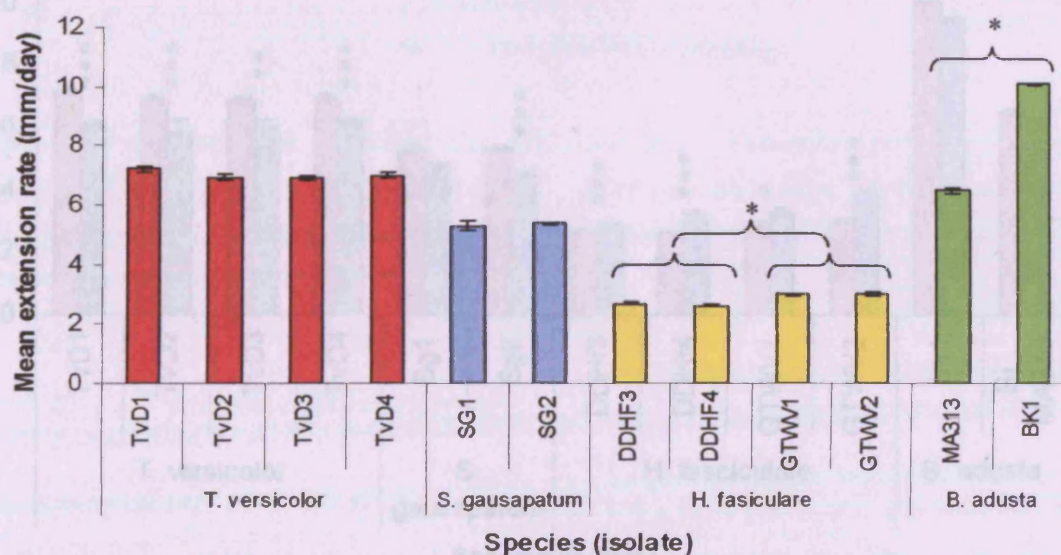


**Figure 3.8** Comparison of mycelial expansion rate ( $\text{mm d}^{-1}$ ) of singly inoculated isolates of four species. Error bars are  $\pm$  SEM. Asterisks indicate significant differences between isolates of the same species. \* $P < 0.05$ . There was significant difference between the two pairs of isolates of *H. fasciculare*, DD=11/4 and GTWV1/2, but not within each pair and also between the two isolates of *B. adusta*, MA313 and MA314.

### 3.3.2 Extension rates

#### 3.3.2.1 Single species inocula

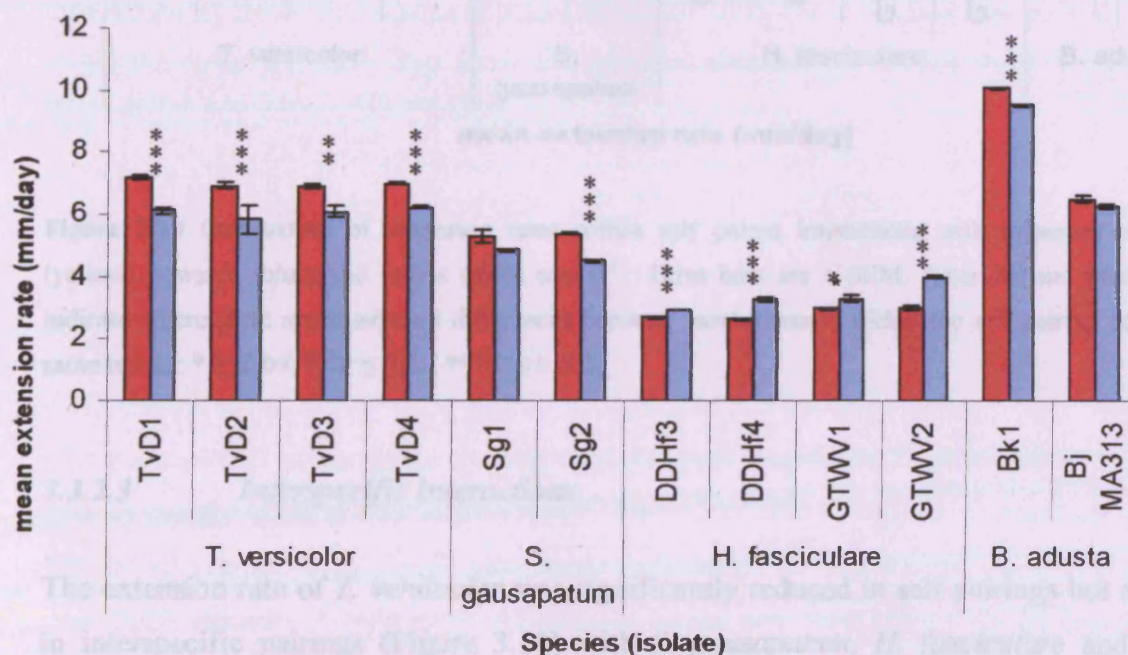
There was a highly significant difference in mycelial extension rate between species ( $P < 0.0005$ ). *Bjerkandera adusta* (Bk1) had the greatest average extension rate ( $10.08 \text{ mm d}^{-1}$ ) though isolate MA313 was significantly ( $P \leq 0.05$ ) lower ( $6.51 \text{ mm d}^{-1}$ ). *T. versicolor*, *S. gausapatum* and *H. fasciculare* had decreasing extension rates with means of  $7.04$ ,  $5.35$  and  $2.82 \text{ mm d}^{-1}$  respectively. With the exception of *B. adusta* the growth rates of isolates of the same species were very similar. There was no significant difference between isolates of *T. versicolor* or *S. gausapatum* ( $P > 0.05$ ). Although the DDHF and GTWV isolates of *H. fasciculare* were not significantly different amongst themselves (i.e. DDHF 3 & 4 and GTWV 1 & 2) they were significantly different from each other ( $P \leq 0.05$ ).



**Figure 3.8** Comparison of mycelial extension rate ( $\text{mm d}^{-1}$ ) of singly inoculated isolates of four species. Error bars are  $\pm$  SEM. Asterisks indicate significant differences between isolates of the same species. \*  $P \leq 0.05$  There was significant difference between the two pairs of isolates of *H. fasciculare*, DDHF3/4 and GTWV1/2, but not within them and also between the two isolates of *B. adusta*, MA313 and BK1.

### 3.3.2.2 Self pairings

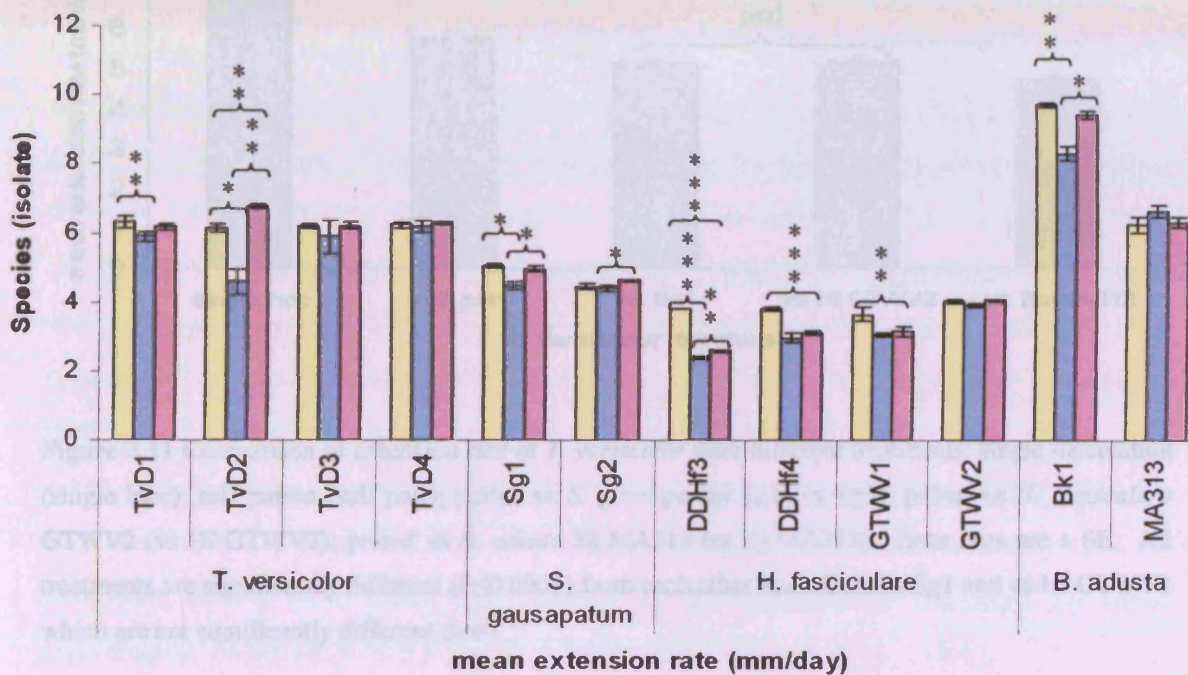
During self paired interactions of *T. versicolor* the overall extension rate of colonies was highly significantly reduced when compared with single inoculations of the same species for all isolates ( $P \leq 0.001$  for TvD1, D2, D4;  $P \leq 0.01$  for TvD3). A similar relationship was observed for *S. gausapatum* and *B. adusta* but the decrease in extension rate was only significant for one of the two replicates tested for each species, Sg2 ( $P \leq 0.001$ ) and Bk1 ( $P \leq 0.001$ ) respectively. However, all isolates of *H. fasciculare* tested showed a significant increase ( $P \leq 0.05$ ) in the overall extension rate in self pairings when compared with single inoculations with isolates DDHf3, DDHf4 and GTWV2 highly significant ( $P \leq 0.001$ ).



**Figure 3.9** Comparison of mycelial extension rate ( $\text{mm d}^{-1}$ ) of single (red) and self paired (blue) inoculations of isolates of four species. Error bars are  $\pm$  SEM. Asterisks indicate significant differences between single and self pairings of the same isolate: \*  $P \leq 0.05$ ; \*\*  $P \leq 0.01$ ; \*\*\*  $P \leq 0.001$ .

There were often differences in extension rate in different directions during self pairings, growth towards the other colony often being inhibited (Figure 3.10). Isolates TvD3, TvD4, HF GTWV2 and Bj MA313 showed no difference between extension rate in any direction. TvD1, Sg1, Sg2 and DDHf4 and GTWV1 all showed some significant differences in extension rate between some of the directions ( $P \leq 0.05$ ) but

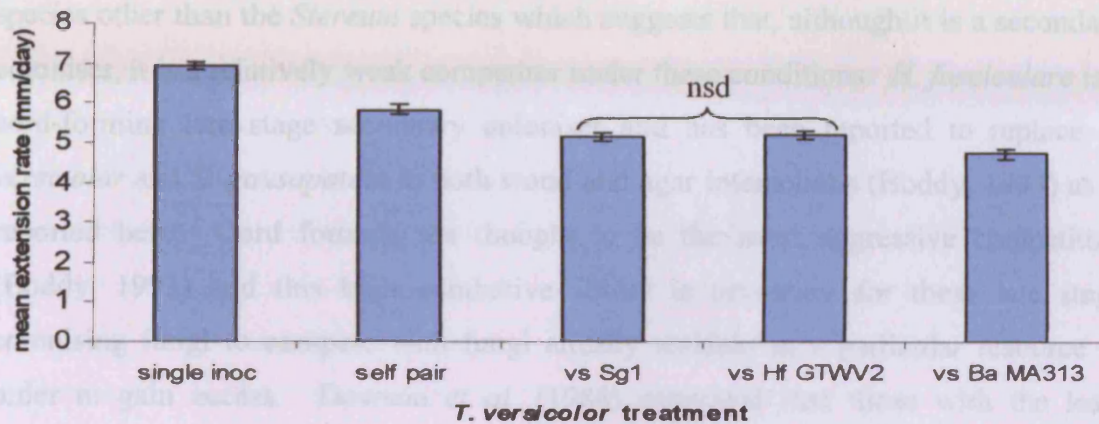
not all. DDHf3 and TvD2 both showed significant differences between all measures ( $P \leq 0.05$ ).



**Figure 3.10** Comparison of extension rates within self paired interactions with measures away (yellow), towards (blue) and radius (pink)  $\text{mm d}^{-1}$ . Error bars are  $\pm$  SEM. Asterisks and brackets indicate where there are significant differences between measurements within the self pairing of the same isolate: \*  $P \leq 0.05$ ; \*\*  $P \leq 0.01$ ; \*\*\*  $P \leq 0.001$ .

### 3.3.2.3 Interspecific interactions

The extension rate of *T. versicolor* was significantly reduced in self pairings but also in interspecific pairings (Figure 3.11) with *S. gausapatum*, *H. fasciculare* and *B. adusta* ( $P \leq 0.001$ ) (Figure 3.11). The Tukey-Kramer *a posteriori* test showed that all treatments were different from each other apart from the pairings with Sg1 and HfGTWV2 where there was no significant difference between them implying that they have equal ability to inhibit the growth of *T. versicolor*.



**Figure 3.11** Comparison of extension rate of *T. versicolor* after different treatments: single inoculation (single inoc); self paired (self pair); paired vs *S. gausapatum* Sg1 (vs Sg1); paired vs *H. fasciculare* GTWV2 (vs Hf GTWV2); paired vs *B. adusta* Bj MA313 (vs Bj MA313). Error bars are  $\pm$  SE. All treatments are significantly different ( $P < 0.0001$ ) from each other apart from vs Sg1 and vs Hf GTWV2 which are not significantly different (nsd).

### 3.4 Discussion

#### 3.4.1 Outcomes of interactions

The outcomes of interactions showed that, in these conditions *H. fasciculare* and *B. adusta* had the greatest combative ability. They were able to replace or deadlock with almost all species with which they were confronted, *H. fasciculare* being replaced only by *B. adusta*. *T. versicolor* appeared to be the next best competitor followed by the *Stereum* species and finally *P. radiata*. In general these outcomes correlate with the ecological strategies of the species concerned. *S. gausapatum* was either replaced by or deadlocked with all species but was never able to replace any competitors. These results are consistent with those found by Rayner and Boddy (1988), and they reflect the ecology of *S. gausapatum* as a primary coloniser: it arrives at and colonises fresh uncolonised resources where little competition is required. The other species studied were secondary colonisers and in general appeared to have greater combative ability with a variety of outcomes depending on the species confronted. *T. versicolor* has been reported to replace *S. gausapatum* and *S. hirsutum* in both wood and agar interactions (Rayner & Boddy, 1988) and to be replaced by *B. adusta* (Owens *et al.*,

1994), which supports the findings in this study. *P. radiata* was replaced by all species other than the *Stereum* species which suggests that, although it is a secondary coloniser, it is a relatively weak competitor under these conditions. *H. fasciculare* is a cord-forming late stage secondary coloniser and has been reported to replace *T. versicolor* and *S. gausapatum* in both wood and agar interactions (Boddy, 1993) as is reported here. Cord formers are thought to be the most aggressive competitors (Boddy, 1993) and this high combative ability is necessary for these late stage colonising fungi to compete with fungi already resident in a particular resource in order to gain access. Dowson *et al.* (1988) suggested that those with the least specialised resource relationships tend to possess the most aggressive combative strategies. This corresponds with the foraging growth habit of *H. fasciculare* and other cord-forming fungi which invade from the forest floor (Boddy, 2001) and have less host specificity when compared to pathogens such as *Armillaria* spp. and *H. annosum*, which have both been shown to be replaced or inhibited by other saprotrophic basidiomycetes (Cox & Scherm, 2006; Woods *et al.*, 2006).

Traditionally data from competition experiments are used to construct combative hierarchies (Holmer & Stenlid, 1997). This representation of differences in combative ability is problematic and does not account for the full complexity of these interactions. If a species *a* is able to replace species *b*, and species *b* can replace species *c*, it does not necessarily follow that species *a* will be able to replace *c* i.e. it is intransitive. *B. adusta* replaced *H. fasciculare*, which replaced *T. versicolor*, and *T. versicolor* replaced *S. gausapatum*. However, *H. fasciculare* and *B. adusta* both deadlocked with *S. gausapatum* rather than replacing them, thus, the hierarchy is intransitive and highlights that a pyramid hierarchy is oversimplified.

A number of factors are involved in determining the growth and outcomes of interactions such as the species involved, the timing of interactions, the size of the inoculum and the environmental conditions. This study has only covered the outcomes of interactions in agar cultures on one type of growth medium. Altering the environmental conditions with respect to growth medium, temperature, pH, water potential and gaseous regime would almost certainly alter the outcomes of some interactions. Although some studies have found that interaction experiments on agar and wood have produced similar results (Rayner & Boddy, 1988; Holmer *et al.*, 1997;



Cox & Scherm, 2006) for some species others have found that this is not the case (Dowson *et al.*, 1988; Holmer & Stenlid, 1993). Wald *et al.* (2004b) studied the interactions of tooth fungi with other wood rotting basidiomycetes in a variety of conditions and found that the outcomes of interactions varied dramatically with altered pH, temperature, water potential and gaseous regime. A combination of all of these factors and the other organisms present within the environment influence the outcomes of interactions in the natural environment and different species are able to cope with them in different ways. It is these differences that drive niche differentiation and lead to specialisation to particular ecological habits.

### 3.4.2 Morphological changes

The morphological changes observed during the interspecific interactions were typical of those reported in the numerous other studies that have looked at similar types of interactions (Boddy *et al.*, 1985; Pearce, 1990; Owens *et al.*, 1994; Holmer *et al.*, 1997; White *et al.*, 1998; Wald *et al.*, 2004a,b). Barrages of aerial mycelium were present in the interaction zones after initial contact and these are likely to be triggered by non-self recognition systems in the fungi. Both species of *Stereum* produced orange pigmentation during interactions, which is an indication of the production of secondary metabolites and is more than likely to be accompanied by increases in enzyme activity, and altered protein synthesis and gene expression (Savoie *et al.*, 2001). *H. fasciculare* produced cords when grown against a competitor species but in general does not produce them when grown alone in agar culture (Boddy, 1993). This production of cords has also been observed in interactions with other species (Wald *et al.*, 2004a) and appears to be characteristic of the response of *H. fasciculare* to confrontation. Indeed, the morphology of *H. fasciculare* changes when grazed by invertebrates to adopt a foraging strategy and produces points of rapid outgrowth as cords with a fanned margin (Tordoff *et al.*, 2006). This response is similar to that during mycelial interactions as in both cases *H. fasciculare* is trying to gain access to new space and resources. Similarly, *T. versicolor* has been reported to produce cords in interactions with *Piptoporus quercinus* at pH 3.75 (Wald *et al.*, 2004a) and also with *Daldinia concentrica* at reduced water potentials, though they have never been seen when growing alone (Boddy *et al.*, 1985). No cords were observed in any of the

interactions produced here but it does imply that there is the genetic capability to produce them under certain circumstances.

### 3.4.3 Extension rates

These experiments showed that generally there was consistency in the extension rates between isolates of the species studied. *T. versicolor* and *S. gausapatum* especially showed very little variation between isolates. However, more variation was observed between isolates of *H. fasciculare* and *B. adusta* which may be due to the isolates originating from different geographical areas. Although the isolates of *T. versicolor* and *S. gausapatum* are distinct individuals they are recorded as having been isolated at the same time and more than likely from the same area thus due to their geographical location they may have local genetic similarities. However, isolates of *H. fasciculare* and *B. adusta* showed more variation. The four isolates of *H. fasciculare* are all distinct individuals and produce incompatibility responses if paired together but isolates DDHf3 and DDHf4 were isolated by the same person and were collected from the same area, as were GTWV1 and GTWV2, but from a different location. The fact that the isolates taken from the same area have similar growth habits and that they are different from the isolates from a different location suggests that there is some geographical genetic variation that may have arisen. If individuals within a limited area do not mix with those from other areas then over time genetically distinct individuals within the same species will evolve. Similarly the two isolates of *B. adusta* used were isolated from different locations at different times which may account for their more dramatic differences in extension rates. However, these differences may also be due to inherent phenotypic plasticity within these particular species.

When comparing the overall extension rates of a species grown alone and when self paired there was often a highly significant difference despite the fact that there were no perceptible changes in morphology or visible evidence of any recognition of an opponent. For *T. versicolor*, *S. gausapatum* and *B. adusta* the self pairings resulted in inhibition of extension rate whereas the growth of *H. fasciculare* was stimulated. These effects are produced before any physical contact has been made between

growing colonies and may indicate that growing mycelium are producing volatile or diffusible chemicals (See Chapter 4). The growing mycelium appears to be able to perceive the presence of other mycelium and responds with slowed growth. This could be a strategy to prevent potentially costly interactions and to concentrate growth in the other direction. However, once contact is made the fungus is able to recognise itself and growth continues as normal. The consistent stimulation of *H. fasciculare* in self pairings may reflect its generally high combative ability. Sensing a potential competitor and stimulating growth may be an aggressive strategy to prevent ingress of competitors. The effects of self pairings on growth of colonies in different directions showed varied results and it seems that no general rule applies to all species. *H. fasciculare* had the most dramatic changes within its own colony and perhaps this ability to adapt its growth significantly in response to outside environmental stimuli is what confers its combative superiority.

#### 3.4.4 Effect of interspecific interactions on extension of *T. versicolor*

*T. versicolor* showed a decrease in extension rate when self paired and then further subsequent reductions in overall extension rate when confronted with a competitor species. The greatest effect was observed during interactions with *B. adusta*, a species with which it eventually deadlocks. Despite the dramatically different outcomes of its interactions with *S. gausapatum* and *H. fasciculare*, replacement and replaced by, respectively, the extension rate of *T. versicolor* appears to be the same in both these situations but still reduced when compared with solitary growth or self pairing. This may be indicative of a common response to interactions by *T. versicolor* regardless of the competitor such as simple self or non-self recognition which triggers the same cascade of signalling and physiological changes. Indeed in the initial stages of interactions of *T. versicolor* with other species, the visible responses are very similar in each case. The eventual outcome of an interaction may be determined by the response of the competitor to the standard response of *T. versicolor* rather than a different response being triggered in *T. versicolor* in the presence of different species.

If gene expression is found to be the same during different interactions then this might suggest that *T. versicolor* has a stock response to confrontation but if it alters it

indicates that different species elicit different responses. The nature of these defence and attack mechanisms may also change throughout the course of an interaction. The outcome of an interaction may be determined at a later stage of the interaction perhaps in response to the changing environment that results from the interaction such as altered enzymes, changes in pH, production of volatiles and pigments which may all elicit different responses from *T. versicolor*.

### 3.4.5 Experimental design

These experiments were carried out in relatively small systems and the number of growing days that can be measured before mycelia meet is limited. It would be interesting to use larger plates to monitor growth over a longer period and discover if there is a point at which mycelia are able to perceive another individual that then triggers an alteration in extension rate. This could be coupled with temporal and spatial analysis of the substrate and the volatiles produced by the fungi to determine which may be responsible for these effects. Similarly, there is evidence that the volume of starting mycelium has an effect on the outcome of interactions (Holmer & Stenlid, 1997) and it seems likely that the timing of interactions is also important.

An established colony has the combative advantage over incoming fungi due to the greater space it occupies. Thus, species which may be able to outcompete others when inoculated simultaneously may be unable to wrest territory from an already established species. Indeed, this is what happens during secondary resource capture.

Interactions have been studied in more realistic systems such as growth on sawdust, wood blocks and inoculations into logs (Wardle *et al.*, 1993; Holmer & Stenlid, 1997; Woods *et al.*, 2006) and are a way of providing conditions closer to the natural environment. These studies have often found different outcomes of interactions for species grown in different resources (Dowson *et al.*, 1988) which might suggest that agar interactions are not ideal. However, these systems are inherently heterogeneous and the principal variables within these environments that influence the outcomes of interactions are not easily identified, separated or controlled. Thus, agar interactions are a valid comparative approach as they allow the manipulation of environmental

conditions. Furthermore, for the study of volatile production and gene expression (Chapters 4-7), agar interactions provide a reproducible controlled environment to test fungi.

While the measuring of extension rates provides some measure of the response of fungi to competitors it would also be interesting to see how this correlates with total biomass and how that is affected by interactions, as species which show little stimulation or inhibition of radial extent may have very different biomass.

### 3.4.6 Data analysis

The comparisons of extension rates within self-pairings and between species grown alone and self pairings required a large number of paired t-tests and two sample t-test respectively. These are relatively low power statistics and it is preferable not to perform high multiples of tests as this reduces the power of the statistics further. As the number of tests performed increases so too does the probability that at least one of those tests will give a positive or significant result by chance alone rather than because the data is truly significant, i.e. a false positive or a type I error. This probability can be calculated as:  $1-(1-\alpha)^N$ , where  $\alpha$  is the confidence level and N is the number of tests. Thus for 10 tests and a desired 95% confidence level (0.05) the probability is 0.4 or 40% chance of finding at least one test is significant due to chance. However, multiple t-tests were most appropriate for the pairwise comparisons required despite the inherent risk of type I errors. There are corrections that can be employed to reduce the risk of type I errors such as the Bonferoni correction which is widely used in ecological and medical studies. This adjusts the  $\alpha$  level according to the number of tests performed ( $\alpha/N$ ) to make the assessment of tests more stringent. However, this is a highly conservative method and while reducing the risk of type I errors it also increases the risk of type II errors, that is rejecting results as non significant when in fact they are significant. A modification of this method is the sequential Bonferoni correction (Holm, 1979) which is slightly less conservative but still highly stringent and carries the same high risk of type II errors. A further problem is that there is some disagreement among statisticians as to which level the Bonferoni correction should be applied. For example, in this study the correction

could be applied to all tests performed within the study as a whole, the set of tests within a table such as the 36 tests performed for Figure 3.10, or all the tests performed for each particular species, or the three tests performed on each individual isolate. When applied at the whole study level paradoxically the more detailed the analysis the less likely it will be to find significant results due to the highly conservative nature of the Bonferoni correction. Consequently, within this study no correction has been used when assessing the significance of results to ensure that significant results are not excluded erroneously. However, significance levels are reported as  $*P \leq 0.05$ ,  $**P \leq 0.01$  and  $***P \leq 0.001$  so that the reader can assess the confidence of each significant result reported and the potential for type I errors is noted. Indeed if individual results were to be used as the basis for further investigation then it would be advisable to repeat tests assessed as significant to only  $P \leq 0.05$  with more replicates to confirm the significance of results.

#### 3.4.7 Selection of *T. versicolor* for continued study

*T. versicolor* was selected from these initial experiments for further study because of the range of outcomes that it produced when interacting with the various other saprotrophic basidiomycetes. It is also abundant in temperal forests within the UK (Rayner & Boddy, 1988). It is also an economically important fungus exploited in the wood pulping industry for its high laccase activity (Monteiro & De Carvalho, 1998) and in bioremediation because it is capable of degrading many hydrocarbons (Kim *et al.*, 1998; Novotný *et al.*, 2004; Walter *et al.*, 2005). The three pairings chosen to study further were: *T. versicolor* paired with *S. gausapatum*, which it replaces; *H. fasciculare* which it is replaced by; and *B. adusta* with which it deadlocks. These species are all abundant in soil and woody substrates found within temperate forests within Britain (Rayner & Boddy, 1988). Thus, these interactions are likely to be taking place frequently within the environment and play important roles in succession and nutrient cycling within the forest ecosystem. Studying the reactions of this fungus to different competitors, which will eventually result in different outcomes, could reveal which are the important pathways and mechanisms involved in the effects observed during interactions.

## 4. Volatile production during interactions

### 4.1 Introduction

Fungi are ubiquitous in the woodland environment and are constantly encountering, and interacting with, other fungi. Interactions may be mediated through direct contact between opposing mycelium or at a distance via volatile and diffusible compounds, and lead to changes in morphology, enzyme activity, protein synthesis and gene expression (Boddy, 2000; Wheatley, 2002; Woodward & Boddy, 2008).

Volatile compounds are produced by a wide range of organisms including plants (Baldwin *et al.*, 2006; Pichersky *et al.*, 2006), bacteria (Bruce *et al.*, 2004), yeasts (Buzzini *et al.*, 2005) and fungi (Wheatley, 2002; Ewen *et al.*, 2004) and commonly include terpenes, phenolics, and hydrocarbon alcohols, aldehydes and ketones. Production of volatiles can be over a range of concentrations (Wheatley *et al.*, 1997) and they have a variety of roles in the environment. The often distinctive odours produced by many organisms are due to volatile organic compounds (VOCs). The fragrance signature of flowers is a composite of volatile chemicals in specific stoichiometric concentrations (Knudsen *et al.*, 1993). For example, at least 13 different volatile compounds have been identified in scent from carnations (Schade *et al.*, 2001). The typical fungal odour is due to the production of 1-octen-3-ol by many fungi (Maga, 1981). Upon drying many fungi lose their aroma and this coincides with the loss of 1-octen-3-ol (Maga, 1981). Many odours consist of several compounds in combination and may also change over time.

Volatile compounds play important roles within the environment and are involved in the interactions between many organisms. Bacterial VOCs inhibit the growth, and in some cases spore germination, of various species of fungi (Bruce *et al.*, 2003; Kai *et al.*, 2007; Zou *et al.*, 2007) and stimulate growth in other species (Mackie & Wheatley, 1999). However, these interactions vary greatly depending on the species producing the volatile, the fungi perceiving them and the environment within which the interaction takes place.

Plants produce VOCs for the attraction of pollinator insects and invertebrates, defence and communication and many of these VOCs can exert an effect on fungi. These can be produced constitutively, such as allicin from garlic (Curtis *et al.*, 2004) and hex-2-enal produced by strawberry plants (Arroyo *et al.*, 2007), which both inhibit mycelial growth. Similarly volatiles derived from broad bean plants both stimulate and inhibit growth of the rust fungus, *Uromyces fabae* (Mendgen *et al.*, 2006). Volatiles may also be produced in response to wounding (Hamilton-Kemp *et al.*, 1992) and infection (Huang *et al.*, 2005; Thelen *et al.*, 2005), and can also aid establishment of mycorrhizal relationships (Akiyama *et al.*, 2005).

Fungi also produce volatiles that have an affect on plants. Volatiles from truffle fungi, *Tuber* spp. alone will inhibit the growth of *Arabidopsis thaliana* and induce an oxidative burst (Splivallo *et al.*, 2007). When plant pathogenic fungi infect plants an oxidative burst and hypersensitive response (HR) are often elicited in the plant as a defence mechanism. This is induced by a number of factors, such as contact and wounding. The most potent inhibitors of growth and elicitors of HR, produced by *Tuber* spp., were the C8 molecules (Splivallo *et al.*, 2007). Similarly, volatile 1-octen-3-ol can induce HR in *A. thaliana*. The concomitant effect is that resistance to the pathogen *Botrytis cinerea* is enhanced (Kishimoto *et al.*, 2007).

Fungi, insects and other invertebrates often have close associations which may be facilitated by the production of fungal volatiles and often only very low concentrations are required to modify insect behaviour (Daisy *et al.*, 2002). Fungi may benefit from the association by producing volatiles that attract insects and other invertebrates, which disperse spores in a process analogous to pollination in plants (Borg-Karlson *et al.*, 1994; Fäldt *et al.*, 1999; Shiestl *et al.*, 2006). Moreover, there is evidence of convergent evolution of volatile production, for example, between the voodoo lily, *Sauromatum guttatum*, and the stinkhorn fungus, *Phallus impudicus* (Borg-Karlson *et al.*, 1994). The production of dimethyl trisulphide and dimethyl disulphide is common to both and they attract the same 'pollinator' species of insects (Borg-Karlson *et al.*, 1994). The rust fungi *Puccinia* spp. produce a floral scent from pseudoflowers that mimics flowers but not necessarily the scent of its host (Raguso & Roy, 1998). Conversely, the plant *Dracula chestertonii* emits a mushroom-like scent, which includes 1-octen-3-ol, and morphologically resembles a mushroom, thereby



attracting fungus gnats for pollination (Kaiser, 2006). Similarly, parasitoid insects use fungal volatile signals to aid foraging and locating hosts, thus they are often attracted to growing fungi (Martínez *et al.*, 2006; Steiner *et al.*, 2007). Other insects and invertebrates which facilitate the spread of infections use volatiles to locate their hosts (Belmain *et al.*, 2002; Cheng *et al.*, 2005) and aid establishment of the fungi in new environments (Bruce *et al.*, 1984; Lin & Phelan, 1992). Furthermore, volatile compounds act as antifeedants in *Gleophyllum odoratum* (Kahlos *et al.*, 1994), and the production of naphthalene by the endophytic fungus, *Muscodor vitigenus*, repels insects (Daisy *et al.*, 2002).

#### 4.1.1 The effects of volatile compounds on fungi

There is a wealth of research into the effects of fungal derived volatiles on other species of fungi in terms of stimulation and inhibition of growth and the control of development. However, very little is known about the bioactivity of volatile compounds and how they produce their effects. Moreover, there is even less known about their production and role during interactions.

*Trichoderma* species produce a range of different volatiles, and when tested against wood decay fungi stimulate growth in some species but inhibit growth in others, thus many studies have focused on their possible use for biocontrol of pest fungi (Bruce *et al.*, 1996; Calistru *et al.*, 1997; Kexiang *et al.*, 2002; Humphris *et al.*, 2002). VOCs isolated from *Trichoderma* spp. inhibit the growth of *Serpula lacrymans* isolates but the extent of inhibition was dependent on the pairings involved (Humphris *et al.*, 2002), and there have been many experiments with different species and isolates that have produced similar results (Calistru *et al.*, 1997; Wheatley *et al.*, 1997; Bruce *et al.*, 2000; Wheatley, 2002).

During the interaction between *Hypholoma fasciculare* and *Resinicium bicolor* VOCs are produced that differ from those detected during solitary growth or self pairings (Hynes *et al.*, 2007), although the precise roles these volatiles play during the interaction are not known. It seems likely therefore, that volatile compounds will be

produced during interspecific interactions between other fungal species, such as *T. versicolor* and *S. gausapatum*, the species of interest within this project.

#### 4.1.2 VOC profiles

Often the volatiles produced by a particular organism create a reproducible profile for an individual species or certain volatile compounds may always be present within a profile, which may aid its detection and identification. Indeed, toxic strains of *Fusarium* spp. can be distinguished from non-toxic strains by the detection of trichodiene, a precursor in the biosynthesis of the mycotoxin tricothecene, and thus it acts as a volatile marker for tricothecene biosynthesis (Demyttenaere *et al.*, 2004). Similarly, strains of *Penicillium roqueforti* that produce PR toxin all generate a specific set of sesquiterpene hydrocarbons. The temperature and growth medium both affected the amount of sesquiterpenes produced but not the profile, therefore these volatile compounds could be used as markers (Jelen, 2002). DeLacy Costello *et al.* (2001) found that there were some volatiles unique to each species and where there were similarities it was likely to be due to similar growth habits or metabolism of the same substrate. However, the abiotic environment, including growth medium, has a large effect on the production of volatiles by many species. Scotter *et al.* (2005) studied six species of fungi, grown on five different culture media and found the ‘fingerprint’ of volatiles produced was strongly dependent on culture medium. Similarly, *Trichoderma* spp. produce different volatiles depending on the growth medium and the isolate involved (Bruce *et al.*, 2000; Wheatley, 2002). Furthermore, Ewen *et al.* (2004) found that *Serpula lacrymans* produced more complex volatile profiles when grown on pine shavings than on glass slides, probably due to compounds being generated during the degradation of the wood. The majority of studies have taken a snapshot sample of volatiles from a single timepoint. However, volatile profiles can alter over time (Sunesson *et al.*, 1995; Nilsson *et al.*, 1996; Korpi *et al.*, 1999). The volatile profile from *Trichoderma aureoviride* changes as growth progresses and the volatiles derived from cultures 7-14 days old are most inhibitory to growth of other fungi (Bruce *et al.*, 1996). Clearly these differences are an important consideration when studying the evolution of volatile compounds *in vitro*.

There is a complex relationship between fungi and volatile-producing antagonists, and the effects that volatiles have may be determined not just by their presence but also by their relative concentrations. Furthermore, many of the effects on growth induced by volatile compounds are transient, and mycelial growth often recovers on removal of an antagonist or transfer to new growth media (Mackie & Wheatley, 1999; Wheatley, 2002; Chitarra *et al.*, 2005). This may have ecological significance. The self-inhibition of conidial germination by *Penicillium paneum* modulated by 1-octen-3-ol is reversible and inhibition occurs only at high spore concentrations (Chitarra *et al.*, 2005). This self-inhibition of conidial germination at high spore concentrations is known as the ‘crowding effect’ (Chitarra *et al.*, 2005). It serves to prevent premature spore germination before dispersal, ensures that conidia only germinate when dispersed to suitable growth substrates, and prevents self competition between spores for space and nutrients.

Although the majority of research has considered simple pairwise interactions between species, or exposure to single known chemicals, interactions are rarely as simplistic as pair wise associations. The interactions that occur between organisms facilitated by volatile compounds are likely to have wider community effects. Synergistic effects of VOCs have been observed, confirming that systems are complex. For example, various pairs of volatile compounds increased inhibition of *Penicillium notatum* growth when compared to single compound treatments (Tunc *et al.*, 2007). Similarly, unsaturated aldehydes produced by plants were most potent inhibitors of *Botrytis cinerea* when combined with epiphytic bacteria (Abanda-Nkpwatt *et al.*, 2006).

In addition to altered growth rates, morphological changes occur at the hyphal level on exposure to VOCs. Calistru *et al.* (1997) showed that volatiles produced by *Trichoderma* spp. induced morphological changes in hyphae of *Aspergillus flavus* and *Fusarium moniliforme*, such as cell wall abnormalities, abnormal vesicle formation and aberrant conidial heads. Similarly, Myung *et al.* (2007) found changes in membrane permeability of *Botrytis cinerea* when exposed to C6 aldehydes which inhibited growth, while Arroyo *et al.* (2007) found similar plasma membrane disorganisation, lysis of organelles and eventually cell death when the pathogen *Colletotrichum acutatum* was exposed to (E)-hex-2-enal derived from strawberry

plants. Zucchi *et al.* (2005) studied the effects of benzene on *Aspergillus nidulans*, using this species as a model to assess its genotoxicity in eukaryotes. Conidial viability was reduced and this was accompanied by DNA alterations and damage. However, Wheatley *et al.* (1997) did not observe morphological changes accompanying altered growth rates of four wood decay fungi exposed to *Trichoderma* VOCs. This may have been due to different effects occurring in different species and perhaps different approaches to studying the morphological effects.

Developmental processes can also be affected by exposure to VOCs, such as reduced conidiogenesis of *Heterobasidion abietinum* after exposure to monoterpenes (Zamponi *et al.*, 2006) and self-inhibition of conidial germination by 1-octen-3-ol produced by *Penicillium paneum* (Chitarra *et al.*, 2005). Some fungi have evolved to use volatiles to stimulate development, such as the obligate biotrophic rust fungus *Uromyces fabae* which develops haustoria, infection structures, on contact with nonenal, decanal and hexenyl acetate which are produced by the host broad bean plants, *Vicia faba* (Mendgen *et al.*, 2006). However, haustoria development is suppressed by the terpenoid farnesyl acetate produced by the same plant (Mendgen *et al.*, 2006). It seems likely that differences in the relative quantity of compounds produced, and their temporal distribution, determines the fungal response.

### 4.1.3 Bioactivity of volatiles

Little is known about which compounds within VOC profiles are responsible for the growth inhibition and stimulation of other organisms. Jelen (2002) found that the aldehyde group of PR toxin, a sesquiterpenoid metabolite produced by *Penicillium roqueforti*, was responsible for its toxic nature, and several studies have implicated aldehydes and ketones in association with the inhibition of basidiomycetes (Wheatley, 2002; Abanda-Nkpwatt *et al.*, 2006). Myung *et al.* (2007) studied the inhibition of *B. cinerea* by six carbon (C6) aldehydes and suggested that aldehydes disrupted hydrogen bonding in the membrane lipid bilayer and caused the changes in membrane permeability observed. Eight carbon (C8) molecules, especially 1-octen-3-ol, have also been implicated in suppressing mycelial growth in many studies (Maga, 1981; Kahlos *et al.*, 1994; Rösecke *et al.*, 2000; Jelen, 2002; Ewen *et al.*, 2004; Chitarra *et*

*al.*, 2005; Combet *et al.*, 2006). Many aromatic compounds and terpenoids produced by fungi (Florjanowicz, 2000; Roy *et al.*, 2003) have been shown to have inhibitory effects on other fungi. In addition, different isomers of the same compounds can have different bioactivities (Prosser *et al.*, 2004), which should be considered when investigating the active compounds within volatile profiles. Germacrene D enantiomers from goldenrod, *Solidago canadensis*, have different effects on insect behaviour (Prosser *et al.*, 2004) and enantiomers of limonene and carvone isolated from plants, have differing antimicrobial activity (Aggarwal *et al.*, 2002).

Alterations of mycelial growth induced by exposure to VOCs are accompanied by altered protein synthesis (Humphris *et al.*, 2002; Wheatley, 2002; Myung *et al.*, 2007). It seems likely that the limits of mycelial growth may be due to alterations in protein production, although suppression of enzyme activity may also occur. Thus, it follows that altered protein production is the result of up or down-regulation of the genes encoding the proteins involved.

#### 4.1.4 Sampling of volatiles

A number of approaches can be employed to sample the VOCs produced by fungi. In general the collection of volatiles involves the isolation of a growing culture and sampling its headspace. Several methods of sampling are available such as liquid-liquid extraction (LLE), solid phase extraction (SPE) and solid phase microextraction (SPME), all of which are based on the principle of allowing analytes to separate between the sample and an extracting phase. Another approach is solid sample injection (SSI) where analytes are directly purged onto a gas chromatography column, which omits the need for absorption and desorption (Ewen *et al.*, 2004). LLE and SPE are both multi-step processes, the preparation of samples often being time consuming. Also, LLE requires the addition of organic solvents to the sample which may give rise to artefacts during sample analysis. Furthermore, if high temperatures are used for desorption this can result in alteration of the volatiles originally collected. SPME, however, does not require solvents, extraction time is short and there is no lengthy sample preparation. A silicone fibre coated with an adsorptive material is exposed to the volatiles in the headspace of a sample or can be dipped in a liquid

sample, the volatiles are adsorbed onto the coating and can then be analysed. Sometimes a stir bar is used as agitation aids diffusion of analytes. There are many types of fibre available each capable of adsorbing different compounds. Both polydimethylsiloxane (PDMS) and polyacrylate (PA) have been used to sample fungal volatiles (Nilsson *et al.*, 1996; Jelen, 2003; Demyttenaere *et al.*, 2004; Ewen *et al.*, 2004; Hynes *et al.*, 2007). Jelen (2003) tested four types of fibre and found that each showed varied efficiency and selectivity but sesquiterpenes were the predominant fraction isolated by all fibres. No single fibre type is capable of adsorbing all analytes, thus the choice of fibre to use is determined by the compounds expected to be found or more than one fibre can be used. However, in experiments where timing of samples is critical it may be logistically unfeasible to test each sample with several fibres. The disadvantage of SPME is that fibres can break easily, there is potential for carry over between samples and high molecular weight compounds can potentially adsorb irreversibly (De Fatima Alpendurada, 2000).

Several studies have compared extraction techniques and most have found that different profiles of volatiles are obtained using different methods (Jelen, 2003; Ewen *et al.*, 2004), although Demyttenaere *et al.* (2004) found that headspace SPME and headspace sorptive extraction (HSSE) produced the same qualitative profiles, but the relative contribution of each compound was slightly different. Clearly, each extraction method may only provide a partial profile of the VOCs, and if possible several extraction techniques should be used. Increasingly SPME has been used because of the rapid extraction times and the portability of SPME probes makes their use in the field possible.

Data derived from SPME fibres should always be treated with some caution as the composition and percentage of each compound present in the sample may not always be represented in the analysis by the same percentage of the relative peaks areas. Differing distribution coefficients between phases, affinity of the fibre coating, composition of the matrix, extraction temperature, pH and exposure time can all have an effect on the final volatile profile detected (Jelen, 2003). Therefore, it is essential to ensure that conditions are kept constant if comparisons are required, to acknowledge that quantifications may not reflect the true concentrations of compounds, and standards should be used if more accurate quantification is required.

The basis of GC-MS analysis is discussed in Appendix A1.1.

#### 4.1.5 Objectives

The objectives of the experiments reported here were to:

- Test the hypothesis that a unique set of volatile compounds are produced during the interaction of *Trametes versicolor* and *Stereum gausapatum*, compared to solitary growth or self pairings.
- Use SPME to sample volatiles from the headspace of growing fungal cultures of *Trametes versicolor* and *Stereum gausapatum* growing alone, self paired and paired against each other.
- Using gas chromatography-mass spectrometry (GC-MS) to identify and quantify the compounds detected and make comparisons between species and pairings.

SPME enables quick and easy sampling. A 100 µm PDMS fibre was used, which is one of the most popular types of fibre, as it is able to withstand high temperatures and extracts non-polar compounds, including polycyclic aromatic hydrocarbons, monoterpenes and sesquiterpenes (De Fatima Alpendurada, 2000). This seemed a good choice of fibre as Wheatley (2002) and McAfee (1999) found that the volatiles produced by *T. versicolor* were mostly aldehydes, ketones, alcohols, monoterpenes and sesquiterpenes. Hynes *et al.* (2007) also detected several sesquiterpenes during the interaction between *Resinicium bicolor* and *Hypholoma fasciculare* using this type of fibre.

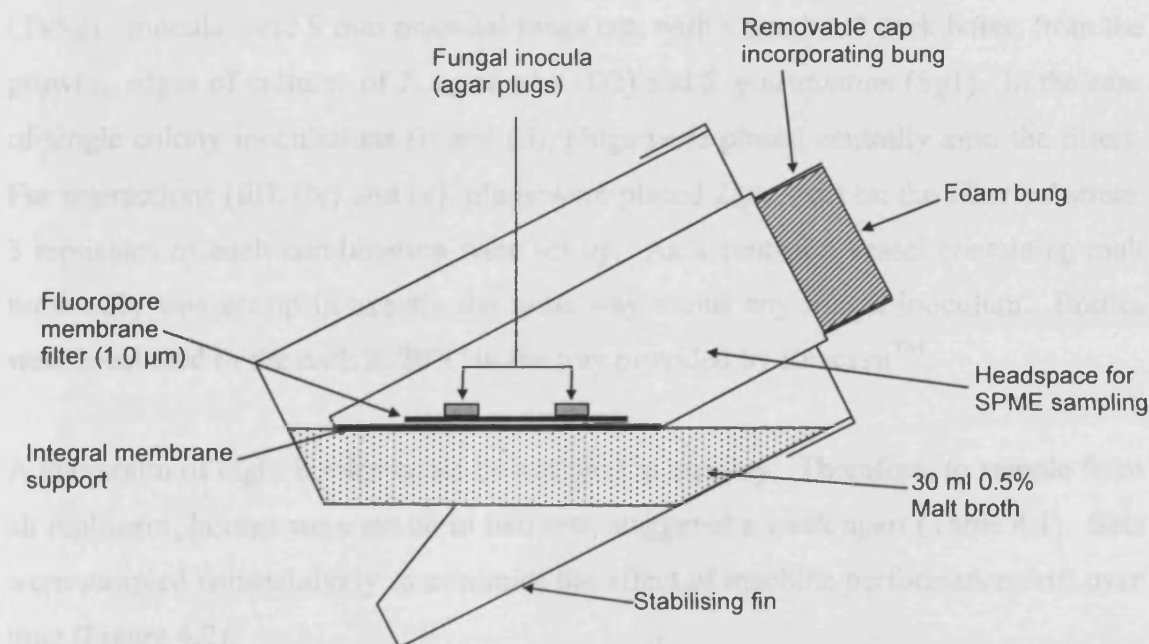
## 4.2 Materials and Methods

### 4.2.1 Growth conditions

Cultures of *T. versicolor* D2 and *S. gausapatum* Sg1 were maintained by subculturing on 0.5% w/v Malt agar (5 g l<sup>-1</sup> Munton & Fison spray malt, 15 g l<sup>-1</sup> Lab M agar No. 2) in the dark at 20°C on 9 mm non-vented Petri dishes (Greiner).

### 4.2.2 Interactions in Reacsyn™ vessel microcosm

Volatile chemical production was studied using a Reacsyn™ fermentation vessel (BioDiversity, Enfield, UK) that allows fungal isolates to be grown within a closed system either alone or confronted with another species (Figure 4.1).



**Figure 4.1** Diagram of Reacsyn™ vessels used for culturing fungi to enable sampling of volatiles during growth



The bottle is designed such that the central headspace section can be accessed and the mycelia growing within it can be removed from the bottle and transferred to a new bottle if necessary. Vessels were not altered for the entirety of the experiment with the system only being opened during the flushing periods.

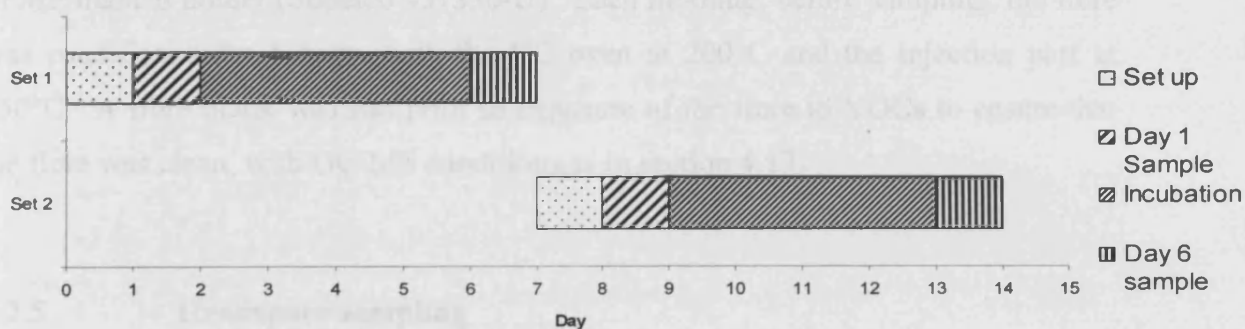
Bottles were set up with 35 ml 0.5% w/v Malt broth (5  $\text{g l}^{-1}$  Muntion & Fison spray malt) in the base of the Reacsyn<sup>TM</sup> vessel. An additional sterile 1.0  $\mu\text{m}$  pore size Fluoropore membrane filter (Millipore, UK) was placed on top of the integral membrane support on the platform to encourage lateral growth of fungi towards one another rather than down through the existing filter into the broth. It also provided a white background which aided observation of pigmentation during interactions.

Five different mycelial combinations were set up (i) *T. versicolor* D2 alone (Tv), (ii) *S. gausapatum* Sg1 alone (Sg), (iii) *T. versicolor* D2 self paired (TvTv), (iv) *S. gausapatum* Sg1 self paired (SgSg) and (v) *T. versicolor* D2 vs *S. gausapatum* (TvSg). Inocula were 9 mm mycelial plugs cut, with a number 3 cork borer, from the growing edges of cultures of *T. versicolor* (D2) and *S. gausapatum* (Sg1). In the case of single colony inoculations (i) and (ii), plugs were placed centrally onto the filters. For interactions (iii), (iv) and (v), plugs were placed 2cm apart on the filter substrate. 3 replicates of each combination were set up. As a control a vessel containing malt broth only was set up in exactly the same way minus any fungal inoculum. Bottles were incubated in the dark at 20°C in the tray provided by Reacsyn<sup>TM</sup>.

A maximum of eight bottles could be sampled in one day. Therefore, to sample from all replicates, bottles were set up in two sets, staggered a week apart (Table 4.1). Sets were sampled consecutively to minimise the effect of machine performance drift over time (Figure 4.2).

**Table 4.1** Allocation of replicates for each combination to experimental sets 1 and 2

Combination	Replicate	Set 1	Set 2
Tv	1	•	
	2	•	
	3		•
Sg	1	•	
	2	•	
	3		•
TvTv	1	•	
	2	•	
	3		•
SgSg	1	•	
	2		•
	3		•
TvSg	1	•	
	2		•
	3		•
Malt	1		•

**Figure 4.2** Gantt chart showing the timespan of experiment

### 4.2.3 Volatile sampling

Head space sampling was performed for all vessels 1 d and 6 d after inoculation (Figure 4.2). At 1 d mycelium had begun to emerge from the inoculum plug, they are assumed to have stopped producing damage VOCs, and the mycelium had not yet made contact with the opponent. The 6 d timepoint was chosen because at this point mycelia had met and pigment production had begun, in the case of the interaction between *T. versicolor* and *S. gausapatum*.

These timepoints mirror the two treatments that were used during the SSH library construction and microarray experiments detailed in Chapters 5 and 6. For SSH and microarray work cultures were harvested on Day 5 of agar interactions. Headspace sampling was carried out on Day 6 however, because the growth substrate within the bottles slows the progress of the mycelial mats towards one another when compared with growth on agar. However, the endpoint is the same i.e. the point at which fungi have made physical contact and typical interaction morphologies are visible.

#### **4.2.4 Fibre conditioning**

Volatiles produced were sampled using a Solid Phase Microextraction (SPME) fibre with a 100µm Polydimethylsiloxane (PDMS) coating (Supelco #57300-U), held in a SPME manual holder (Supelco #57330-U). Each morning, before sampling, the fibre was conditioned for 1 hour, with the GC oven at 200°C and the injection port at 250°C. A fibre blank was run prior to exposure of the fibre to VOCs to ensure that the fibre was clean, with GC-MS conditions as in section 4.17.

#### **4.2.5 Headspace sampling**

The Reacsyn™ bottle to be sampled was flushed through in a laminar flow hood, by removing the cap of the bottle for 10 min prior to fibre exposure, and then resealed. The fibre was then inserted through the foam bung of the Reacsyn™ vessel and held in place using a clamp stand. The fibre was exposed for 1 hour and then immediately manually injected into the GC-MS.

#### **4.2.6 Volatile compound separation and detection**

##### **4.2.6.1 Fungal volatiles**

Volatiles were analysed by GC-MS analysis (GC8000, Thermofinnigan, Hemel Hempstead, UK; MD 800, Thermofinnigan). Fungal volatile samples were injected manually and desorbed at 220°C in a split/splitless injection port in splitless mode for

2 min (purge 2 min, split 2 min) and resolved on a 30 x 0.25 mm I.D, 0.25  $\mu\text{m}$  VF23ms (Varian, Palo Alto, CA, USA) polar column with helium carrier gas (55 KPa). The temperature program was as follows: start 45°C, increasing at 3°C min<sup>-1</sup> to 200°C, then held at 200°C for 5 min. Mass spectra were recorded with Electron Ionisation (EI+) in scan mode from  $m/z = 35.00$  to 400.00 with scan time 0.30 s, interscan delay 0.1 s, at a source temperature of 200°C and interface at 280°C.

#### 4.2.6.2 *Calibration and performance checks*

To monitor the performance of the GC and check consistency, a Polar Test mixture (Cat. No. 47302 Supelco, Bellefonte, PA) was run through the machine occasionally. This consists of known compounds in known concentrations, thus the resulting chromatogram and mass spectra could be compared with the literature to assess the operational status of the machine. Deviation from the predicted chromatogram and spectra indicated a fault with the machine.

The Polar Test mixture (1 $\mu\text{l}$ ) was injected using an autosampler (AS 800, CE instruments) in a split/splitless injection port in split mode for 2 min, (purge 2 min, split 0), split ratio 50:1. Autosampler settings were: Injection volume - 1.0  $\mu\text{l}$  sample, 1.0  $\mu\text{l}$  air; Pre-injection washing - 5  $\mu\text{l}$  Hexane for 5 wash cycles; Sample volume - 1.0  $\mu\text{l}$  for 2 wash cycles; Post-injection washing - 5  $\mu\text{l}$  Hexane for 5 wash cycles. An isothermal program was used at 120°C for 24 min. Mass spectra were recorded with EI+ in scan mode from  $m/z = 35.00$  to 400.00 with scan time 0.35 s, Interscan delay 0.05 s, solvent delay 2 min, at a source temperature of 200°C and interface at 280°C. Retention window was 2.00 to 24.00 min.

#### 4.2.6.3 *External standard*

For this experiment the external standard used was a mixture of two terpenes and one sesquiterpene: (1S) (-) Verbenone  $\text{C}_{10}\text{H}_{14}\text{O}$  FW=150.22 (Aldrich 218251); (1R) (-) Fenchone  $\text{C}_{10}\text{H}_{16}\text{O}$  FW=152.24 (Aldrich 196436);  $\alpha$  - Humulene  $\text{C}_{15}\text{H}_{24}$  FW=204.35 (Fluka 53675), dissolved in Hexane at 50 $\mu\text{g cm}^{-3}$  for each compound. It was injected directly into the GC. This standard was used because a previous experiment

analysing the volatiles produced by interacting saprotrophic basidiomycetes, *Hypholoma fasciculare* and *Resinicium bicolor* (Hynes *et al.*, 2007), found that the major compounds produced during an interaction were sesquiterpenes.

The terpene standard mixture (1 $\mu$ l) was injected using an autosampler (AS 800, CE instruments) in a split/splitless injection port in split mode for 2 min (purge 2min, split 0). Autosampler settings were the same as those used for the Polar test mix (Section 4.1.7.2). The temperature program was as follows: Start 40°C, increasing at 5°C min<sup>-1</sup> to 165°C. Mass spectra were recorded with EI+ in scan mode from m/z = 28.00 to 450.00, with scan time of 0.45 s, interscan delay 0.05, solvent delay of 2 min, at a source temperature of 200°C and interface at 280°C.

#### 4.2.7 Data analysis

Masslab Version 1.4 (Finnigan) GC-MS software was used to record data from the GC-MS and produce chromatograms, mass spectra and to integrate peaks. Chromatograms come off the GC and mass spectra are derived from each peak within the chromatograms.

##### 4.2.7.1 Peak assignment

In the first instance, chromatograms for the three replicates of each treatment were aligned and the scales standardised. This allowed comparison between treatments to find common peaks and to compare the intensity of the peaks between replicates. Peaks with the same (or very close) retention times were regarded as homologous if the time discrepancies were not more than  $\pm 1$ -2 s. However, all mass spectra were analysed to confirm they represented the same compounds. Peaks that appeared in only one of the three replicates were reported but considered artefacts and were not included in further analysis.

#### 4.2.7.2 *Production of mass spectra for individual peaks*

Spectra for the individual peaks were produced with background subtracted using the combine function in MassLab.

#### 4.2.7.3 *Peak Identification*

Individual peak spectra were compared to the National Institute of Standards and Technology (NIST) v2.1 mass spectral database using the MassLab library function. Spectra were also visually inspected to identify characteristic fragmentation patterns and to confirm that library matches were plausible before making putative identifications.

#### 4.2.7.4 *Quantification*

**Integration.** The external standard comprising three terpenes (Section 4.1.7.3), of known concentrations, was run each day to monitor machine function and to provide an estimate of the concentration of compounds detected by the GC-MS. The integration function of MassLab was used to calculate the area under each peak in the chromatograms. The integration parameters were optimised and the same set of parameters used to integrate all chromatograms.

**Normalisation.** The terpene mix external standards from each sampling day were normalised against themselves and an average peak area (that represents 50 ng in “standard terpene units” (stu)) for all three external standard peaks was used to normalise against the experimental peaks, and calculate the amount of each compound evolved. To justify the use of an average value for normalisation rather than a single peak, the ratio of peaks were tested using a Chi-squared test to confirm that variation between the three peaks was consistent.

**Comparison of amounts of volatiles produced.** The concentration of volatile evolved for each peak (as concentration in “terpene standard units”), was compared between treatments using one-way analysis of variance (ANOVA) together with Tukey-

Kramer *a posteriori* tests, with  $H_0$ : no significant difference between treatments. Data were tested for normality using Anderson-Darling significance testing and Bartlett's test for equality of variances to ensure that the assumptions of ANOVA were upheld.  $\text{Log}_{10}$  transformations of data were performed prior to analysis where the assumptions were not met.

Two sample t-tests were used to test whether the concentrations of particular peaks changed between Days 1 and 6 and also to test whether the size of colony has an affect on volatile concentration, by comparing the peaks for single and paired inocula treatments of the same species e.g. Sg compared with SgSg.  $\text{Log}_{10}$  transformation of data was performed where the assumptions of normality and equality of variance were not upheld prior to analysis. Minitab<sup>®</sup> 14.13 (Minitab Inc.) was used for statistical analysis.

### 4.3 Results

Chromatograms are produced by the GC for each sample run. Peaks within these chromatograms represent each compound as it is eluted from the column into the MS. Mass spectra are then acquired for each peak from the chromatogram and compared with the library databases.

#### 4.3.1 Mycelial growth

Inocula within vessels sampled after 1 d did not show any obvious growth of mycelia. However, after 6 d lateral mycelial growth was observed across the membrane together with downward growth into the broth. *S. gausapatum* produced aerial mycelium, while *T. versicolor* produced little visible aerial mycelium. In all paired inocula treatments the mycelium had met at the centre between agar plugs after 6 d. For self paired treatments TvTv and SgSg mycelial growth did not appear to be different from that of the single inocula treatments. In the interspecific pairing TvSg there was marked orange pigmentation at the interaction zone after 6 d.

### 4.3.2 Fibre Blank

Fibre blanks run at the start of each sampling day produced chromatograms without peaks (Figure 4.3) and thus confirmed that the fibre had been correctly conditioned. There was an initial spike between retention time 1.6-1.9 min on all fibre blank runs followed by the chromatogram trace gradually declining to a consistent level of background noise.

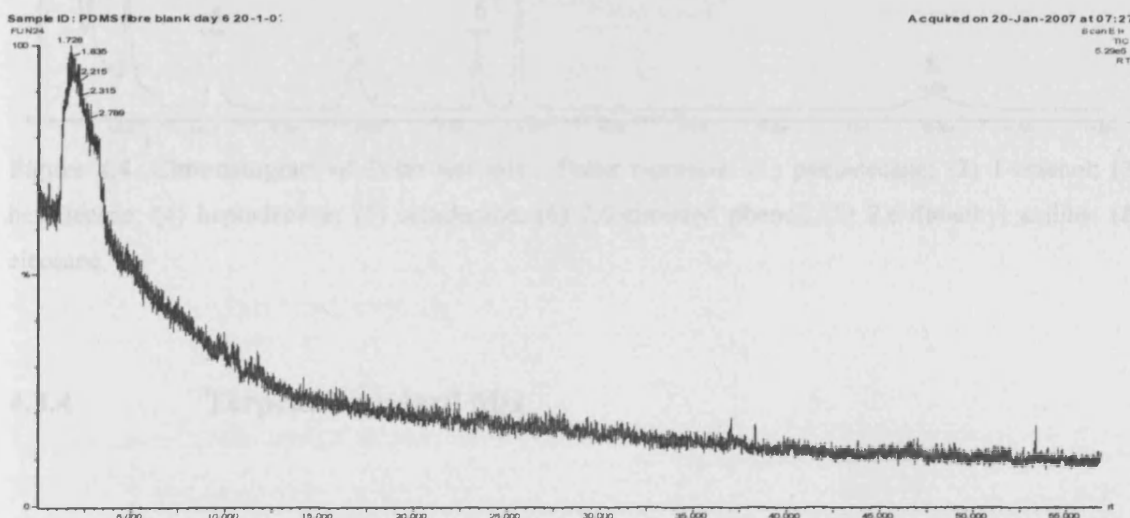
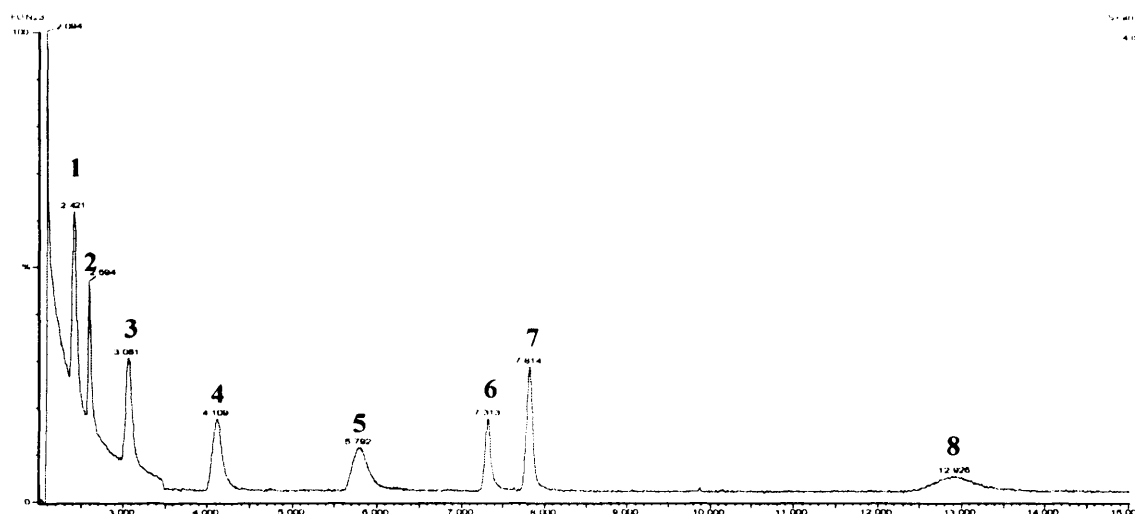


Figure 4.3 Chromatogram for PDMS 100µm fibre blank run

### 4.3.3 Polar Test mix

Eight peaks were detected (Figure 4.4) which represent pentadecane, 1-octanol, hexadecane, octadecane, 2,6-dimethyl phenol, 2,6-dimethyl aniline, eicosane respectively. In general the elution of peaks was in the order stated by the manufacturer (Supelco, Bellefonte, CA). However, when analysed by comparison with the NIST database, peaks 6 and 7 at retention times 7.3 and 7.8 min represented 2,6-dimethylphenol and 2,6-dimethylaniline respectively, which according to the manufacturer notes should have eluted in the opposite order. This discrepancy is due to a different column used by the manufacturer. There was no apparent peak tailing or reduction in peaks to indicate sub-optimal machine function.

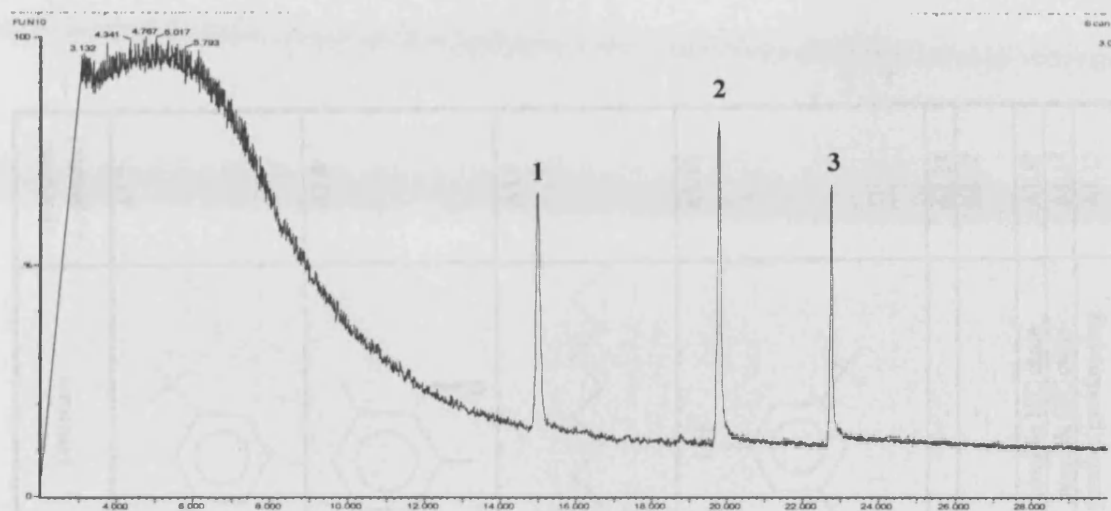




**Figure 4.4** Chromatogram of Polar test mix. Peaks represent: (1) pentadecane; (2) 1-octanol; (3) hexadecane; (4) heptadecane; (5) octadecane; (6) 2,6-dimethyl phenol; (7) 2,6-dimethyl aniline; (8) eicosane.

#### 4.3.4 Terpene Standard Mix

Three peaks were consistently observed in all replicates (Figure 4.5) at average retention times 14.9, 19.8 and 22.7 min which represent the three constituents of the standard mix, (1R) (-) Fenchone (mw=152.24),  $\alpha$  - Humulene (mw=204.35) and (1S) (-) Verbenone (mw=150.22) respectively. Peak areas for each compound were different despite 50 ng of each compound being loaded into the GC-MS. The differences in peak area are due to differences in sensitivity to ionisation between each of the compounds which may affect how much of each is detected and recorded. The ratios of peak areas relative to each other were consistent across replicates (see normalisation, Section 4.3.8). However, peak areas varied between replicates, thus emphasising the need for the use of an external standard for normalisation of the experimental chromatograms, to take into account the different levels of detection when running the machine on any particular day.



**Figure 4.5** Representative chromatogram for terpene test mix. Peaks represent 50 ng of: (1) (R) (-) fenchone; (2)  $\alpha$ -humulene; (3) (1S) (-) verbenone.

#### 4.3.5 Malt broth blank

For the malt broth control blank three peaks were observed at average retention times 12.1, 24.2 and 26.9 min on both Days 1 and 6 (Figure 4.6, Peaks 1-3). An additional peak was detected on Day 6 at retention time 34.6 min (Figure 4.6, Peak 4). By comparison with the NIST v1.2 library and visual inspection of the spectra the compounds were putatively identified for peaks 1-4 as benzene, 1,3-bis(1,1-dimethylethyl), 2,6-dimethylbenzaldehyde, 3-dodecene, and phenol 3,5-bis(1,1-dimethylethyl) respectively (Table 4.2). The database produced a number of matches with good forward and reverse scores and visual inspection of spectra found these to be the closest matches. However, to confirm which stereoisomers they were would require further analysis. For spectra see Appendix A1.3, Figures A1.7-A1.10.

Table 4.2 Summary of peak analysis for all treatments on days 1 and 6

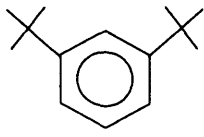
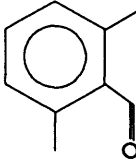

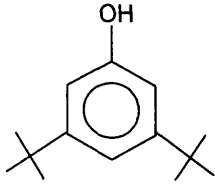
Peak	RT	Code	Day1					Day6					Putative identity	Formula	mw	Structure	Spectrum Appendix1			
			Malt	Tv	Sg	TvTv	SgSg	TvSg	Malt	Tv	Sg	TvTv						SgSg	TvSg	
1	12.1	P	•	•	•	•	•	•	•	•	•	•	•	•	•	1-3-bis(1,1-dimethylethyl) benzene  (possibly mixed peak when detected in TvSg)	C <sub>14</sub> H <sub>22</sub>  (204)	190		A1.7
2	24.2	P	•	•	•	•	•	•	•	•	•	•	•	•	•	2,6-dimethylbenzaldehyde	C <sub>9</sub> H <sub>10</sub> O	134		A1.8
3	26.9	P	•	•	•	•	•	•	•	•	•	•	•	•	•	3-dodecene	C <sub>12</sub> H <sub>24</sub>	168		A1.9
4	34.6	P		•	•	•	•	•	•	•				•		phenol 3,5-bis(1,1-dimethylethyl)	C <sub>14</sub> H <sub>22</sub> O	206		A1.10
5	24.7			•	•	•	•	•								?	-	-	-	A1.11
6	27.7	Art					•									?	-	max m/z = 174	-	A1.12
7	28.6			•	•	•	•	•								?	-	-	possible H/C chain	A1.13
8	29.1			•	•	•	•	•								?	-	-	possible H/C chain	A1.14
9	38.7	Art					•									?	-	max m/z = 148	possible pyridine ring	A1.15

Table 4.2 (continued) Summary of peak analysis for all treatments on days 1 and 6

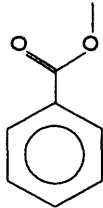
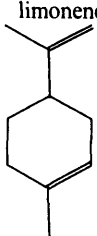
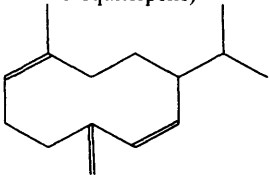
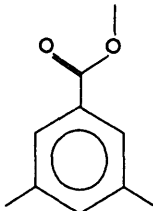
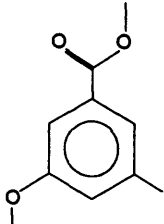
Peak	RT	Code	Day1					Day6					Putative identity	Formula	mw	Structure	Spectrum Appendix1				
			Malt	Tv	Sg	TvTv	SgSg	TvSg	Malt	Tv	Sg	TvTv						SgSg	TvSg		
10	13.1	I														•	?	-	max m/z = 204	possible benzene ring	A1.16
11	13.6	I														•	sesquiterpene	C <sub>15</sub> H <sub>24</sub>	204	possibly similar to α-4-dimethyl-3-cyclohexene acetaldehyde	A1.17
12	14.9	I														•	sesquiterpene	C <sub>15</sub> H <sub>24</sub>	204	Germacrene D or similar bicyclic sesquiterpene	A1.18
13	16.6	Sg														•	benzoic acid methyl ester (syn. Clorius)	C <sub>8</sub> H <sub>8</sub> O <sub>2</sub>	136		A1.19
14	17.1	I														•	?	-	-	possible benzene ring	A1.20
15	21.9	I														•	sesquiterpene	C <sub>15</sub> H <sub>24</sub>	204	possible monoterpene basic structure best match was to limonene 	A1.21 A1.22
16	20.4	I														•	sesquiterpene	C <sub>15</sub> H <sub>24</sub>	204	Germacrene (or similar bicyclic sesquiterpene) 	A1.23 A1.24 A1.25
17	21.9	I														•	?	-	-	possible benzene ring	A1.26

Table 4.2 (continued) Summary of peak analysis for all treatments on days 1 and 6

Peak	RT	Code	Day1					Day6					Putative identity	Formula	mw	Structure	Spectrum Appendix I	
			Malt	Tv	Sg	TvTv	SgSg	TvSg	Malt	Tv	Sg	TvTv						SgSg
18	26.465	Sg																A1.27
19	29.214	I															possible benzene ring	A1.28
20	30.087	I															possibly similar to 2,5, cyclo p-benzoquinone	A1.29 A1.30
21	31.6	Sg																A1.31

RT = retention time

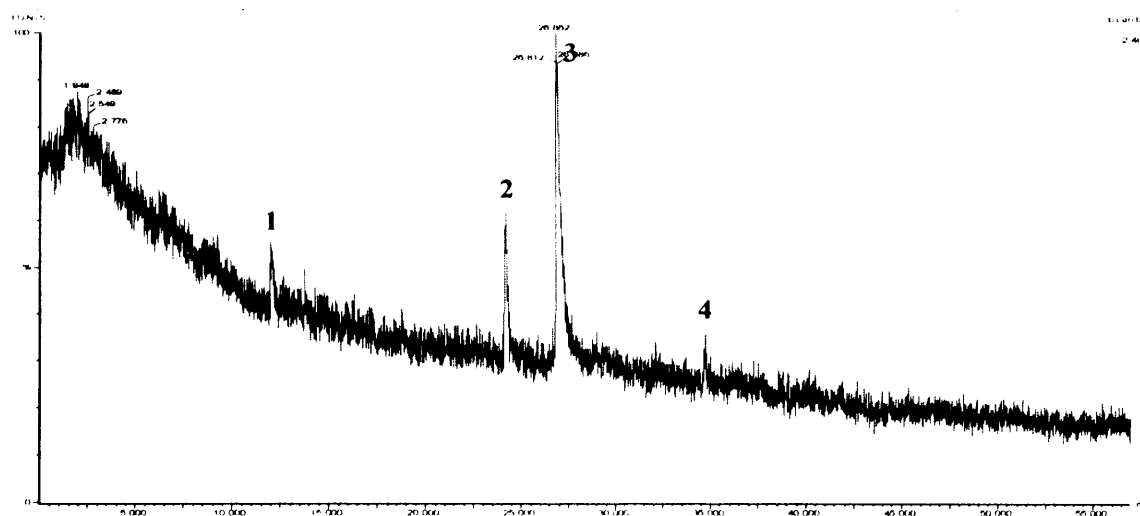
P = plasticiser volatile produced by Reacsyn vessel

Art = artefact

I = volatiles produced during an interspecific interaction

Sg = volatiles produced when *S. gausapatum* present

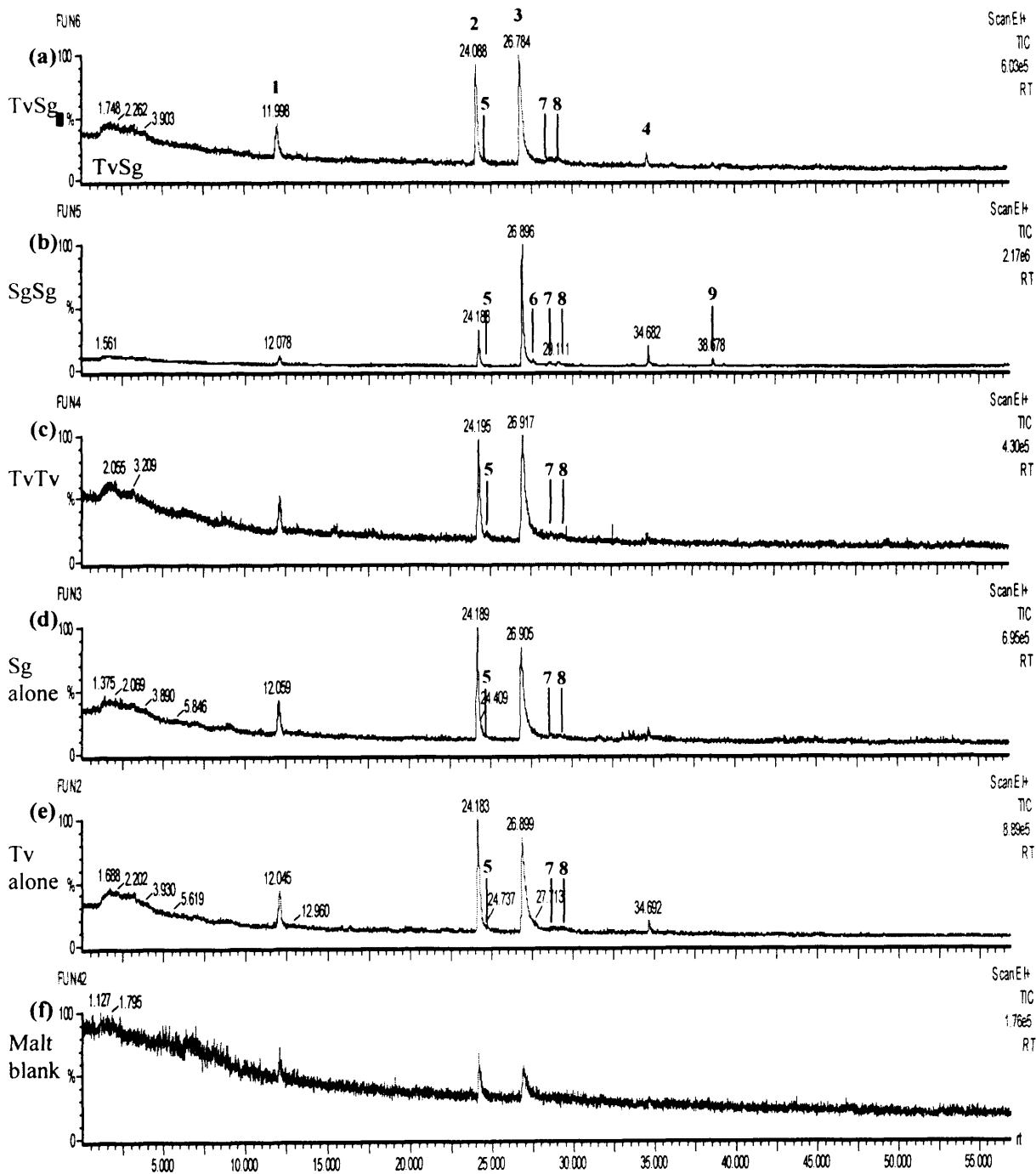
● = presence of peak in a treatment



**Figure 4.6** Representative chromatogram for malt bottle blank day 6. Peaks probably represent: (1) 1,3-bis(1,1-dimethylethyl)benzene; (2) 2,6-dimethylbenzaldehyde; (3) 3-dodecene; (4) 2,4-bis(1,1,dimethylethyl)phenol.

#### 4.3.6 VOCs produced during mycelial interactions – Day 1

Four peaks were observed consistently at average retention times 12.1, 24.2, 26.9, 34.7 min (Peaks 1-4) for all treatments (Figure 4.7a-f). Comparison of retention times and spectra with library databases together with visual inspection of spectra confirmed that these were homologous peaks to those detected in the malt broth blanks and represent the same compounds 1,3-bis(1,1-dimethylethyl)benzene, 2,6-dimethylbenzaldehyde, 3-dodecene, 2,4-bis(1,1,dimethylethyl)phenol respectively. There were five very small additional peaks detected on Day 1. Peak 5 at retention time 24.7 min appears as a shoulder on Peak 2 and is present in all treatments with the exception of the malt blank. (Appendix A1.2, Figures A1.2-A1.6 for chromatograms). However, identification of the compound was not possible (Appendix A1.3, figure A1.11 for spectrum). Peaks 7 and 8 at retention times 28.6 and 29.1 min respectively were most pronounced in self pairings of *S. gausapatum* (SgSg) (Figure 4.7b) but could be seen in all treatments to some extent, excluding malt blank. Although identification of peaks was not possible, the spectra reveal that the compounds are most likely hydrocarbon chains due to the decreasing slope of fragments (See Appendix A1.3, Figures A1.13, A1.14). Peaks 6 and 9, at retention times 27.5 and 38.7



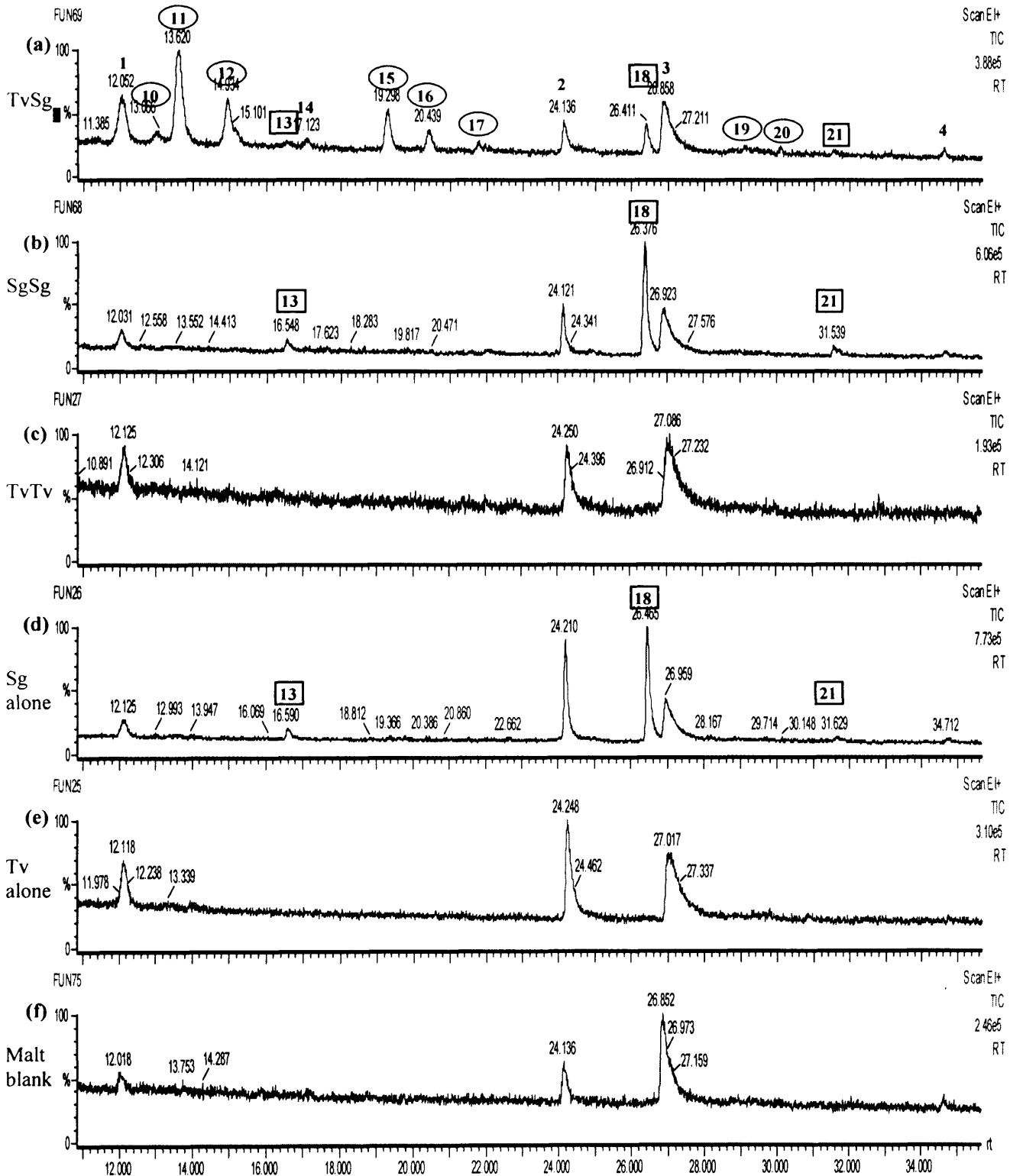
**Figure 4.7** Representative chromatograms for day 1 samples for all treatments: a) TvSg; b) SgSg; c) TvTv, d) Sg alone; e) Tv alone; f) malt blank. Peaks 1-4 are present in each treatment and represent : (1) 1,3-bis(1,1-dimethylethyl) benzene; (2) 2,6-dimethylbenzaldehyde; (3) 3-dodecene; (4) 2,4-bis(1,1-dimethylethyl) phenol. Peaks 5-8 in chromatogram (d) are peaks only present in one replicate and were considered artefacts. Larger chromatograms are in Appendix A1.3 (Figures A1.2-A1.6).

min, respectively, were very small and only present in one replicate of the self pairing of *S. gausapatum* (SgSg) (Figure 4.7b) so were considered artefacts. It is possible that these peaks are genuine but were below the level of detection for the other replicates. Peak 6 had a maximum  $m/z$  of 174 and the closest match from the database was with benzene, 1,3-diisocyanatomethyl ( $mw=174$ ) (See Appendix A1.3, Figure A1.12). Peak 9 had a maximum  $m/z$  of 148 and matches with the database suggest that it may contain a pyridine ring structure (see Appendix A1.3, Figure A1.15).

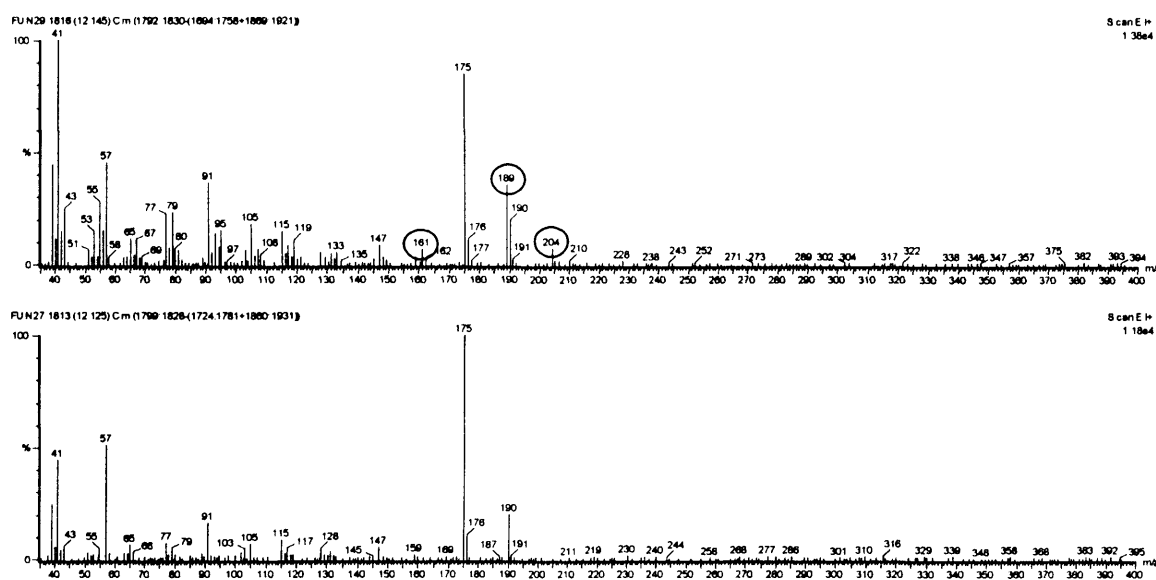
#### 4.3.7 VOCs produced during mycelial interactions - Day 6

A total of 16 peaks were detected in all treatments on Day 6 sampling. Peaks 1-3 had been detected in the malt blank and on Day 1 were present at approximately the same retention times. However, Peak 4, previously found at average retention time 34.7 min was absent from treatments Tv alone and TvTv (Figure 4.8c,e) but found in all other treatments. Analysis confirmed that Peaks 2-4 represented the same compounds as detected in Sections 4.3.5 and 4.3.6. However, analysis of Peak 1 from the interspecific interaction treatment TvSg (Figure 4.8a) produced a spectrum with an  $m/z$  maximum of 204, rather than  $m/z$  max = 190 as in the previous analysis (Section 4.3.5) that identified the compound with  $mw = 190$ . Many of the constituent peaks within appear to match with the spectra for Peak 1 in other treatments but their intensities are different (Figure 4.9) and there are additional peaks at 189 and 204. This discrepancy may indicate a different compound present in the interspecific interaction at the same elution time as the compound from other treatments, thus resulting in overlapping peaks. If this is the case confident identification of the peak is not possible unless the co-eluting compounds can be separated and analysis repeated.





**Figure 4.8** Representative chromatograms for Day 6 samples for all 5 treatments: a) TvSg; b) SgSg; c) TvTv; d) Sg alone; e) Tv alone; f) malt blank. □ Peaks only present in treatments involving *S. gausapatum* (Peaks 13, 18, 21); ○ Peaks only present in the interspecific interaction (TvSg) (Peaks 10, 11, 12, 15, 16, 17, 19, 20).



**Figure 4.9** Mass spectra for Peak 1 from both TvSg (top) and TvTv (bottom) treatments found at retention time 12.1 min. The mass spectrum for TvSg has additional peaks at 161, 189 and 204 and peaks that are shared between spectra are in general greater intensity in TvSg.

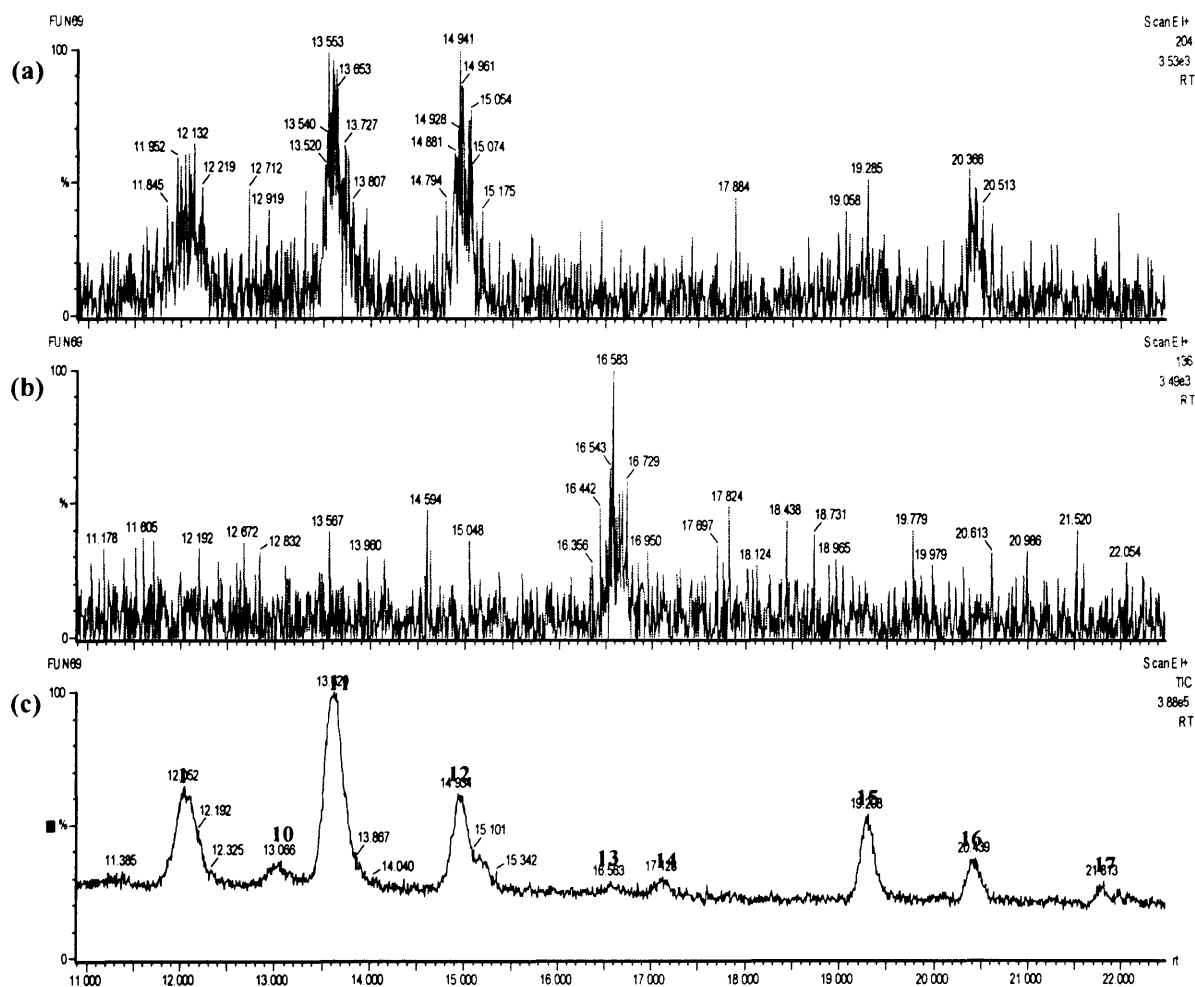
#### 4.3.7.1 *Treatments involving S. gausapatum*

A further three peaks were observed only in treatments involving *S. gausapatum*, i.e. TvSg, SgSg and Sg alone (Figure 4.8a,b,d □): Peaks 13, 18 and 21 were observed at average retention times 16.6, 26.5 and 31.6 min. Analysis putatively identified Peak 13 as benzoic acid, methyl ester, Peak 18 as methyl-3,5-dimethyl benzoate (or an isomer of) and Peak 21 as benzoic acid, 3-methoxy, -methyl ester (or an isomer of) (Table 4.2). See Appendix A1.3 for spectra, Figures A1.19, A1.27 and A1.31.

#### 4.3.7.2 *Interspecific interaction*

The interspecific interaction (TvSg) produced a total of 16 peaks (Figure 4.8a), 9 of which were unique to this treatment (Peaks 10, 11, 12, 14, 15, 16, 17, 19 and 20), i.e. were not found in the single species treatments (Figure 4.8a □). All peaks were observed in all four replicates, with the exception of Peak 17 which was present in only two out of four replicates.

A number of monoterpenes and sesquiterpenes were expected to be produced based on finding from Hynes *et al.* (2007) and others. Sesquiterpenes have  $mw = 204$  and monoterpenes  $mw = 136$ . An initial filter of the interspecific interaction chromatogram for these size fragments showed a number of peaks for  $m/z = 204$  which may indicate the presence of sesquiterpenes between 12 and 20 min (Figure 4.10a). A peak was also present for  $m/z = 136$  at approximately 16 min, indicating a monoterpene compound (Figure 4.10b), which was confirmed by the identification of peak 13 as a monoterpene (Table 4.2). Analysis of individual peaks confirmed these initial hypotheses.



**Figure 4.10** Chromatograms showing the distribution of (a) 204 and (b) 136 fragments and (c) the chromatogram for TvSg Day 6 between the same retention times 11-22 min. Peaks in (a) and (b) indicate where high concentrations of fragments with  $m/z$  ratios of 204 and 136 were detected.

It was not possible to identify Peaks 10 and 11 but they may be sesquiterpenes as peaks at 204 were found in spectra for both peaks (See Appendix A1.3, Figures A1.16 and A1.17). The compound for Peak 10 may have a benzene ring structure within it as the fragmentation pattern of 91, 77, 67, 55 is characteristic of this structure. Although no good matches with the database could be found for Peak 11 the spectrum did match well with that of  $\alpha$ ,4-dimethyl-3-cyclohexene-1-acetaldehyde (mw=137; Appendix A1, Figure A1.17), which may indicate that the compound for Peak 11 has a similar basic structure but is a larger molecule with mw = 204.

Peaks 12 and 16, at retention times 14.9 and 20.4 min respectively, also had an m/z maximum of 204 indicating that they are both sesquiterpenes (Table 4.2). The spectra for both peaks best matched germacrene D from the database (See Appendix A1.3, figure A1.18 and A1.23) and the mass spectra themselves look very similar. Their different elution times but very similar spectra suggests that they could be different enantiomers of germacrene, but this would need to be confirmed by further analysis. Other sesquiterpenes also had very similar spectra such as  $\zeta$ -cadinene and 1H-cyclopenta 1,3-cycloprop-1,2-benzene, octahydro-7-methyl 3-, and these also have very similar structures to germacrene (Appendix A1.3, Figures A1.24 and A1.25). Thus, a definite identification of Peaks 12 and 16 cannot be made but they are likely to be bicyclic sesquiterpenes.

It was not possible to identify Peaks 14 and 17, at average retention times 17.1 and 21.9 min respectively, but the compounds may include benzene ring structures due to the characteristic fragment series 91, 77, 67, 55 (Appendix A1.3, Figures A1.21 and A1.26). Peak 15 had an m/z maximum of 204 (Appendix A1, Figure A1.16) but no good matches were found with the databases. However, mass spectra partly matched those of several monoterpenes (mw = 136) such as D-limonene, 1-methyl-4-(1-methylethenyl)-cyclohexene, 1-methyl-4-(1-methylethenyl) cyclohexanol acetate,  $\alpha$ -myrcene and camphene (Appendix A1.3, Figure A1.22) suggesting that Peak 15 could have a basic structure similar to a monoterpene (Table 4.2).

Peak 19, at retention time 29.2 min, was relatively small and it was difficult to produce high quality spectra. The spectra produced from replicates were consistent with m/z maxima of 108 and major peaks at 94, 91, 79, 77 and 67 (Appendix A1.3,

Figure A1.28) which might indicate an aromatic compound, however, no matches were found in the database. Peak 20, at retention time 30.1 min, was not identified but the closest match within the database was to p-benzoquinone,2,3,5-trimethyl-6-(3-methyl-2-butenyl) (Appendix A1.3, Figures A1.29 and A1.30), with m/z maximum of 218 which may suggest a related compound for Peak 20 (Table 4.2).

#### 4.3.8 Normalisation

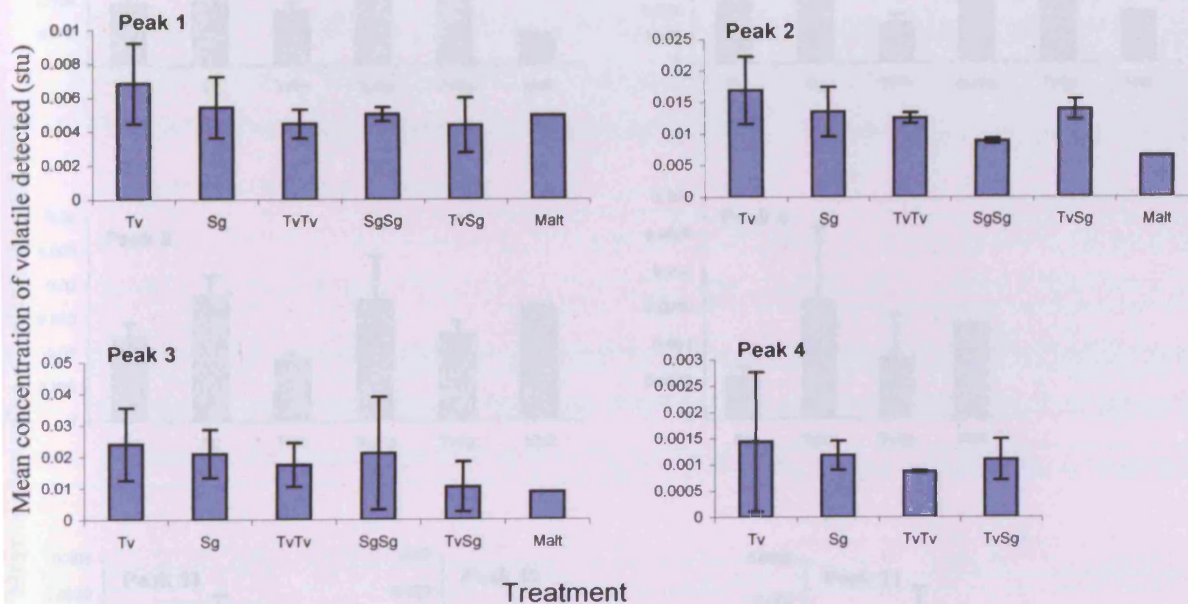
There was no significant difference between the peak ratios between replicates of the terpene standard control mix ( $P > 0.05$ ) and  $H_0$ : no significant difference between peak ratios between replicates, was accepted. Thus, the average peak area was used to normalise chromatograms produced on the same day.

#### 4.3.9 Quantification

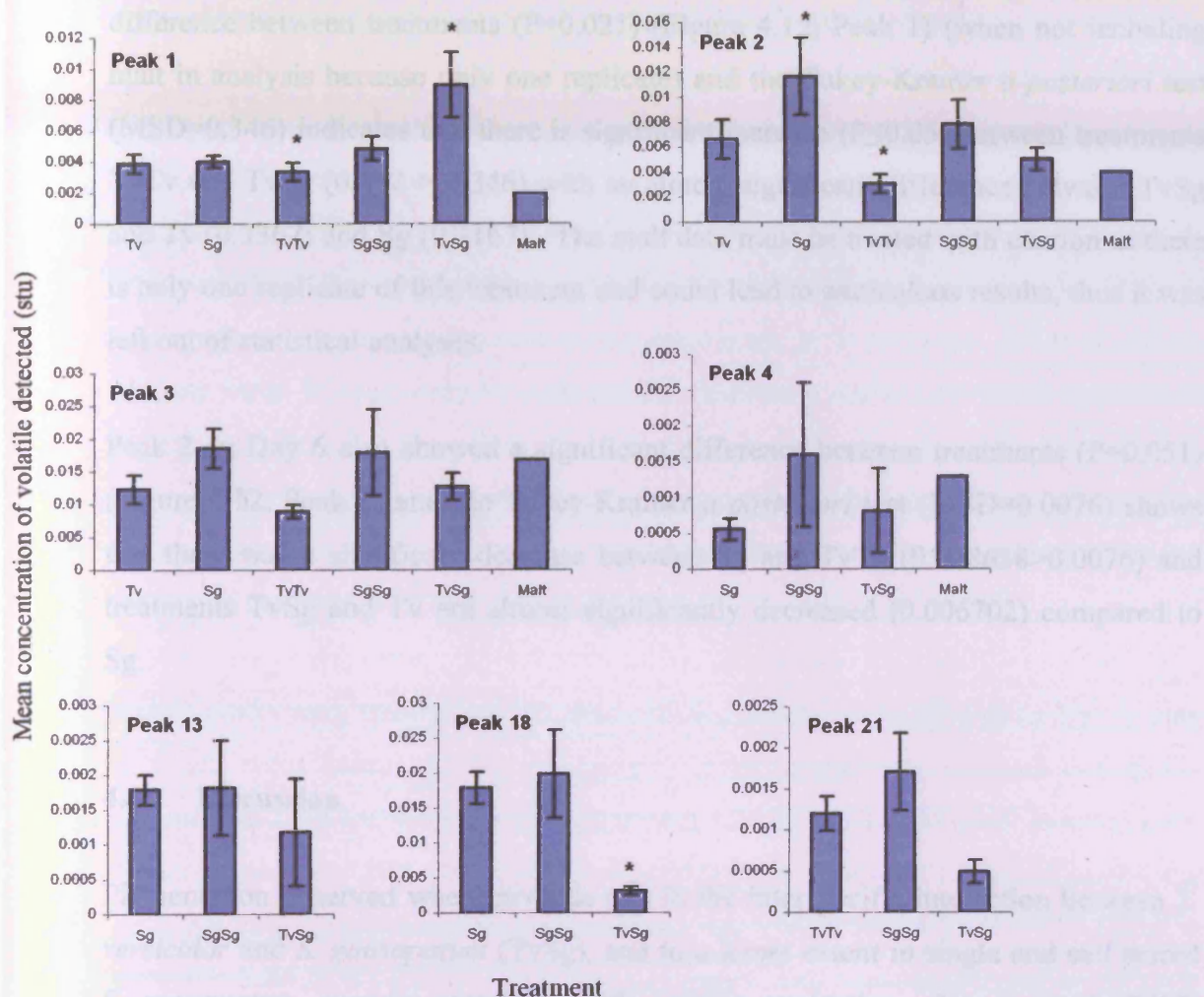
The amount of compound detected for peaks ranged between 0.492 ng (Day 6, TvSg, Peak 21) and 23.99 ng (Day1, Tv, Peak 3) (Figures 4.11 and 4.12).

Peaks 1-4 were present on both days but there was no overall significant difference in concentration between Days 1 and 6 ( $P > 0.05$ ) for any of the treatments (Figure 4.11 and 4.12). Furthermore the production of volatiles was unaffected by colony size. There was no significant difference ( $P > 0.05$ ) in concentration between the corresponding peaks from single inocula and same species pairing treatments i.e. Sg and SgSg ( $P > 0.05$ ).

Peaks 13 and 21, which were only found in treatments involving *S. gausapatum*, showed no significant ( $P > 0.05$ ) difference in concentration between treatments ( $P > 0.05$ ). However, Peak 18 also only found in treatments involving *S. gausapatum* showed a significant ( $P \leq 0.05$ ) decrease in concentration in the interspecific pairing (TvSg) when compared to the single and paired single species (Sg and SgSg) treatments ( $P = 0.001$ ) (Figure 4.12, Peak 18).



**Figure 4.11** Comparison of the amounts of volatiles detected for each peak on Day 1 where peaks were observed in more than one treatment. Treatments are: *T. versicolor* alone (Tv), *S. gausapatum* alone (Sg), *T. versicolor* self paired (TvTv), *S. gausapatum* self paired (SgSg) and *T. versicolor* vs *S. gausapatum* (TvSg). Error bars are  $\pm$  SEM.



**Figure 4.12** Comparison of the amounts of volatiles detected for each peak on Day 6 where peaks were observed in more than one treatment. Treatments are: *T. versicolor* alone (Tv), *S. gausapatum* alone (Sg), *T. versicolor* self paired (TvTv), *S. gausapatum* self paired (SgSg) and *T. versicolor* vs *S. gausapatum* (TvSg). Error bars are ± SEM. Asterisks indicate a significant difference ( $p < 0.05$ ) between the amount of volatile detected for the treatment labelled and other treatments for that peak using one way ANOVA. Multiple asterisks indicate where the significant difference is between only certain treatments if Tukey-Kramer *a posteriori* tests has indicated as such. Log<sub>10</sub> transformation of data was required for Peaks 1 and 18.

For the majority of peaks there was no significant difference in concentration between treatments ( $P > 0.05$ ) on either day. However, Peak 1 on day 6 showed a significant difference between treatments ( $P = 0.021$ ) (Figure 4.12, Peak 1) (when not including malt in analysis because only one replicate) and the Tukey-Kramer *a posteriori* test ( $MSD = 0.346$ ) indicates that there is significant increase ( $P \leq 0.05$ ) between treatments TvTv and TvSg ( $0.402 > 0.346$ ) with an almost significant difference between TvSg and Tv ( $0.3362$ ) and Sg ( $0.3167$ ). The malt data must be treated with caution as there is only one replicate of this treatment and could lead to anomalous results, thus it was left out of statistical analyses.

Peak 2 on Day 6 also showed a significant difference between treatments ( $P = 0.051$ ) (Figure 4.12, Peak 2) and the Tukey-Kramer *a posteriori* test ( $MSD = 0.0076$ ) shows that there was a significant decrease between Sg and TvTv ( $0.008638 > 0.0076$ ) and treatments TvSg and Tv are almost significantly decreased ( $0.006702$ ) compared to Sg.

#### 4.4 Discussion

Pigmentation observed where mycelia met in the interspecific interaction between *T. versicolor* and *S. gausapatum* (TvSg), and to a lesser extent in single and self paired *S. gausapatum*, may be associated with volatile production. Hynes *et al.* (2007) observed pigment production during the interaction between *H. fasciculare* and *Resinicium bicolor*. Two groups of volatile compounds were detected at different times, which coincided with the different timings of pigment production by both of the competitor species involved. Furthermore, Savoie *et al.* (2001) observed mycelial barrages with pigmented zones during interactions of white rot basidiomycetes with *Trichoderma harzianum*, and for some species this was associated with increases in laccase activity. Similarly, *P. radiata* is known to produce pigments and this has been shown to be associated with changes in metabolism (Griffith *et al.*, 1994; Rayner *et al.*, 1994).

The absence of Peaks 6 and 9 in some replicates on Day 1, and the total absence of peaks 5-9 on Day 6 may not have been due to lack of production, but low



concentrations of the volatile compounds present. Despite the relative sensitivity of SPME compared to other headspace sampling techniques some compounds may have dropped below the level of detection resulting in the absence of peaks.

The detection of Peaks 13, 18 and 21 only when *S. gausapatum* was present i.e. grown alone, self paired or paired against *T. versicolor*, suggests that the compounds were a product of constitutive growth and were not produced in response to the interaction. They may be associated with the synthesis of pigments by *S. gausapatum*. Benzoic acid based compounds were detected in culture broth of *Stereum* spp. (Li *et al.*, 2006), together with a sesquiterpene compound, and were shown to have nematicidal properties. Perhaps then these benzoic acid based compounds produced by *S. gausapatum*, despite being produced in normal growth rather than being induced by a defence response, may play a role in the inhibition of invertebrates and other species of fungi in the vicinity of *S. gausapatum*.

Sixteen peaks were detected during the interspecific interaction (TvSg) on Day 6, nine of which were unique to the interaction. Four compounds detected during the interspecific interaction were also putatively identified as aromatic hydrocarbons (Peaks 14, 17, 19, 20). Aromatic hydrocarbons are produced by many plants and fungi and exposure to aromatic hydrocarbons can inhibit fungal growth (Wheatley *et al.*, 1997; Said *et al.*, 2004). Exposure to benzene and benzene-derived compounds can induce mycelial and DNA damage (Zucchi *et al.*, 2005). Therefore, these may have been generated as part of a defence or aggressive response by either fungus.

The five sesquiterpene compounds, detected in the interspecific interaction, between approximately 13 – 20 min retention time, correspond with the study by Hynes *et al.* (2007) which found 19 sesquiterpenes eluting between 12.5 and 21 minutes. The exact identity of the sesquiterpenes could not be determined. Where there were close matches with the library databases better identification could be made by comparisons with standards consisting of homologous series of isomers and compounds similar to the putative identity of the compound of interest. Compounds which were only identified as possible sesquiterpenes and did not yield any close matches with the databases could possibly be compounds unique to these species and this interaction and thus not described previously. Several studies have discovered new

sesquiterpenes, produced by fungi, not previously described in other species (Reina *et al.*, 2004; Yoo *et al.*, 2006).

Sesquiterpenes are well known to be produced by plants (Knudsen *et al.*, 1993; Hakola *et al.*, 2005; Baldwin *et al.*, 2006; Kaiser, 2006) and fungi (Nilsson *et al.*, 1996; Stahl, 1996) and are used by invertebrates for communication (Sonenshine, 1985), to locate plant or animal hosts (Belmain *et al.*, 2002), and by plants and fungi to attract insects for propagule dispersal (Fäldt *et al.*, 1999; Schiestl *et al.*, 2006). Plants also produce sesquiterpenes as antifeedants (Kahlos *et al.*, 1994; Stadler & Sterner, 1998) and in response to pathogens (Mendgen *et al.*, 2006) but they may also be involved in the establishment of mycorrhizal relationships (Akiyama *et al.*, 2005). Similarly, many plants and fungi produce sesquiterpenes with antifungal activity (Abraham, 2001; Roy *et al.*, 2003; Wu *et al.*, 2005). Indeed the production of antifungal sesquiterpenes and other volatile compounds by *Trichoderma* species contributes to its potential for biocontrol applications (Kexiang *et al.*, 2002; Reithner *et al.*, 2005).

Germacrene D was a close match for the compounds corresponding to Peaks 16 and 12 (Table 4.2). This hydrocarbon is a biosynthetic precursor of many other sesquiterpenes (Bülow & König, 2000) and has strong effects on insect behaviour (Røsteliën, *et al.*, 2000; Mozuraitis *et al.*, 2002). Thus, its detection in the context of the interspecific interaction between *T. versicolor* and *S. gausapatum* may be a consequence of the biosynthesis of other sesquiterpenes taking place. Those compounds detected may be Germacrene D or very closely related compounds resulting from its rearrangement to produce new compounds. The presence of Germacrene D may act also as an attractant for invertebrates during interactions, which could influence the progress and outcomes of interactions and could be investigated in the future. Furthermore, the bioactivity of Germacrene and many other compounds is affected by their stereochemistry and optical activity (Maga 1981; Prosser *et al.*, 2004). If the effects of individual compounds on fungal growth and interactions were eventually investigated it would be necessary to determine the chirality of compounds using enantioselective GC-MS.

Many species of fungi are capable of producing sesquiterpene and aromatic hydrocarbon compounds. Within this study it was not possible to attribute the generation of particular compounds during the interaction to either species. The potentially antifungal VOCs detected may be produced by *S. gausapatum* in response to confrontation with *T. versicolor*, which has a greater combative ability and will eventually overgrow it as a defence response. Alternatively, the VOCs may be produced by *T. versicolor*, conferring its superior combative ability by facilitating the replacement of *S. gausapatum* due to the toxic effect. It seems likely however that both are taking place.

The outcomes of interactions can vary depending on the growth substrate (Wald *et al.*, 2004a; Griffith & Rayner, 1994), and the production of volatiles can also vary depending on the nutrient resources available (Wheatley *et al.*, 1997; Bruce *et al.*, 2000; Scotter *et al.*, 2005). The outcome of interactions may in part be determined by the volatiles produced during the interaction. These studies were performed on a limited nutrient medium and perhaps on a more complex growth medium further compounds would have been detected. The same interaction on a wood substrate would be expected to produce more compounds as there are more complex nutrients available for assimilation and conversion, by extracellular enzymes, into volatile compounds, which could then have an effect on the outcome of the interaction. Furthermore, Heilmann-Clausen and Boddy (2005) showed that wood previously colonised by saprotrophic fungi can be inhibitory to later fungi even when the original coloniser is dead. Lignin-derived phenols are inhibitory to *Lentinus* spp. (Shuen & Buswell., 1992), and it is perhaps the derivatives of lignin breakdown, produced during initial colonisation, that cause the inhibition of later growth observed by Heilmann-Clausen and Boddy (2005).

#### 4.4.1 Quantification

The reduction of Peaks 13, 18 and 21, although only significant for Peak 18, during the interspecific interaction (TvSg) may be due to inhibition of production of these compounds by *S. gausapatum* in the presence of *T. versicolor*, or the compounds produced by *S. gausapatum* may have been degraded by *T. versicolor*. Indeed,



exposure of fungi to VOCs has been shown to alter protein synthesis (Myung *et al.*, 2007; Humphris *et al.*, 2002; Wheatley, 2002). Also, many fungi are capable of degrading aromatic hydrocarbons (Kim *et al.*, 1998; Kamada *et al.*, 2002; Qi *et al.*, 2002; Demir, 2004; Prenafeta-Boldú *et al.*, 2006), a property which gives white rot fungi the ability to degrade lignin and has been exploited for bioremediation of chemical waste and contamination (Tortella *et al.*, 2005; McErlean *et al.*, 2006; Ryan *et al.*, 2007). This degradation is often carried out by phenoxidising enzymes such as laccase and peroxidase (Ohkuma *et al.*, 2001; Baldrian, 2004). Perhaps this is what caused the apparent reduction in Peaks 2, 13, 18 and 21 in the presence of *T. versicolor*, a fungus known to have high laccase activity (Baldrian, 2004). Indeed, perhaps a major determinant of the outcomes of interactions is the relative abilities of each fungus to metabolise potentially inhibitory compounds produced by competitors during interactions. Some fungi are self-inhibitory (Bottone *et al.*, 1998) and this may be because they are good at producing inhibitory chemicals but poor at degrading them.

Investigation of the expression of genes, the activity of enzymes involved in the biosynthesis of these compounds, and the enzymes responsible for their degradation during the interaction, could offer insight into the cause of the effects observed. Furthermore, more replicates could provide more accurate quantification and would confirm if this effect is only true for Peak 18 or for all compounds detected.

#### 4.4.2 Plasticiser volatiles

Although the four peaks derived from the Reacsyn™ vessel (Peaks 1-4) cannot provide information about the volatile compounds produced in response to the interaction, they may have had an effect in this study. In general, the levels of plasticiser compound detected were consistent between treatments (Figure 4.12) and sampling days suggesting that ‘breathing’ of the bottles after sampling did not affect the levels of detection. Indeed Hynes *et al.* (2007) used one of these plasticisers as an internal standard for normalisation of their results, however, in this study levels of plasticisers although generally consistent, were too variable to use for quantification.

Superficially, the significant increase of peak 1 in TvSg compared to TvTv (day 6) implies greater production of benzene, 1-3-(1,1-dimethylethyl). However, the analysis of these peaks showed that there were potentially two compounds present with overlapping peaks, detected at the same retention time. Therefore, it is likely that the increased volume detected for this peak is due to the additive effect of two compounds produced in TvSg at the same retention time, rather than increased production of benzene, 1-3-(1,1-dimethylethyl) or increased degradation in the other treatments.

Peaks 2 and 4 were also identified as aromatic hydrocarbons and Peak 3 as a long chain hydrocarbon and as previously discussed these can have effects on the growth of fungi. The significant decrease in Peak 2 between treatments TvTv and Sg on Day 6 may be due to *T. versicolor* being able to degrade this compound, 2,6-dimethyl benzaldehyde, as it appears to be reduced in treatments involving *T. versicolor* when compared with those with *S. gausapatum*. The greater reduction in Peak 2 with TvTv could be due to a larger biomass of *T. versicolor* present in this treatment, which could result in greater degradation of the compound compared to those with a single colony of *T. versicolor*. A similar qualitative effect was observed for Peak 3, and Peak 4 was absent in treatments Tv and TvTv, which could indicate that this compound was reduced below detectable levels through degradation by *T. versicolor*. Although this effect was only statistically significant for Peak 2 it could be interesting to investigate further with more replicates to give more accurate quantification as *T. versicolor* and many other white rot fungi have been shown to be capable of degrading hydrocarbons.

#### 4.4.3 Quantification and normalisation method

The aims of this project were principally to detect if volatiles were produced differentially during the interaction between *T. versicolor* and *S. gausapatum*, as compared to growth alone, and to putatively identify the compounds involved. Although estimates of the quantity of compounds detected were made, they cannot be taken as absolute measures of the amounts of volatiles produced. However, they do provide an indication of changes in relative concentration. The concentration of

volatiles present in a headspace sample does not necessarily equate to how much is adsorbed on to the fibre, desorbed and then detected by the GC-MS, because each compound will have a different affinity for the SPME fibre and susceptibility to fragmentation. Ideally an internal standard would be used, by spiking reactions with a known compound and concentration. However, this was not possible because the addition of a compound to the fungal cultures could affect the interaction and the VOCs produced. Therefore, an external standard (injected into the GC separately) of three terpenes was used in this study for normalisation of data. Although equal concentrations of each of the compounds were loaded, the peaks detected were not equal, which illustrates the point that the properties of different compounds will affect how much is detected. By using the average of three compounds, rather than just one, to normalise takes this variation into account to a certain extent, but for non-terpenoid compounds the approximation is less valid. Therefore, changes in the amount of volatile compounds detected can only really be compared between treatments for the same compound, as the relative amounts of different compounds detected will be subject to bias due to the different properties of each compound.

The use of an external standard for normalisation is designed to account for variation in the detection rate of the machine between sampling days. However, there may also have been variation in the detection rate of the GC-MS throughout the day. The external terpene standard was run at the end of each sampling day and therefore represents the detection rate at the end of the day. Normalisations may have been more accurate if the standard was run at the beginning and end of each day of sampling to record how the detection rate changed during the day and experimental runs could then be normalised on a gradient scale. However, this was not possible due to time and expense. Running the standard at the end of the sampling day, however, provides a more conservative estimate for quantification. It is assumed that if the detection level does change, it will be deterioration during the day due to septum coring and inlet liner contamination following multiple sample injections. The septum is a rubber seal over the injection port. Injection of the SPME fibre cuts small cores from this septum when it is pushed through, which can then contaminate and potentially block the inlet liner.

Several peaks were present in only one (of three) replicate and were recorded as artefacts. These peaks were often small and may have represented compounds genuinely produced by the fungi but at low concentrations. Thus, any reduction in detection sensitivity in replicate runs would result in their absence from chromatograms. If it was desired to investigate these peaks further then more replicates, together with longer fibre exposure time, could be used to sample greater concentrations of the less abundant volatile compounds.

#### 4.4.4 Volatile sampling method

Although the large number of sesquiterpenes detected during the interaction indicates that these are important compounds during interactions it should be noted that the PDMS SPME fibre used is particularly good at detecting these types of molecules; other compounds that play key roles during interactions may not have been detected. In other studies, oxygenated sesquiterpenes and shorter chain aldehydes and ketones have been detected from fungi (Jelen, 2003) and found to have inhibitory effects, but none were detected here. Similarly, 1-octen-3-ol is detected from many species of fungi (Maga, 1981; Kahlos *et al.*, 1994; Chitarra *et al.*, 2005) and has an inhibitory effect on growth and development (Chitarra *et al.*, 2005), but in this study the majority of compounds detected were much larger, which is likely to be due to the method used. The headspace sampling method used, the choice of SPME fibre and the GC program all contribute to determining which compounds are detected. The use of other volatile sampling methods to complement this study of the interaction between *T. versicolor* and *S. gausapatum* would help assemble a more comprehensive profile of the volatiles generated during the interaction. Jelen (2003) compared several methods of volatile sampling and found that simultaneous distillation extraction (SDE) and SPME produced different profiles: mostly oxygenated sesquiterpenes were found with SDE; and different SPME fibres varied in their efficiency and selectivity of the compounds they adsorped. Similarly, Ewen *et al.* (2004) found thermal desorption on Tenax produced the most comprehensive profiles of volatiles from *Serpula lacrymans* and *Coniophora puteana* when compared with SPME. Although in contrast, Demettynare *et al.* (2004) compared extraction methods and found that headspace solvent extraction (HSSE) and SPME produced the same

qualitative patterns from headspace profiles, but the relative contribution of each compound varied.

#### 4.4.5 Experimental platform

The Reacsyn™ vessels were used because they allow headspace sampling of growing fungi and simultaneous removal of growth medium from the base of the vessel. Thus, synchronous analysis of volatile and diffusible compounds produced during the interaction can be performed. In this study a sample of broth was removed at the time of each volatile sampling, but the analysis of these samples was not within the scope of this project. The volatiles produced by the Reacsyn™ vessel were mainly benzene derived compounds and these have been shown to have an inhibitory effect on many fungi (Zucchi *et al.*, 2005). Thus, there is potential for inhibition of growth of the fungi by the compounds derived from the Reacsyn™ vessel. Moreover, the fungi could potentially have used these compounds as substrates for synthesis of the other volatiles detected during the sampling. Ideally in future these experiments could be carried out in glass vessels on agar, if the broth is not intended to be analysed, to prevent any interference. The Reacsyn™ vessels are also designed so that the growing fungus can be transferred between vessels containing different media. It would be interesting to study if the transfer of fungi, growing alone or interacting, to another vessel containing culture medium previously grown on by another species, would induce changes in the volatile profile detected. Similarly, it would also be interesting to see how the volatile profile changes over time with respect to the constituent compounds and their relative concentrations. If compounds are produced in response to mycelial contact during interactions, then perhaps the production of volatiles will cease when one species has completely overgrown the other, and there are no more new contacts being made.

#### 4.4.6 Future work

An important aspect of future work would be to use standards to identify more conclusively the compounds detected during the interaction between *T. versicolor* and



*S. gausapatum*, and study volatile production during the course of the interaction. The influence of individual compounds on fungal growth and interactions, in the absence of physical contact between mycelium, and their effect on invertebrates, would also be interesting points of study. Investigation of the underlying mechanisms of enzyme activity, protein synthesis and gene expression during volatile generation would also give interesting insight into the relationship between the interacting species and how the changes that take place, and the overall outcomes of interactions, are effected.

## 5. Suppression Subtractive Hybridisation (SSH)

### 5.1 Introduction

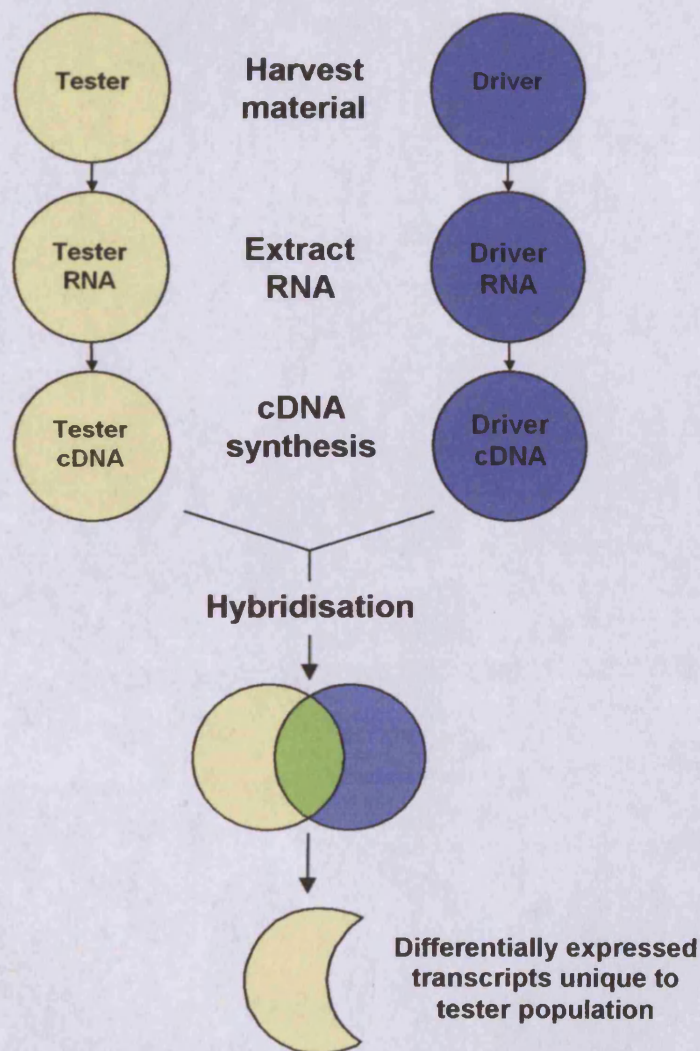
Suppression subtractive hybridisation is a method by which genes expressed in two groups of cells or cells subjected to different treatments, can be compared and those differentially expressed between the two sets isolated. A subtractive cDNA library can then be constructed composed of only differentially expressed genes. This approach has been used in many different fields of biology to identify differentially expressed transcripts between two sets of cells, from cancer research (Liu *et al.*, 2007) to ecology (Morales & Thurston, 2003), and can be used alone for gene discovery or to complement DNA microarrays (Cao *et al.*, 2004).

The SSH method has the advantage over some similar techniques of requiring less hybridisation steps and requires a relatively small amount of starting material. It also enriches for low and medium abundance transcripts, which can often be underrepresented or missed by other techniques. Both of these features are important in this project as it may be that only very subtle changes in gene expression cause some of the changes seen during interactions between fungi.

To date there have been very few studies applying this technique to fungi, but where it has been used it has mainly been with respect to differences in the developmental stages of fungi (Dogra & Breuil, 2004; Lu *et al.*, 2005), responses to growth on different media (Morales & Thursdton, 2003; Ouziad *et al.*, 2005) or the interaction of a pathogen with its plant host (Beyer *et al.*, 2002; Broeker *et al.*, 2006). There is only one other study using this technique to investigate interspecific interactions of fungi (Carpenter *et al.*, 2005) in which they studied mycoparasitism of *Sclerotinia sclerotiorum* by *Trichoderma hamatum* and used SSH to successfully identify differentially expressed genes.

Briefly, the basis of suppression subtractive hybridisation is that two populations of cells are isolated and RNA extracted. These may be different types of cells or the same type of cell harvested at different timepoints, developmental stage or subjected

to different treatments. The reference population is known as the driver or control population, while the treated or different population is the tester. cDNA is synthesised from mRNA for each of the two populations separately then hybridisation of the two populations is performed. Those transcripts that are common to both tester and driver, i.e. not differentially expressed, will hybridise and can then effectively be removed from the population. The end result is a set of differentially expressed transcripts which are amplified and can then be cloned. Figure 5.1 summarises this process in a Venn diagram, it is the yellow section of the populations which are of interest.



**Figure 5.1** Simplified summary of Suppression subtractive hybridisation (SSH).

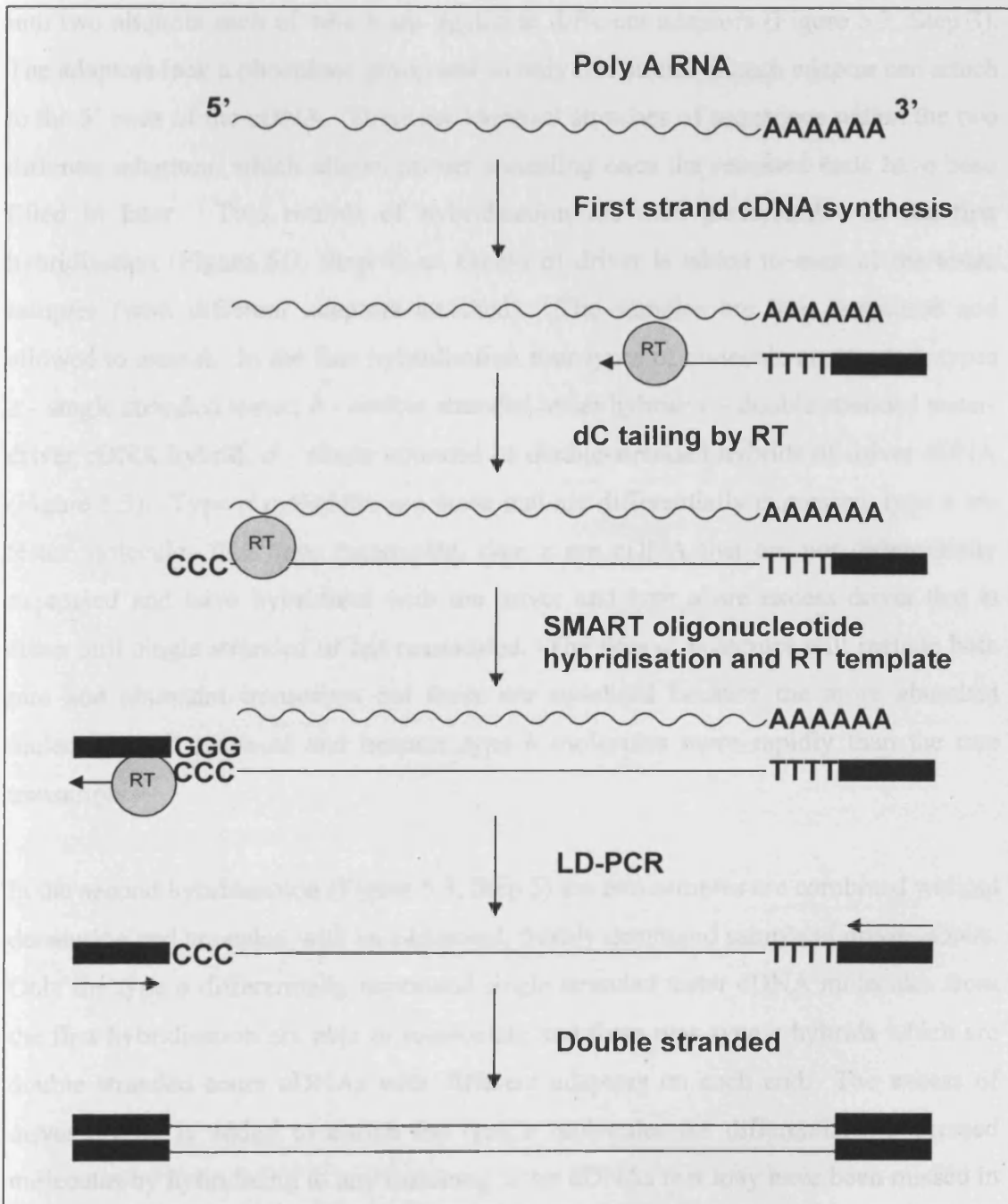
For this study the Clontech PCR-Select cDNA subtraction kit was used to perform SSH which is based on the method by Diatchenko *et al.* (1996). A minimum of 2 µg total RNA is required as starting material for the Clontech PCR-select cDNA subtraction. Extractions did not produce sufficient material, therefore Clontech SMART cDNA synthesis was used to synthesise cDNA for the subtraction, using a relatively small amount of starting material available. This method produces a large amount of cDNA and enriches for full-length cDNAs. Conventional cDNA synthesis uses reverse transcriptase (RT) to produce ss cDNA from mRNA templates. However, conventional cDNA synthesis can leave the 5' ends of mRNAs underrepresented because the RT is not always able to transcribe the entire sequence.

### 5.1.1 SMART cDNA synthesis

SMART™ (Switching Mechanism at 5' End of RNA Template) cDNA synthesis (Figure 5.2) uses the properties of the Moloney Murine Leukemia Virus Reverse Transcriptase (MMLV RT) to create full length cDNA which can then be exponentially amplified. The MMLV RT has the property that it adds 3 to 5 deoxycytidine nucleotides to the 3' end of the first strand cDNA when the 5' end of the mRNA template is reached, and also that it is capable of switching between templates and continuing transcription.

Firstly a modified oligo(dT) primer is used in the first strand synthesis. The RT synthesises the first strand in the 3' to 5' direction and when it reaches the 5' end the enzyme adds a few additional nucleotides to the 3' end, particularly deoxycytidine. This dC tag at the end of the first strand is then paired with the SMART oligonucleotide, which has an oligo(G) sequence at the 3' end. This creates a longer template, which the RT continues to transcribe (Chenchik *et al.*, 1998) to the end of the oligonucleotide by switching strands. Thus, a full length single stranded cDNA of the mRNA template is created, which has a complementary sequence to the SMART oligonucleotide at the 3' end, and sequences complementary to the oligo A sequence at the 5' end. These known sequences, incorporated at both ends of the ss cDNA, act as priming sites for amplification of the full length cDNA by long distance PCR (LD-PCR). If for some reason the RT is unable to transcribe efficiently the whole length

of the mRNA, then the addition of the deoxycytidine nucleotides at the end is also less efficient, and prevents the binding of the SMART oligo(dG). The result is that the short cDNAs will lack the priming sites at both ends, which will prevent their exponential amplification, along with any other contaminating genomic DNA or non-poly A RNA.



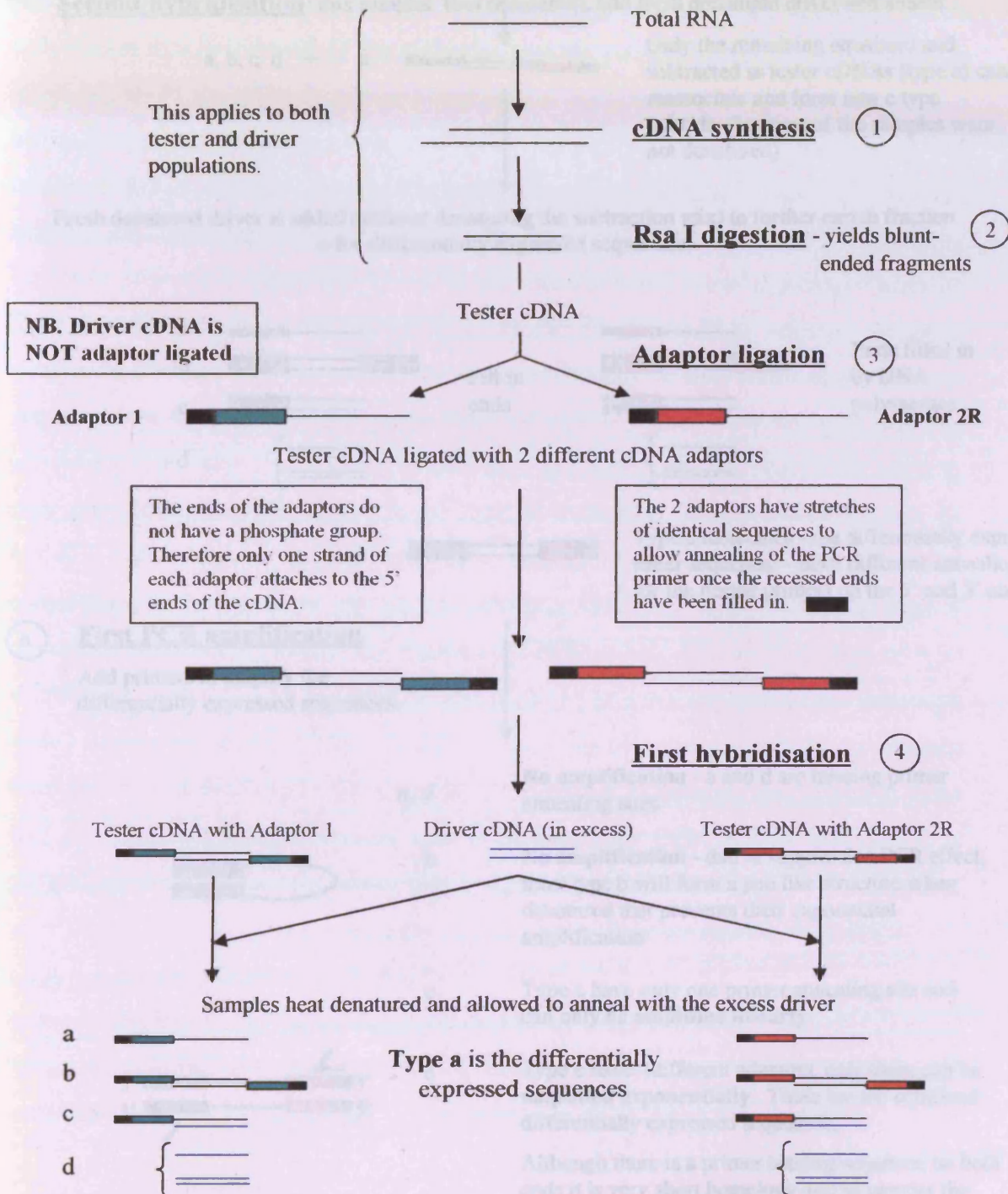
**Figure 5.2** The basis of SMART™ cDNA synthesis. RT = MMLV Reverse transcriptase; PolyA = poly adenylated; dC = deoxycytidine; SMART = Switching mechanisms at 5' end of RNA template; LD-PCR = long distance-PCR.

### 5.1.2 PCR-select cDNA subtraction

Once enough starting material from the SMART<sup>TM</sup> cDNA synthesis has been obtained then SSH can be performed (Figure 5.3, Step 1). Firstly the two populations of cDNA are digested with *RsaI* a restriction enzyme, which has a 4 bp recognition site and produces blunt ended fragments (Figure 5.3, Step 2). The tester cDNA is then divided into two aliquots each of which are ligated to different adaptors (Figure 5.3, Step 3). The adaptors lack a phosphate group and so only one strand of each adaptor can attach to the 5' ends of the cDNA. There are identical stretches of sequences within the two different adaptors, which allows primer annealing once the recessed ends have been filled in later. Two rounds of hybridisation are then performed. In the first hybridisation (Figure 5.3, Step 4) an excess of driver is added to each of the tester samples (with different adaptors attached). The samples are heat denatured and allowed to anneal. In the first hybridisation four types of molecule are created: types *a* - single stranded tester; *b* - double stranded tester hybrid; *c* - double stranded tester-driver cDNA hybrid; *d* - single stranded or double-stranded hybrids of driver cDNA (Figure 5.3). Type *a* molecules are those that are differentially expressed, type *b* are tester molecules that have reannealed, type *c* are cDNA that are not differentially expressed and have hybridised with the driver and type *d* are excess driver that is either still single stranded or has reannealed. The type *a* molecules will include both rare and abundant transcripts but these are equalised because the more abundant molecules will reanneal and become type *b* molecules more rapidly than the rare transcripts.

In the second hybridisation (Figure 5.3, Step 5) the two samples are combined without denaturing and annealed with an additional, freshly denatured sample of driver cDNA. Only the type *a* differentially expressed single stranded tester cDNA molecules from the first hybridisation are able to reassociate and form new type *e* hybrids which are double stranded tester cDNAs with different adaptors on each end. The excess of driver cDNA is added to enrich the type *e* molecules for differentially expressed molecules by hybridising to any matching tester cDNAs that may have been missed in the first hybridisation.

Figure 5.3 Molecular basis of PCR-Select cDNA subtraction



The concentration of high and low abundance sequences is equalised among the type a molecules because reannealing is faster for the more abundant molecules due to the second order kinetics of hybridisation.

At the same time the ss type a molecules are significantly enriched for differentially expressed sequences, as cDNAs that are not differentially expressed form type c molecules with the driver.

Figure 5.3 (continued) Molecular basis of PCR-Select cDNA subtraction

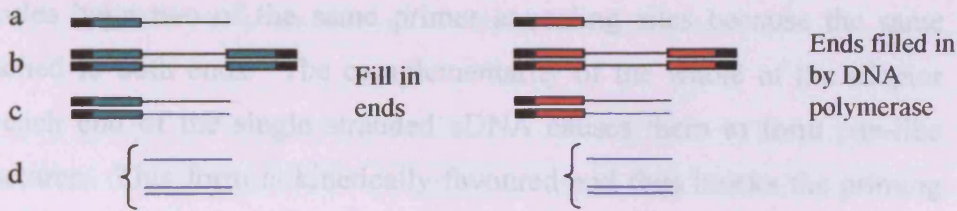
5

**Second hybridisation:** mix samples (not denatured), add fresh denatured driver and anneal.

a, b, c, d + e

Only the remaining equalised and subtracted ss tester cDNAs (type a) can reassociate and form new e type hybrids (because of the samples were not denatured)

Fresh denatured driver is added (without denaturing the subtraction mix) to further enrich fraction e for differentially expressed sequences.



e Type e molecules - the differentially expressed tester sequences - have different annealing sites for the nested primers on the 5' and 3' ends.

6

**First PCR amplification**

Add primers to amplify the differentially expressed sequences.

a, d

No amplification - a and d are missing primer annealing sites.

b

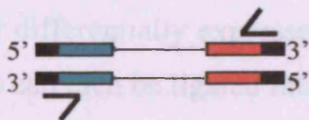
No amplification - due to suppression PCR effect, most type b will form a pan like structure when denatured that prevents their exponential amplification

c

Type c have only one primer annealing site and can only be amplified linearly

e

Type e have 2 different adaptors, only these can be amplified exponentially. These are the equalised differentially expressed sequences.



Although there is a primer binding sequence on both ends it is very short homology and so negates the PCR suppression effect.

7

**Secondary PCR amplification** performed using nested primers to further reduce any background PCR products and to enrich for differentially expressed sequences.

8

cDNAs inserted into cloning vector



Once the hybridisations have been carried out suppression PCR (Figure 5.3, Step 6) is used preferentially to amplify those fragments with both adapters attached. DNA polymerase fills in the ends of the molecules and the entire population of molecules is subjected to PCR with one primer matching the ends of both adaptors. The type *e* molecules have different priming sites within the two different adaptors on each end of the molecule and will be amplified exponentially. This round of PCR will not amplify all fragments. Type *d* have no primer annealing sites. Type *a* and *c* only have one primer annealing site so will be amplified linearly rather than exponentially. Type *b* molecules have two of the same primer annealing sites because the same adaptor is attached to both ends. The complementarity of the whole of the adaptor sequences on each end of the single stranded cDNA causes them to form pan-like secondary structures. This form is kinetically favoured and thus blocks the priming sites preventing amplification. Some type *b* molecules will however be able to amplify with the one primer but the resulting molecules will also carry the complementarity, and form pan-like structures. Thus any amplification of type *b* molecules is minimal. This is the suppression PCR effect. The amplification of type *e* molecules with different adaptors at both ends can proceed exponentially. Although there is some homology of the primers on the ends of both adaptors it is relatively short (not the whole length of the adaptor as in type *b* molecules) and although there will be some suppression due to this it is relatively little, unless the cDNA is particularly short. This only serves then to enrich for the longer fragments which tend to be less efficiently hybridised, amplified and cloned than the smaller fragments.

Next a secondary PCR (Figure 5.3, Step 7) is performed with nested primers to enrich further for differentially expressed sequences and reduce background. The end set of transcripts can then be ligated into a T/A cloning vector (Figure 5.3, Step 8).

### 5.1.3 Subtraction verification

Verification and assessment of the efficiency of the subtraction can be achieved by performing forward and reverse subtractions for the tester/driver pair of samples. A forward subtraction (tester minus reference) gives only those genes unique to the

interaction, while a reverse subtraction (reference minus tester) isolates genes that are not produced during interactions. For a forward subtraction, adaptors are ligated to the tester cDNA and the driver has no adaptors (Figure 5.3, Step 3). In the reverse subtraction this must be performed in reverse, with the tester as driver and the driver as tester i.e. driver (reference) minus tester (interacting). If subtractions are performed in both directions, a gene from the forward subtracted SSH library (those already thought to be unique to interactions only) identified by the microarray analysis to be significantly up or down-regulated under different interaction conditions, can be compared with the reverse subtracted library. Genes in the forward subtracted library should not be present in the reverse subtracted library.

After a subtractive library has been constructed it is important to confirm that clones are genuinely differentially expressed, as the SSH process is unlikely to be 100% efficient, and false positives are likely, especially when the cells from which the two RNA populations are being compared are very similar. One of the conventional methods for screening the clones is to use northern blot analysis on randomly selected clones but this can be time consuming and inefficient. In this study the large number of clones in the subtracted library makes a high-throughput screening procedure the most appropriate. The subtractive libraries generated can be coupled with cDNA microarray technology for high-throughput screening to verify the subtraction and allows the simultaneous comparison of the expression profiles of thousands of clones in one experiment. By using RNA from the same type of tester and driver populations i.e. *T. versicolor* grown alone and *T. versicolor* vs *S. gausapatum* to probe an array made with the subtractive library it was possible to verify which clones are differentially expressed and assess the success of the SSH procedure (see Chapter 7).

### 5.1.4 Objectives

The creation of subtractive libraries was part of the approach of this project for discovering genes differentially expressed during the interspecific interaction between *T. versicolor* and *S. gausapatum*. The specific aims of this section were to:

- Isolate genes differentially expressed during the interspecific interaction between *T. versicolor* and *S. gausapatum* by using suppression subtractive hybridisation (SSH) to create subtractive cDNA libraries
- Perform forward and reverse subtractions for the tester/driver pair to determine the efficiency of the subtraction

These were then used to:

- Obtain expressed sequence tags (ESTs) for a portion of clones within both libraries and annotations applied if possible (Chapter 6)
- Use the SSH libraries to create cDNA microarrays to allow high throughput screening of clones with probes derived from *T. versicolor* interacting with three different species (Chapter 7)

## 5.2 Materials and Methods

### 5.2.1 Growth of mycelium for RNA extraction

Material was grown up and harvested for RNA extraction as described in Section 2.2. Mycelium was kept on ice during harvesting then flash frozen in liquid nitrogen and stored at  $-80^{\circ}\text{C}$  until required.

### 5.2.2 RNA extraction

RNA was extracted as described in Section 2.3 using TRIreagent (Sigma-Aldrich, Dorset, UK). The end product was 100  $\mu\text{l}$  extracted RNA which was stored at  $-80^{\circ}\text{C}$ . The product (10  $\mu\text{l}$ ) was analysed for the presence of RNA by gel electrophoresis on a 1 % agarose/EtBr gel as described in Section 2.6.

### 5.2.3 SMART cDNA synthesis

The Clontech PCR-Select<sup>TM</sup> subtraction protocol requires a minimum of 2 $\mu\text{g}$  total RNA be used as starting material for an efficient subtraction. Extraction of RNA from harvested mycelium yielded insufficient RNA, therefore the Clontech SMART cDNA synthesis (Alto palo, US) kit was used to synthesise enough cDNA to carry out the subtraction. This allows synthesis of cDNA with as little as 500ng total RNA as starting material.

#### 5.2.3.1 *First Strand cDNA synthesis*

For both Tester and Driver samples, reagents (Table 5.1) were combined in a sterile 0.5 ml reaction tube.

**Table 5.1** Experimental set up for first strand synthesis for tester and driver samples. Volumes are  $\mu\text{l}$ .

Reagent	Tester	Driver
RNA sample (Driver or Tester) (500 ng)	2	2
3' SMART CDS Primer II A (12 $\mu\text{M}$ )	1	1
SMART II A Oligonucleotide (12 $\mu\text{M}$ )	1	1
dH <sub>2</sub> O	1	1
Total volume	5	5

Tube contents were mixed, centrifuged briefly and incubated at 65°C in a hot-lid thermal cycler for 2 min. Additional reagents (Table 5.2) were then added to each tube at room temperature.

**Table 5.2** Reagents added to tester and driver samples for first strand synthesis.

Reagent	Tester	Driver
5X First-Strand Buffer	2	2
DTT (20 mM)	1	1
dNTP (10 mM)	1	1
BD PowerScript Reverse Transcriptase	1	1

Tubes were vortexed and centrifuged briefly, then incubated at 42°C for 1 hour in an air incubator. Following incubation this first strand reaction product was diluted by adding 40  $\mu\text{l}$  TE buffer (10 mM Tris [pH 7.6], 1 mM EDTA) because total RNA was used as starting material. Tubes were then incubated at 72°C for 7 min and stored at -20°C.

### 5.2.3.2 *cDNA Amplification by LD-PCR*

According to the manufacturers instructions each 100  $\mu\text{l}$  reaction will produce a yield of 1-3  $\mu\text{g}$  ds cDNA after PCR and clean up steps. Two reactions per sample are recommended, along with an extra tube to be used for optimisation of the number of cycles for the samples and conditions used. However, after previous attempts at the SSH protocol it was found that the yield was probably much lower and after the series of later steps and clean-ups insufficient material was left to perform the hybridisations and subtractions. Therefore a total of six reactions were carried out for both tester and driver samples to maximise yield. These reactions were carried out in three sets of

two reactions, however, rather than all simultaneously to prevent wastage of limited reagents in case a particular run was unsuccessful. The six reactions were amalgamated at the end of the procedure. For a set of two reactions, three tubes were set up for both tester and driver samples and labelled  $T_A$   $T_B$   $T_X$  and  $D_A$   $D_B$   $D_X$ .  $T_X$  and  $D_X$  were additional tubes to be used for the LD-PCR optimisation while tubes A and B were replicate reactions.

Approximately 0.5  $\mu$ g Total RNA was used as starting material for the first strand synthesis for both tester and driver samples. Diluted ss cDNA (2  $\mu$ l) from the previous step (section 5.2.3.1) was used as template for the LD-PCR reactions made up to 10  $\mu$ l with sterile dH<sub>2</sub>O. A master mix was prepared as follows per reaction: dH<sub>2</sub>O, 74  $\mu$ l; 10X Advantage 2 PCR Buffer, 10  $\mu$ l; 50X dNTPs (10 mM of each dNTP), 2  $\mu$ l; 5' PCR Primer II A, 2  $\mu$ l; 50X BD Advantage 2 Polymerase mix, 0.5  $\mu$ l. 90  $\mu$ l of master mix was aliquotted into each reaction tube and was followed immediately by thermal cycling according to the following programme: 95°C 1 min; [95°C 5s, 65°C 5s, 68°C 6min]  $\times$  cycles; 4°C  $\infty$  in a PE2700 PCR machine (Applied Biosystems, CA, USA).

**Optimisation of LD-PCR.** The LD-PCR reaction was optimised to ensure the double stranded cDNA remained in the exponential stage of amplification. Undercycled cDNA gives a poor yield and overcycled cDNA is poor template for the subtraction reaction. All tubes were initially subjected to 15 cycles of the above programme. Tubes  $T_A$   $T_B$  and  $D_A$   $D_B$  were removed from the thermal cycler and stored temporarily at 4°C. Aliquots (5  $\mu$ l) were removed from tubes  $T_X$  and  $D_X$  and stored at 4°C. Tubes  $T_X$  and  $D_X$  were then returned to the thermal cycler and subjected to further cycles with 5  $\mu$ l aliquots being removed from each tube after each subsequent 3 cycles up to 33 cycles in total. Aliquots were analysed by gel electrophoresis on a 1.2% agarose/EtBr. The optimum number of cycles for LD-PCR is one less than is required for a plateau to be reached. For both tester and driver the optimum number of cycles was determined (see Section 5.3.1) and then tubes  $T_A$ ,  $T_B$ ,  $D_A$  and  $D_B$  were returned to the thermal cycler and subjected to enough further cycles to bring them up to their optima.

### 5.2.3.3 *Purification of LD-PCR reactions*

LD-PCR products were purified to remove unincorporated nucleotides and enzymes. The PCR-Select™ protocol recommends the use of Clontech chromatography columns. However, this purification method was inefficient and resulted in a large loss of product. QIAquick PCR Purification columns (Qiagen, Crawley, UK) were used as a substitute for the purification. These purification columns are as much as 80% efficient in returning product.

Replicates of tester and driver PCR reactions were amalgamated then purification carried out (section 2.4). cDNA was eluted in 30 µl Buffer EB. Purified cDNA was stored at -20°C until required.

### 5.2.4 *RsaI Digestion and purification*

Digestion with *RsaI* generates shorter blunt-ended ds cDNA fragments, which are necessary for both adaptor ligation and for the later subtraction. The eluted volume of purified cDNA (from Section 5.2.3.3) was 35 µl. If the chromatography columns had been used the end eluate would have been 360 µl in TNE buffer (10mM Tris-HCl, 10 mM NaCl, 0.1 mM EDTA). For simplicity, the eluted volumes were made up to 360 µl with Buffer EB (10 mM Tris-HCl pH 8.5) from the QIAquick kit, so that the volumes in later steps in the protocol would not have to be adjusted to accommodate this change in clean-up procedure.

36 µl 10X *RsaI* restriction buffer and 1.5 µl *RsaI* were added to both tester and driver reactions and incubated at 37°C for 3 hours in an air incubator.

*RsaI* digested reactions were purified to remove enzymes using QIAquick PCR purification columns (Qiagen) as previously described (Section 2.4).

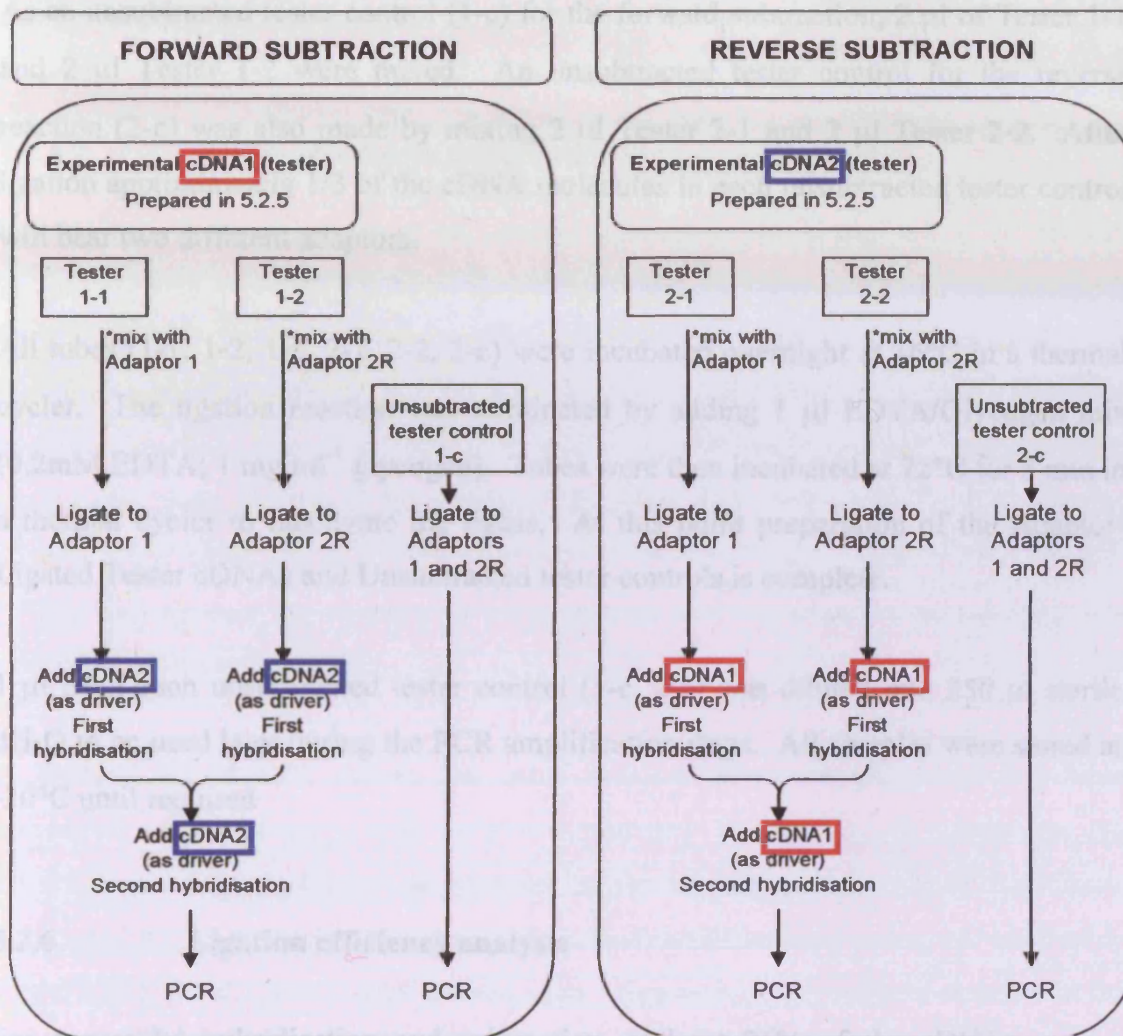
### 5.2.5 Adaptor ligation

For adaptor ligation the tester population was split into two and each subset was ligated with a different cDNA adaptor (Adaptor 1 or Adaptor 2R) (Figure 5.4). The driver population, however, has no adaptors. The adaptors have been designed to lack a phosphate group. Consequently, only one strand of each adaptor will attach to the 5' ends of the cDNA. Adaptors 1 and 2R are different overall but have homologous regions, which allow the PCR primer to anneal once the recessed ends have been filled in (Figure 5.3). Forward and reverse subtractions were both performed (Figure 5.4). For each direction of subtraction, the tester cDNA was subdivided and half ligated with Adaptor 1 (forward 1-1, reverse 2-1) and the other with Adaptor 2R (forward 2-1, reverse 2-2). In the reverse subtraction the roles of the cDNA populations are reversed, driver becomes tester and tester become driver. To avoid confusion, cDNA populations were renamed: Tester = cDNA 1; Driver = cDNA 2.

#### 5.2.5.1 Adaptor ligation method

*Rsa*I digested experimental cDNA (1  $\mu$ l) was diluted with 5  $\mu$ l sterile dH<sub>2</sub>O. A ligation master mix was prepared as follows per reaction: 3  $\mu$ l sterile dH<sub>2</sub>O, 2  $\mu$ l 5X ligation buffer, 1  $\mu$ l T4 DNA Ligase (400 units  $\mu$ l<sup>-1</sup>) (Clontech, Palo Alto, USA). Reagents were combined as follows (Table 4.2) for the adaptor ligation reaction mixtures.





**Figure 5.4** Summary of the preparation of adaptor-ligated tester cDNAs for hybridisation and PCR, for forward and reverse subtractions. cDNA populations are renamed to avoid confusion when the roles are reversed in the reverse subtraction: Tester cDNA = cDNA1; Driver cDNA = cDNA2.

**Table 5.3** Adaptor Ligation experimental set up. Four reactions were set up in 0.5 ml PCR tubes. All volumes are  $\mu$ l.

Subtraction	Forward		Reverse	
Tester labels (Figure 5.4)	1-1	1-2	2-1	2-2
Diluted cDNA 1	2	2	-	-
Diluted cDNA 2	-	-	2	2
Adaptor 1 (10 $\mu$ M)	2	-	2	-
Adaptor 2 (10 $\mu$ M)	-	2	-	2
Master mix	6	6	6	6
Total	10	10	10	10

As an unsubtracted tester control (1-c) for the forward subtraction, 2  $\mu$ l of Tester 1-1 and 2  $\mu$ l Tester 1-2 were mixed. An unsubtracted tester control for the reverse reaction (2-c) was also made by mixing 2  $\mu$ l Tester 2-1 and 2  $\mu$ l Tester 2-2. After ligation approximately 1/3 of the cDNA molecules in each unsubtracted tester control will bear two different adaptors.

All tubes (1-1, 1-2, 1-c, 2-1, 2-2, 2-c) were incubated overnight at 16°C in a thermal cycler. The ligation reaction was terminated by adding 1  $\mu$ l EDTA/Glycogen mix (0.2mM EDTA; 1 mg ml<sup>-1</sup> glycogen). Tubes were then incubated at 72°C for 5 min in a thermal cycler to inactivate the ligase. At this point preparation of the Adaptor-Ligated Tester cDNAs and Unsubtracted tester controls is complete.

1  $\mu$ l from each unsubtracted tester control (1-c, 2-c) was diluted into 250  $\mu$ l sterile dH<sub>2</sub>O to be used later during the PCR amplification steps. All samples were stored at -20°C until required

### 5.2.6 Ligation efficiency analysis

For successful hybridisation and subtraction, at least 25% of the cDNAs require adaptors at both ends. PCR on the adaptor-ligated tester controls was used to verify this by amplifying fragments that span the adaptor/cDNA junction (cross-junction, XJ) and comparing it to the amplification of internal cDNA fragments (internal, INT) using primers for constitutively expressed gene as a reference. By using only one of these internal primers together with a primer corresponding to the common primer site on both Adaptors 1 and 2R, it is possible to compare the relative amounts of product from each reaction. Only those cDNAs with the Adaptor attached will be amplified, and therefore the intensity of the bands from the PCR with cross-junction primers should give an estimate of the percentage of cDNAs with Adaptors attached, when compared to the reference product when both internal primers are used.

The internal primers provided with the Clontech PCR-Select kit are G3PDH primers that are designed to work with human, rat and mouse models. However, as fungi are

being studied it was necessary to design more suitable primers for this purpose (5.2.6.1).

#### 5.2.6.1 *Design of primers to a constitutively expressed gene*

For analysis of the efficiency of the adaptor ligation reactions and to test the success of subtractions, a pair of primers was designed to amplify a sequence present in all mycelium and constitutively expressed. The sequences/partial sequences for the invariant  $\beta$ -tubulin gene of several basidiomycetes (*Trametes versicolor*, *Coprinus cinerea*, *Paxillus involutus*, *Pleurotus sajor-caju*, *Melampsora lini*, *Microbotryum violaceum*) were found on the GenBank database and their amino acid sequences aligned using ClustalW in Bioedit Sequence Alignment Editor Version 7.0.5.3 (Hall, 1999). Sequences from several species were used so that primers could subsequently also be used in related fungi.

A forward and reverse primer pair were designed from the alignment that were conserved across all genes with as little degeneracy as possible. *T. versicolor*, the fungus under investigation, was included in the alignment, thus where there were occasional differences between the sequences of the different species, the nucleotide found in the *T. versicolor* sequence was used. This yielded the sequences required for the forward and reverse tubulin primers. No degeneracy was introduced in the final primer designs to avoid any reduction in primer efficiency.

Primers were analysed for hairpins and dimerisation using Oligo Analyser 3.0 software ([www.bioinformatics.com](http://www.bioinformatics.com)). Primers were synthesised by Sigma-Genosys (Haverhill, UK).

The primer sequences were as follows:

Forward:	<b>TubCor1</b>	5'- ACAGGTGCCAAGTTCTGG -3'	$T_m = 61.4^\circ\text{C}$
Reverse:	<b>TubCor2</b>	5'- GTAGTGACCCTTCGCCCA -3'	$T_m = 63.8^\circ\text{C}$

Primers were tested with a 25  $\mu\text{l}$  PCR reaction as in Section 2.4 with *T. versicolor* DNA as template, annealing temperature at  $65^\circ\text{C}$ , for 30 cycles.

### 5.2.6.2 *Ligation efficiency analysis method*

Each adaptor-ligated tester cDNA (1  $\mu$ l) (i.e. 1-1, 1-2, 2-1, 2-2) was diluted into 200  $\mu$ l sterile dH<sub>2</sub>O. Then reagents were combined in an appropriate order (Table 5.4):

**Table 5.4** Ligation efficiency analysis PCR set up. XJ = cross-junction primer amplification, INT = internal primer amplification.

Subtraction	Forward				Reverse			
Tube label	1	2	3	4	5	6	7	8
Amplification	XJ	INT	XJ	INT	XJ	INT	XJ	INT
dil.Tester 1-1 (adaptor 1)	1	1	-	-	-	-	-	-
dil.Tester 1-2 (adaptor 2R)	-	-	1	1	-	-	-	-
dil.Tester 2-1 (adaptor 1)	-	-	-	-	1	1	-	-
dil.Tester 2-2 (adaptor 2R)	-	-	-	-	-	-	1	1
TubCor2 (10 $\mu$ M)	1	1	1	1	1	1	1	1
TubCor1 (10 $\mu$ M)	-	1	-	1	-	1	-	1
PCR Primer 1 (10 $\mu$ M)	1	-	1	-	1	-	1	-
<b>Total</b>	<b>3</b>	<b>3</b>	<b>3</b>	<b>3</b>	<b>3</b>	<b>3</b>	<b>3</b>	<b>3</b>

A master mix was prepared as follows for each reaction: Sterile dH<sub>2</sub>O 18.5  $\mu$ l; 10X buffer 2.5  $\mu$ l; dNTPs (10 mM) 0.5  $\mu$ l; *Taq* polymerase (purified in house) 0.125  $\mu$ l. The master mix was aliquotted (22  $\mu$ l) into each of tubes 1-8 (Table 5.4). Reaction mixtures were incubated in a thermal cycler at 75°C for 5 min to extend the adaptors by filling in the missing strand of the adaptors: this also creates binding sites for the PCR primers (Figure 5.3). Incubation was followed immediately by thermal cycling with the following programme. 94°C 30 s; {94°C 10 s; 65°C 30 s; 68°C 2.5 min} for 30 cycles on a PE2700 PCR machine (Applied Biosystems, CA, USA). Products (5  $\mu$ l) were analysed by gel electrophoresis on a 2.0% agarose/EtBr gel.

### 5.2.7 **First Hybridisation**

An excess of driver cDNA was added to each adaptor-ligated tester cDNA during the first hybridisation. The samples were heat denatured and then allowed to anneal, thereby allowing sequences common to both tester and driver populations, i.e. non-

target cDNAs, to hybridise. The ss cDNAs that remain are dramatically enriched for differentially expressed sequences (Figure 5.3).

For each experimental subtraction reagents were combined in the order shown in a specific order (Tables 5.5 and 5.6).

**Table 5.5** Subtraction reaction mixture for forward subtraction

Subtraction	Forward	
	Hyb1	Hyb2
<b>Tube label</b>		
<b>RsaI-digested driver cDNA (cDNA 2)</b>	1.5	1.5
<b>Adaptor 1 ligated tester 1-1 (cDNA 1)</b>	1.5	-
<b>Adaptor 2R ligated tester 1-2 (cDNA 1)</b>	-	1.5
<b>4X Hybridisation buffer</b>	1	1
<b>Total</b>	4	

**Table 5.6** Subtraction reaction mixture for reverse subtraction

Subtraction	Reverse	
	Hyb3	Hyb4
<b>Tube label</b>		
<b>RsaI-digested tester cDNA (cDNA 1)</b>	1.5	1.5
<b>Adaptor 1 ligated tester 2-1 (cDNA 2)</b>	1.5	-
<b>Adaptor 2R ligated tester 2-2 (cDNA 2)</b>	-	1.5
<b>4X Hybridisation buffer</b>	1	1
<b>Total</b>	4	4

All reactions were incubated in a thermal cycler at 98°C for 1.5 min and then a further 8 hours at 68°C. The lids of the PCR tubes were covered with parafilm to prevent evaporation from tubes during the extended incubation period. The second hybridisation was performed immediately following the 8 hour incubation.

### 5.2.8 Second Hybridisation

The two samples from the first hybridisation for each subtraction were mixed together in the presence of excess denatured driver DNA and allowed to anneal. Those ss cDNAs, each with a different adaptor ligated to them, enriched in the first

hybridisations could then reassociate and form new hybrids that are the differentially expressed cDNAs with different adaptors on each end (Figure 5.3).

**Table 5.7** Second Hybridisation reaction mixtures. All volumes are  $\mu\text{l}$ .

<b>Subtraction</b>	<b>Forward</b>	<b>Subtraction</b>	<b>Reverse</b>
<b>2<sup>nd</sup> Hyb. Sample name</b>	<b>Hyb1</b>	<b>2<sup>nd</sup> Hyb. Sample name</b>	<b>Hyb3</b>
<b>1<sup>st</sup> Hyb. samples mixed</b>	Hyb 1 and Hyb 2	<b>1<sup>st</sup> Hyb. Samples mixed</b>	Hyb 3 and Hyb 4
<b>Driver cDNA</b>	1	<b>Tester cDNA</b>	1
<b>4X Hybridisation buffer (room temp)</b>	1	<b>4X Hybridisation buffer (room temp)</b>	1
<b>dH<sub>2</sub>O</b>	2	<b>dH<sub>2</sub>O</b>	2
<b>Total</b>	4	<b>Total</b>	4

Hybridisation mixtures (Table 5.7) were prepared and 1  $\mu\text{l}$  of each was denatured by incubation in a thermal cycler at 98°C for 1.5 min. This freshly denatured driver was removed from the thermal cycler and mixed simultaneously with Hyb1 and Hyb2 (Hyb3 and Hyb4 in the case of the reverse subtraction). To ensure that the two hybridisation samples mix together only in the presence of freshly denatured driver a micropipettor was set to 15  $\mu\text{l}$  and hybridisation sample 2 drawn up into the tip. Then a small air space was drawn up into the tip. The denatured driver was then drawn up in the same tip so that hybridisation sample 2 and the denatured driver were separated by an air space in the tip and were not yet mixed. The entire contents of the pipette tip was then transferred into the tube containing hybridisation sample 1 and mixed by pipetting up and down. The reaction was incubated at 68°C overnight in a thermal cycler. This procedure was repeated for the reverse subtraction using Hyb3 and Hyb4 and an excess of denatured tester cDNA.

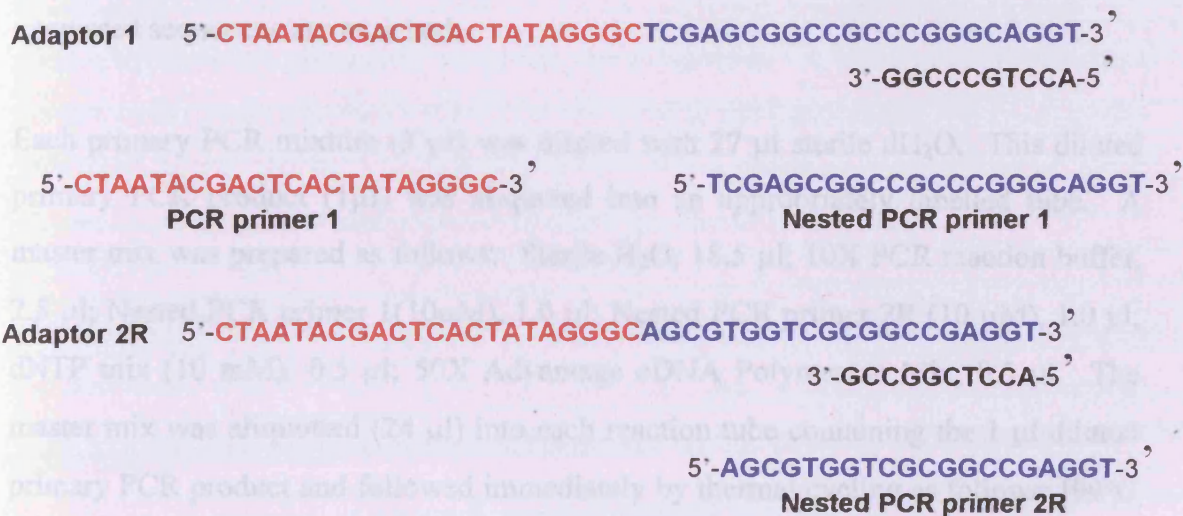
Following the overnight incubation, 200  $\mu\text{l}$  dilution buffer pH 8.3 (20 mM HEPES [pH 6.6], 20 mM NaCl, 0.2 mM EDTA [pH 8.0]) was added to each reaction tube and mixed by pipetting, followed by incubation in a thermal cycler at 68°C for 7 min and stored at -20°C.

### 5.2.9 PCR amplification

Following hybridisation, the samples were selectively enriched by PCR for differentially expressed sequences with different adaptors on each end. The differentially expressed transcripts may have varied in abundance in the original mRNA sample, but the enrichment by PCR equalises the products to be present in roughly equal proportions.

#### 5.2.9.1 Primary PCR

Prior to amplification the samples are incubated for 5 min at 75°C to fill in the missing strands of the adaptors, thus creating a binding site for PCR primer 1 (Figure 5.5). In this first amplification a general primer with sites on both types of adaptor is used. Therefore, only ds cDNAs with different adaptor sequences on each end are exponentially amplified. All other molecules present within the sample cannot be amplified (Figure 5.3).



**Figure 5.5** Sequences of the PCR-Select cDNA adaptors and PCR primers.

PCR was performed on both the forward and reverse subtracted testers from the second hybridisation, Hyb1 and Hyb3 respectively (Table 5.7), and the corresponding unsubtracted tester controls, 1-c and 2-c together with the positive control supplied with the kit (a subtracted mixture of Hae III-digested  $\phi$ X174 DNA.

Each diluted sample (1  $\mu$ l) was aliquotted into a 0.2 ml PCR tube and a master mix prepared as follows for each reaction: Sterile dH<sub>2</sub>O, 19.5  $\mu$ l; 10X PCR reaction buffer, 2.5  $\mu$ l; dNTP mix (10 mM), 0.5  $\mu$ l; PCR primer 1 (10  $\mu$ M), 1.0  $\mu$ l; 50X Advantage cDNA Polymerase Mix 0.5  $\mu$ l. Master mix (24  $\mu$ l) was aliquotted into each tube with the 1  $\mu$ l template. Tubes were incubated in a thermal cycler at 75°C for 5 min to extend the adaptors, followed immediately by thermal cycling as follows: 94°C 25 s; [94°C 10 s, 66°C 30 s, 72°C 1.5 min] for 27 cycles in a PE2700 PCR machine (Applied Biosystems, CA, USA). PCR products (8  $\mu$ l) were analysed by gel electrophoresis on a 2.0 % agarose/EtBr gel.

### 5.2.9.2 *Secondary PCR*

The secondary PCR was commenced immediately after analysing the primary PCR products. The amplification stage enriches the differentially expressed sequences further using nested PCR. By priming from sites from within the amplified region of the primary PCR, any background PCR products are reduced and the differentially expressed sequences are enriched.

Each primary PCR mixture (3  $\mu$ l) was diluted with 27  $\mu$ l sterile dH<sub>2</sub>O. This diluted primary PCR product (1 $\mu$ l) was aliquoted into an appropriately labelled tube. A master mix was prepared as follows: Sterile H<sub>2</sub>O, 18.5  $\mu$ l; 10X PCR reaction buffer, 2.5  $\mu$ l; Nested PCR primer 1(10 $\mu$ M), 1.0  $\mu$ l; Nested PCR primer 2R (10  $\mu$ M), 1.0  $\mu$ l; dNTP mix (10 mM), 0.5  $\mu$ l; 50X Advantage cDNA Polymerase Mix, 0.5  $\mu$ l. The master mix was aliquotted (24  $\mu$ l) into each reaction tube containing the 1  $\mu$ l diluted primary PCR product and followed immediately by thermal cycling as follows: [94°C 10 s; 68°C 30 s; 72°C 1.5 min] for 12 cycles in a PE2700 PCR machine (Applied Biosystems, CA, USA). Each reaction (8  $\mu$ l) was analysed by gel electrophoresis on a 2.0 % agarose/EtBr gel. Reaction products were stored at -20°C until required.

### 5.2.9.3 *Purification of PCR products*

Prior to vector ligation PCR products were purified using QIAquick PCR purification columns (Qiagen) as described in 2.5. The method was amended slightly so that the final elution step was with 15  $\mu$ l Buffer EB (10mM Tris-HCl) + 15  $\mu$ l dH<sub>2</sub>O. This



effectively reduced the the final concentration of the eluate to 5 mM Tris-HCl rather than 10 mM. This modification was made because in the later vector ligation step it was desired that the whole sample be ligated to the plasmid. Therefore, the sample would have to be concentrated to at least half the volume, which would double the end concentration of Tris-HCl. A higher Tris-HCl concentration could have inhibitory effects on downstream reactions. By halving the concentration of the elution buffer this effect is minimised.

### 5.2.10 Vector Ligation

Forward and reverse subtracted experimental testers were cloned using the pGEM®-T Easy vector system (Promega) which is an A/T cloning vector. The cut vector has 3'-T overhangs added to the 3' ends. This improves the efficiency of ligation of the PCR product into the vector because of the tendency of *Taq* polymerases to add As to the end of PCR products independently of what the template is. The 3'-T overhangs also prevent re-circularisation of the vector.

Two controls were performed alongside these ligations. A positive control, where control Insert DNA supplied with the kit was used in the ligation reaction to assess the efficiency of the ligation. A negative control using dH<sub>2</sub>O as a substitute for insert allowed the number of false positives due to background to be assessed.

Ligation reactions were set up (Table 5.8) in 0.5 ml Eppendorf tubes. The 2X rapid ligation buffer was vortexed vigorously before each use. All reactions were incubated at room temperature for 1 hour and then stored at -20°C.

**Table 5.8** Plasmid ligation reactions set up.

	Forward 1-1	Reverse 2-1	Positive Control	Background Control
<b>2X Rapid Ligation Buffer</b>	5	5	5	5
<b>PGEM-T Easy Vector (50 ng)</b>	1	1	1	1
<b>PCR product</b>	2	2	-	-
<b>Control Insert DNA</b>	-	-	2	-
<b>T4 DNA Ligase (3 Weiss units <math>\mu\text{l}^{-1}</math>)</b>	1	1	1	1
<b>dH<sub>2</sub>O</b>	1	1	1	3
<b>Total volume</b>	10	10	10	10

### 5.2.11 Transformation of ligation reactions

High efficiency XL 10-Gold Ultracompetent cells (Stratagene Ltd., Cambridge, UK) competent cells were used for the transformation of the experimental ligation reactions to obtain high transformation yields. Due to the expense of the ultracompetent cells, they were not used for the transformation of the positive and background controls from the vector ligation. Instead XL1-Blue Subcloning-Grade competent cells (Stratagene Ltd., Cambridge, UK) were used. Although the XL1-Blue cells did not produce the same magnitude of colonies as the XL10-Gold cells, they still provided an assessment of the ligation efficiency. Efficiency of the ligation is assessed based on the proportions of blue to white colonies produced rather than the overall number of colonies.

#### 5.2.11.1 Transformation of Forward and Reverse subtraction vector ligation reactions

Several transformations were performed for both forward and reverse subtractions.

XL 10-Gold Ultracompetent Cells (Stratagene Ltd., Cambridge, UK) (50  $\mu$ l) were thawed on ice and aliquotted into pre-chilled 15 ml Falcon polypropylene tubes standing on ice.  $\beta$ -mercaptoethanol mix (2  $\mu$ l) was added to each aliquot of cells and swirled gently. Cells were incubated on ice for 10 min, swirling every 2 min. The ligation mixture (2  $\mu$ l) was added to the cells, swirled gently and incubated on ice for a further 30 min. Cells were heat-pulsed at 42°C for 30 s in a water bath and incubated on ice for a further 2 min. NZY<sup>+</sup> broth (0.95 ml; Section 2.11.1), preheated at 42°C was added and the tubes incubated at 37°C for 1 hour with shaking at 225-250 rpm in an Orbital incubator (Gallenkamp, Loughborough, UK).

For blue-white colour screening of colonies, LB agar (Section 2.11.2) plates containing 50  $\mu$ g ml<sup>-1</sup> ampicillin (Sigma-Aldrich Ltd., Dorset, UK), were prepared by spreading 100  $\mu$ l of 10 mM IPTG (isopropyl-1-thio- $\beta$ -D-galactopyranoside) and 100  $\mu$ l of 2% X-gal (5-bromo-4-chloro-3-indolyl- $\beta$ -D-galactopyranoside) onto solidified LB agar plates, 30 min prior to plating the transformations. These were pipetted into a 100  $\mu$ l pool of SOC medium (Section 2.11.3) and then the mixture spread across the

plate, for consistent colour development across the plate. The SOC medium prevents precipitation that might occur if the IPTG and X-gal were mixed directly.

Aliquots of the transformation mixture (100  $\mu$ l) were spread onto plates and incubated at 37°C for 17 h to allow growth of colonies and colour development. Plates were stored at 4°C wrapped in cling film for up to 8 weeks.

#### **5.2.11.2 Transformation of control vector ligation reactions**

The following protocol was carried out for both the positive and background control vector ligation reactions.

XL1-Blue Subcloning grade cells (50  $\mu$ l; Stratagene Ltd., Cambridge, UK) were thawed on ice and aliquotted into pre-chilled 15 ml Falcon polypropylene tubes also standing on ice. The ligation mixture (2  $\mu$ l) was added to an aliquot of cells, swirled gently and incubated on ice for 20 min. Cells were heat-pulsed at 42°C for 45 s in a water bath and incubated on ice for a further 2 min. SOC medium (0.95 ml; section 2.11.3) preheated at 42°C was added and the tubes incubated at 37°C in an orbital incubator (Gallenkamp, Loughborough, UK) for 30 min with shaking at 225-250 rpm.

Aliquots of the transformation mixture (200  $\mu$ l) were spread onto LB agar plates containing ampicillin (50  $\mu$ g ml<sup>-1</sup>) and prepared with X-Gal and IPTG for blue/white screening as described for the transformation with XL10-Gold cells in section 5.2.12.1. Plates were incubated for 17 h at 37°C, then stored at 4°C wrapped in cling film.

#### **5.2.12 Screening of transformants**

Clones are screened using blue/white selection where white colonies are those that contain plasmids with inserts, while blue colonies contain empty plasmids.

To confirm that white colonies contained plasmids with inserts, PCR was performed on 10 white colonies and a blue control colony using M13F/R primers. The pGEM-T Easy vector has M13 priming sites on either side of the insertion site in the plasmid.

This allows the insert, if present, to be amplified and its size assessed. Some vector sequence will also be amplified, which must be subtracted from the product size to give the size of the insert. A 236 bp product is expected from empty vectors, thus it can be inferred that PCR products exceeding 263 bp contain inserts. M13 primers were as follows: M13F - GTTTCCCAGTCACGACGTTG; M13R - TGAGCGGATAACAATTTACACAG.

Colonies were picked into 200  $\mu$ l LB broth (section 2.11.2) containing ampicillin (50  $\mu$ g ml<sup>-1</sup>) and incubated for 3-4 h at 37°C with shaking at 200 rpm in an orbital incubator (Gallenkamp, Loughborough, UK). The characteristic smell of bacterial growth was used to confirm cultures had grown. This liquid culture (1  $\mu$ l) was used in a 25  $\mu$ l PCR reaction as template. The rest was stored at 4°C for up to 1 week. A master mix was prepared as follows: dH<sub>2</sub>O 18.9  $\mu$ l; 10X PCR reaction buffer, 2.5  $\mu$ l; dNTPs (10 mM), 0.5  $\mu$ l; M13F (10  $\mu$ M), 1.0  $\mu$ l; M13R (10  $\mu$ M), 1.0  $\mu$ l; *Taq* polymerase (purified in-house), 0.125  $\mu$ l. All reagents and reaction tubes were kept on ice during preparation. 24  $\mu$ l of master mix was aliquotted into each reaction tube already containing the 1  $\mu$ l template.

Thermal cycling was commenced according to the following programme: [94°C 1 min; 50°C 1 min; 72°C 2 min] for 40 cycles; 72°C 7 min; 4°C  $\infty$ . 5  $\mu$ l of each reaction was analysed on a 1.5 % agarose/EtBr gel and run in 1X TAE buffer.

### 5.2.13 Miniprepping for Sequencing

Ten clones were picked at random to be submitted for sequencing. Sequencing requires a large amount of plasmid DNA, which must be separated from cell debris. By growing a colony in a 3 ml overnight culture and then performing a mini-prep purification step, the required high-copy plasmid DNA can be obtained. A QIAprep Spin Plasmid kit (Qiagen) was used according to the manufacturers instructions as follows.

Liquid cultures (50  $\mu\text{l}$  of the 200  $\mu\text{l}$ ) grown up for colony PCR was used to inoculate 3 ml LB broth containing 50  $\mu\text{g ml}^{-1}$  ampicillin. Cultures were incubated at 37°C overnight with shaking at 250 rpm in an orbital incubator (Gallenkamp, Loughborough, UK). A portion of the liquid culture (0.5 ml) was retained and stored at 4°C for up to 2 weeks. The remaining 2.5 ml of this liquid culture was decanted into two 1.5 ml Eppendorfs and centrifuged for 3 min at 4300 g in an Eppendorf Minispin microcentrifuge to pellet cells. The supernatant was discarded and the pellet resuspended in 250  $\mu\text{l}$  Buffer P1. Buffer P2 (250  $\mu\text{l}$ ) was added and the tubes inverted 4-6 times to mix. The solution at this point becomes viscous and slightly clear. Buffer N3 (350  $\mu\text{l}$ ) was added and the tube was immediately inverted gently 4-6 times. The solution becomes cloudy and very viscous. Tubes were then centrifuged for 10 min at 11300 g as above. Supernatants were applied to QIAprep columns and centrifuged for 1 min at 11300 g as above and the flow-through discarded. This was repeated until all of the supernatant had been spun through the column. Columns were washed by adding 0.75 ml Buffer PE and allowing them to stand for 5 min at room temperature, followed by centrifuging for 1 min. The flow-through was discarded and the wash step repeated. Columns were centrifuged for an additional min at 11300 g to remove any residual buffer. The columns were transferred to clean 1.5 ml Eppendorf tubes and 50  $\mu\text{l}$  of 10 mM Tris-HCl, pH 8.5 were added to the centre of the column, allowed to stand for 5 min and centrifuged for 1 min at 11300 g as above to elute the DNA. The purified plasmid was quantified using Genequant spectrophotometer. Samples require a yield  $>30 \mu\text{g ml}^{-1}$  for sequencing.

#### 5.2.14 Sequencing

Preliminary samples were processed by the Cardiff University Molecular Biology Support unit. The clones were sequenced on an ABI Prism 3100 Capillary Sequencer (Applied Biosystems, Foster City, CA, USA). Sequencing reactions were performed using the BigDye Terminator Cycle Sequencing Kit (Applied Biosystems) using M13F primers (5'-GTAAAACGACGGCCAGT-3'). Further sequencing was carried out at the Edinburgh NERC Sequencing Facility (details in Chapter 6).

### **5.2.15 Sequence Analysis**

Sequences were examined using CHROMAS software (version 2.3 Technelysium Pty Ltd, Tewantin, Qld, Australia) to check sequence quality. The vector and nested PCR primers 1 and 2R were identified and removed from the sequence leaving only the SSH insert sequence.

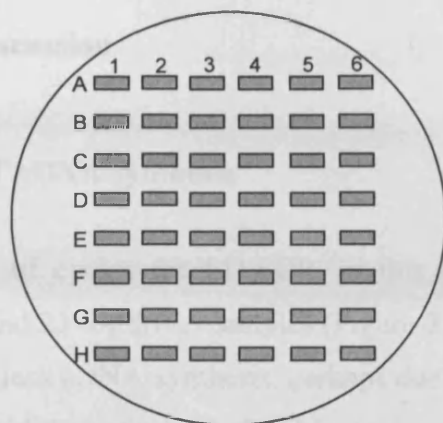
### **5.2.16 Database Similarity searching**

All sequences were then submitted to BLASTN and BLASTX searches using the BLAST Network Service (National Centre for Biotechnology Information, NCBI website 2005) to be compared with all genome databases to find any sequence similarities with known genes or proteins. All sequences were subjected to BLAST similarity searches against the non-redundant nucleotide database on the NCBI website.

### **5.2.17 Storage of clones**

#### ***5.2.17.1 Temporary storage on patch plates***

Following each transformation all white colonies were picked from agar plates and transferred to 90 mm diameter LB/Amp50 agar plates in small patches following a template in the same configuration as a 96-well plate (Figure 5.6). Each agar plate fits 48 patches, i.e. half a 96-well plate. Plates were incubated overnight at 37°C and then wrapped in clingfilm and stored at 4°C for up to 8 weeks.



**Figure 5.6** Layout of patch plate for temporary storage of clones. Grey areas indicate areas of bacterial growth.

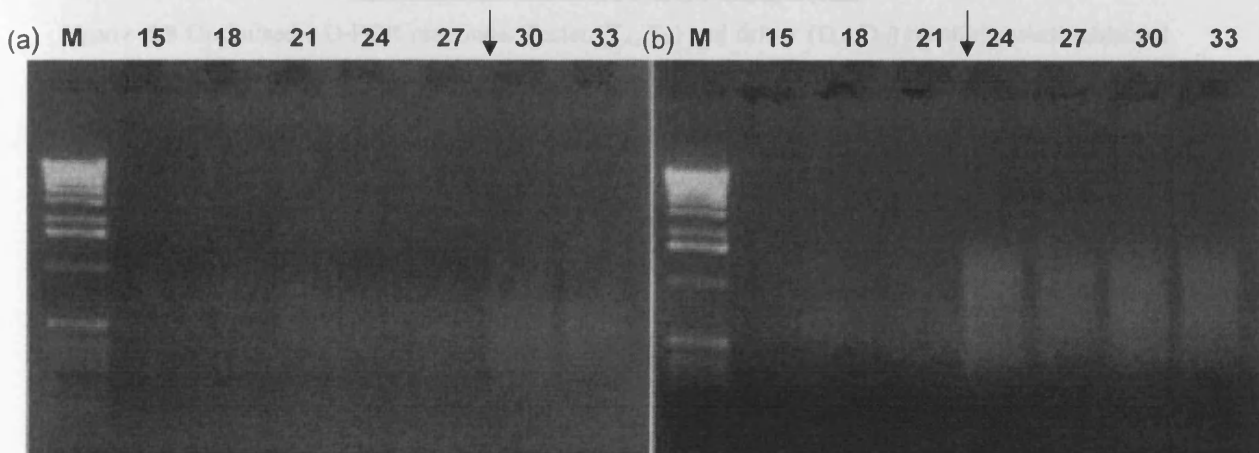
### 5.2.17.2 Long term storage in glycerol stocks

For longer term storage of clones, a few cells were transferred into 150  $\mu\text{l}$  LB broth containing ampicillin ( $100 \mu\text{g ml}^{-1}$ ) in each well of a sterile U-bottomed 96-well plate (Alpha Laboratories Ltd, Hampshire, UK). Plates were wrapped in clingfilm, or stacked together if more than one plate was prepared at a time and then wrapped. The stack was wrapped in tin foil and incubated static at  $37^\circ\text{C}$  overnight in an air incubator. Each well was topped up with 100  $\mu\text{l}$  of a 50 % LB:50 % glycerol solution and pipetted to mix. Plates were heat sealed with foil lids (Alpha Laboratories Ltd, Hants., UK) and stored at  $-80^\circ\text{C}$ .

### 5.3 Results and Discussion

#### 5.3.1 SMART cDNA synthesis

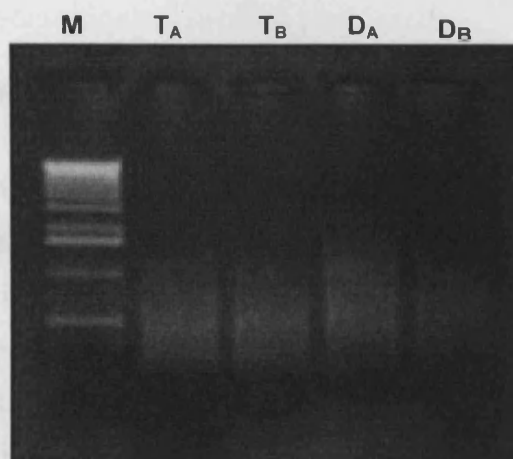
The optimum number of cycles for LD-PCR, in this case, for the tester samples (Figure 5.7a) was 29, and 23 for driver samples (Figure 5.7b). Tester samples required more cycles indicating less cDNA synthesis, perhaps due to less starting material, and again, highlights the need for optimisation at this stage.



**Figure 5.7** Optimisation of LD-PCR. Aliquots taken from reaction mixtures after cycles 15-33 for (a) Tester ( $T_x$ ) and (b) Driver ( $D_x$ ). M = 500 ng 1Kb ladder (Invitrogen). Arrows indicate where the plateau starts.

There was some variation in the optimum number of cycles (Tester - 29, 29 and 26; Driver - 23, 23, 20) for each of the three separate LD-PCR optimisations performed, probably due to slight differences in reaction conditions thus highlighting the need for optimisation with each set of replicates (Figure 5.8)

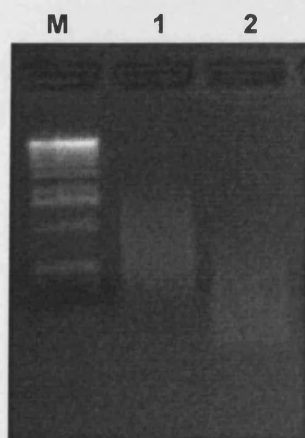




**Figure 5.8** Optimised LD-PCR reactions. Tester ( $T_A$ ,  $T_B$ ) and driver ( $D_A$ ,  $D_B$ ) reactions were subjected to 29 and 23 cycles respectively. M = 500 ng 1kb ladder (Invitrogen).

### 5.3.2 *RsaI* digestion

Following *RsaI* digestion, there was an overall reduction in the average size of cDNA, with undigested cDNA ranging in size between 0.5-2.5 kb, while digested cDNA ranged between 0.1-2 kb (Figure 5.9). The average size range of cDNA was slightly smaller than that described in the manufacturers notes, which expects mammalian and non-mammalian cDNA to be in the ranges 0.5-10 kb and 0.5-3 kb respectively. The reduced size of the fungal cDNA could be due to shorter mRNA: either due to smaller full length transcripts or minor degradation or impurities in the RNA extract resulting in smaller cDNA products.



**Figure 5.9** Comparison of undigested tester cDNA (1) with *RsaI*-digested tester cDNA (2). M = 500 ng 1kb ladder (Invitrogen).

### 5.3.3 Ligation efficiency analysis

#### 5.3.3.1 *Design of primers to a constitutively expressed gene*

Conserved areas from the alignment of  $\beta$ -tubulin were used for primer design (Figure 5.10, marked in red). Although, the amino acid sequences in these regions were identical for all species aligned, there was some variation in the codon usage. A decision was made to design primers primarily for use with *T. versicolor*, but which could also subsequently be used in related fungi. However, where there was variation, the nucleotide found in the *T. versicolor* sequence was used in the primer rather than creating degenerate bases within the primer which could potentially reduce the overall efficiency of the primer.

The primer pair designed was as follows:

Forward:     **TubCor1**     5'- ACAGGTGCCAAGTTCTGG -3'  
Reverse:     **TubCor2**     5'- GTAGTGACCCTTCGCCCA -3'

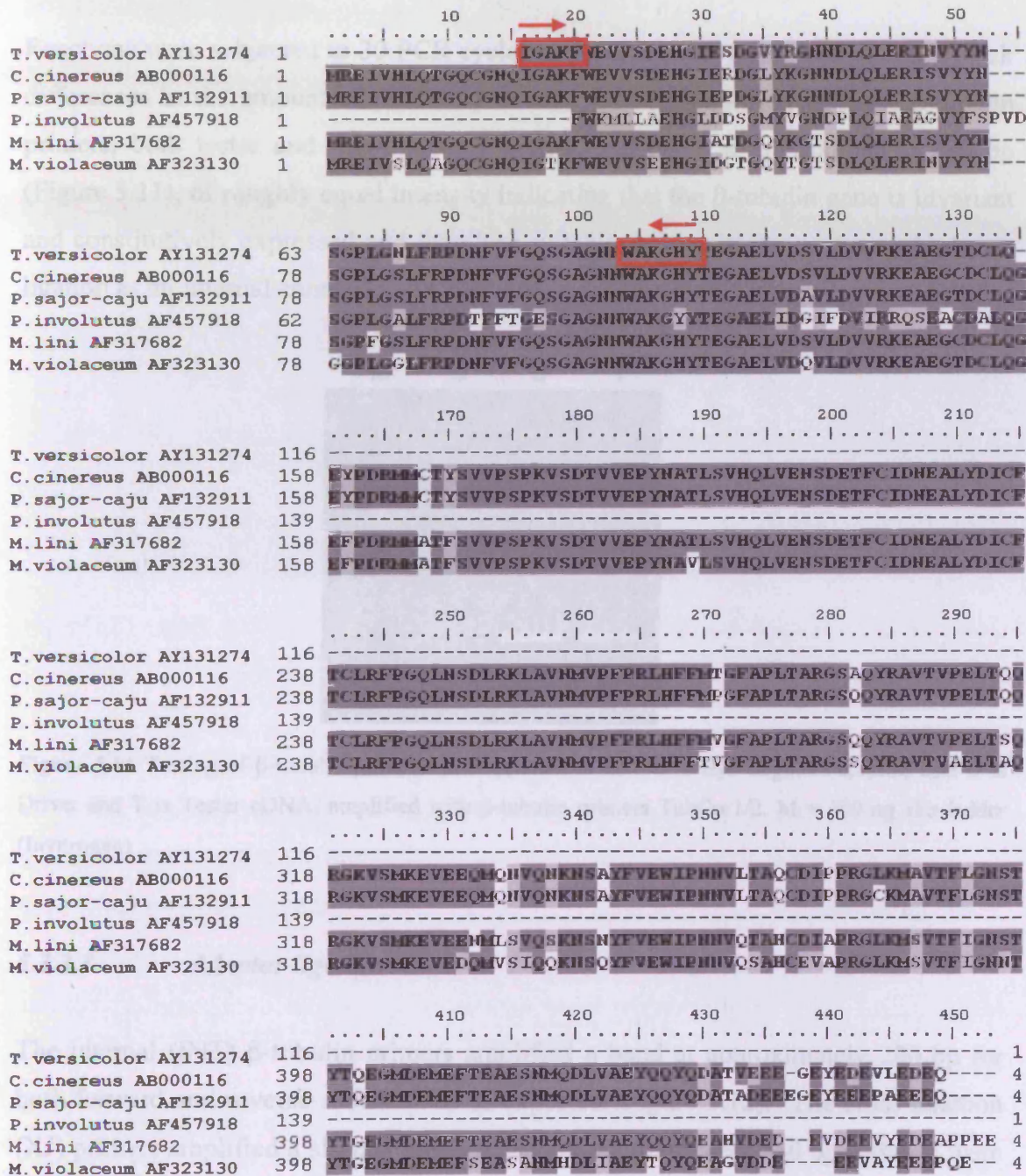
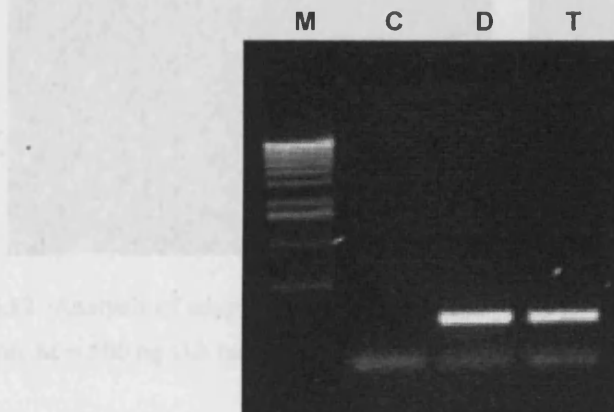


Figure 5.10 Alignment of beta-tubulin gene amino acid sequences for basidiomycetes *T. versicolor*, *C. cinerea*, *P. sajor-caju*, *P. involutus*, *M. lini*, *M. violaceum* produced using Bioedit Sequence Alignment Editor. Areas from which primers were designed are marked in red. Codes alongside species names are Genbank accession numbers.

### 5.3.3.2 Testing $\beta$ -tubulin primers

Reactions were subjected to 30 PCR cycles to prevent overcycling which could mask differences in the amount of product produced. When amplified with the  $\beta$ -tubulin primers, both tester and driver cDNA produced a band at approximately 280 bp (Figure 5.11), of roughly equal intensity indicating that the  $\beta$ -tubulin gene is invariant and constitutively expressed and therefore suitable for use in the analysis of adaptor ligation as an internal control.

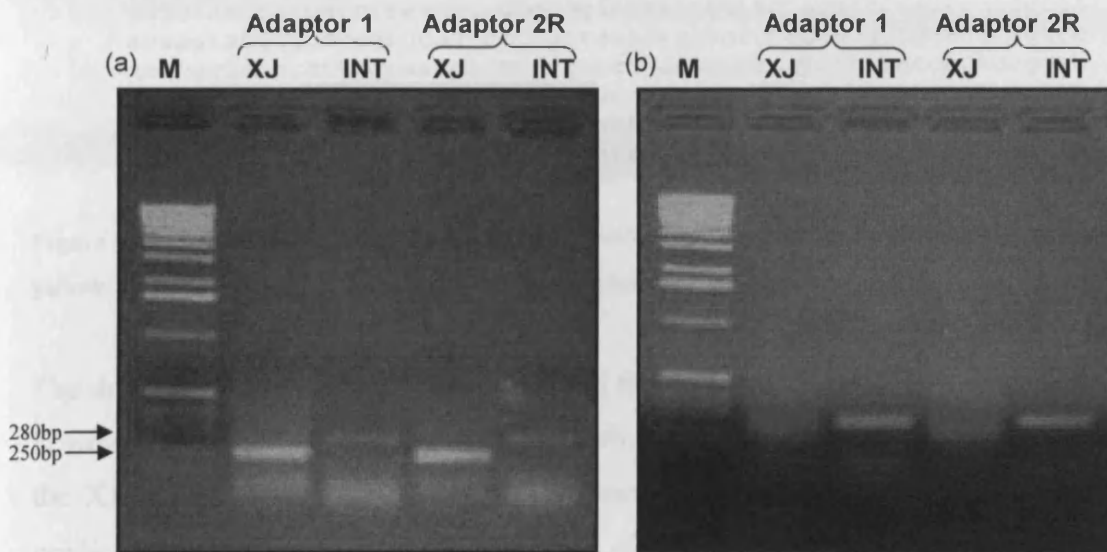


**Figure 5.11** Testing of  $\beta$ -tubulin primers. PCR product in lane C is H<sub>2</sub>O negative control, lane D is Driver and T is Tester cDNA, amplified with  $\beta$ -tubulin primers TubCor1/2. M = 500 ng 1kb ladder (Invitrogen)

### 5.3.3.3 Adaptor ligation

The internal (INT)  $\beta$ -tubulin primers amplified a band at approximately 280 bp for both forward and reverse subtractions as expected (Figure 5.12). The cross-junction (XJ) primers amplified a slightly smaller band at approximately 250 bp. Bands were of equal intensity for both adaptors 1 and 2R within each subtraction indicating that both adaptors were ligated with similar efficiency. The presence of an XJ band confirms that there has been adaptor ligation, however the ligation analysis for the forward subtraction (Figure 5.12a) shows that bands from the XJ amplification are much more intense than the INT bands. It might be expected for this relationship to be the other way round as this implies that adaptor ligation was more than 100% efficient which is highly unlikely as the expected level of ligation is much less. This discrepancy may be due to a difference in the efficiency of the PCR reactions with the

different sets of primers resulting in unequal amplification and may account for the large difference in the amount of PCR product.



**Figure 5.12** Analysis of adaptor ligation efficiency for (a) for forward subtraction and (b) for reverse subtraction. M = 500 ng 1kb ladder (Invitrogen).

Another explanation could be that there is an inherent property of the  $\beta$ -tubulin gene to favour adaptor ligation and thus an unequal proportion of the  $\beta$ -tubulin cDNA fragments will have adaptors attached and thus there will be more cDNA fragments with adaptors than there are left in the pool. However, closer inspection of the *T. versicolor*  $\beta$ -tubulin gene sequence from which the TubCor1/2 primers were designed shows that there is a *RsaI* cutting site within the sequence (Figure 5.13), which would result in a proportion of the  $\beta$ -tubulin cDNAs in the tester cDNA pool being cut in the earlier *RsaI* digestion step (Section 5.3.2). Consequently, the proportion of full length  $\beta$ -tubulin cDNAs that can be amplified by the internal TubCor1/2 primers in the tester cDNA pool would be reduced and would result in a smaller product. However, cut  $\beta$ -tubulin cDNAs may still be amplified with the XJ primer pair if adaptors have ligated to the cut fragments. Thus the relative intensities of bands are not informative as to the proportion of fragments with adaptors attached. However, it can be inferred that there has been adaptor ligation to a reasonable level as there are substantial amounts of XJ band products.

```

>Trametes versicolor AY131274
gatcgggtgagagggcgtcggacacgatggggcgctggatatgattgtctgacaccctc
gaggttgtctccgatgagcacggcatcgagtcggacgggtgtttaca
ggggcaacaacgacctccagctcgagcggatcaacgtctactacaacgaagtggcgcga
acaagtatgtgccccgtgcagtcctcgttgatctggagcctggaaccatggactccgtcc
gctcggggcccccttggcaacctcttcgccccgacaacttcgtctttggtcagagcggag
ctggttaacaactgggctgaagggtcactacaccgaggggtgccgagctcgttgactccgttc
tcgacgtcgtccgcaaggaggctgagggcactgactgcctgcagggtaagctttattccg
tgtgtgacgacgctgcgtgacacgccgatatcaatctgcacaa

```

**Figure 5.13**  $\beta$ -tubulin gene sequence from *T. versicolor*. The *RsaI* cutting site at catg is highlighted in yellow, primers TubCor1 (pink) and TubCor2 (green) are also highlighted.

The driver samples that were adaptor ligated for the reverse subtraction (Figure 5.11b), however, show the inverse relationship which INT bands appearing more intense than the XJ bands. This is unexpected as the same relationship as in Figure 5.11a was predicted since the same differences in PCR efficiency and the cutting of the  $\beta$ -tubulin cDNAs should apply to both the tester and driver cDNA pools equally. Thus, the relatively low intensity XJ bands implies that the adaptor ligation was much less efficient for the driver cDNA pool, although this could also be due to more dilute template. However it was apparent that there had been some ligation in both samples and the subtraction was continued to prevent wasting of samples. If there had been insufficient ligation of adaptors then this would be apparent at the PCR amplification stages, as priming sites are located on the adaptors, and the PCRs would be unsuccessful if adaptors were absent.

### 5.3.4 Hybridisation

There were no control steps for this stage of the SSH procedure.

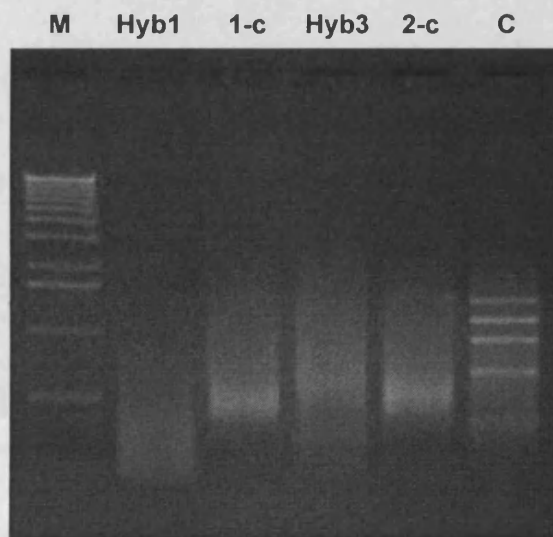
### 5.3.5 PCR amplification

Two rounds of amplification of the subtracted cDNA pools enriches the differentially expressed cDNA and reduces non-target background.

### 5.3.5.1 Primary PCR

This amplification was the first step in enriching for differentially expressed sequences. PCR products appear as smears rather than distinct bands because the samples were comprised of many different cDNAs over a wide size range.

Smears for the unsubtracted tester controls for both forward and reverse subtractions (1-c and 2-c respectively) ranged over a larger size distribution and were more intense than their corresponding subtracted testers (Figure 5.14). More intense bands would be expected for the unsubtracted samples as the subtraction removes common templates from the sample resulting in an overall reduction in template. The result from the control subtracted cDNA was also as described in the user manual.

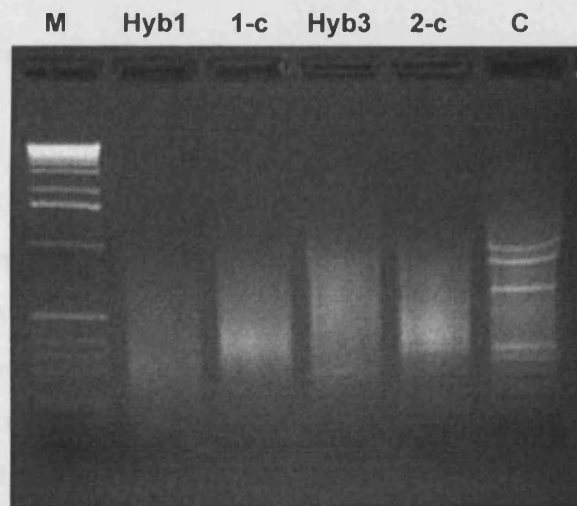


**Figure 5.14** Primary PCR products. Hyb1 and Hyb3 are the forward and reverse subtracted samples respectively. 1-c and 2-c are the corresponding unsubtracted tester controls. The control (C) is a subtracted mixture of HaeIII-digested  $\Phi$ X174 DNA. M = 500 ng 1kb ladder (Invitrogen).

### 5.3.5.2 Secondary PCR

The secondary nested PCR reaction further enriched for differentially expressed sequences by using primers within the amplified fragments from the primary PCR, thus one would expect bands to be of a greater intensity than those from primary PCR. This step also equalises cDNAs that were originally more or less abundant in the mRNA extract.

The smears for all samples were more intense and the difference in intensity between smears for subtracted and unsubtracted controls was also less marked following the nested secondary PCR reactions (Figure 5.15). The greater intensity of the PCR products indicates that the secondary PCR reaction was successful. The control subtracted cDNA resembled that in the user manual, also indicating successful PCR. Successful PCR reactions indicated that the subtraction was successful, and that the end product, of an equalised enriched sample of differentially expressed sequences, could be used to construct a subtractive library, and further used for microarray analysis as planned.



**Figure 5.15** Secondary PCR. Hyb1 and Hyb3 are the forward and reverse subtracted samples respectively. 1-c and 2-c are the corresponding unsubtracted tester controls. The control (C) is a subtracted mixture of HaeIII-digested  $\Phi$ X174 DNA. M = 500 ng 1kb ladder (Invitrogen).

### 5.3.6 Transformation and cloning

#### 5.3.6.1 Control vector ligation reactions

Transformations with the positive control ligations were approximately 50% efficient, with numbers of white colonies ranging between 49-58% indicating a good ligation reaction. Negative background control ligations when transformed produced significantly fewer colonies overall and of those only 5% were white, indicating a 5%



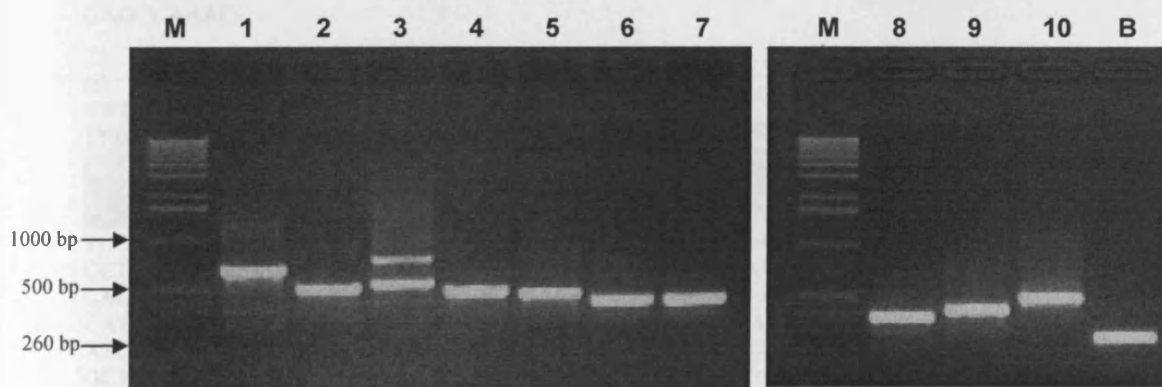
false positive rate. Ligation reactions were more efficient when 2X ligation buffer was used rather than 10X.

### 5.3.6.2 Forward and reverse vector ligation reactions

Transformations of forward and reverse vector ligation reactions were in general less efficient than the positive control transformations, with only up to 20% white colonies in each transformation. In total 3939 clones from the forward subtraction and 4560 from the reverse subtraction were picked (total 8499), grown as liquid cultures in 96 well plates and stored as glycerol stocks at  $-80^{\circ}\text{C}$ .

### 5.3.7 Screening of transformants

White colonies all produced bands of different sizes on an agarose gel, ranging from approximately 300-700 bp, thus confirming a different fragment size in each insert (Figure 5.16). The blue colony produced a band at approximately 260 bp, which confirms that the vector was empty in this particular colony, as the expected product is 263 bp for empty vector. Lane 3 (Figure 5.16) shows a double band in the PCR product, which suggests that the template was mixed perhaps due to accidental transfer of a neighbouring colony during picking.



**Figure 5.16** Clone PCR. Ten different white colonies and one blue colony were screened using PCR with M13F/R primers to confirm white colonies contained insert and blue colonies had empty vector. Lanes 1-10 are white colonies picked, B is a blue colony, M = 500 ng 1kb ladder (Invitrogen).

### 5.3.8 Sequencing of clones

Sequences confirmed that cDNA inserts varied in size significantly between clones as indicated from gel electrophoresis screening of clones (section 5.3.6, Figure 5.16). Insert size ranged from just 65 bp (Figure 5.17 b) to 360 bp (Figure 5.17 a). In some cases the insert included the poly A tail of the cDNA (Figure 5.17c), thus the insert is likely to represent a non-coding region of a cDNA and unlikely to produce matches with the nucleotide databases.

(a)

>W1 Insert: 360 bp

```
CACTATAGNNTTTAATTGGGCCCCNACGTCGCATGCTCCCCGGCCGCCATGGAGGCCGCGGGAATTCGA
TTAGCGTGGTTCGCGGGCCGAGGTACCTCGGCCTCCACNACCTCATCAGGTCTGAAAGCGCAGCCGCC
ACGCCGAGGGTGTATGGTAGTACCGGGGAGACAGCGCAGCCTGAAGTATATGGAGACGCAAGTAG
GAAATTTCCAGGATGTATGATGAAAGTGTACCTGCCCGGGCGGCCGCCCGGGCAGGTACCGCTGGGG
CCGTGTGGGGCGGTAGAACCGGATTATGTTCTCGTTCTGGTCGAGCAGCNANATGTCATTGTACAAG
CCCAGCCCAGATGGTGCCTTACACTTGTGATTCGCGCTTGGATTTGGACTCTCGTCATATCGTAT
TCCTCTTTCATGCGTCTTCCGCCGCTAATACACTGTAGCATACTAGTACCTCGGCCGCGACCACGCTA
ATCACTAGTGAATTCGCGGCCGCTGCAGGTCGACCATATGGGAGAGCTCCCAACGCGTTGGATGCA
TAGCTTGAGTATTCTATAGTGTACCTAAATAGCTTGGCGTAATCATGGGTCATAGCTGNTTTCCTGT
GTGAAATTGTTATCCGCTCACAANTTCCACACAACATACGAGCCCCGAAAGCATAAC
```

(b)

>W8 Insert: 65 bp

```
GTAGNGGCCAGTGAATTGTAATNGACTCACTATAGNTNTNAATTGGGCCCCGACGTCGCATGCTCCCC
GCCGCCATGGCCGCGCGGGAATTTCGATTAGCGTGGTTCGCGGCCGAGGTAACCTCGGCCTCCACAACC
TCATCAGGTCTTGAAAGCGCAGCCGCGACGCCGAGGGTGTATGGTAGTACCTCGGCCGGGCGGCCGC
TCGA AATCACTAGTGAATTCGCGGCCGCTGCAGGTCGACCATATGGGAGAGCTCCCAACGCGTTGG
ATGCATAGCTTGAGTATTCTATAGTGTACCTAAATAGCTTGGCGTAATCATGGTCATAGCTGTTTCC
TGTGTGAAATTGTTATCCGCTCACAATCCACACAACATACGAGCCGGAAGCATAAAGTGTAAAGCC
TGGGGTGCCTAATGAGTGAGCTAACTCACATTAATTGCGTTGCGCTCACTGCCCGCTTCCAGTCGGG
AAACCTGTGCTGCCAGCTGCATTAATGAATCGGCCAACGCGCGGGGAGAGGGCGGTTTGCATTTGGG
CGCTTCCGCTTCCCTCGCTACTGACTCGCTGCGCTCGGTCGTTTCGGCTTGCGGCGAGCGGTATCA
GCTCACTCAAAGCGGTAATACGGTTTATCCACAGAAATCAGGGGGATAACGCAGGAAAAANAATGT
GAGCCAAAC
```

(c)

>W6 Insert: 107 bp

```
TNGCGCCAGTGAATTGTATCGACTCACTATAGGGNGAATTGGGCCCCGACGTCGCATGCTCCCCGGCC
GCCATGGCGGCCGCGGTAATTCGATTAGCGTGGTTCGCGGCCGAGGTAACCTCGCGCTCGAGCTTATAT
AGGGAGATCTATCCGACCAATTGTAACCTTATACAGCAGCGGCTTGGAAATCGATGTTACAGTGTCCGAA
AAAAAAAAAAAAAAAAAAGTACCTCGGCCGGGCGGCTCGAAATCACTAGTGAATTCGCGGCCGCC
TGCAGGTCGACCATATGGGAGAGCTCCCAACGCGTTGGATGCATAGCTTGAGTATTCTATAGTGTC
CCTAAATAGCTTGGCGTAATCATGGTCATAGCTGTTTCTGTGTGAAATTGTTATCCGCTCACAATTC
CACACAACATACGAGCCGGAAGCATAAAGTGTAAAGCCTGGGGTGCCTAATGAGTGAGCTAACTCA
CATTAAATTGCGTTGCGCTCACTGCCCGCTTCCAGTCGGGAAACCTGTCGTGCCAGCTGCATTAATGA
ATCGGCCAACGCGCGGGGAGAGCGGTTTGCATTTGGGCGCTCTTCCGCTTCCCTCGCTCACTGACTC
GCTGCGCTCGGTGCTTCCGCTGCGGCGAGCGGTATCAGCTCACTCAAAGGCGGGTAATACGGNTTAT
CCNCANAATCAGGGGATAACGCAGGAAANAACATGTGANCCAAAAGGCCAGCNAAGGCCAGNA
ACCGTAAAAANGNCCCCGTTTGTGGGGTTT
```

**Figure 5.17** Examples of the forward subtraction clone sequences from clones screened in figure 5.15. Highlighted sequences are: yellow - pGEM T-easy vector; pink – nested primer sequences; blue – forward subtracted cDNA insert.

Once the inserts had been separated from surrounding vector sequences they were submitted as queries for BLAST similarity searches. Only one of the sequences submitted, however, showed any significant matches, which is probably due to the fact that the full genome of *T. versicolor* has not been sequenced and annotated, and fungi in general are underrepresented among the genome databases available. Furthermore, the nature of the SSH procedure is that the subtracted cDNA is composed of generally smaller fragments due to the earlier cutting with *RsaI* and hence it may reduce the likelihood of finding a good match with the databases. More in depth sequence analysis of all clones is performed in Chapter 6.

#### 5.4 Conclusion

The Clontech PCR-Select cDNA subtraction kit that was used is designed primarily for mammalian work, however, the principles of the technique are the same and can be applied to analysis of fungal gene expression. The process itself is lengthy and each step requires optimisation, which can be a handicap when starting material is scarce. However, following optimisation, each stage of the SSH protocol appears to have worked satisfactorily and controls, where applicable, gave the results expected based on the manufacturer's guidelines. The size distribution of the cDNA populations appeared to be slightly smaller than that suggested by the manufacturer's guidelines but this is perhaps just an inherent difference in the size of the transcripts in this fungal species. Furthermore, despite perhaps a poor choice of internal primers for the analysis of adaptor ligation, the later PCR amplification stages of the SSH process worked well for both of the subtractions indicating that there was sufficient adaptor ligation, and that subtractions and subsequent enrichment of the differentially expressed transcripts were successful.

## 6. Sequencing of SSH library

### 6.1 Introduction

Functional genomics is the process of assigning functions to gene sequences produced from genomic projects. Mutant phenotype screening or biochemical analyses of gene products, can be used to assign functions to individual genes. However, the majority of annotation is achieved using homology searches, whereby functions are assigned to sequences derived from expressed sequence tag (EST) libraries and genome sequencing projects, based on similarity to other genes, that have been already well characterised. Currently, the scientific community is encouraged to submit sequences to public databases. GenBank (USA), EMBL nucleotide sequence database (Europe) and DNA database of Japan (DDBJ) are annotated databases of all the publicly available DNA sequences, and they collaborate to share submitted sequence information (Kulikova *et al.*, 2006). These databases contain sequences from genome projects, EST libraries and peptide sequences, and the availability of these sequences makes broad similarity searches possible. Within GenBank there are approximately 61 million sequence entries with fungi only representing 3.5 % of entries, and basidiomycetes less than 1 %.

To date only a few fungal DNA genomes have been completely sequenced and made publicly available, including *Saccharomyces cerevisiae*, *Neurospora crassa* and *Aspergillus nidulans*, and currently, basidiomycetes are poorly represented within the nucleotide databases. However, the Fungal Genome Initiative (FGI), coordinated by the Broad Institute (Cambridge, MA, USA) has identified key fungal species on which to concentrate sequencing efforts, to increase the number of complete fungal genome sequences available. The basidiomycetes *Puccinia graminis*, *Ustilago maydis* and *Coprinopsis cinereus* have been sequenced, provisionally annotated and are available in Genbank. *C. cinerea*, is a filamentous basidiomycete with a typical mushroom fruit body, and therefore is most likely to show sequence similarity to *Trametes versicolor*, than *P. graminis* and *U. maydis*, which are both specialist plant pathogenic fungi.

ESTs are important resources for transcriptome investigation. ESTs are short unedited sequences of nucleotides (usually 100-800 nucleotide bases long) derived from single pass sequencing of clones from cDNA libraries. These can be generated rapidly from either the 3' or 5' ends of cDNA clones. High throughput analysis in this way can yield large amounts of information about transcriptionally active genes in a particular organism, tissue or cell, at a particular time.

The generation of ESTs is relatively simple and inexpensive. High-throughput EST generation enables investigation of the transcriptome without necessarily requiring the whole genome sequence of the study organism. This enables gene discovery, and complements genome annotation and gene structure identification. Furthermore, when the genome sequence of an organism does become available, a collection of cDNA sequences provides the best tool for identifying genes within the DNA sequence. The number of ESTs submitted to dbEST, a division of the GenBank database (Benson *et al.*, 2007) and the largest publicly available EST database (Boguski *et al.*, 1993), is increasing exponentially. Currently it holds over 46 million EST sequences from 1397 organisms, with fungi represented by 1,189,107 ESTs. In addition, Unigene, also curated by GenBank, is a non-redundant database of gene clusters derived from ESTs, which avoids redundancy and overlap of sequences from within dbEST when searching the databases. However, although ESTs can generate a lot of information about transcriptionally active genes it is important to note that there are limitations. ESTs can only provide information about the mRNA sequence and there may be important information found in introns of those genes. Furthermore, although large numbers of ESTs can be generated rapidly there is usually considerable redundancy in libraries, as the cDNA template used can be partial or full length. ESTs can also be contaminated with vector sequence and the sequencing is often prone to errors, especially at the ends of sequences (Aaronson *et al.*, 1996). In addition, ESTs can be subject to sampling bias which can result in less abundant transcripts being under-represented. Techniques such as SSH can be used to enrich for rare transcripts and isolate differentially expressed genes before ESTs are generated.

However, for the data generated by ESTs to be biologically informative the analysis of large sets of ESTs is necessary, as individual raw ESTs alone cannot provide much information about the transcriptome.

Initially analysis involves the pre-processing of ESTs to remove poor sequences and vector and primer contamination. Base calling software such as Phred (Ewing & Green, 1998; <http://www.phrap.org>) is used to process raw sequence chromatograms and generate EST sequences (Figure 6.1, Step 1). There is often vector and primer contamination within EST sequences, and to fully analyse the sequences within a library it is necessary to remove these contaminating sequences prior to clustering (Figure 6.1, Step 2). Various software programmes are available for trimming vector from EST sequences, such as BLAST or Cross\_match, which scan ESTs for known vector and primer sequences and then remove them.

Redundancy arises within EST libraries, as particular genes may be transcribed numerous times within a particular cell or tissue, leading to many ESTs derived from the same gene. Furthermore, EST sequences vary in length and may come from any region within a gene. Consequently, some sequences may also be non-coding. Redundancy can be reduced by grouping ESTs into clusters (Figure 6.1, Step 3), based on sequence similarity, which also serves to increase the overall length of sequences, which may improve the chance of downstream annotation. Consensus sequences (or contigs) are generated from clusters, which represent putative genes (Figure 6.1, Step 4). Software such as CLOBB (Clustering on the basis of BLAST; Parkinson *et al.*, 2002) and Phrap ([www.phrap.org](http://www.phrap.org)) are among the numerous programs available for this EST clustering and assembly. Once consensus sequences have been obtained, then possible functions can be assigned to putative genes by homology searches against nucleotide and peptide databases (Figure 6.1, Step 5) using BLAST (Altschul *et al.*, 1990). BLASTN is used to query ESTs against non-redundant nucleotide sequence databases. BLASTX is used to translate conceptually the EST sequence, in all six reading frames, into a putative peptide, which is then compared to peptide sequence databases, to identify sequences with protein coding regions similar to proteins within the databases. TBLASTx converts a nucleotide

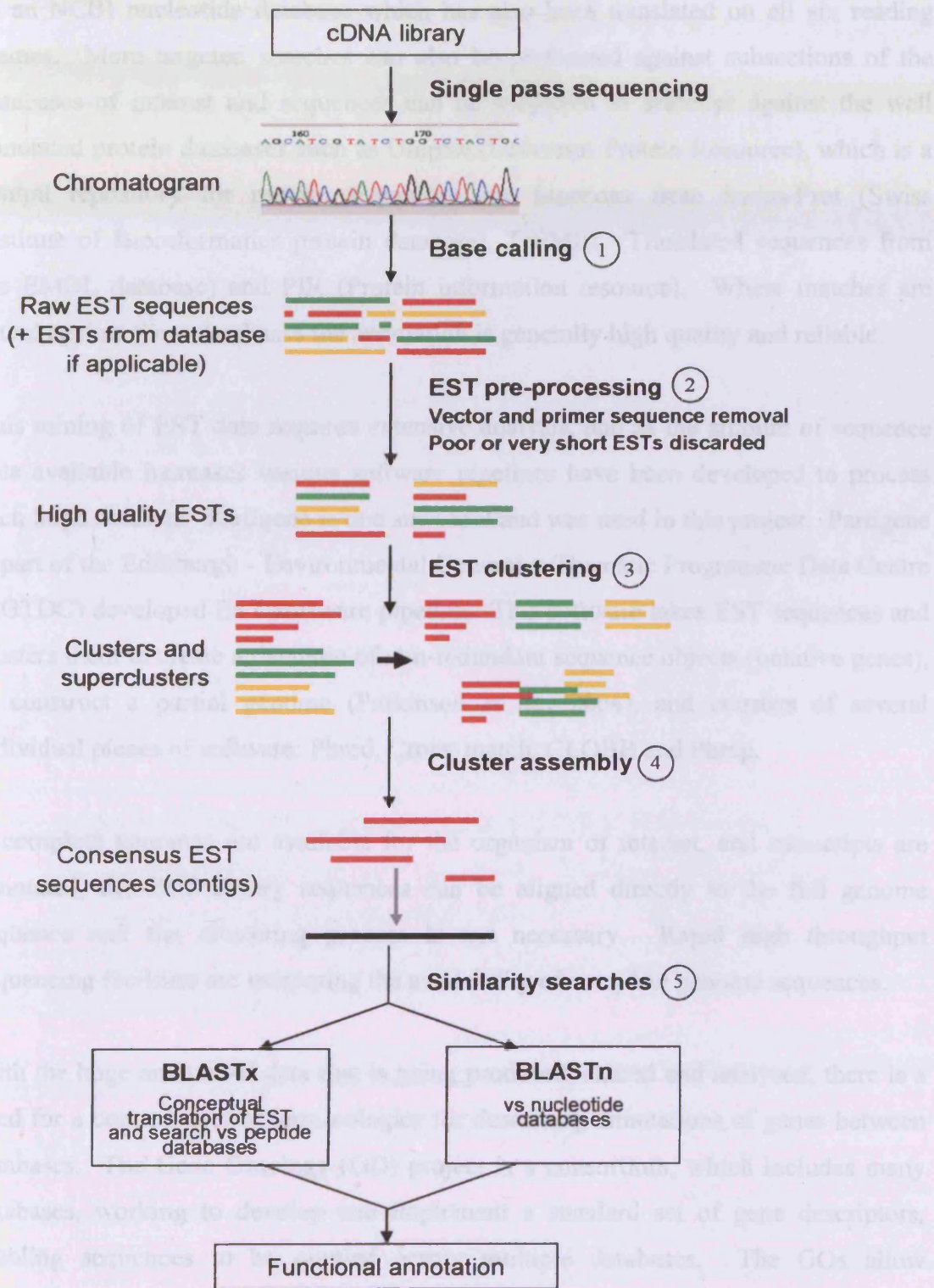


Figure 6.1 Summary of the basic steps involved in EST analysis.

query sequence into peptide sequences in all 6 reading frames and then compares this to an NCBI nucleotide database which has also been translated on all six reading frames. More targeted searches can also be performed against subsections of the databases of interest and sequences can be subjected to searches against the well annotated protein databases such as Uniprot (Universal Protein Resource), which is a central repository for protein sequences and functions from Swiss-Prot (Swiss Institute of Bioinformatics protein database), TrEMBL (Translated sequences from the EMBL database) and PIR (Protein information resource). Where matches are found against these databases the annotation is generally high quality and reliable.

This mining of EST data requires extensive analysis, and as the amount of sequence data available increases various software pipelines have been developed to process such large datasets. Partigene is one such tool and was used in this project. Partigene is part of the Edinburgh - Environmental Genomics Thematic Programme Data Centre (EGTDC) developed EST-software pipeline. This software takes EST sequences and clusters them to create a database of non-redundant sequence objects (putative genes), to construct a partial genome (Parkinson *et al.*, 2004), and consists of several individual pieces of software: Phred, Cross\_match, CLOBB and Phrap.

If complete genomes are available for the organism of interest, and transcripts are annotated, the EST library sequences can be aligned directly to the full genome sequence and the clustering process is not necessary. Rapid high throughput sequencing facilities are increasing the availability of complete genome sequences.

With the huge amount of data that is being produced, shared and analysed, there is a need for a common set of terminologies for describing annotations of genes between databases. The Gene Ontology (GO) project is a consortium, which includes many databases, working to develop and implement a standard set of gene descriptors, enabling sequences to be queried across multiple databases. The GOs allow researchers to assign properties to the genes they are annotating at different levels, depending on the depth of annotation required. GOs are principally divided into three sections: biological process – a recognised series of events or molecular functions; molecular function – that describes activities that occur at the molecular level such as binding; and cellular component – that describes the part of a cell in which the gene



functions. A single gene can be associated with all of these groupings, and within these can be active in one or more biological processes, cell components or molecular functions. GOs can be linked to consensus sequences to assign putative functions using a program called Blast2GO (Conesa *et al.*, 2005).

### 6.1.1 Objectives

The specific objectives of this chapter were to:

- Obtain EST sequences for the set of forward and reverse subtracted SSH clones, that were used for microarray analysis
- Analyse EST libraries by pre-processing, clustering and generating contig consensus sequences to represent putative genes
- Use cluster analysis to verify the efficiency of the SSH used to construct the libraries
- Apply annotations and gene ontologies to putative gene sequences, to identify the biological processes and molecular functions with which they are associated, and their locations within cells.
- Submit ESTs to dbEST

## 6.2 Materials and Methods

Ten 96 well plates of glycerol stocks (960 clones) from both the forward and reverse subtracted libraries (1920 total) were prepared for sequencing as follows:

### 6.2.1 PCR with clones from glycerol stocks

A master mix for 100 samples was made up for each 96 well plate, allowing 4 extra reactions for pipetting discrepancies. Reagents for one 100  $\mu$ l reaction were as follows: dH<sub>2</sub>O, 75.6  $\mu$ l; 10x PCR reaction buffer, 10.0  $\mu$ l; M13F (10  $\mu$ M), 1.0  $\mu$ l; M13R (10  $\mu$ M), 1.0  $\mu$ l; *Taq* polymerase (purified in house), 0.125  $\mu$ l. All reagents were kept on ice during preparation and the glycerol stock plate was taken out of the freezer to thaw briefly, just before required. Master mix (100  $\mu$ l) was pipetted into each well of a 96-well PCR plate (ABgene Ltd., Epsom, UK), then 4  $\mu$ l of the glycerol stock was pipetted into the corresponding wells of the PCR plate using a multichannel pipette. Wells were sealed with cap strips (ABgene Ltd), labelled and then thermal cycling was according to the following programme: 95°C 10 min; [95°C 1 min, 56°C 1 min, 72°C 3 min] for 35 cycles; 72°C 10 min; 4°C  $\infty$ , in a PE2700 PCR machine (Applied Biosystems, CA, USA).

### 6.2.2 Purification of colony PCR products

PCR products were purified using a Millipore Montage Multiscreen  $\mu$ 96 plate (Millipore, LSKM PCR10). All of the samples (100  $\mu$ l) were transferred by pipetting into the corresponding wells of the millipore plate. Plates were transferred to a vacuum manifold (Packard Bioscience, US) and vacuum applied until the whole sample was drawn through (approximately 10 min) leaving empty wells. The bottom of the plate was blotted on absorbent paper and 30  $\mu$ l sterile polished H<sub>2</sub>O pipetted into each well. Plates were then shaken for 8 min on a DPC<sup>®</sup> Micromix 5 (Promega) (Function 9, Amplitude 50). A portion of each sample (5  $\mu$ l) was transferred to a fresh 96 well plate, sealed with a foil lid and stored at -20°C until it was sent to the Edinburgh Sequencing facility, part of the NERC Molecular Genetics Facilities. The

remaining sample (25  $\mu$ l) was transferred to another 96 well plate, sealed with a foil lid and also stored at -20°C until required for microarray printing (Chapter 7).

### 6.2.3 Sequencing

Purified colony PCR products were single pass sequenced using a ABI3730 sequencer and M13F primer (GTTTTCCCAGTCACGACGTTG) at the Edinburgh Sequencing Facility. Files were returned as chromatogram files (.abi) and raw sequence files (.seq).

### 6.2.4 Partigene

Firstly, raw sequences were stripped of contaminating vector sequence then, the Partigene software pipeline (Parkinson *et al.*, 2004) was used to process EST sequences to create a database of non-redundant sequence objects (putative genes) to construct a partial genome. Three cluster analyses were performed: *T. versicolor* EST sequences from this project alone (TVC); *T. versicolor* ESTs from this project and *Saccharomyces cerevisiae* ESTs from Genbank (TYC); *T. versicolor* ESTs from this project and 5606 *T. versicolor* ESTs from Genbank (NCBI) (TTC). Statistical analyses were performed using Minitab 14.0.

#### 6.2.4.1 Cross\_match

Cross\_match was used to locate and remove pGEM T-Easy vector and M13 primer sequences from ESTs leaving only insert

#### 6.2.4.2 CLOBB

Vector/primer trimmed sequences were clustered based on sequence similarity using CLOBB (Parkinson *et al.*, 2002). Clusters of sequences, with a minimum overlap of 30 bp, were identified and related clusters were identified as 'superclusters'. Sequences with no matches were identified as 'singletons'.

### 6.2.4.3 *Phrap*

Clusters were assembled into consensus sequences (Contigs) using Phrap (P. Green<sup>©</sup>, 1994-1999) (Forcelevel 10).

### 6.2.5 **BLAST similarity searches**

Bulk BLAST searches were performed on a pool of Bio-Linux machines using Condor (Thain *et al.*, 2005).

BLASTn searches were performed with all contigs and singletons against the cDNA database for *Saccharomyces cerevisiae* from Ensembl ([www.ensembl.org](http://www.ensembl.org)) and Basidiomycota corenucleotide and EST sequences from Genbank (NCBI).

BLASTx searches were also performed with all contigs and singletons against: the Uniprot peptide database ([www.ebi.uniprot.org](http://www.ebi.uniprot.org)); the *S. cerevisiae* peptide database downloaded from Ensembl; and 71530 peptide sequences for Basidiomycota from Genbank (NCBI).

tBLASTx searches were performed against the non-redundant (nr) nucleotide database from Genbank (NCBI).

Blast results were parsed to produce an .xml file with only the top hit for each search included. E-values were used to assess the significance of BLAST search results. E-values  $\leq 0.0001$  (1E-04) were considered to be significant hits.

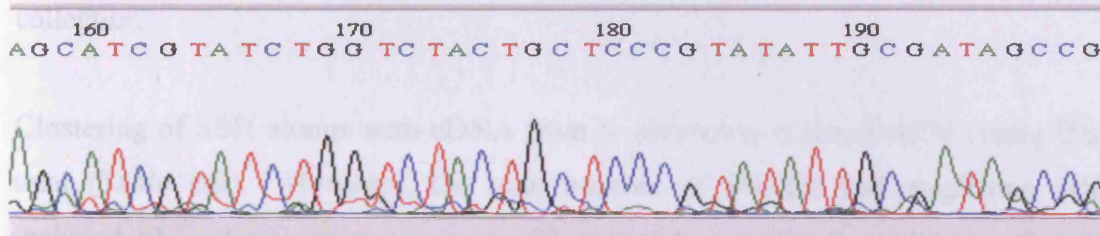
### 6.2.6 **Blast2GO**

The web-based gene ontology analysis tool Blast2GO (Conesa *et al.*, 2005; [www.blast2go.de](http://www.blast2go.de)) was used to search for gene ontologies corresponding with contig BLAST search results. Cluster sequences were imported into Blast2GO in a concatenated FASTA file format and subjected to BLAST and InterPro scans. Gene ontologies were then mapped onto these results and annotations applied. Gene ontologies recovered were separated according to level 2 classifications: biological process, molecular function and cell component, then further separated into level 3 classifications.

## 6.3 Results

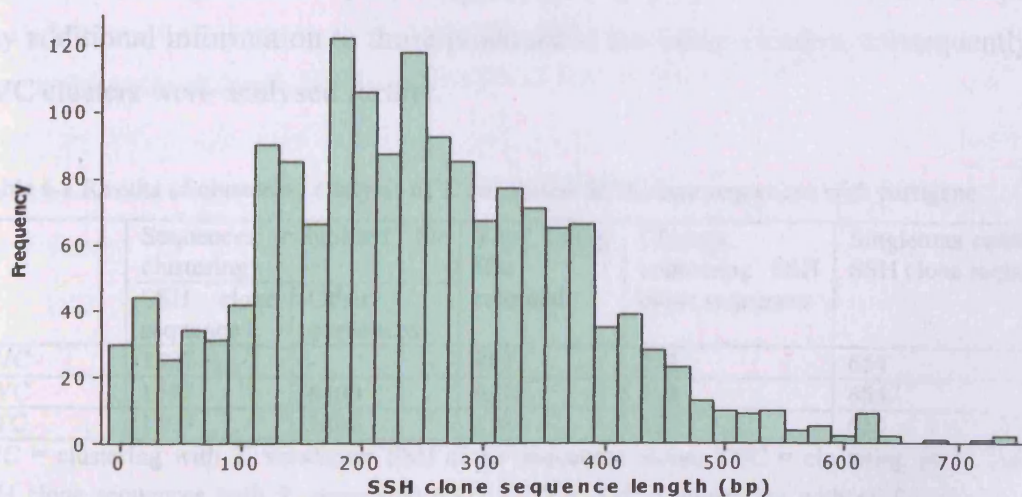
### 6.3.1 Sequencing

Chromatograms (Figure 6.2) returned from sequencing indicated that the sequences were of variable quality and many appeared to contain runs of A nucleotides, indicating that those clone fragments were from the non-coding poly A tail of cDNAs. Ninety-six sequencing reactions failed completely, yielding a total of 1824 SSH clone sequences.



**Figure 6.2** Example of a high quality sequence chromatogram. Note the distinct peaks for each base, which enable accurate base calling. A – adenine; C – cytosine; T – thymine; G – guanine.

Once vector and primer sequences had been removed, SSH clones sequences were between 1 – 749 bp long, with mean sequence length 244 bp and median 237 bp (Figure 6.3).



**Figure 6.3** Frequency distribution for SSH clone sequence length (base pairs - bp) after vector and primer sequence removal. Mean sequence length = 244 bp, median = 236.50 bp, StDev = 126.88 bp.

### 6.3.2 Clustering analysis with Partigene

Only 1439 of the 1824 *T. versicolor* SSH clone sequences entered into partigene went into clustering analysis, as poor sequences and sequences less than 50 bp long were omitted. This total comprised 789 forward and 650 reverse subtracted SSH clone sequences. Cluster analysis of *T. versicolor* SSH clones alone produced 228 clusters (containing >1 sequence) and 654 singletons (containing only 1 sequence), resulting in a total of 882 unique contig IDs i.e. all singleton sequences and cluster consensus sequences combined (Table 6.1). Redundancy of the EST library was calculated to be 55% (number of ESTs in clusters/total number of ESTs; Sterky *et al.*, 1998). Therefore, any new sequence has a 55% chance of already being represented in the collection.

Clustering of SSH clones with cDNA from *S. cerevisiae* returned 6826 contig IDs in total (Table 6.1). However, the total number of clusters and singletons, which included SSH clone sequences, was 228 and 654 respectively, indicating that SSH clone sequences and *S. cerevisiae* cDNA sequences had segregated and no clustering between these two sets of sequences had occurred. This was confirmed by inspection of the contents of clusters. Similarly, clustering of *T. versicolor* SSH clones with *T. versicolor* ESTs downloaded from Genbank returned 6566 contig IDs, with 227 clusters and 655 singletons consisting of *T. versicolor* SSH clone sequences (Table 6.1). This indicates that there was segregation between the two sets of sequences submitted for sequence analysis. Clustering analyses TYC and TTC did not provide any additional information to those produced in the initial clusters, consequently only TVC clusters were analysed further.

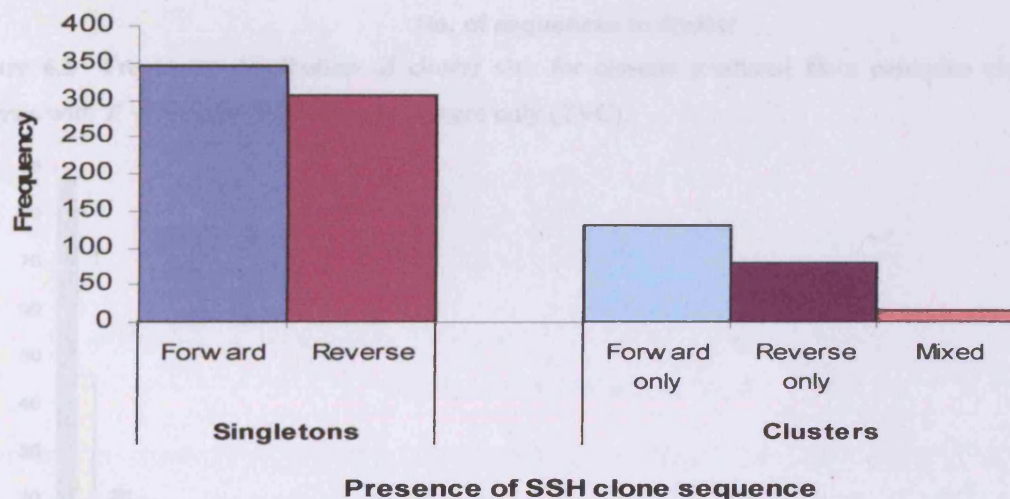
**Table 6.1** Results of clustering analysis of *T. versicolor* SSH clone sequences with partigene

	Sequences submitted for clustering		Total contig IDs returned	Clusters containing SSH clone sequences	Singletons containing SSH clone sequences
	SSH clone sequence	Other sequences			
TVC	1597	-	882	228	654
TYC	1597	6400	6826	228	654
TTC	1597	5606	6566	227	655

TVC = clustering with *T. versicolor* SSH clone sequences alone; TYC = clustering of *T. versicolor* SSH clone sequences with *S. cerevisiae* ESTs (TYC); TTC = clustering with of *T. versicolor* SSH clone sequences with *T. versicolor* ESTs.

### 6.3.3 Analysis of clustering of *T. versicolor* SSH clone sequences

Of the 228 clusters within the 882 contig IDs produced by partigene, 132 contained forward subtracted clones only, 80 contained reverse subtracted clones only and 16 were mixed. The 654 singletons comprised 346 forward and 308 reverse subtracted clone sequences (Figure 6.4).



**Figure 6.4** Representation of forward and reverse subtracted SSH clone sequences within the singletons and clusters identified using partigene clustering of all *T. versicolor* SSH clone sequences

Clusters contained an average of 3.4 sequences with a range between 2 - 29 sequences in total (Figure 6.5). Clusters containing only forward subtracted SSH clones tended to have fewer sequences within them (mean no. of sequences in cluster = 2.86) compared with clusters containing only reverse subtracted SSH clones (mean no. of sequences in cluster = 3.62) (Figure 6.6). Although there was one large cluster of 27 sequences that contained only forward subtracted clones (Figure 6.6). Where clusters were mixed they contained either predominantly forward or reverse clones (Figure 6.7), with the exception of one cluster (cluster 13), which was divided equally (4 forward + 4 reverse).

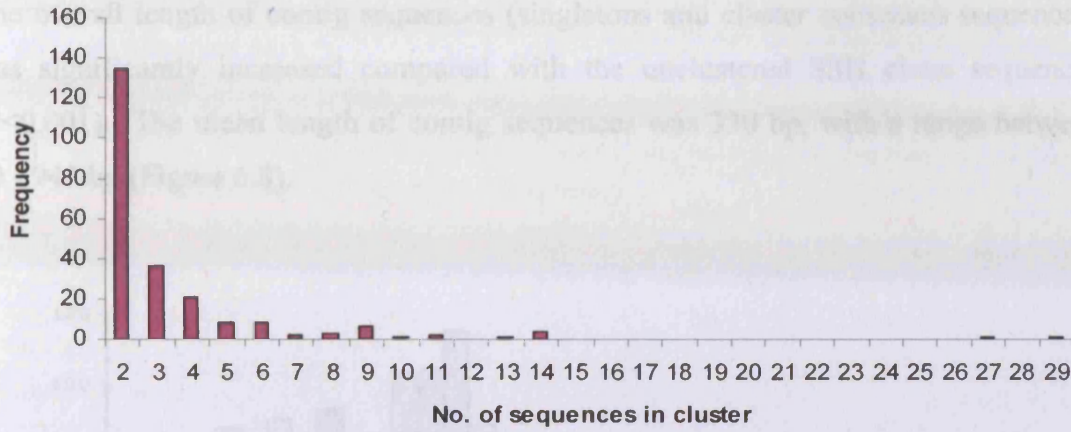


Figure 6.5 Frequency distribution of cluster size for clusters produced from partigene clustering analysis with *T. versicolor* SSH clone sequences only (TVC).

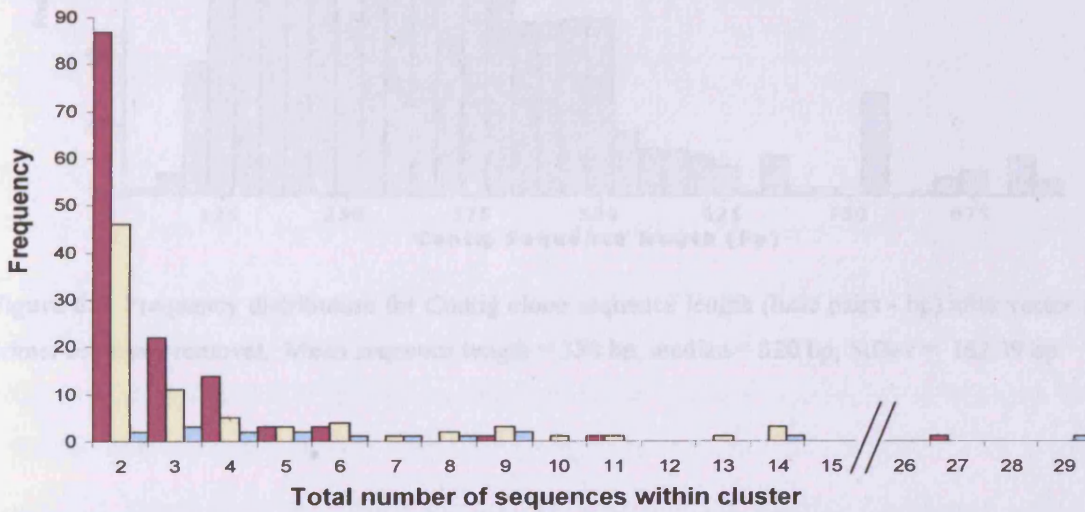


Figure 6.6 Frequency distribution of cluster size for clusters containing only containing forward subtracted SSH clones (red), reverse subtracted SSH clones only (yellow) and mixed clusters (blue).

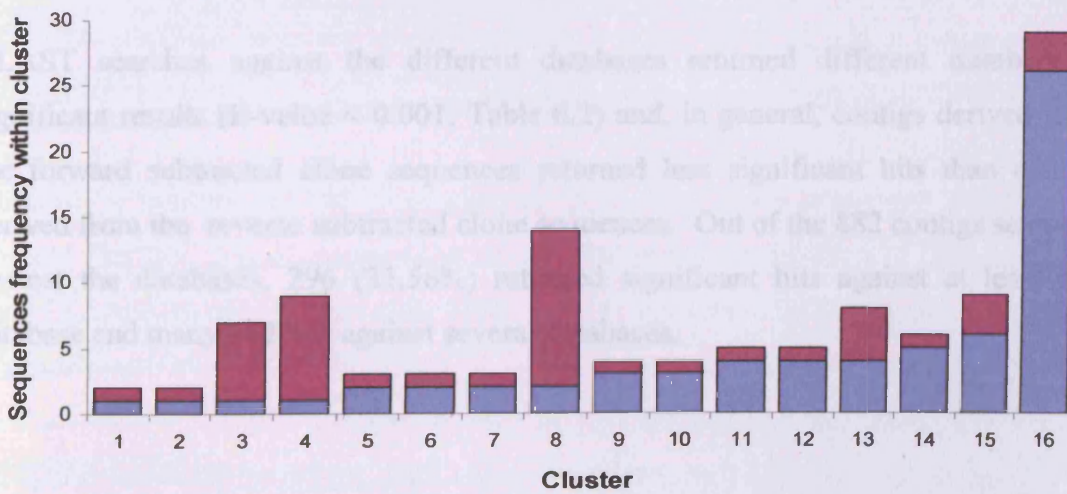
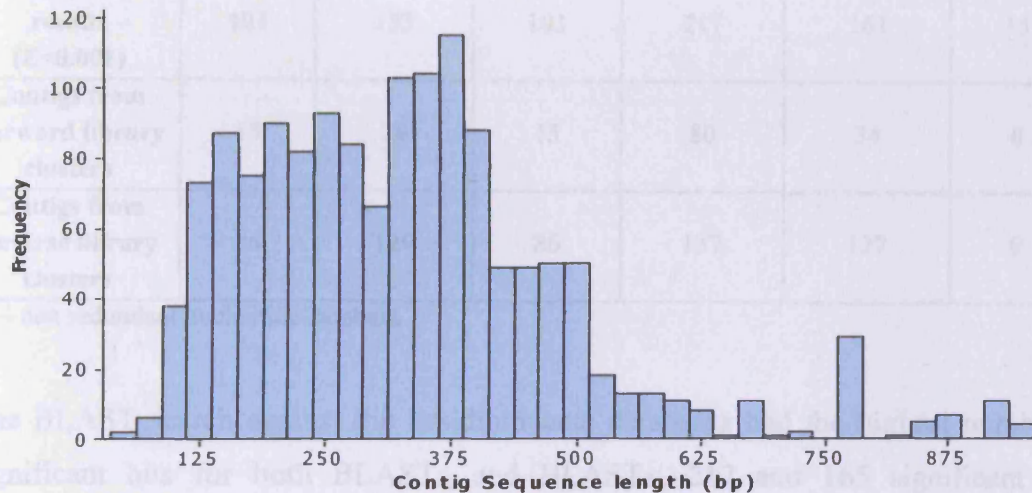


Figure 6.7 Distribution of forward and reverse SSH clone sequences within mixed clusters. Note that apart from cluster 13 all clusters contain predominantly forward or reverse clone sequences. Red = Reverse SSH clone sequence; Blue = Forward SSH clone sequence.



The overall length of contig sequences (singletons and cluster consensus sequences) was significantly increased compared with the unclustered SSH clone sequences ( $P < 0.001$ ). The mean length of contig sequences was 330 bp, with a range between 50 - 941 bp (Figure 6.8).



**Figure 6.8** Frequency distribution for Contig clone sequence length (base pairs - bp) after vector and primer sequence removal. Mean sequence length = 330 bp, median = 320 bp, StDev = 162.39 bp.

### 6.3.4 BLAST search results

BLAST searches against the different databases returned different numbers of significant results (E-value < 0.001; Table 6.2) and, in general, contigs derived from the forward subtracted clone sequences returned less significant hits than contigs derived from the reverse subtracted clone sequences. Out of the 882 contigs searched against the databases, 296 (33.56%) returned significant hits against at least one database and many had hits against several databases.

**Table 6.2** Summary of significant results returned from BLAST searches of 882 submitted contig sequences vs different databases

	Uniprot	Genbank nr	Uniprot	Basidiomycete databases		<i>S. cerevisiae</i> databases	
	Peptide	Nucleotide	Peptide	Corenucl + ESTs	Peptide	cDNA	Peptide
	BLASTx	tBLASTx	BLASTx	BLASTn	BLASTx	BLASTn	BLASTx
<b>Total significant results (E&lt;0.001)</b>	101	153	101	217	161	15	87
<b>Contigs from Forward library clusters</b>	15	24	15	80	34	6	15
<b>Contigs from Reverse library clusters</b>	86	129	86	137	127	9	72

nr – non redundant nucleotide database

The BLAST search against the basidiomycete databases had the highest number of significant hits for both BLASTn and BLASTx, 217 and 165 significant hits, respectively (Table 6.2). However, the descriptions returned for significant hits in general were not informative. All 217 significant hits returned for BLASTn were either undescribed EST mRNA sequences from various species or sequences from genome sequencing projects with no functional annotations available. In general, BLASTx searches against the *S. cerevisiae* and Uniprot peptide databases, produced fewer significant hits but where there were hits, they were informative and provided descriptions of putative gene function. tBLASTx searches against the Genbank non-redundant database returned more significant results, many of which mirrored those returned from Uniprot.

Analysis of contigs derived from clusters with 10 or more sequences within them showed that the largest cluster (TVC00014, Table 6.3), consisting of 29 sequences, was *Taq* polymerase. The only other contig for which a significant result was returned was TVC00429, consisting of 14 sequences, which was putatively identified as a peroxidase. Other contigs returned significant BLAST hits with cDNA clone ESTs and provided no information about their function (Table 6.3) or no significant hits were retrieved.

**Table 6.3** Blast results for contigs with ten or more sequences within them

ContigID	Seq#	F	R	Putative function	E-value	Database
TVC00014	29	26	3	DNA polymerase I, thermostable (EC 2.7.7.7) (Taq polymerase 1)	1.00E-124	UniprotX
TVC00017	27	27		<i>Trametes versicolor</i> cDNA clone	2.00E-30	BasidN
TVC00429	14	2	12	Peroxidase	4.00E-10	tBLASTx
TVC00653	14	-	14	none found	-	-
TVC00870	14	-	14	none found	-	-
TVC00991	13	-	13	none found	-	-
TVC00031	11	11		none found	-	-
TVC00807	11	-	11	<i>Pleurotus ostreatus</i> cDNA clone,	1.00E-69	BasidN
TVC00568	10	-	10	none found	-	-

Seq# - Total number of sequences within cluster

F- No. of sequences from Forward SSH clones

R- No. of sequences from Reverse SSH clones

UniprotX – BlastX results vs Uniprot peptide database

BasidN – BlastN result vs Basidiomycota DNA database

TBLASTx – tBlastX results vs the NCBI non-redundant database

The forward library yielded significant hits for 105 contigs but very few that allowed annotation as most results were to other ESTs or genome sequences. The majority of results from the basidiomycete databases did not yield informative descriptions of gene function, most were described as hypothetical or predicted proteins. Uniprot and *S. cerevisiae* peptide and tBLASTx searches yielded significant results for a total of 25 contigs with informative descriptions of putative function (Figure 6.4). Where there were hits from more than one database the descriptions were the same and the Uniprot description and E-value is reported. Of those that were annotated, a number of potentially stress-related genes were identified (Table 6.4), such as peroxidase, aryl alcohol dehydrogenase, heat shock proteins, ubiquitin-conjugating enzymes and translationally controlled tumour proteins (TCTP). Cytochrome oxidase, a vacuolar membrane protein, a putative actin and a yippee-like protein were also identified (Table 6.4). The most common annotation was for a putative peroxidase (10 contigs).

A total of 191 contigs from the reverse library produced significant hits overall, with the results from the Uniprot (86) and *S. cerevisiae* (72) peptide and tBLASTx vs nr (129) databases again providing 107 informative annotations (Table 6.5). The most abundant annotations were for a peroxidase (from *Musa acuminata*), ribosomal proteins and cytochrome c oxidase, and other putative functions included ATP synthase, beta tubulin, cell division cycle proteins, proteases, catalase, zinc transporters, protein synthesis, metabolism enzymes and respiratory enzymes. Four

contigs were identified as *Taq* DNA polymerase (3 from the forward library, 1 from the reverse library). As in the forward library, peroxidase was the most abundant functional annotation (14 contigs).

**Table 6.4** Summary of the significant BLAST results for the Forward library with informative annotation

Contig ID	Seq#	Putative function	E-value	Database
TVC00357	1	Yippee-like protein – zinc binding	8.00E-04	Uniprot
TVC00534	2	HBS1-like protein (heat shock protein)	3.00E-07	Uniprot
TVC00534	1	Actin 9 - cytoskeleton	7.00E-10	Uniprot
TVC00117	1	Aryl alcohol dehydrogenase	1.00E-14	Uniprot
TVC00180	1	Ubiquitin-conjugating enzyme E2	32.00E-05	Uniprot
TVC00101	4	Cytochrome c oxidase	2.00E-21	Uniprot
TVC00144	3	Cytochrome c oxidase	2.00E-55	Uniprot
TVC00047	3	Cytochrome c oxidase	1.00E-11	Uniprot
TVC00224	2	Translationally controlled tumour protein	1.00E-10	Uniprot
TVC00181	1	Acidic proline-rich protein PRP25	3.00E-04	Uniprot
TVC00395	1	Vacuolar membrane protein	3.00E-07	Uniprot
TVC00091	2	DNA polymerase I, thermostable	4.00E-39	Uniprot
TVC00014	26	DNA polymerase I, thermostable	1.00E-124	Uniprot
TVC00027	1	DNA polymerase I, thermostable	5.00E-55	Uniprot
TVC00122	1	Peroxidase	5.00E-08	tBLASTx
TVC00337	1	Peroxidase	3.00E-07	tBLASTx
TVC00455	1	Peroxidase	6.00E-08	tBLASTx
TVC00264	1	Peroxidase	3.00E-11	tBLASTx
TVC00232	1	Peroxidase	3.00E-09	tBLASTx
TVC00260	1	Peroxidase	2.00E-07	tBLASTx
TVC00191	1	Peroxidase	9.00E-06	tBLASTx
TVC00432	1	Peroxidase	2.00E-04	tBLASTx
TVC00403	1	Peroxidase	7.00E-06	tBLASTx
TVC00458	1	Peroxidase	4.00E-04	tBLASTx
TVC000356	1	Golgi transport related	4.00E-10	tBLASTx

Seq# - Total number of sequences within cluster

UniprotX – BlastX results vs Uniprot peptide database

tBLASTx – tBlastX results vs the NCBI non-redundant database

**Table 6.5** Summary of the significant BLAST results for the reverse subtracted library with informative annotation

Contig ID	Seq#	Putative function	E-value	Database
TVC00655	3	1,3-beta-glucan synthase component bgs2	7.00E-15	UniprotX
TVC01166	1	2-oxoisovalerate dehydrogenase beta subunit, mitochondrial precursor	3.00E-15	UniprotX
TVC01211	1	30S ribosomal protein S2	2.00E-06	UniprotX
TVC00914	1	40S ribosomal protein S4	1.00E-55	UniprotX
TVC00789	1	50S ribosomal protein L21, mitochondrial precursor	7.00E-05	UniprotX
TVC00799	1	60S ribosomal protein L17	6.00E-12	UniprotX
TVC00712	1	60S ribosomal protein L19	3.00E-07	UniprotX
TVC00695	2	60S ribosomal protein L38	5.00E-13	UniprotX
TVC00582	3	60S ribosomal protein L38-1	7.00E-05	UniprotX
TVC01123	1	60S ribosomal protein L39	1.00E-18	UniprotX
TVC00835	2	60S ribosomal protein L44	5.00E-39	UniprotX
TVC01120	1	Acyl-CoA fatty acid desaturase	2.00E-24	UniprotX
TVC00801	1	Acyl-CoA fatty acid desaturase	1.00E-20	UniprotX
TVC01230	2	Acyl-CoA fatty acid desaturase	3.00E-15	UniprotX
TVC00863	1	Aldehyde reductase I	2.00E-47	UniprotX
TVC01129	1	Amino acid transporter	4.00E-13	tBLASTx
TVC00577	1	Aminomethyltransferase, mitochondrial precursor	9.00E-08	UniprotX
TVC00855	1	AMP deaminase 2	5.00E-28	UniprotX
TVC01018	1	Aorsin precursor	1.00E-08	UniprotX
TVC01107	1	Arginine biosynthesis bifunctional protein argJ	3.00E-04	UniprotX
TVC01083	1	Aspartyl-tRNA synthetase	8.00E-09	UniprotX
TVC00808	1	ATP synthase beta chain, mitochondrial precursor	2.00E-08	UniprotX
TVC01223	1	Beta-glucan synthesis-associated protein KRE6	5.00E-19	UniprotX
TVC00765	1	C-8 sterol isomerase	2.00E-33	UniprotX
TVC00884	1	Catalase	7.00E-13	UniprotX
TVC00832	2	Catalase	4.00E-34	UniprotX
TVC01101	1	Cell division control protein 16	2.00E-11	UniprotX
TVC00951	1	Cell division control protein 3	2.00E-10	UniprotX
TVC01222	1	Chloroplast 50S ribosomal protein L6	1.00E-09	UniprotX
TVC01200	1	Clathrin coat assembly protein AP50	3.00E-28	UniprotX
TVC00932	1	Cullin-1	1.00E-07	UniprotX
TVC01047	1	Cytochrome c oxidase subunit 1	1.00E-49	tBLASTx
TVC01187	1	Cytochrome c oxidase subunit 1	3.00E-11	UniprotX
TVC00590	1	Cytochrome c oxidase subunit 1	3.00E-16	UniprotX
TVC00973	1	Cytochrome c oxidase subunit 1	6.00E-26	UniprotX
TVC01140	1	Cytochrome c oxidase subunit 1	8.00E-72	UniprotX
TVC00689	5	Cytochrome c oxidase subunit 1	1.00E-31	UniprotX
TVC00724	2	Cytochrome c oxidase subunit 2	1.00E-39	UniprotX
TVC00650	1	Cytochrome P450 51	1.00E-05	UniprotX
TVC01234	1	Cytochrome P450 51	7.00E-05	UniprotX
TVC01196	1	DNA polymerase I, thermostable	3.00E-68	UniprotX
TVC00802	1	Electron transfer protein 1, mitochondrial precursor	2.00E-04	UniprotX
TVC00985	1	Elongation factor 1-alpha	8.00E-33	UniprotX
TVC00784	1	Elongation factor 2	1.00E-112	UniprotX
TVC01145	1	Elongation factor 2	3.00E-23	UniprotX
TVC00674	1	Eukaryotic initiation factor 4A	1.00E-09	UniprotX
TVC00574	9	Glycogen debranching enzyme	9.00E-15	UniprotX
TVC00770	1	Glycolipid 2-alpha-mannosyltransferase	6.00E-17	UniprotX
TVC00952	1	GPI transamidase component GAB1 homolog	9.00E-08	UniprotX

**Table 6.5 (continued)** Summary of the significant BLAST results for the reverse subtracted library with informative annotation

Contig ID	Seq#	Putative function	E-value	Database
TVC00936	1	GrpE protein homolog, mitochondrial precursor	4.00E-16	UniprotX
TVC01076	1	GrpE protein homolog, mitochondrial precursor	1.00E-04	UniprotX
TVC00638	2	GrpE protein homolog, mitochondrial precursor	2.00E-13	UniprotX
TVC00575	1	GTP-binding protein YPTC1	9.00E-19	UniprotX
TVC01073	1	High-affinity zinc transport protein ZRT1	8.00E-18	UniprotX
TVC00856	1	Histidinol-phosphate aminotransferase	4.00E-07	UniprotX
TVC01110	1	Hypothetical 107.7 kDa protein in TSP3-IPP2 intergenic region	7.00E-12	UniprotX
TVC01231	1	Hypothetical 49.1 kDa protein in ND3 intron	2.00E-06	UniprotX
TVC00968	1	Hypothetical protein C1861.01c in chromosome II	8.00E-04	UniprotX
TVC00812	1	Inosine-5'-monophosphate dehydrogenase	3.00E-09	UniprotX
TVC01046	1	Intersectin 1	5.00E-06	UniprotX
TVC00573	2	Intron-encoded DNA endonuclease a14 precursor	3.00E-34	UniprotX
TVC00743	2	intronic ORF at intron 6 of cox1	8.00E-53	BasidX
TVC01241	1	large subunit ribosomal RNA gene	3.00E-29	tBLASTx
TVC01209	1	large subunit ribosomal RNA gene	5.00E-16	tBLASTx
TVC00587	1	large subunit ribosomal RNA gene	4.00E-12	tBLASTx
TVC01008	1	Low-affinity zinc transport protein ZRT2	1.00E-05	UniprotX
TVC01057	1	Methoxy mycolic acid synthase 1	7.00E-05	UniprotX
TVC00917	1	Mitochondrial intermediate peptidase, mitochondrial precursor	5.00E-51	UniprotX
TVC00643	2	Mitogen-activated protein kinase	1.00E-17	UniprotX
TVC00679	1	NADPH oxidase homolog 1	8.00E-15	UniprotX
TVC01149	1	Peroxidase	5.00E-12	tBLASTx
TVC01031	1	Peroxidase	5.00E-10	tBLASTx
TVC01000	1	Peroxidase	6.00E-07	tBLASTx
TVC00760	1	Peroxidase	3.00E-06	tBLASTx
TVC01148	1	Peroxidase	5.00E-06	tBLASTx
TVC00749	1	Peroxidase	7.00E-06	tBLASTx
TVC01109	1	Peroxidase	2.00E-05	tBLASTx
TVC01039	2	Peroxidase	8.00E-06	tBLASTx
TVC00678	2	Peroxidase	9.00E-04	tBLASTx
TVC00982	3	Peroxidase	2.00E-11	tBLASTx
TVC00811	3	Peroxidase	1.00E-10	tBLASTx
TVC00959	6	Peroxidase	2.00E-09	tBLASTx
TVC00830	9	Peroxidase	3.00E-05	tBLASTx
TVC00429	14	Peroxidase	4.00E-10	tBLASTx
TVC01172	1	Phenylalanyl-tRNA synthetase beta chain	2.00E-18	UniprotX
TVC00567	1	Phosphoglucomutase	4.00E-11	UniprotX
TVC00902	1	Pre-mRNA processing splicing factor 8	3.00E-31	UniprotX
TVC00844	1	Probable acyl-CoA desaturase	1.00E-04	UniprotX
TVC00641	2	Probable dolichyl pyrophosphate Glc1Man9GlcNAc2 alpha-1,3-glucosyltransferase	5.00E-10	UniprotX
TVC00841	1	Probable ornithine aminotransferase	4.00E-05	UniprotX
TVC00838	1	Probable reductase	9.00E-14	UniprotX
TVC00834	2	Probable small nuclear ribonucleoprotein Sm D3	6.00E-27	UniprotX
TVC00603	3	Putative dioxygenase C576.01c	2.00E-23	UniprotX
TVC00611	2	Putative endonuclease segE	3.00E-04	UniprotX
TVC01229	1	Putative helicase C6F12.16c	6.00E-20	UniprotX
TVC00900	1	Putative propionyl-CoA carboxylase beta chain, mitochondrial precursor	5.00E-35	UniprotX
TVC00825	1	Retinal-specific ATP-binding cassette transporter	5.00E-09	UniprotX
TVC00600	1	Septin homolog spn1	3.00E-21	UniprotX

**Table 6.5 (continued)** Summary of the significant BLAST results for the reverse subtracted library with informative annotation

Contig ID	Seq#	Putative function	E-value	Database
TVC01192	1	Septin homolog spn1	4.00E-04	UniprotX
TVC00775	1	serine/threonine kinase receptor associated protein	5.00E-08	tBLASTx
TVC01250	1	Synaptic glycoprotein SC2	7.00E-13	UniprotX
TVC00769	1	Synaptic glycoprotein SC2	7.00E-08	UniprotX
TVC00740	1	Threonyl-tRNA synthetase, cytoplasmic	3.00E-24	UniprotX
TVC00969	1	Tubulin beta-2 chain	4.00E-11	UniprotX
TVC00737	1	Tumor necrosis factor ligand superfamily member 6	0	UniprotX
TVC00948	1	Ubiquinol-cytochrome c reductase complex 14 kDa protein	8.00E-19	UniprotX
TVC01191	1	Ubiquitin-conjugating enzyme E2 15	2.00E-22	UniprotX

Seq# - Total number of sequences within cluster

UniprotX – BlastX results vs Uniprot peptide database

BasidX – BlastX results vs basidiomycete peptide database

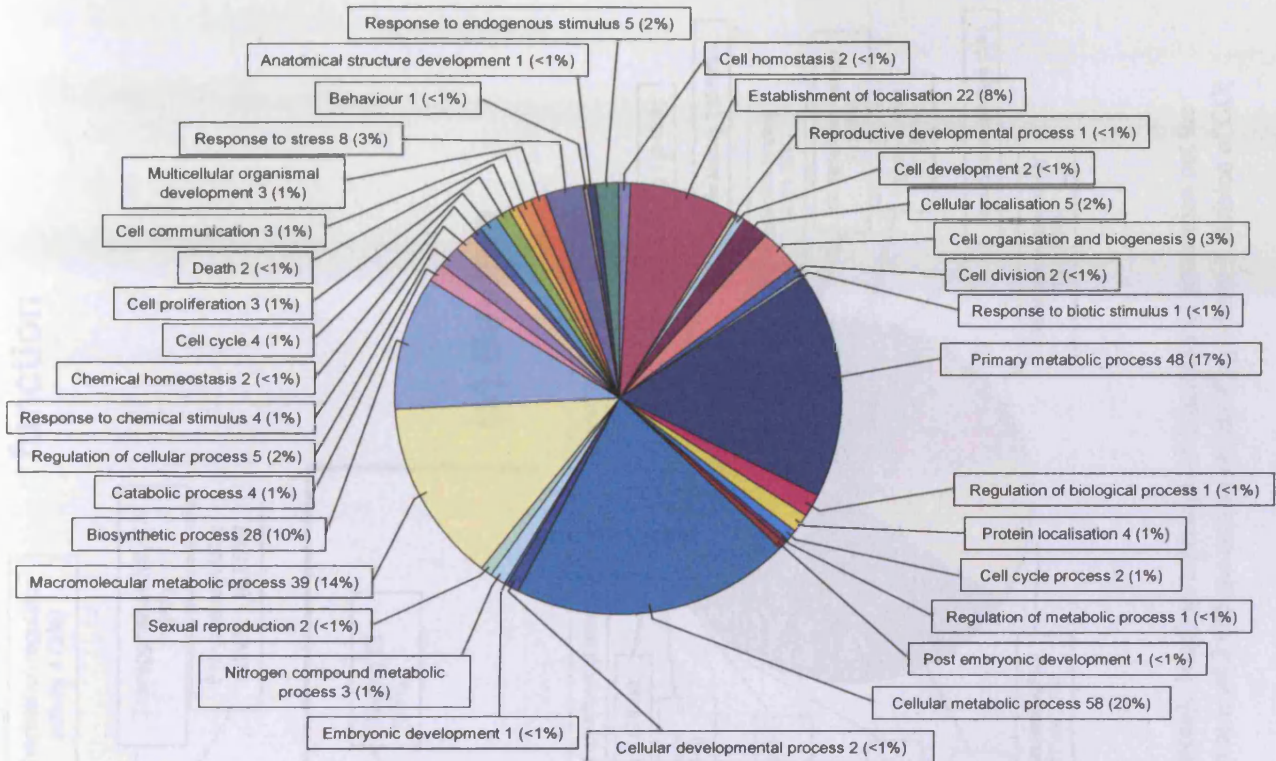
TBLASTx – tBlastX results vs the NCBI non-redundant database

### 6.3.5 Gene Ontology

Ninety-eight of the 882 contigs submitted to Blast2go had gene ontologies (GOs) associated with them. These 98 were from within the 101 significant Blast hits against the Uniprot database (Table 6.2). Not all significant Blast hits had GOs associated with them. Many contigs had multiple ontological annotations, with between 1-11 GOs being assigned to a single contig sequence, and there was overlap in the classifications contigs were allocated to.

#### 6.3.5.1 Biological process

Seventy-two contigs were associated with biological process GOs (Figure 6.9). Single contigs often had more than one GO associated with them and the percentages in pie charts (Figure 6.9) are the percentage of the relative frequency of annotation; the number is the number of gene objects (contigs) within each class. The most abundant annotation classes were primary metabolism (17%), cellular metabolism (20%), macromolecular metabolism (14%) and biosynthesis (10%).



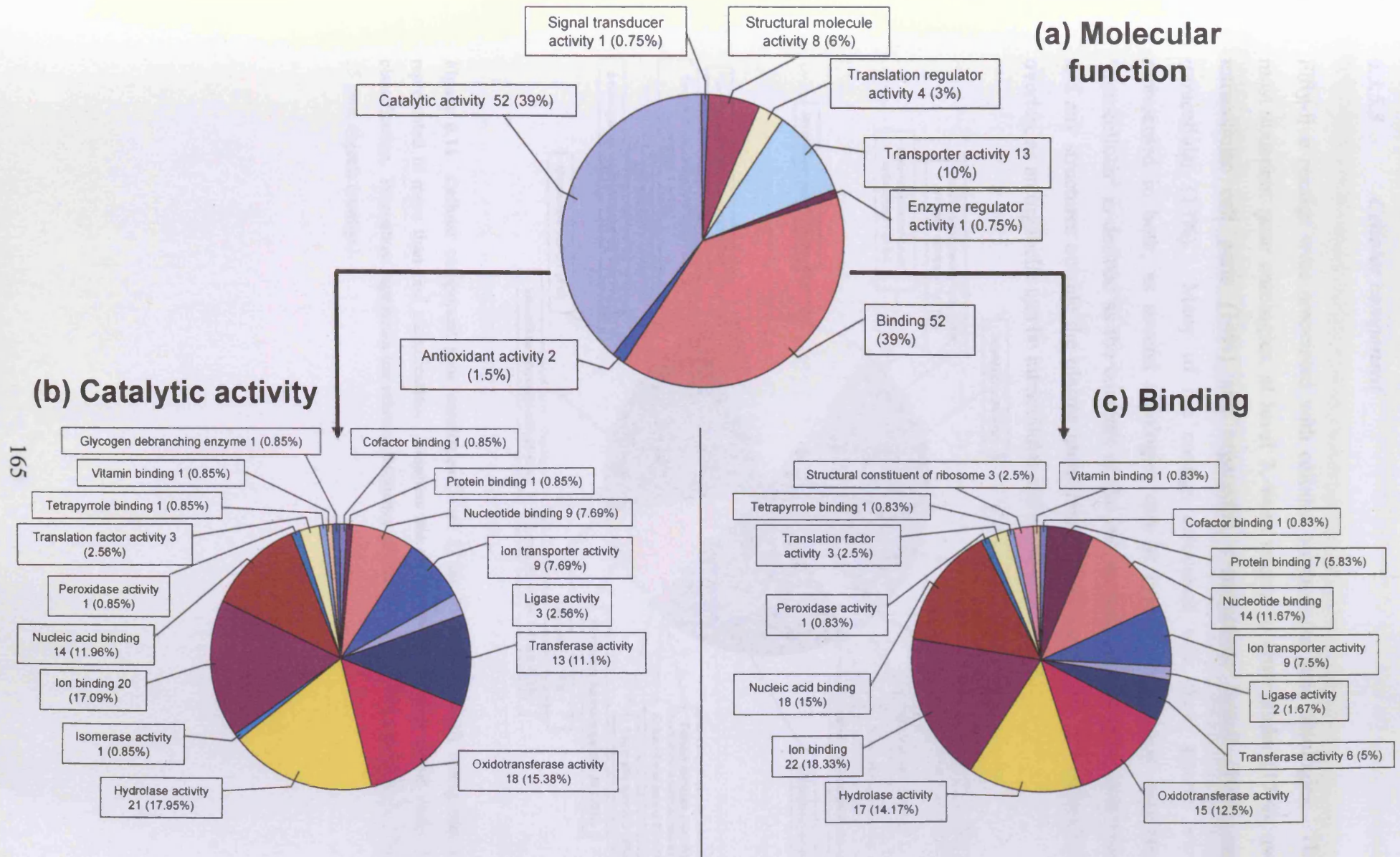
**Figure 6.9** Biological process gene ontologies (level 3) for 72 contigs. Each contig may be represented in more than one classification. Numbers are the number of contigs within each GO classification. Percentage represents the relative frequency of each annotation, not a percentage of the 72 gene objects (contigs).

### 6.3.5.2 Molecular function

Seventy-eight contigs were annotated with involvement in molecular functions (Figure 6.10 a). Single contigs were often represented in more than one classification, hence the percentage is the proportion of the relative frequency of each annotation classification, and the number is the number of contigs within each classification. Binding and catalytic activity were the major ontology groups applied to contigs, with the majority (52) of the 78 contigs associated with both ontologies. The 52 contigs represented in binding and catalytic activity were not necessarily the same contigs, although there was some overlap.

When the level 2 ontologies binding and catalytic activity, for the 52 contigs described by each, were divided further to level 3 ontologies (Figure 6.10 b,c), the largest groups within both were ion binding, hydrolase activity, oxidoreductase activity and nucleic acid binding (Figure 6.10 b, c)

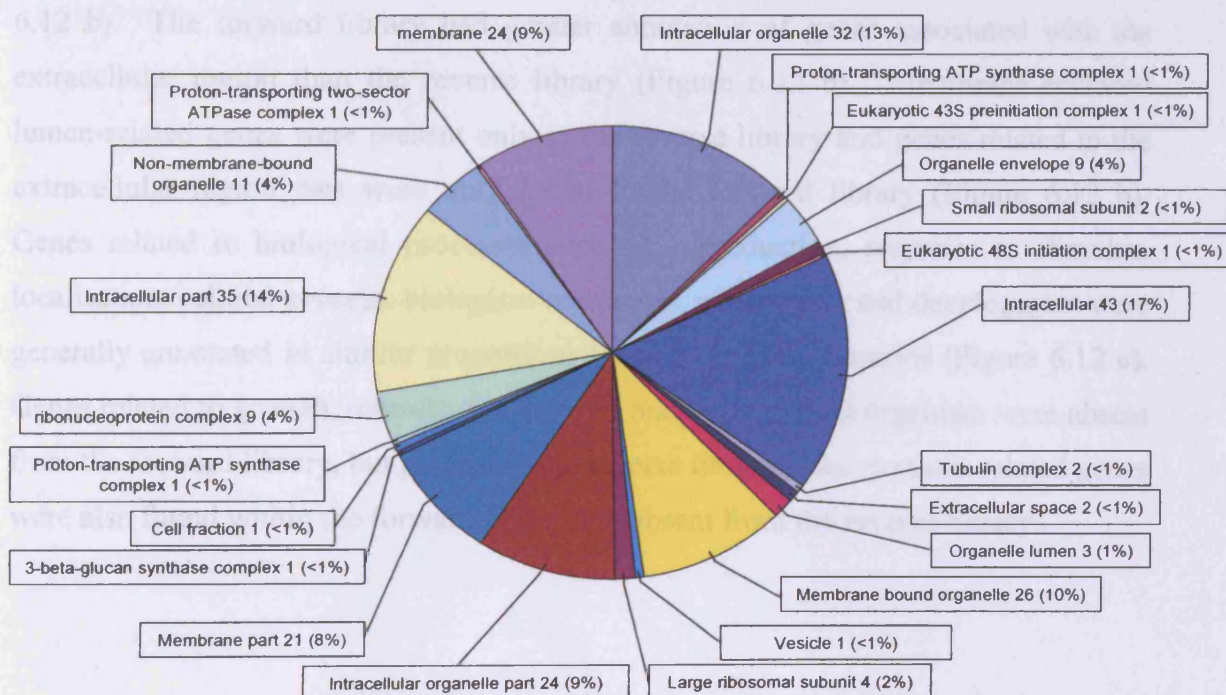




**Figure 6.10** Molecular function gene ontologies (GOs) for all *T. versicolor* contig sequences (clusters + singletons). Numbers represent the frequency of annotation not the total number of contigs as some may be allocated to more than one group. (a) Molecular function of all contigs at level 2 GO annotation; (b) Binding – level 3 division of GO; (c) Catalytic activity – level 3 division of GO.

## 6.3.5.3 Cellular component

Fifty-five contigs were associated with cellular components gene ontologies. The most abundant gene ontologies, at level 3, were related to intracellular (17%), and intracellular cell parts (14%) and organelles - membrane bound (10%) and intracellular (13%). Many of the contigs associated with these groups were represented in both, as several ontologies can be applied to a single sequence. 'Intracellular' is defined as the contents of the cell excluding the plasma membrane and any structures outside the plasma membrane. These ontologies also potentially overlap, as an organelle can be intracellular and membrane bound.

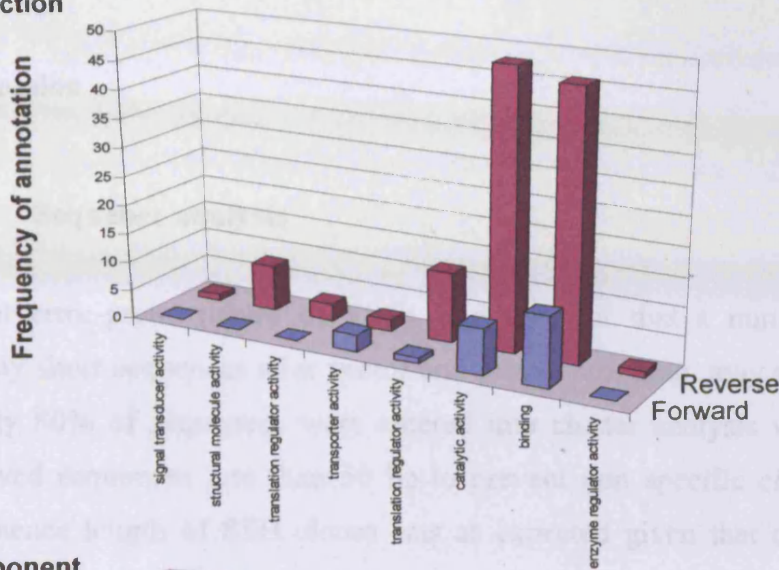


**Figure 6.11** Cellular component gene ontologies (level 3) for 55 contigs. Each contig may be represented in more than one classification. Numbers are the number of contigs within each GO classification. Percentage represents the relative frequency of each annotation, not a percentage of the 55 gene objects (contigs).

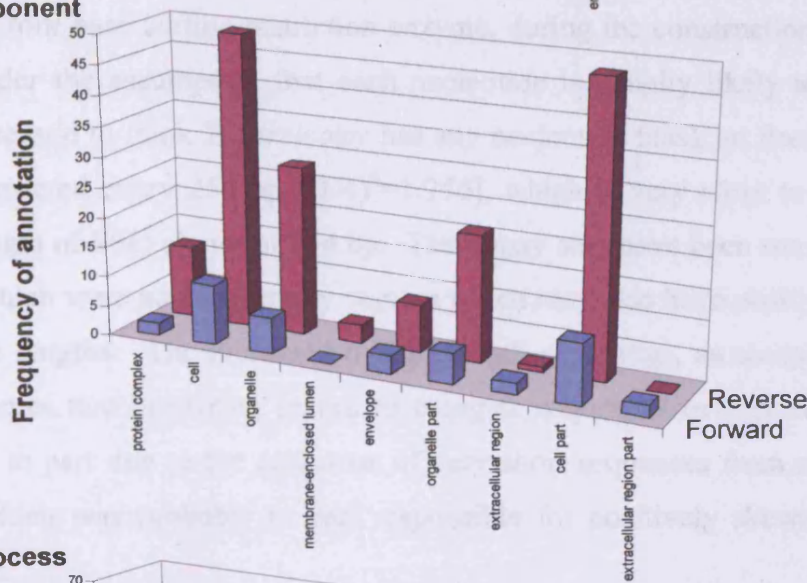
#### 6.3.5.4 *Forward and Reverse SSH libraries*

Where molecular function classifications were represented in both forward and reverse libraries (transporter activity, translation regulator activity, catalytic activity and binding) the relative frequencies were similar, with catalytic activity and binding the most abundant in both forward and reverse libraries (Figure 6.12 a). The reverse library also had genes associated with signal transduction, structural molecule activity, translation regulation and enzyme regulation, which were not found in the forward library (Figure 6.12 a). The relative frequency of classifications within the cellular component were also similar between forward and reverse libraries (Figure 6.12 b). The forward library had greater annotation of genes associated with the extracellular region than the reverse library (Figure 6.12 b). Membrane-enclosed lumen-related genes were present only in the reverse library and genes related to the extracellular region part were only found in the forward library (Figure 6.12 b). Genes related to biological processes such as, reproduction, response to stimulus, localisation, cellular process, biological regulation, metabolism and development were generally annotated in similar proportions between the two libraries (Figure 6.12 c). Genes related to growth, reproductive process and multicellular organism were absent from the forward library, but present in the reverse library. Homeostasis related genes were also found within the forward library but absent from the reverse library.

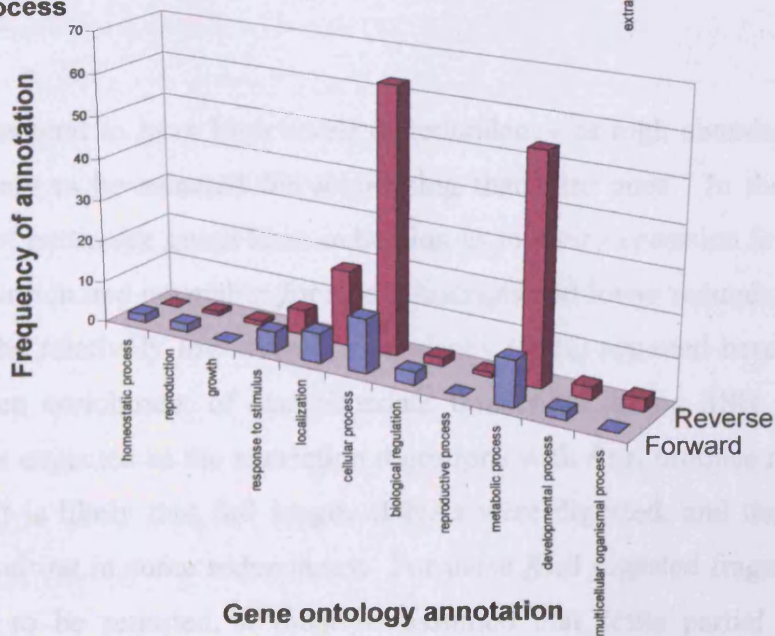
(a) Molecular function



(b) Cellular component



(c) Biological process



Gene ontology annotation

Figure 6.12 Graphs showing the relative proportions of each function class in forward and reverse subtracted libraries for each of the level 2 Gene Ontologies: (a) Molecular function; (b) Cellular component; (c) Biological process.

## 6.4 Discussion

### 6.4.1 Sequence analysis

The inherent error-prone nature of ESTs, and the fact that a number of clones produced only short sequences after vector and primer stripping, may account for the fact that only 80% of sequences were entered into cluster analysis with partigene, which removed sequences less than 50 bp to prevent non specific clustering. The average sequence length of SSH clones was as expected given that cDNA was cut with *RsaI*, a four base cutting restriction enzyme, during the construction of the SSH library. Under the assumption that each nucleotide is equally likely to be present (there is no reason to think *T. versicolor* has any nucleotide bias), an *RsaI* cutting site would be expected every 256 bp  $[(1/4)^4=1/256]$ , which is very close to the average sequence length of SSH clones at 244 bp. There may also have been some very short sequences which were actually empty vectors which may also have positively skewed the sequence lengths. The increased overall length of contigs, as compared to SSH clones, indicates that clustering served to elongate sequences overall, although this may also be in part due to the exclusion of very short sequences from clustering by partigene, which was probably in part responsible for positively skewing the SSH clone lengths.

ESTs libraries tend to have high levels of redundancy as high abundance transcripts are more likely to be selected for sequencing than rare ones. In these cases high redundancy of particular genes is an indication as to their expression level. However, SSH should enrich and normalise for rare transcripts and lower redundancies might be expected. The relatively low overall redundancy (55%) reported here indicates that there has been enrichment of less abundant transcripts during SSH. A degree of redundancy is expected as the restriction digestions with *RsaI* produce relatively short fragments. It is likely that full length cDNAs were digested, and then reunited by clustering resulting in some redundancy. For these *RsaI* digested fragments from the same cDNA to be reunited, it must be assumed that some partial digestion has occurred, which will allow overlap of sequences. Many clusters with only 2 constituent sequences were found, which may be due to this phenomenon.

The similar redundancy levels between the forward (52%) and reverse (50.2%) libraries indicates that the SSH subtraction was of equal efficiency for the two libraries. Although the data appear to show a larger number of singletons and clusters derived from the forward SSH library sequences, the failed 96 well plate of sequencing was from the reverse library, which may account for this discrepancy. Furthermore, the general segregation of forward and reverse SSH clones into clusters and the low number of mixed clusters (those with forward and reverse sequences within them) implies that the subtraction was good, as one might expect more overlap between forward and reverse sequences if the subtraction was unsuccessful. Mixed clusters may have arisen from inefficient subtraction, or if the ESTs were from gene families which had sufficient homology to overlap and be clustered together, despite being different, but related genes. If this was the case then those related genes could be expressed under different circumstances, be present in the different libraries, but still cluster together. It would be interesting to look at the expression profiles of the sequences within these clusters to see if they are different during the microarray analysis.

Although clusters were generally smaller, the greater total number of clusters from the forward library, suggests that a larger number of putative genes were identified from clustering analysis than in the reverse library. Fewer, and generally larger, clusters from the reverse library indicates that those putative genes identified are fewer in number, but perhaps more abundant, which might be consistent with the reverse library consisting of predominantly housekeeping genes.

The large number of singletons from the clustering analysis may represent unique and rare transcripts, which are enriched by SSH. However, a number of these singletons are also likely to be poor sequences that were not filtered during pre-processing, or sequences with a few bases errors which prevented their clustering. The clustering with CLOBB in the partigene pipeline is highly stringent and only a few base differences may lead to sequences being left out of clusters. High stringency produces more reliable clusters, but may reduce the overall number of clusters derived from the analysis.

The segregation of sequences during the clustering of SSH clones with *S. cerevisiae* ESTs indicated that the *T. versicolor* SSH sequences were distinct from those of *S. cerevisiae*, which is perhaps expected as the two species, although both fungi, are evolutionarily very distant (James *et al.*, 2006) and the ascomycetes and basidiomycetes are thought to have diverged at least 400 million years ago (Taylor & Berbee, 2006). Therefore in the future it could be beneficial to relax the clustering parameters to allow clustering of these sequences, given the knowledge that they are likely to be more divergent. However, it was perhaps surprising that the clustering analysis of SSH clones with *T. versicolor* ESTs from Genbank did not result in the mixing of sequences from the two groups within clusters. The ESTs from Genbank were derived from an EST project in Concordia University (Canada) and it is possible that the isolates of *T. versicolor* were genetically distinct due to their geographical separation. The isolate used in this study was from the UK, and there may be allelic differences, which would prevent clustering. However, some homology in conserved genes would be expected. Furthermore, when contigs were submitted for BLAST homology searches there were matches found with *T. versicolor* cDNA clone sequences from Concordia University, indicating that the clustering analysis was not able to match up sequences where there were indeed homologies. Again, this may be due to the high stringency of the CLOBB software used for clustering within the partigene pipeline. This analysis could perhaps be repeated with an alternative clustering program. There may also be chimeric sequences present within the SSH clones which would prevent clustering with other *T. versicolor* ESTs, although this would be expected to be the case for only a small proportion of sequences. As the clustering of SSH sequences with other sets of ESTs did not add to the clusters from those produced with just SSH sequences (TVC), only those from the SSH were carried forward for further analysis.

Clustering analysis is useful for EST analysis, especially in non-model organisms, although there is clearly potential for error. If the complete genome sequence for *T. versicolor* were available it would enable the direct alignment of the SSH sequences with full length gene sequences within the genome and remove the need for clustering. Full length gene sequences for expressed genes could be found, which would improve the chance of being able to annotate transcripts functionally.

### 6.4.2 Functional annotation

Although the return of significant BLAST results was not high (33.56 % overall), this is perhaps not unexpected, as fungi are generally underrepresented within the nucleotide and peptide databases and the complete genome sequence of *T. versicolor* is not available. The contigs from the reverse library are those reduced or absent from the interaction, many of which are likely to be housekeeping genes. This may explain the greater number of significant BLAST hits, as compared with the forward library contigs. The forward library should contain genes differentially expressed during the interaction and may include many genes which have not previously been identified and characterised. If this is the case less significant hits for annotation would be expected. Where BLASTn results against nucleotide databases were significant they were not particularly informative as the majority of returns were from genome sequencing projects or from other unidentified cDNA clone ESTs. BLASTx and tBLASTx searches produced more significant results. The conceptual translation of sequences into peptides means that any variation in codon usage in *T. versicolor*, compared with other species within the database, should not prevent matches with the database, which might occur with BLASTn searches. As previously discussed with respect to clustering, the low number of significant BLAST results against the *S. cerevisiae* nucleotide and peptide databases probably reflects the genetic distance between *T. versicolor* and *S. cerevisiae* and highlights the need for annotated full genome sequences of more closely related fungi to be available. The Uniprot database represents well characterised genes and annotations and although there were relatively few significant hits against this database, where there were hits they were generally useful for assigning function to putative genes. The Uniprot, tBLASTx and BLASTx vs *S. cerevisiae* gave the most informative annotations and underlines the need to select databases wisely.

The assignment of gene ontologies (GOs) to putative genes was low, relative to the number of significant BLAST results returned. However, generally, GOs were assigned to those contigs which returned significant hits against the Uniprot database. GOs are only assigned to well characterised genes and therefore a large number of GOs assigned to these libraries would not be expected. Molecular function is perhaps the most informative of the gene ontologies as it refers to specific activities within the



cell, which may offer more insight into the processes active in the mycelium. The biological process ontology is a rather broad classification defined as ‘a series of events accomplished by one or more ordered assemblies of molecular functions’. However, both of these classifications, together with the cellular component GOs provide some information about the main processes active in both libraries. In this case, binding and catalytic activity were predominant, which might be expected in general housekeeping processes. A high catalytic activity might be expected within regions of mycelial growth where opposing mycelia are potentially sensing each other, interacting and competing, particularly in *T. versicolor*, which has well documented extracellular enzyme activity (Baldrian, 2004). The gene ontologies are developed from genes that have mainly been studied and functionally annotated in other organisms, hence any functions or locations derived from GOs should be treated as guidelines for functional annotation as some genes may have different roles and locations within other organisms.

Putative genes from the reverse library were generally assigned putative functions as housekeeping genes. This would be expected as the reverse subtracted library should contain only genes which are not expressed in *T. versicolor* during an interaction. Functions such as respiration (cytochrome oxidase, ATPase), metabolism (hexose degradation, glycogen debranching, zinc uptake), the cytoskeleton (tubulin, septin, actin), protein synthesis (ribosomal proteins, elongation factors) and cell division are all likely to be involved in ‘normal’ growth of *T. versicolor*. However, the expression of genes involved in these process may also change during interactions, and this may be shown during the microarray analysis. Catalase activity was identified in the reverse library, which is usually associated with coping with oxidative stress. This might not be expected to be present in ‘housekeeping’ genes. However, mycelium is damaged during the harvesting for use in constructing the SSH libraries, which might induce some sort of defence response, similar to the oxidative burst produced by plants in response to wounding and interactions (Splivallo *et al.*, 2007). Although mycelium was harvested quickly, and flash frozen, perhaps there was sufficient time for a defence response to be triggered in *T. versicolor* growing alone, during harvesting.

The forward subtracted library should consist of putative genes active during the interaction of *T. versicolor* and *S. gausapatum*. Although the majority of BLAST results for the forward library were non-informative genome sequences or ESTs, the hits against the Uniprot database and the tBLASTx results, which included stress response genes, may represent the sorts of genes that are active during interactions. Mycelium harvested from interacting *T. versicolor* was also subject to the same possibility of induction of stress responses. However, proportionally, 'stress' genes are better represented in the forward library, suggesting that their expression is primarily due to the interaction. Some of the genes identified are thought to play roles in constitutive growth in some organisms, but this does not necessarily negate a potential role for them during this fungal interaction. Many of the genes identified are only from small clusters (1-3 sequences) and perhaps these are low abundance transcripts active during the interaction, which might not have been detected without the enrichment of the SSH. Many of the genes are relatively common, often highly conserved and are well characterised. This may account for why these genes produced significant hits against the Uniprot database, a database of proteins predominantly from organisms distantly related to basidiomycetes, and were able to be putatively identified. Genes specific to basidiomycetes may not have been identified or studied yet, making functional annotation more difficult as they may be too divergent from other genes within the databases.

Peroxidase was the most abundant function found in both forward and reverse libraries, although it was proportionally better represented within the forward library (Forward: 10 of 25 contigs (40%) (Table 6.4); Reverse: 14 of 107 (13%) (Table 6.5)). Peroxidases are produced by many white-rot fungi (Martínez, 2002; Baldrian, 2004) and are enzymes which use H<sub>2</sub>O<sub>2</sub> to catalyse the oxidation of a variety of inorganic and organic compounds (Martínez, 2002). Peroxidases are involved in the degradation of lignin (Kersten & Cullen, 2007) and are also capable of degrading aromatic hydrocarbons (Babarová *et al.*, 2006) and also in coping with oxidative stress (Silar, 1999). There are different types of peroxidases, including lignin peroxidases and manganese peroxidases (Leonowicz *et al.*, 1999) and their production is dependent on the environmental conditions and the presence of competitors (White & Boddy, 1992; Schlosser *et al.*, 1997; Score *et al.*, 1997; Chi *et al.*, 2007). During interspecific interactions high levels of peroxidase activity have been detected (Bruno

& Sparapano, 2006), which can have heterogeneous patterns of activity (White & Boddy, 1992) and in some cases activity is increased in mixed cultures and particularly localised to the confrontation zone between species (Chi *et al.*, 2007). Silar (2005) showed that some fungi accumulate H<sub>2</sub>O<sub>2</sub> when challenged, similar to the oxidative burst produced by plants. If this is the case then it is likely that a competitor would benefit from the increased production of peroxidases, which may already be being produced for lignin degradation, in order to detoxify the reactive oxygen species produced by the competitor. Peroxidases have been characterised in several species of fungi (Martínez, 2002), including *T. versicolor* (Collins *et al.*, 1999), and it is likely that there are several different genes encoding peroxidases in fungi. The full genome sequence of *Phanerochaete chrysosporium* is available and this has made the discovery of genes much easier. This species has a large and complex family of structurally related peroxidases (Kersten & Cullen, 2007) but there is not necessarily coincident transcriptional regulation of these genes at the same time. Kersten and Cullen (2007) suggest that these structurally related genes may encode proteins with subtle differences in function. This diversity may equip the fungus to deal with a variety of different environments. There are several different clusters that were identified as putative peroxidases here and these may represent slightly different but related peroxidases, or simply sequences that were not able to cluster together because the cDNA was totally digested. One of the contigs identified in the reverse library as a putative peroxidase contained 14 sequences within the cluster, implying that this is a highly expressed gene during constitutive growth. This is perhaps expected as *T. versicolor* is a lignin degrading white-rot fungus and its ligninolytic enzyme production is well documented and exploited for wood pulping and bioremediation. It would be interesting to use 5'RACE to obtain the full length cDNA and characterise the gene and study its expression further.

Aryl alcohol dehydrogenase (AAD) has been detected and characterised in several fungi, predominantly white rot causing species, including *Phanerochaete chrysosporium* (Muheim *et al.*, 1991; Reiser *et al.*, 1994), *Bjerkandera adusta* (Muheim *et al.*, 1990) and *Pleurotus eryngii* (Guillen & Evans, 1994). AAD is found intracellularly, where it reduces aromatic compounds in the presence of NADPH as a cofactor (Muheim *et al.*, 1991; Gutierrez *et al.*, 1994; Delneri *et al.*, 1999), and this allows it to degrade lignin by redox cycling of aromatic compounds, which provide

H<sub>2</sub>O<sub>2</sub> to ligninolytic peroxidases (Gutierrez *et al.*, 1994). In *S. cerevisiae* AAD expression is induced in response to exposure to chemicals that cause an oxidative shock, such as diamide and diethyl meleic acid ester, although the presence of H<sub>2</sub>O<sub>2</sub> had no effect (Delneri *et al.*, 1999). Whereas in *P. chrysosporium* AAD expression correlates with the appearance of lignin peroxidase-specific transcripts in growing cultures (Reiser *et al.*, 1994). AAD has also been implicated in the biosynthesis of aflatoxin by *Aspergillus* spp. (Yu *et al.*, 1995; Cary *et al.*, 1996; Erlich *et al.*, 2004), which involves at least 16 different enzymes (Yu *et al.*, 1995) and is encoded by the aflatoxin biosynthesis pathway gene cluster (Erlich *et al.*, 2004). NorA, a gene found in *Aspergillus* spp., has 49% identity to an aryl-alcohol dehydrogenase (aad) gene from *P. chrysosporium* and its expression is elevated in *Aspergillus parasiticus*, when grown in medium conducive to aflatoxin biosynthesis (Cary *et al.*, 1996). There are several potential roles for AAD in the context of the interaction between *T. versicolor* and *S. gausapatum*. An AAD gene may be expressed by *T. versicolor* in response to the stress of interacting with *S. gausapatum*, and it could play a role in degrading pigments and other toxic compounds produced by *S. gausapatum*. It could also be involved in the production of inhibitory compounds by *T. versicolor* for combat with *S. gausapatum*. It is likely that this gene is also expressed during constitutive growth where lignin degrading enzymes are required, but perhaps it is also upregulated during interactions and thus was present in the forward library. It may be absent from the reverse library because fungi were grown on malt extract medium, rather than wood (i.e. a lignin rich substrate) and hence its expression may not be induced.

Heat shock proteins are highly conserved and are produced in response to heat and after exposure to other environmental stresses (Lindquist, 1992). They tend to perform essential molecular chaperone function in cells and facilitate interactions between proteins during intracellular transport, and their synthesis can be induced at different stages of fungal development (Georg & Gomes, 2007). HBS1 is a member of the heat shock protein subfamily B suppressor 1 (HBS1) and is involved in gene expression, signal transduction, GTP binding and protein biosynthesis (Carr-Schmid *et al.*, 2002) and the HBS1-like (HSB1L) protein identified may have a similar role. In eukaryotes HBS1 is thought to be involved with 'No-go decay' in yeast, which is a mechanism for clearing cells of stalled translation elongation complexes, which might occur as a result of damaged mRNAs or ribosomes (Doma & Parker, 2006). In this

process mRNAs with stalls in translation are recognised and targeted for endonucleolytic cleavage. Similarly, this could be a mechanism of post-translational control. HSB1L has been used as a housekeeping gene in some studies (Thellin *et al.*, 1999; Silver *et al.*, 2006), which might suggest that it is a housekeeping gene that has appeared in the forward library erroneously, as the subtraction is unlikely to have been 100% efficient. However, the gene is uncharacterised and it may have as yet unknown roles during an interaction. Furthermore, there may be increased expression of genes during interactions, which requires more translational machinery during that time.

Proline-rich proteins are well known in plants where they are components of the plant extracellular matrix and are involved in crosslinking in the plant cell wall during development, which may increase wall strength. This can occur rapidly in response to elicitors and perhaps acts as a barrier to pathogen ingress (Bradley *et al.*, 1992). In *S. cerevisiae*, the gene VRP1 encodes a proline rich protein. *Vrp1* mutants show altered cell shape and size, and have aberrant chitin and actin localisation. Thus, this protein is implicated with the actin cytoskeleton and cytokinesis in yeast (Bradley *et al.*, 1992) and may have a similar role in *T. versicolor*.

The most common role of ubiquitin is labelling proteins for proteasomal degradation, but it also has roles in post-translational modification of proteins and intracellular protein localisation (Pines & Lindon, 2005). Indeed, a proteasome-mediated pathway may be involved in the metabolism and regulation of ligninolytic activities in *T. versicolor* (Staszczak, 2002). The ubiquitin-conjugating enzyme (E2) that was identified in the forward library is likely to have a role in catalysing the covalent attachment of ubiquitin molecules to other proteins. In *S. cerevisiae* the RAD6 gene encodes a ubiquitin-conjugating (E2) enzyme and is required for DNA repair and meiosis (Prakash, 1989), and also regulates yeast-hypha morphogenesis in the human pathogen, *Candida albicans*. Its expression is increased in response to UV light, during sporulation and during recombination in meiosis (Madura *et al.*, 1990). However, it was not induced by heat and starvation, which otherwise induce stress responses in yeast. This may imply that RAD6, in yeast at least, is primarily involved in DNA damage repair, rather than coping with stress (Madura *et al.*, 1990). A gene was identified in *Colletotrichum gloeosporioides*, which is very similar (82% identity)

to another *S. cerevisiae* E2 enzyme (UBC4-UBC5), which is particularly active in stressed yeast cells (Liu & Kolattukudy, 1998). This gene was expressed during conidial germination and appressorial differentiation, which implies that there is ubiquitin-dependent protein degradation involved in these processes (Liu & Kolattukudy, 1998). Furthermore, a similar ubiquitin-conjugating E2 enzyme was found to be active during the ectomycorrhizal interaction between the basidiomycete, *Tricholoma vaccinum* and its host spruce, *Picea abies* (Krause & Kothe, 2006). There is a structural and functional homolog to the yeast RAD6 gene in *Schizosaccharomyces pombe*, which is distantly related to *S. cerevisiae*. This gene and its function appear to be conserved across eukaryotes (Reynolds *et al.*, 1990) and perhaps a similar role is found in *T. versicolor*. DNA damage occurs following exposure of fungi to some volatile compounds (Zucchi *et al.*, 2005) and this gene may be involved in DNA repair during these interactions.

Translationally controlled tumour protein (TCTP), is a highly conserved protein, which was originally described in mammalian tumour cells, and a putative homologue was identified here from the forward library. In yeast it may be involved in interactions between mitochondria and microtubules, and may be needed for correct localisation of mitochondria during cell division (Rinnerthaler *et al.*, 2006), although its exact cellular function is yet to be elucidated. In *S. cerevisiae* it is highly expressed during active growth, but down regulated in stress situations (Rinnerthaler *et al.*, 2006). There is also translocation of this enzyme from the cytoplasm to the mitochondria on exposure of *S. cerevisiae* to mild oxidative stress. (Rinnerthaler *et al.*, 2006).

Yippee-like (YPLE) proteins are putative zinc binding proteins, similar to an intracellular *Drosophila* protein (Yippee) which interacts with hemolin, a part of the immunoglobulin superfamily, found in the moth *Hyalophora cecropia* (Roxström-Lindquist & Faye, 2001). There is a YPLE gene family consisting of up to five members, genes appear to be conserved and can be found in 68 different species (Hosono *et al.*, 2004), however, its function is, as yet, unknown.

The identification of four clusters as *Taq* polymerase indicates that there was some contamination from the enzyme used for colony PCR to produce products for

sequencing. PCR products were purified prior to sequencing but perhaps plasmid purifications by mini-prepping might have decreased contamination further, although in this case the scale of amplification and the cost required would be prohibitive. The *Taq* polymerase used was that purified in-house rather than commercial *Taq* which again may have increased the chance of contamination, if some remnants of the *Taq* plasmid, from which the enzyme was overexpressed in *E. coli*, were still present in the *Taq* polymerase mixture put into PCR reactions.

The serine-threonine protein kinase gene identified could have a regulatory function and would potentially be interesting for further study of the temporal and spatial signalling activity in *T. versicolor*, during the interaction. Its presence in the reverse library indicates that it is either absent or downregulated during the interaction. Although the nucleic acid binding gene ontology was well represented, there were no apparent transcription factors, which would also be interesting for further study.

## 6.5 Conclusion

The forward and reverse SSH libraries represent a snapshot of the mRNA composition of mycelia at a certain time. The forward library was enriched for genes upregulated during the interaction between *T. versicolor* and *S. gausapatum*, and the annotation of putative functions has highlighted some interesting candidates that may be involved with the interaction. Examining the expression profiles of these genes during the different fungal interactions using cDNA microarrays will confirm whether these genes are truly differentially expressed during interactions. Furthermore, expression profiles for these putative genes will help to make informed decisions about which genes are important in the interaction and which to study further. Those contigs it was not possible to annotate may also show similar expression profiles and could direct to closer examination of certain sequences to verify clustering analysis. Contigs from the reverse library are those that are either down regulated or absent from the interaction, but their expression may change under different interaction circumstances. Since putative functions could be assigned to many of these contigs, this will help to elucidate some of the mechanisms operating during constitutive growth in basidiomycetes, still relatively unstudied, but may also contribute to our knowledge about the mechanisms of interactions, and which processes are being shut down during an interaction.

## 7. Microarrays

### 7.1 Introduction

There are a number of different methods for studying gene expression. Previously experimental approaches looked at individual genes on a gene-by-gene basis, and the genes studied were often chosen based on educated guesses about which genes might be involved in a particular pathway of interest, or on genes identified from large mutant screens. While these both can yield good results they can be highly labour intensive and eventually the chosen gene may prove not to be differentially expressed in the circumstances studied. Microarray technology has become increasingly popular as it allows the simultaneous global assessment of tens of thousands of genes in a single experiment. Often this is used to determine different patterns of gene expression in a particular type of cell or organism when subjected to different treatments, over time, with different phenotypes or at different developmental stages. Rather than picking candidate genes prior to an investigation, this experimental approach identifies a large set of differentially expressed genes from which particular genes can be selected for further investigation from a significantly better informed standpoint. However, with the advantages that studying thousands of genes at the same time brings there is also the issue of an almost overwhelming volume of data produced by an experiment of this nature, and this remains one of the largest challenges for researchers when tackling microarray technology.

The microarray process can be separated into three main parts: (i) Array fabrication - the production of a matrix of ordered DNA material spotted onto and attached to a solid substrate support; (ii) Probe preparation and hybridisation - two differently labelled fluorescent probes, produced from cells subjected to two different treatments, or of different phenotypes, are co-hybridised to the slide; (iii) Data collection, normalisation and analysis - the relative amount of hybridisation to each spot by the different probes is assessed by measuring the fluorescence of each spot, and this is used to infer different levels of expression (Figure 7.1)



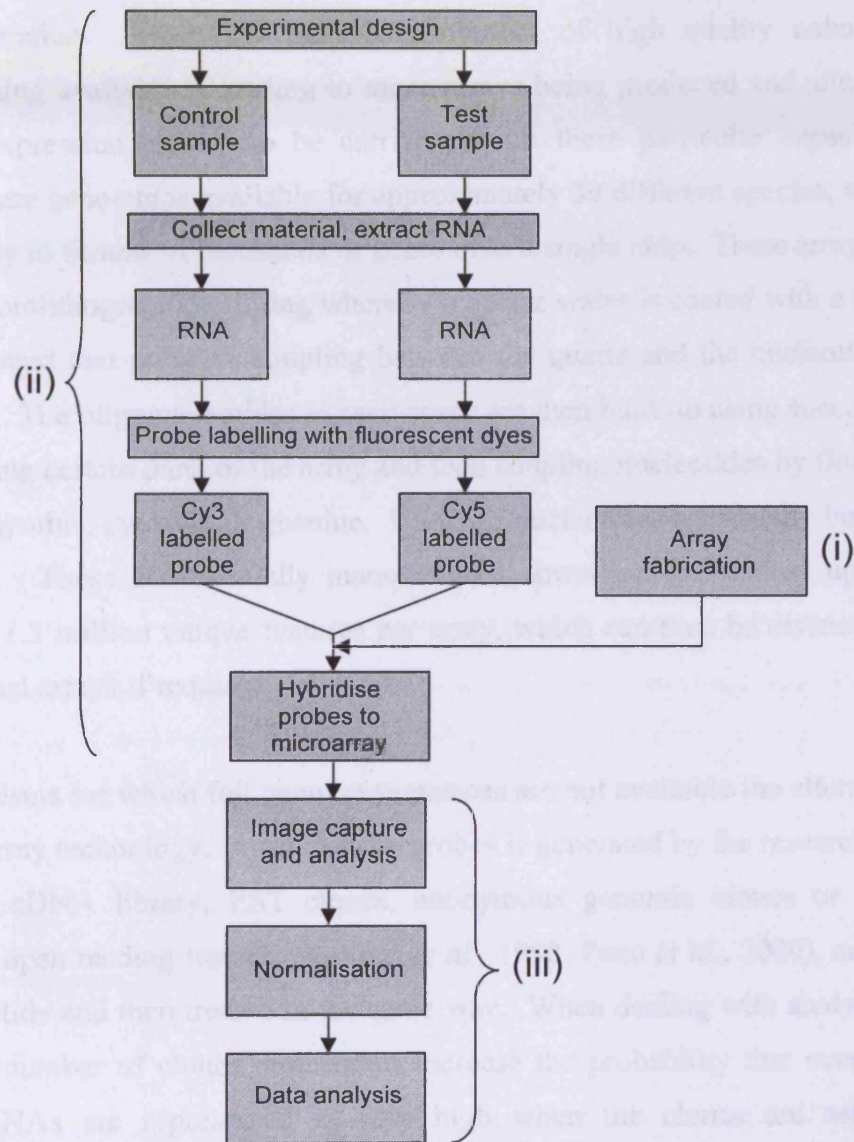


Figure 7.1. Summary of the main stages in microarray analysis.

**7.1.1 Array Fabrication**

There are different microarray platforms currently available for use. Perhaps one of the most popular is the Affymetrix GeneChip<sup>®</sup> oligonucleotide microarray consisting of oligonucleotides constructed from sequence databases. These “gene-chips” are available for many model organisms ranging from multicellular organisms such as

humans, *Drosophila melanogaster*, *Arabidopsis thaliana* and *Danio rerio* to unicellular organisms such as brewer's yeast (*Saccharomyces cerevisiae*) and bacteria (*Escherichia coli*, *Bacillus subtilis*). These types of array are reliant on good sequence information. Thus, the increasing number of high quality annotated genomes becoming available is leading to more arrays being produced and allowing genome-wide expression studies to be carried out on these particular organisms. Currently there are gene-chips available for approximately 30 different species, which have the capacity to fit tens of thousands of genes onto a single chip. These arrays are produced by photolithographic printing whereby a quartz wafer is coated with a light-sensitive compound that prevents coupling between the quartz and the nucleotide of the DNA probe. The oligonucleotides in each space are then built up using successive rounds of masking certain parts of the array and then coupling nucleotides by flooding with adenine, thymine, cytosine or guanine. Up to 25 nucleotides are usually built up onto the quartz. These commercially manufactured arrays can be printed up to a density of over 1.3 million unique features per array, which can then be divided into smaller individual arrays if required.

For those organisms for which full genome sequences are not available the alternative is DNA microarray technology. A set of gene probes is generated by the researcher in the form of a cDNA library, EST clones, anonymous genomic clones or DNA amplified from open reading frames (Welford *et al.*, 1998; Penn *et al.*, 2000), and are printed onto a slide and then treated in the same way. When dealing with analysis of this nature the number of clones required to increase the probability that even low abundance mRNAs are represented is very high when the clones are selected randomly from a cDNA library. Producing an array of this size is not feasible in many cases, including this project. The SSH method used to generate the cDNA clones for the arrays in this project reduces the number of clones necessary to ensure that low abundance transcripts are represented. SSH was used so that only those transcripts whose expression is altered during interactions are included on the array, and housekeeping genes are omitted.

There are various different types of materials available for array fabrication depending on the desired application. In general, microarrays are produced by printing PCR-amplified cDNA clones suspended in a high salt or denaturing print buffer, onto poly-

L-lysine or aminosilane coated glass microscope slides using a robot. The slide surface and the print buffer both have an effect on the hybridisation efficiency, and printing consistency, and thus reproducibility of results. For this experiment aminosilane coated slides were used. Their surface provides available amine groups for ionic bonds to form between the phosphate backbone of the spotted DNA and the solid substrate. Following this initial ionic attachment DNA is covalently fixed to the slide by baking or UV irradiation. Typically PCR products are double stranded but denaturing the fragments allows them to be used for hybridisation experiments. DMSO (50%) is used as the printing buffer as it denatures the DNA, allowing better binding to the slide and providing more single stranded targets for hybridisation. Also, it is hygroscopic, which reduces evaporation from the slide and allows array slides to be stored for extended periods (Hegde *et al.*, 2000).

Many other factors may also affect the quality and consistency of microarray printing with respect to both the size and morphology of spots and the end hybridisation efficiency. The type of robotic system used, the types of pins used for spotting and the environmental conditions during printing (temperature, humidity) all play a role in the success of the microarray. Thus, to ensure consistency of the results, it is vital that all these factors are kept constant.

### 7.1.2 Probe preparation

Labelling with fluorescent probes has become the standard practice when using microarrays, rather than using radioactive labelling which is more hazardous and time consuming. The most commonly used fluorophores are Cy3 and Cy5 which are most reactive and give greatest labelling efficiency. By binding these fluorescent probes to cDNA the levels of hybridisation to the microarray can be assessed by laser excitation at different wavelengths for the two dyes and the intensity of the signal recorded for each spot. Both Cy3 and Cy5 are photosensitive and care is required when handling them to minimise exposure to light, which may result in degradation and ultimately inefficient probe labelling. There are several methods for fluorescently labelling probes including direct and indirect cDNA labelling, cDNA labelling with fluorescent dendrimers, direct mRNA labelling and direct or indirect labelling of amplified RNA.

RNA amplification may be necessary if the amount of starting material available is very small but there is a risk of unequal amplification of transcripts that may leave some of the less abundant transcripts under-represented.

In the direct labelling method, fluorescently modified nucleotides are incorporated into cDNA during first strand synthesis from the starting RNA. However the modified nucleotides tend to be bulky and incorporation efficiency during cDNA synthesis may be low. In addition, the Cy5 molecule is larger than the Cy3 molecule and may result in differential incorporation of the two dyes. Consequently the use of the indirect labelling method (sometimes called post-labelling), the method used in this project, is often favoured. This method involves cDNA synthesis with modified aminoallyl-modified nucleotides, followed by covalent coupling of the NHS-ester of the appropriate fluorescent Cy dyes to the active amino groups of the modified cDNA (Soundy *et al.*, 2001). The aminoallyl nucleotides are less bulky so are incorporated equally in the two probes, and with greater efficiency during reverse transcription thus yielding longer cDNA fragments and resulting in better probe labelling yields (Burke *et al.*, 2001). The fluorescent dendrimer method involves the hybridisation of a fluorescent dendrimer with hundreds of dye molecules per complex to cDNA, post synthesis (Manduchi *et al.*, 2002).

### 7.1.3 Hybridisation

The two different fluorescently labelled cDNA populations are co-hybridised in equal concentrations onto slides. The degree of hybridisation by each cDNA population is assessed by laser excitation of the two different channels and the signal intensity assessed. These measurements are made by comparing the intensity of fluorescence between the background and the spots on the microarray. Thus, it is important to minimise background fluorescence and non-specific binding of labelled cDNA to areas of the slide other than the spot areas. This can be achieved by blocking the slide with a solution of bovine serum albumin. This binds to the free amine groups on the aminosilane surface of the array and prevents non-specific binding of the labelled cDNA to the surface, which would also reduce the amount of labelled cDNA available to hybridise to spots. Many factors can affect hybridisation efficiency, such

as temperature, humidity, length of hybridisation, pH etc. Accordingly these parameters should remain constant within an experiment to ensure reproducibility and consistency.

#### 7.1.4 Data collection, normalisation and analysis

A hybridised array is scanned using a confocal laser scanner which excites the fluorophores with different wavelengths of light. 633 nm and 543 nm are used for Cy5 and Cy3 respectively and the images for each channel are stored. The images produced for each channel are analysed by placing a grid over the images corresponding to the spots within the array. The foreground is differentiated from background by a process called segmentation, spots are quality flagged and poor or empty spots can be removed. The intensities within each spot are calculated along with the local background intensity as background interference, which may arise from dust contamination on the slide or artefacts from slide washing, may not be uniform across the whole slide. The background intensity is then subtracted from the spot intensity and differential expression is identified by calculating a ratio (experimental/control) of the fluorescence intensity of the two channels, i.e. the control and experimental cDNA populations hybridised to each spot (Hegde *et al.*, 2000). A ratio of 1 indicates equal hybridisation of both labelled cDNA populations whereas a ratio greater than 1 indicates increased expression in the experimental population. A ratio of less than 1 indicates decreased expression in the experimental population.

Before comparisons can be made between arrays, normalisation of the data is required to remove systematic variation arising from differences in the efficiency of labelling and detection of probes, unequal amounts of cDNA, dye biases and differences in scanning. There are a number of approaches to normalisation (Quackenbush, 2002) including: (i) global normalisation which uses the total signal from all spots on the array and assumes equal signal in each spot; (ii) housekeeping or invariant gene normalisation which uses constantly expressed genes as standards to normalise between arrays; (iii) normalisation using exogenous RNA, which is spotted in known amounts onto arrays and the differences in signal intensity are used for normalisation; (iv) linear regression which assumes that the majority of genes will not change

between samples which may be the case in closely related samples; (v) non-linear regression or locally weighted scatterplot smoothing (LOWESS) which takes into account gene intensity and spatial information. Methods (i) to (iii) are not ideal as signals may depend on the spot location within the array and hybridisation efficiency may not be constant across the whole slide and invariant genes may not be as constantly expressed as once thought (Lee *et al.*, 2002). LOWESS normalisation is preferable as it performs a large number of local regressions in overlapping windows allowing normalisation to be performed taking variation across the slide into account. However, it assumes the majority of genes do not change and may be inappropriate to use with SSH. However, there is no standard way to normalise microarray data for analysis and the method used must be determined by examining the data.

Following normalisation, data are analysed to identify genes which are differentially expressed. Previously most studies have used a 2 fold change as a threshold for defining differential expression either up or down (Chen *et al.*, 1997), however, this may be statistically inefficient and increase the probability of false positives or negatives. Consequently, statistical approaches, such as t-tests and ANOVA, are being used increasingly to create lists of those genes with statistically significant differential expression. Although a more stringent method, the problem of multiple hypothesis testing arises where by the chances of type I and type II errors can be high when studying thousands of genes simultaneously.

### 7.1.5 Replication

Replication of experiments is necessary to take account of any variation within an experiment, thus allowing accurate, reliable conclusions to be drawn from data analysis. Variation can arise from the experimental procedures used at each stage, (i.e. RNA extraction, labelling, hybridisation), for which technical replicates are required, but also from variation between biological samples being used to represent a particular treatment or phenotype, for which biological replicates are required. Biological replicates are most important as there may be some variability between gene expression in the same tissue type in different samples. Furthermore, by using

independent biological replicates, and taking each through the whole probe-making and hybridisation process individually, technical replication is also achieved.

### 7.1.6 Microarray standards

With the versatility of microarray analysis comes the challenge of interpreting the huge amounts of data it produces and making it accessible to others. There are a number of different platforms that can be used to carry out microarray analysis, from the experimental protocols, to the data analysis methods, which may make the verification of results and repeating of experiments difficult. What may appear to be a similar result with respect to up or down regulation of a particular gene may not be so if two laboratories are using different methods.

To try to tackle this problem the Microarray Gene Expression Data (MGED) Society (<http://www.mged.org>) was formed to aid the sharing of microarray data by establishing a set of standards for microarray annotation, with a view to producing comprehensive databases of the details of all microarray experiments (Ball & Brazma, 2006). To this end the Minimum Information About a Microarray Experiment (MIAME) document has been produced (Brazma *et al.*, 2001), which outlines a set of criteria for faithfully recording the details of microarray experiments in unambiguous language so that potentially any experiment could be reproduced by another group. Briefly, this minimum information is divided into six parts: (i) **Experimental design**, the set of hybridisation experiments as a whole; (ii) **Array design**, each array used and each element on the array; (iii) **Samples**, samples used, extract preparation and labelling; (iv) **Hybridisations**, procedures and parameters; (v) **Measurements**, images, quantification and specifications; (vi) **Normalisation controls**, types, values and specifications (Brazma *et al.*, 2001)

The MGED ontology (Stoeckert & Parkinson, 2003; Whetzel *et al.*, 2006) sets out a defined set of terms for describing and recording the details of experiments to avoid ambiguity. Similarly, they also recommend using MAGE-TAB (Rayner *et al.*, 2006) format based on tab-delimited spreadsheets to record these details, to make data more easily collatable and usable by others. The MGED Society also has a working group

trying to establish ways in which to record how data normalisation and transformation has been carried out in individual studies.

### 7.1.7 Objectives

The objectives of these experiments were to:

- Produce cDNA microarrays from the SSH libraries generated from the interaction between *T. versicolor* and *S. gausapatum* (Chapter5)
- Assess the success of the SSH subtraction by probing arrays with RNA from the same pairing used to generate the SSH libraries
- Test the hypothesis that there are differentially expressed genes common to interactions regardless of the outcome, by probing cDNA arrays with RNA from *T. versicolor* interacting with different competitors, with which different interaction outcomes occur. These were *S. gauspatum* (replaced by *T. versicolor*), *B. adusta* (deadlocks) and *H. fasciculare* (replaces *T. versicolor*)



## 7.2 Materials and Methods

### 7.2.1 Array Fabrication

#### 7.2.1.1 *Colony PCR and screening*

Ten 96 well plates of glycerol stocks of clones from both forward and reverse subtracted libraries (1920 clones in total) were amplified and purified as described in Sections 6.2.1 and 6.2.2.

Clones were screened to confirm the presence of inserts and to detect any mixed products or failed PCRs which might produce anomalous results downstream in the microarray process. A portion of each reaction (5 $\mu$ l) was mixed with 4  $\mu$ l loading dye in a separate 96 well plate and then analysed on a 2% agarose/EtBr stretch gel run in 1XTAE buffer. Hyperladder I (Bioline Ltd., London, UK) (5  $\mu$ l, 720 ng) was used as a marker. Stretch gels were used because the gel combs are in an 8x12 configuration and the wells are spaced so that a multichannel pipette may be used to load the gel.

PCR products were inspected and recorded as either good, mixed, empty vector or failed PCR. The number of poor PCR products, i.e. mixed or empty vector or failed PCR, was low. Consequently, all PCR products were printed onto the microarray rather than cherry picking the good ones. The poor ones may act as useful tools in the analysis.

#### 7.2.1.2 *Transfer to 384 well plates*

The pins of the microarray printing machine are compatible with a 384 well plate format, therefore, PCR products needed to be transferred into this format. Transfers were performed using a Multiprobe<sup>®</sup> II HT EX (PerkinElmer LAS (UK) Ltd.) robot. Dimethyl sulfoxide (DMSO; 5  $\mu$ l) was transferred into each of the 384 wells followed by 5 $\mu$ l of each PCR product, transferred from sets of 4 x 96 well plates into each 384 plate. Plates were sealed with adhesive foil lids and stored at -20°C until required.

### 7.2.1.3 *Invariant Genes*

Included with the PCR products to be printed onto the arrays were six PCR products produced using the TubCor primers (Chapter 5, Section 5.2.6.1) that amplify the  $\beta$ -tubulin gene. As this gene is thought to be equally expressed in the experimental treatments used here (see Chapter 5, also used for assessment of subtraction) it acted as a control for assessing the microarray, since its expression should not change between treatments. Six replicates of this gene were interspersed with the clone PCR products.

### 7.2.1.4 *Printing the array*

Each amplified clone PCR product suspended in DMSO (50%) was spotted onto 25 x 75 mm aminosilane-coated Corning® UltraGAPS™ slide (Corning Life Sciences, NL) using a robotic Flexys array printer (Genomic Solutions, Ltd., Cambridgeshire, UK) with solid pins, having 120  $\mu$ m tips delivering approximately 340 pl. Three replicates of each clone were printed onto each slide. Spots were printed in a 12x4 metagrid consisting of 12x12 subgrids. A landmark was printed in each corner of each subgrid, surrounded by blank spots. Furthermore two Lucida Microarray ScoreCard (Amersham Plc., Buckinghamshire, UK) control spots were printed in the top left hand corner of each subgrid (Figure 7.2).

L	B	1	2	3	4	5	6	7	8	B	L
B	B	9	10	11	12	13	14	15	16	B	B
SC	SC	17	18	19	20	21	22	23	24	B	B
25	26	27	28	29	30	31	32	33	34	35	36
37	38	39	40	1	2	3	4	5	6	7	8
9	10	11	12	13	14	15	16	17	18	19	20
21	22	23	24	25	26	27	28	29	30	31	32
33	34	35	36	37	38	39	40	1	2	3	4
5	6	7	8	9	10	11	12	13	14	15	16
B	B	17	18	19	20	21	22	23	24	B	B
B	B	25	26	27	28	29	30	31	32	B	B
L	B	33	34	35	36	37	38	39	40	B	L

**Figure 7.2** Layout of subgrids on each microarray slide. L = landmark, B = Blank, SC = Scorecard. Numbers 1-40 are spotted clones.

The scorecard consisted of different types of control: calibration, ratio and negative control. Each control was spotted a total of four times on each microarray slide: in two separate subgrids and twice within each subgrid (Figure 7.2). Calibration control samples hybridise with labelled samples that contain the mRNA spike mix, and the resulting signal levels represent the concentration range. Calibration curves of the signal intensity vs the concentration range allow the upper and lower detection limits to be determined. Ratio control samples allow the experimental raw signal ratios and normalisation method to be assessed. When controls hybridise with labelled samples containing the mRNA spike mix the resulting signal levels should result in ratios close to those defined (Table 7.1). For the calibration and ratio controls the mRNA spike mixes complement the DNA spotted onto the array. Negative controls allow the evaluation of signal levels from non-specific hybridisation.

**Table 7.1** Lucidea Universal Scorecard control samples printed onto each microarray slide. Calibration controls (CC) allow the mRNA concentration detection range to be assessed. Ratio controls (RC) allow raw signal ratios and the normalisation method to be assessed. Negative controls (NC) allow assessment of the degree of non-specific hybridisation.

Control Type	Control Name	mRNA in spike (pg/1 $\mu$ l spike)			Target Ratio
		Test spike mix	Reference spike mix	Utility spike	Test/Reference
Calibration	CC1	15000	15000	0	1:1
Calibration	CC2	5000	5000	0	1:1
Calibration	CC3	1500	1500	0	1:1
Calibration	CC4	500	500	0	1:1
Calibration	CC5	150	150	0	1:1
Calibration	CC6	50	50	0	1:1
Calibration	CC7	15	15	0	1:1
Calibration	CC8	5	5	0	1:1
Calibration	CC9	1.5	1.5	0	1:1
Calibration	CC10	0.5	0.5	0	1:1
Ratio	RC1	50	150	0	1:3 Low
Ratio	RC2	150	50	0	3:1 Low
Ratio	RC3	500	1500	0	1:3 High
Ratio	RC4	1500	500	0	3:1 High
Ratio	RC5	15	150	0	1:10 Low
Ratio	RC6	150	15	0	10:1 Low
Ratio	RC7	500	5000	0	1:10 High
Ratio	RC8	5000	500	0	10:1 High
Negative	NC1	0	0	0	0
Negative	NC2	0	0	0	0

Printed slides were stored in the dark in a vacuum sealed dessicator at room temperature.

### 7.2.2 Making probes for microarray

For each microarray probe, RNA extracts from test and control mycelium are required. For each slide and probe a separate pair of test and reference fungal interactions were grown, extracted and taken through the entire probe-making process independently, providing both biological and technical replicates. Three to five biological replicates were used for each of the three interaction experiments: (i) *T. versicolor* (TvD2) vs *S. gausapatum* (Sg1) (5 replicates); (ii) *T. versicolor* vs *B. adusta* (MA313) (3 reps); (iii) *T. versicolor* vs *H. fasciculare* (GTWV2) (3 replicates). A reference set of *T. versicolor* alone was grown alongside each set of pairings so that the control was subjected to the same conditions to minimise variation.

#### 7.2.2.1 Growth of mycelium for RNA extraction

Mycelium was grown up and harvested for RNA extraction as described in section 2.2. For pairings of (i) *T. versicolor* vs *S. gausapatum* and (ii) *T. versicolor* vs *B. adusta*, both inoculum plugs were plated at the same time. However, for pairings of *T. versicolor* vs *H. fasciculare*, the *H. fasciculare* plugs were plated 2 d prior to adding the opposing *T. versicolor* plugs, ensuring that opposing mycelia met at the centre of the plate.

#### 7.2.2.2 RNA extraction

RNA was extracted, as described in Section 2.3, using TRIreagent. Following extraction, RNA was denatured at 65°C and immediately returned to ice, then vortexed, centrifuged briefly and stored at -80°C. The product (5 µl) was checked for the presence of RNA by gel electrophoresis on a 1 % agarose/EtBr gel.

### 7.2.2.3 Screening of RNA extracts for contamination with competitor species

Although during the harvest of mycelium from interactions every care was taken only to take mycelium from *T. versicolor*, there was a potential risk of contamination with the opposing species. To confirm that there was no contamination, a few microlitres of the extracted RNA was first DNase treated to remove residual DNA and then subjected to RT-PCR to make conventional cDNA. This cDNA was tested by PCR with species-specific primers designed to the opposing species.

**DNase treatment.** For the DNase digestion and cDNA synthesis, 2  $\mu\text{l}$  of each RNA sample was used. Although this may not have represented an equal RNA concentration it did provide a sample of the RNA for testing by RT-PCR while conserving RNA for the labelling. A digestion master mix for each reaction was made up as follows per reaction:  $\text{dH}_2\text{O}$ , 14  $\mu\text{l}$ ; RQ1 DNase 10X buffer (Promega, Southampton, UK), 2  $\mu\text{l}$ ; RQ1 RNase-Free DNase 1 unit  $\mu\text{l}^{-1}$  (Promega), 2  $\mu\text{l}$ . The 2  $\mu\text{l}$  total RNA was added to make a total reaction volume of 20  $\mu\text{l}$ . Tubes were incubated in a thermal cycler at 37°C for 30 min. RQ1 DNase Stop Solution (Promega; 2  $\mu\text{l}$ ) was added to the reaction and it was incubated at 65°C for 10 min to inactivate the DNase. All reagents were kept on ice throughout.

**cDNA synthesis.** First strand cDNA was synthesized from the DNase treated RNA using M-MLV RNase H<sup>-</sup> Reverse Transcriptase (Promega). RNase H activity is removed from this enzyme, which eliminates the degradation of RNA templates, and provides a higher yield and a greater percentage of full-length first-strand synthesis products.

DNase treated RNA (19  $\mu\text{l}$ ) was pipetted into a 0.5 ml PCR tube and 1  $\mu\text{l}$  Oligo (dt) (500  $\mu\text{g ml}^{-1}$ ; Promega) added. The tube was incubated at 70°C for 10 min, followed by incubation on ice for 10 min. To this mixture the following were added: 6  $\mu\text{l}$  5X 1<sup>st</sup> Strand buffer; 2  $\mu\text{l}$  0.1M dithiothreitol; 1  $\mu\text{l}$  10 mM dNTPs, and the tube incubated at 42°C for 2 min. M-MLV RNase H<sup>-</sup> Reverse Transcriptase (1  $\mu\text{l}$ ) was added to the tube and then it was incubated at 42°C for a further 50 min, followed by incubation at 70°C for 15 min to inactivate the enzyme. This produces single strand cDNA. cDNA was stored at -80°C.

**Design of species specific primers.** Species-specific primers already existed for *S. gausapatum* (Dai Parfitt pers. comm.) but not for *B. adusta* and *H. fasciculare*. Briefly, to design primers for these species genomic DNA was extracted from pure cultures of each, the ITS region amplified using ITS1F/4 primers, bands extracted from gels, sequenced in both directions with ITS 1F/4 primers and then the sequences were aligned using Bioedit Sequence Alignment Editor (Version 7.0.5.3; Hall, 1999). From these sequence alignments species specific primers were designed and used to test for contamination within the RNA samples.

**DNA extraction.** Mycelium was scraped from the surface of an agar plate culture of *B. adusta* and *H. fasciculare*, wrapped in foil and then immersed in liquid nitrogen for at least 5 min. The frozen mycelium was transferred to a pre-chilled mortar and using liquid nitrogen, ground to a fine dust. Extraction buffer (200 mM Tris HCl, 250 mM NaCl, 25 mM EDTA, 0.5% SDS, pH 8.5; 600  $\mu$ l) was added and ground to a paste. This mixture of ground mycelium and buffer was thawed and transferred to a 1.5 ml Eppendorf tube. The mortar was washed with 600  $\mu$ l 0.4% w/v dried skimmed milk (Marvel, UK) and the washings transferred to the Eppendorf tube. The tube was vortexed for 15 s and shaken for 30 min in a chest shaker, followed by centrifugation at 11400 g for 5 min in an Eppendorf Minispin microcentrifuge (Eppendorf, Cambridge, UK). The supernatant was transferred to a fresh 1.5 ml Eppendorf tube and centrifuged at 11400 g for 5 min as above. Again the supernatant was transferred to a new 1.5 ml Eppendorf tube and half the supernatant volume of 3M sodium acetate (pH 5.2) added. This was left to stand at  $-20^{\circ}\text{C}$  for 10 mins, then centrifuged at 11400 g for 5 min. The supernatant was transferred to a new 1.5 ml Eppendorf and an equal volume of isopropanol added. This was allowed to stand at room temperature for 5 min and then centrifuged at 11400 g for 5 min. The supernatant was removed and discarded and the remaining pellet washed with 500  $\mu$ l 70% v/v ethanol. The tube was centrifuged at 11400 g for 5 min and the supernatant discarded. The pellet was air dried for approximately 30 min and resuspended in 50  $\mu$ l sterile distilled water. The DNA extract (5  $\mu$ l) was checked on a 1.2% agarose/EtBr gel for the presence of DNA.

**PCR.** The ITS region is a region of the genome that is variable enough to distinguish between different fungal species and it is from the sequences within this region that

the generic fungal primers ITS 1F (Gardes & Bruns, 1993) and ITS 4 (White *et al.*, 1990) were designed. To ensure that enough material would be available for sequencing three replicated 25  $\mu$ l PCR reactions were made. Furthermore, to ensure successful PCR reactions, 3 dilutions of the DNA template were used in these replicates.

Extracted DNA (1  $\mu$ l) was used as template for each 25  $\mu$ l reaction. A master mix for the number of samples required plus one was prepared as follows: sterile distilled H<sub>2</sub>O, 18.9  $\mu$ l ; 10X PCR reaction buffer, 2.5  $\mu$ l; dNTPs (10 mM), 0.5  $\mu$ l; ITS 1F (10  $\mu$ M), 1.0  $\mu$ l; ITS 4 (10  $\mu$ M), 1.0  $\mu$ l; *Taq* DNA polymerase (Qiagen), 0.125  $\mu$ l. This was followed immediately by thermal cycling, in a PE2700 PCR machine (Applied Biosystems, CA, USA), according to the following programme: 96°C 15 mins; [94°C 1 min, 50°C 1 min, 72°C 1 min] for 40 cycles. 5  $\mu$ l of each PCR reaction was analysed on a 1.2 % agarose/EtBr gel run in 1X TAE buffer to check for products of the correct size of approximately 500 bp.

**Gel Extraction.** The QIAquick gel extraction kit (Qiagen Ltd., Crawley, UK) was used to purify DNA from the fragment bands ready for sequencing.

The remaining 20  $\mu$ l of each PCR reaction (60  $\mu$ l in total) were run on a 1.2 % agarose/EtBr gel and viewed on a UV transilluminator. A razor blade was used to excise bands from the gel. Gel pieces were transferred to pre-weighed 15 ml falcon tubes and the weight of gel slices determined. Three volumes of Buffer QG were added to 1 volume gel (100 mg = approx. 100  $\mu$ l). Tubes were incubated at 50°C for 10 min in a water bath and vortexed every 2-3 min, until the gel slice completely dissolved. After the gel slices had dissolved the buffer was yellow, indicating pH  $\leq$  7.5, the optimal pH for DNA binding. One gel volume of isopropanol was then added to the sample and mixed but not centrifuged. This step increases the yield of DNA fragments <500 bp and >4 kb. A QIAquick spin column was placed in a 2 ml collection tube and 800  $\mu$ l of the sample applied to the column and centrifuged at 11400 g for 1 min in an Eppendorf Minispin microcentrifuge (Eppendorf, Cambridge, UK). The maximum volume of the column reservoir is 800  $\mu$ l, therefore if there was more than 800  $\mu$ l of sample the rest was loaded subsequently and centrifuged again through the same column until all of the sample had been passed through the column.

The flow through each time was discarded and the column placed back into the same collection tube. A further 500 µl of Buffer QG was applied to the column and centrifuged at 11400 g for 1 min to remove any residual agarose from the column. The column was then washed by adding 750 µl of Buffer PE to the column and centrifuged at 11400 g for 1 min. The flow through was discarded and the column centrifuged for an additional 1 min to remove residual buffer. The column was then placed in a clean 1.5 ml Eppendorf tube and 30 µl sterile dH<sub>2</sub>O added to the centre of the QIAquick membrane. This was left to stand for 1 min at room temperature and then centrifuged for 1 min to elute the DNA.

**Sequencing and Alignment.** PCR products were submitted for sequencing, as described in sections 5.2.13 and 5.2.14, in both directions with primers ITS1F and ITS4. The resulting sequences for each species were aligned using Bioedit Sequence Alignment Editor (Version 7.0.5.3; Hall, 1999). ClustalW Multiple Alignment (Thompson *et al.*, 1994) was performed and the alignment was used to design primers. Those sections of sequences that contained many sequencing errors, represented by Ns, generally at the beginning of the ITS4 sequences and the end of the ITS1F sequences, were ignored during primer design.

**Primer Design.** Primers were designed from the alignments of the sequences (Figure 7.2) according to the following set of rules.

**Length:** Between 20-35 nucleotides

**G/C content:** 40-60% and equal in each primer

**T<sub>m</sub>:** similar T<sub>m</sub> values for each primer. Estimated using  $T_m = 2^\circ C \times (A+T) + 4^\circ C \times (G+C)$ . Start annealing temp is 5°C below T<sub>m</sub>.

**Sequence:** (i) Avoid complementarity of 2 or 3 bases at 3' ends of primer pairs to reduce primer-dimer formation; (ii) Avoid mismatches between the 3' end of the primer and the target-template sequence; (iii) Avoid runs of 3 or more G or C at the 3' end; (iv) Avoid a 3'-end T. Primers with a T at the 3' end have a greater tolerance of mismatch; (v) Avoid complementary sequences within a primer sequence and between the primer pair.

Proposed primers were analysed with IDT SciTools OligoAnalyzer 3.0 software (<http://www.idtdna.com/analyzer/Applications/OligoAnalyzer/Default.aspx>) to check



for hairpins, self-dimers and heterodimers. Primers were also submitted as a blastn query to check for matches to other sequences in the database.

**Table 7.2** Species specific primers used to test extracted *T. versicolor* RNA for contamination by opposing species

Primer	Primer sequence (5' to 3')	No. bases	Specific for:	Annealing temperature (°C)	No. of cycles	Product size
SgauF	GCGGGGGTCTCTTCGTTA	18	<i>S. gausapatum</i>	65-59 (0.2 steps)	30	520 bp
ITS4	TCCTCCGCTTATTGATATGC	20				
BkF	GTTCGCGCACTTGTAGGT	18	<i>B. adusta</i>	52	40	458 bp
BkR	ACACTAGAATACCCTCCACA	20				
HfF	CACCTTTTGTAGACCTGGATT	21	<i>H. fasciculare</i>	54	40	482 bp
HfR	AGTGCTATAAACGGCAAATAG	21				

**PCR of cDNA with species specific primers.** A master mix for the number of samples required plus one was prepared as follows: dH<sub>2</sub>O, 18.9 µl; 10X PCR reaction buffer, 2.5 µl; dNTPs (10 mM), 0.5 µl; Forward Primer (10 µM), 1.0 µl; Reverse Primer (10 µM), 1.0 µl; *Taq* DNA polymerase (purified in house), 0.125 µl. cDNA (1 µl) was used as template for each 25 µl reaction.

This was followed immediately by thermal cycling in a PE2700 PCR machine (Applied Biosystems, CA, USA) according to the following programme: 96°C 15 min; [94°C 1 min, T<sub>a</sub> 1 min, 72°C 1 min] for 40 cycles, where T<sub>a</sub> is the annealing temperature for the primer used (Table 7.2). Products (5 µl) were analysed on a 1.2 % agarose/EtBr gel in 1X TAE buffer alongside 500ng 1Kb Invitrogen ladder to check for products of the correct size.

#### 7.2.2.4 Probe making

**RNA purification.** Once it was confirmed that there was no contamination of the total RNA extracts with competitor species, the RNA samples were purified using Qiagen RNeasy kit (Qiagen, Crawley, UK) to remove residual proteins, according to the manufacturer's instructions. RNA samples were made up to 100 µl with RNase-free water and 350 µl buffer RLT added and mixed by pipetting. Absolute ethanol (250 µl) was then added to each tube. The resulting 700 µl solution was immediately

applied to the top of an RNeasy column placed in a 2 ml collection tube. The column was centrifuged at 8000 g at room temperature for 15 s. The column was transferred to a new collection tube, 500  $\mu$ l buffer RPE applied to the column and centrifuged at 8000 g at room temperature for 15 s, and the flow-through discarded. A further 500  $\mu$ l buffer RPE were then added to the column and centrifuged at 8000 g at room temperature for 2 min. The column was transferred to a new 2 ml collection tube and centrifuged at 8000 g for a further 1 min. Finally the column was transferred to a sterile 1.5 ml Eppendorf tube, 30  $\mu$ l RNase-free water applied to the membrane surface and centrifuged at 8000 g at room temperature for 1 min. A further 30  $\mu$ l RNase-free water was applied to the membrane again and centrifuged at 8000 g for 1 min to ensure maximum elution of RNA.

**Total RNA assessment.** To assess the concentration and quality of the total RNA, 1  $\mu$ l of each RNA sample was used to make a 1 in 50 dilution. This diluted RNA was analysed using an Ultrospec spectrophotometer and UVette<sup>TM</sup> cuvette. (Pathlength 10 mm, unit:  $\text{ng } \mu\text{l}^{-1}$ , Dilution factor: 50). Wavelengths measured were 230 nm, 260 nm, 280 nm, which represent the following:  $A_{260}$ =RNA,  $A_{280}$ =proteins and  $A_{230}$ =residual organic contamination, e.g. trizol, chloroform. The ratios of 260/230 and 260/280 should be close to or above 1.8 if RNA quality is good. In some cases 2 $\mu$ l RNA was run out on gels to check for quality. The two large ribosomal bands should be visible. In addition, the 28S:16S ratio should be about 2.0 to indicate high quality intact RNA, i.e. the larger 28S band should be twice as bright as the 16S band. 10  $\mu$ g of high quality RNA was required for producing the microarray labels.

**Reverse Transcription – making the modified cDNA.** Anchored oligo (dT) (Sigma-Genosys Ltd., Suffolk, UK) 1  $\mu$ l 100mM, 2  $\mu$ l 100mM random hexamers, 10  $\mu$ g total RNA made up to 13.8  $\mu$ l with HPLC grade water and 1  $\mu$ l of Universal ScoreCard mRNA spike (either test or reference; Amersham Biosciences, Buckinghamshire, UK) were mixed in a 0.2 ml thin-walled PCR tube to give a total volume of 17.8  $\mu$ l. The mixture was vortexed and centrifuged briefly. The tube was heated at 70°C for 10 min in a thermocycler. A reverse transcriptase enzyme mix was made up, keeping reagents on ice at all times. For each reaction the following were combined: 6  $\mu$ l 5X First-Strand Buffer (Invitrogen RT buffer), 3  $\mu$ l 0.1 M DTT, 1.2  $\mu$ l 100 mM aa-dUTP/dNTP mix (fresh). 10.2  $\mu$ l of this mix was added to the PCR tube and a further

2  $\mu$ l Superscript II (Invitrogen, Paisley, UK) added to bring the total volume to 30  $\mu$ l. This was mixed gently by pipetting but not vortexed. The tube was incubated at 42°C for 3 hours. 10  $\mu$ l 1 M NaOH and 10  $\mu$ l 0.5 M EDTA pH 8.0 were added, and the tube vortexed briefly and centrifuged. The EDTA compromises the activity of the RT. The resulting total volume was 50  $\mu$ l. Next the reaction tube was incubated at 65°C for 15 min. This incubation step completely inactivates the enzyme. 25  $\mu$ l 1 M HEPES pH 7.0, were added to produce a total volume of 75  $\mu$ l and the mixture vortexed briefly and centrifuged. The reaction was transferred to a 1.5 ml Eppendorf tube and then made up to a total volume of 300  $\mu$ l by adding 225  $\mu$ l HPLC grade water.

**Precipitation.** To precipitate the cDNA 33  $\mu$ l 3M sodium acetate (pH 5.2; 0.11X) and 800  $\mu$ l chilled absolute ethanol were added to cDNA and vortexed. This was incubated overnight at -80°C or until cDNA recovery was required.

**cDNA Recovery.** To recover the cDNA, tubes were centrifuged at 21000 g for 30 min at 4°C in a Beckman™ Coulter™ Allegra 2IR Centrifuge (Beckman Coulter Ltd., High Wycombe, UK). The supernatant was removed and the pellet washed twice in ice cold 70% ethanol. The pellet was aspirated until effectively dry then resuspended in 5  $\mu$ l filtered sterile HPLC water. To ensure complete resuspension of the pellet, the tube was vortexed and centrifuged briefly, then the tubes placed in a water bath at 65°C for 30 s and then immediately put back on ice. NaHCO<sub>3</sub> (pH 9.0 0.3 M) (3  $\mu$ l) was added and the tube vortexed and then centrifuged briefly. The pH of the NaHCO<sub>3</sub> is critical so fresh aliquots were frozen and the pH checked before use.

**Coupling reaction.** The Cy dyes (Monofunctional NHS Esters: Cy3, 25-8010-80; Cy5, 25-8010-79; Amersham Biosciences, Buckinghamshire, UK) and DMSO were pre-warmed to room temperature for approximately 20 min. Cy dye packs were resuspended in 4  $\mu$ l DMSO immediately prior to adding to the cDNA. This is enough for two labelling reactions with each dye (2x2  $\mu$ l). (N.B. dye packs can be split further to use for more labelling reactions by resuspending in more DMSO). Cy3 was used for labelling the reference cDNA populations and Cy5 for the tester cDNA population. The resuspended Cy dyes (2  $\mu$ l) were added to their respective cDNAs. This was vortexed briefly and centrifuged to gather all reactants to the bottom of the

tube and incubated in the dark at room temperature for at least 1 hour. The reaction was stopped by adding 5  $\mu$ l 4M Hydroxylamine hydrochloride and gently mixed by pipetting, centrifuged briefly and incubated in the dark, at room temperature, for 15 min. HPLC grade water (35  $\mu$ l) was added to make up to 50  $\mu$ l.

**Label purification.** When making probes it is important that all unincorporated CyDye, unlabelled nucleotides and primers are completely removed. CyScribe GFX purification columns (Amersham Biosciences, Buckinghamshire, UK) and QIAquick purification columns (Qiagen, Crawley, UK) were both used with equal success.

**GFX Columns** were used as follows: Capture buffer (500  $\mu$ l) was added to each purification column and the resuspended labelled cDNA added and mixed by pipetting up and down 5 times. Columns were centrifuged at >13,000 g for 30 s in an Eppendorf Minispin microcentrifuge (Eppendorf, Cambridge, UK) and the run-through discarded. 600  $\mu$ l wash buffer was then added and the columns centrifuged at >13,000 g for 30 s and the run through discarded. This wash step was repeated twice for a total of 3 washes. The empty column was centrifuged for 1 min to remove any residual ethanol on the column. Columns were transferred to a fresh 1.5 ml Eppendorf tube and 60  $\mu$ l pre-warmed (65°C) elution buffer added to the top of the column and incubated for 5 min at room temperature. The column was centrifuged at >13,000 g for 1 min and the eluate retained. This was the clean labelled probe.

**QIAquick columns** were used as described in section 2.5.

**Label assessment to assess incorporation.** It is essential that labelled probes are sufficiently clean with no degradation or unincorporated product in order for them to be used for hybridisation. The level of dye incorporation into the probe was assessed before proceeding any further. A 1.5% agarose “John gel” was made up by pouring molten agarose into a 25x75 mm mould which has four raised squares at one end, which produce wells when the gel is turned out. A microscope slide was placed over the top, the gel allowed to set and then the gel turned out onto the slide. The gel was placed in an electrophoresis tank that had previously been thoroughly cleaned to remove all traces of ethidium bromide. Labelled cDNA (1  $\mu$ l) was mixed with 1  $\mu$ l 50% v/v glycerol and then loaded into the well of the gel. The gel was run for 30 min at 100 V then removed and scanned using a GeneTAC<sup>TM</sup>LSIV carousel scanner

(Genomic solutions, Huntingdon, UK) with the accompanying software, GeneTAC GT LS Version 3.11 (Genomic solutions, Huntingdon, UK) to assess the size distribution of the labelled product and produce a composite image of the two channels.

Labelled probes were also assessed using an Ultrospec 2100 pro spectrophotometer to estimate the amount of cDNA present (260 nm) and the amounts of Cy3 (550 nm) or Cy5 (650 nm) present. The following calculations were performed to quantify the amount of label incorporated into the cDNA to ensure equal amounts of each fluorescently labelled cDNA were hybridised to the slide.

**1) cDNA yield (ng) =  $A_{260} \times 37 \text{ ng } \mu\text{l}^{-1}$**  (1  $A_{260}$  unit of ssDNA =  $37 \mu\text{g ml}^{-1}$ )  $\times$   
volume ( $\mu\text{l}$ )

**2) Probe yield (pmol dye incorporated):**

$\text{Cy}^{\text{®}3} = A_{550} \times \text{volume } (\mu\text{l}) / 0.15$  ( $\text{Cy}^{\text{®}3}$  extinction coefficient at  $\text{OD}_{550} = 150,000/\text{Mcm}$ )

$\text{Cy}^{\text{®}5} = A_{650} \times \text{volume } (\mu\text{l}) / 0.25$  ( $\text{Cy}^{\text{®}5}$  extinction coefficient at  $\text{OD}_{650} = 250,000/\text{Mcm}$ )

**3) Frequency of Incorporation (FOI):**

$\text{FOI} = \text{pmol dye incorporated} \times 324.5$  (average molecular weight of 1 kb of DNA in  $\text{g mol}^{-1}$ )/ ng cDNA

Amount to load 50 pmol =  $50/(\text{Probe yield for Cy dye}/\text{volume } \mu\text{l})$

The suitability of each labelled probe for hybridisation is assessed based on these calculations and on the John gel images. For hybridisation the frequency of incorporation (FOI) should be approximately between 20 and 50. This is the number of molecules of Cy dye that have incorporated into the modified cDNA. Probes with values greater than this will not produce a good hybridisation and should not be used. A minimum of 30 pmoles of labelled cDNA should be used for each hybridisation but at least 50 pmoles is preferable. High quality labelling reactions should produce John

gel images which show no unincorporated dye which would appear at the leading edge of the gel separate from the main label smear.

#### 7.2.2.5 *Hybridisation*

***Preparing probe for hybridisation.*** The required amount of each labelled cDNA for each channel was mixed together in a fresh 1.5 ml Eppendorf. If this volume exceeded 19  $\mu$ l the sample was dried down to a volume of  $\leq 19$   $\mu$ l using an Eppendorf Concentrator 5301 (Jencons PLS, Leighton Buzzard, UK) speedvac at 60°C in the dark. The dried down sample was made up to 19  $\mu$ l with HPLC grade water (Chromasolv, Sigma) and 1  $\mu$ l poly A (100  $\mu$ M) was added.

***Preparing substrate for hybridisation – Blocking the slide.*** Blocking buffer was prepared on the day of use and contained 5X SSC, 0.1% SDS, 1% w/v BSA. Slides to be hybridised were incubated for 45 min, in a Coplin jar filled with blocking buffer standing in a water bath at 42°C. Each slide was washed by dipping in four changes of sterile filtered water, each for 1 min, turning the slide onto its opposite end each time it was changed. Washed slides were dried quickly using compressed air and stored in a slide box in the dark (i.e. foil wrapped). Blocked slides were kept for up to 1 hour before hybridisation.

***Microarray Hybridisation.*** Hybridisation buffer (50% formamide (deionised min99.5%), 10X SSC, 0.2% SDS) (1ml) was prepared fresh on the day of use and warmed to 37°C in a water bath until the SDS was in solution, as this can sometimes precipitate. The labelled cDNA probe (section 7.2.2.4) was denatured in a heat block at 95°C for 3 min and then immediately placed on ice. The tube was centrifuged briefly to remove any condensation from the lid and again placed back on ice. Hybridisation buffer (20  $\mu$ l) was added to the labelled cDNA (20 $\mu$ l) and mixed by pipetting. The 40  $\mu$ l of the sample was then pipetted in a line along the long side of a new untreated microscope slide. The blocked microarray was placed face down on to this slide resulting in the hybridisation mixture being slowly drawn across the slide. The slides were turned over so that the microarray slide was on the bottom and the sandwich placed in a humidity chamber at 42°C overnight. This contained a small

amount of water in the bottom of the hybridisation chamber to maintain humidity while the platform for the slides remained completely dry.

**Washing the microarray.** After the overnight incubation the slides were separated whilst immersed in Wash Buffer 1 (1X SSC, 0.2% SDS) at room temperature. Microarray slides were incubated in a fresh aliquot of Wash Buffer 1 in a Coplin jar at 55°C for 10 min. The slide was dipped 5 times and then transferred to Wash Buffer 2 (0.1X SSC, 0.1% SDS) at 55°C for 10 min. This was repeated twice more for a total of 3 washes with Wash Buffer 2. Slides were then transferred to 0.1X SSC for 1 min at room temperature, dipped 5 times and then transferred to a further wash with 0.1X SSC for 1 min. Following this final wash the slide was removed and dried using compressed air. Slides were stored in foil-wrapped slide boxes in a desiccator in the dark until ready to be scanned.

**Scanning the microarray.** Slides were scanned as soon as possible following hybridisation and washing as the fluorophores degrade over time and signals may diminish if scanning is left too long. Microarray slides were scanned using a ScanArray<sup>TM</sup> Express HT microarray scanner (Perkin Elmer Precisely, MA, USA) and the accompanying ScanArray<sup>TM</sup> Express software. Slides were scanned initially at 50 µm resolution to locate the position of spots on the slide and to test different levels of gain for each of the Cy3 and Cy5 channels. The laser scans the Cy3 channel at 543nm and the Cy5 channel at 633nm. The final gain levels are set such that they are high enough to pick up spots with weak signals while not flaring out those highly labelled spots so that the signal is saturated. Once the appropriate gain levels were set for each channel, slides were then scanned at a higher resolution of 5µm to produce a better image. Data were stored as two (Cy3 and Cy5) TIFF (Tagged Image File Format) images. Scanned slides were stored in the dark in a vacuum sealed desiccator, at room temperature.

#### 7.2.2.6 *Image analysis*

Imagene (Version 5.5.3, Standard version, Copyright Biodiscovery Inc.) is a spot finding program that allows a grid to be placed over the scanned slide images and signal intensities to be generated, by measuring pixel intensity within spots and in the

background and then subtracting background. Based on a set of user-defined parameters, spots can then be quality flagged, and a tab-delimited text file of signal intensities with quality flags assigned can be produced.

First the images for Cy3 and Cy5 channels of each slide were imported into Imagene as .tif files. Because the slides were printed using a Flexys array printer, each image had to be rotated 90° anticlockwise to correspond with the csv file produced when the slide was printed. This is the file that contains the information about what has been printed in each spot. Then the two images were aligned with one another and a grid overlaid. For the slides used in this experiment there are 4 metarows and 12 metacolumns and within each grid there are 12 subrows and 12 subcolumns. The grid was fitted to the image and each sub grid and some individual spots were adjusted to ensure a good alignment of the grid with the spots. This manual aligning of spots is required because printing may not always be uniform, due to the possible misalignment of the printing pins. Once the grid was fitted the gene IDs were loaded and the template saved. This template was used for subsequent slides but adjustments were always made to the grid and spot positions, as it cannot be assumed that all slides will be printed in exactly the same way as each other.

The spots were then quantified and flagged according to the following filters:

- **Spot finding:** Find negative spots: ON, Enforce grid constraints: ON, Local flexibility: 3.0 pixels, Global Flexibility: 50%;
- **Segmentation:** Background buffer: 3.0, Background width: 3.0, Signal Percentages: Low: 50%, High: 100%, Background percentages: Low: 0%, High: 100%;
- **Quality Flags:** Empty spots Threshold: 1.0, Poor spots: ON, Negative Spots: ON, Parameters: Background: test against subgrid only: 0.9995, Ignored percentage: 25.0, Open perimeter percentage: 25.0, Offset: 60.0.

During this process Imagene assesses whether spots are empty, good or bad and obtains values for each spot, by subtracting the background intensity around each spot from the intensity within the spot. It then uses a number of parameters to assess the quality of a spot, that can be set by the user, and flag spots that are deemed to be empty, good or bad. For each slide the flagging was checked and in some cases



misflagged spots were altered manually. Automatically flagged spots appear green and are coded as follows: Empty spot – 2 or X; Poor spot – 3 or +; Negative spot – 4 or - ; Manual flags override auto flags, they appear red and are coded as follows: 1 – flag spots; Empty spot – 5 or X; Poor spot – 6 or +; Negative spot – 7 or - .

Once quality flagging is complete then two tab-delimited text files of signal intensities with quality flags assigned for each channel is produced, which can be exported to an analysis package such as GeneSpring. A snapshot image is also produced of the array.

### 7.2.2.7 *Analysis of data with GeneSpring*

Data were imported into GeneSpring (Version GX 7.3: Agilent Technologies UK Ltd., Cheshire, UK) together with annotations (Chapter 6). Technical replicates of each SSH clones spotted (3 replicates per slide) were averaged. Signal intensity was calculated for each spot by subtracting the local background signal from the spot signal. Signal ratios were calculated for each spot (Test Cy5/Control Cy3). Ratios represent the relative level of expression between samples. If:  $Cy5/Cy3=1$ , there is no difference in gene expression between samples;  $Cy5/Cy3>1$ , there is increased gene expression in the test sample (i.e. the interaction) compared with the control;  $Cy5/Cy3<1$ , there is decreased gene expression in the test sample as compared with the control.

**Box plots of data.** Box plots were plotted for the raw data within each array and compared between arrays. These display the central tendency and variability of the data for each slide. Boxplots that are not centred around  $M=0$ , where  $M = \log_2(Cy3/Cy5)$  the signal intensity, that are significantly different from biological replicates show that the data requires normalisation. Poor slides were removed from the dataset and the filtered data was normalised.

**Normalisation of data.** Normalisation is used to adjust for the systematic bias in the measured fluorescence intensities but to retain the intrinsic biological variations in the data. This may be due to difference in labelling efficiency, spatial effects, print tip

effects or scanning parameters. There are a number of potential normalisation methods that can be used, such as:

**Global normalisation:** the bias is assumed to be constant across the chip and the total signal is assumed to be equal for each channel. Data are adjusted to make the total signal the same for both Cy3 and Cy5

**Normalisation to percentiles:** adjusts the 50<sup>th</sup> percentile (median) for each data set so that they are all centred around the same point, but the distribution of the data is unaltered.

**Exogenous standard normalisation:** exogenous DNA is spotted onto microarrays and then probed with known concentrations of mRNA spiked within labelled samples. The resulting signals are used to produce calibration curves to normalise the data from individual arrays.

**Invariant gene normalisation:** data are normalised according to the expression levels of invariant genes within the array, whose expression should not change.

**Locally weighted scatter plot smoothing (Lowess) analysis:** assumes that the majority of genes are not differentially expressed (therefore not necessarily suitable for verification of an SSH library)

**Print tip Lowess:** corrects for systematic variation as in basic Lowess but also corrects for spatial variation between spotting pins.

Landmarks and blank spots, which might skew the data set, were removed from the dataset. Normalisations were performed manually, using GeneSpring and LimmaGUI. LimmaGUI is a graphical user interface for linear modelling of 2-colour spotted microarray experiments (Wettenhall & Smyth, 2004). Global normalisation was performed manually. GeneSpring was used for median polishing and inspecting invariant genes. The lucidea internal scorecard calibration controls (CC1-CC10) were used to construct calibration curves for each slide and ratio controls were used to assess the raw values of the experimental ratios and to verify normalisations.

LimmaGUI was used for Lowess and print tip Lowess analyses. The effects of each normalisation were assessed by inspection of boxplots, MA plots (see below) and principal component analysis (PCA) plots of the array data. The choice of normalisation was based on which method produced box plots that minimised experimental variation, i.e. obvious differences in data due to dye bias etc. (and produced boxplots of similar distribution) but that did not remove all variation which may be due to biological variation rather than systematic variation.

**MA plots** were generated to assess the distribution of the raw and normalised data sets from experimental samples. The MA plot of data shows the intensity dependent ratio with the relative gene expression (M, the log intensity ratio from the two channels), vs the average expression (A, the log median intensity), where:

$$M = \log_2 \left( \frac{\text{Cy5}}{\text{Cy3}} \right)$$
$$A = \frac{(\log_2 \text{Cy5} + \log_2 \text{Cy3})}{2}$$

Ideally MA plots should have evenly distributed M values around 0 across the range of intensities (Dudoit *et al.*, 2002). MA plots of data before and after normalisation were compared to observe if normalisation had created datasets centred around M=0.

**Principal component analysis** (PCA) is a multivariate statistical technique for studying complex data sets by reducing the dimensionality and identifying components which account for most of the variation. Normalisations were aimed at getting separation between the three experiments (TvSg, TvBk and TvHf) in PCA plots, as there are assumed differences between groups, although some overlap was expected between groups.

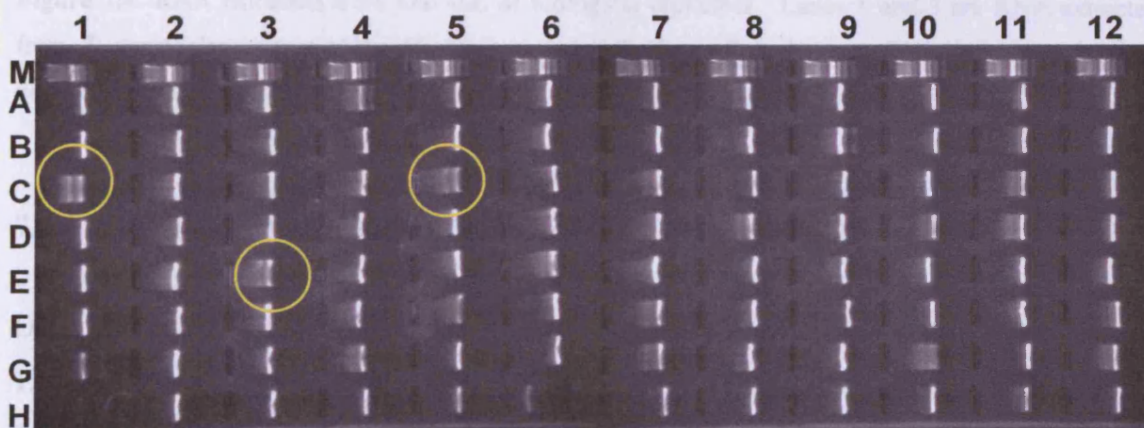
**Data filtering.** Gene lists were generated by filtering on expression level for both 1.4- and 2-fold changes up and down in at least 2 out of 3 arrays for each experiment. Data was also filtered on confidence using statistical differences between groups using a parametric test (t test), at 95% (p=0.05) and 90% (p=0.1) confidence levels using the Benjamini and Hochberg false discovery rate. The distribution of gene ontology (GO) terms in the lists of differentially expressed genes was compared with

the distribution of GO terms assigned to contigs from the forward and reverse subtracted libraries (Chapter 6).

## 7.3 Results

### 7.3.1 Clone PCR screening

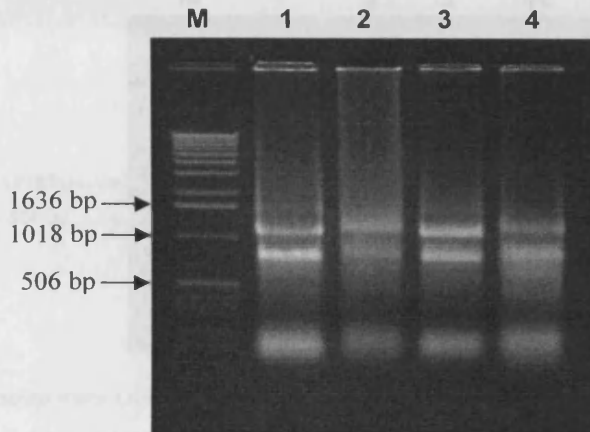
In general all PCR products showed different insert sizes ranging from approximately 300 bp to 1Kb (Figure 7.3). Some colonies had obviously been picked erroneously as a number of clones showed PCR products of 263 bp indicating an empty vector while others showed double bands indicating a mixed PCR product resulting perhaps from cross contamination. Out of a total of 1920 clones screened 16 clones had empty vectors, 98 were mixed and 6 were failed PCRs. Due to the relatively small number of erroneous clones they were not cherry picked and the poor PCR products were also spotted onto the array to act as negative controls



**Figure 7.3** Screening of clone PCR products. Positions on the gel correspond to the wells of a 96 well pcr plate. Fragments are all different sizes ranging from between approximately 300bp-1Kb. Examples of mixed products at C1, E3, C5. M=Hyperladder I. 1.2% agarose/EtBr stretch gel.

### 7.3.2 RNA extraction

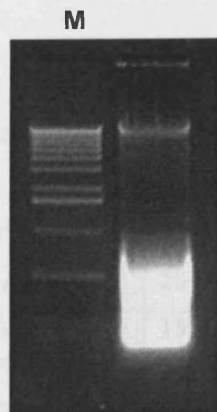
RNA extracts (Figure 7.4) showed distinctive double bands at approximate sizes 1100 bp and 800 bp which represent the 28S and 18S ribosomal RNA respectively. A smaller band at a lower molecular weight is tRNA and mRNA forms a background smear. In general RNA extracts from the interspecific interaction yielded less RNA as less material can be collected from each plate.



**Figure 7.4** RNA extracted from two sets of biological replicates. Lanes 1 and 3 are RNA extracted from *T. versicolor* grown alone (Reference material), lanes 2 and 4 are RNA extracted from *T. versicolor* interacting with *S. gausapatum*. M = 10  $\mu$ l 1 Kb ladder (10 ng  $\mu$ l<sup>-1</sup>)

### 7.3.3 DNA extraction for sequencing of opposing species

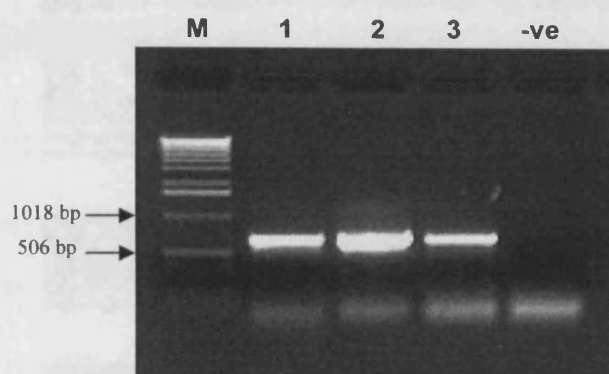
DNA extracts from all species appeared as a high molecular weight band of DNA at  $\geq$  12 Kb, with the RNA as a smear over a range of molecular weights from approx 200bp-10Kb (Figure 7.5).



**Figure 7.5** DNA extracted from *Bjerkandera adusta*. M=10 $\mu$ l 1Kb ladder (Invitrogen) 10 ng  $\mu$ l<sup>-1</sup>. 1.2% agarose/EtBr gel.

### 7.3.4 PCR on species DNA with ITS1F/4

DNA extracts were amplified with general fungal PCR primers, ITS1F/4 at three concentrations: neat, 1/10 and 1/100 dilution. Bands at ~600 bp indicate successful PCR reactions (Figure 7.6) for all species with the general fungal primers ITS1F/4. These bands were cut out and then the fragments sequenced.



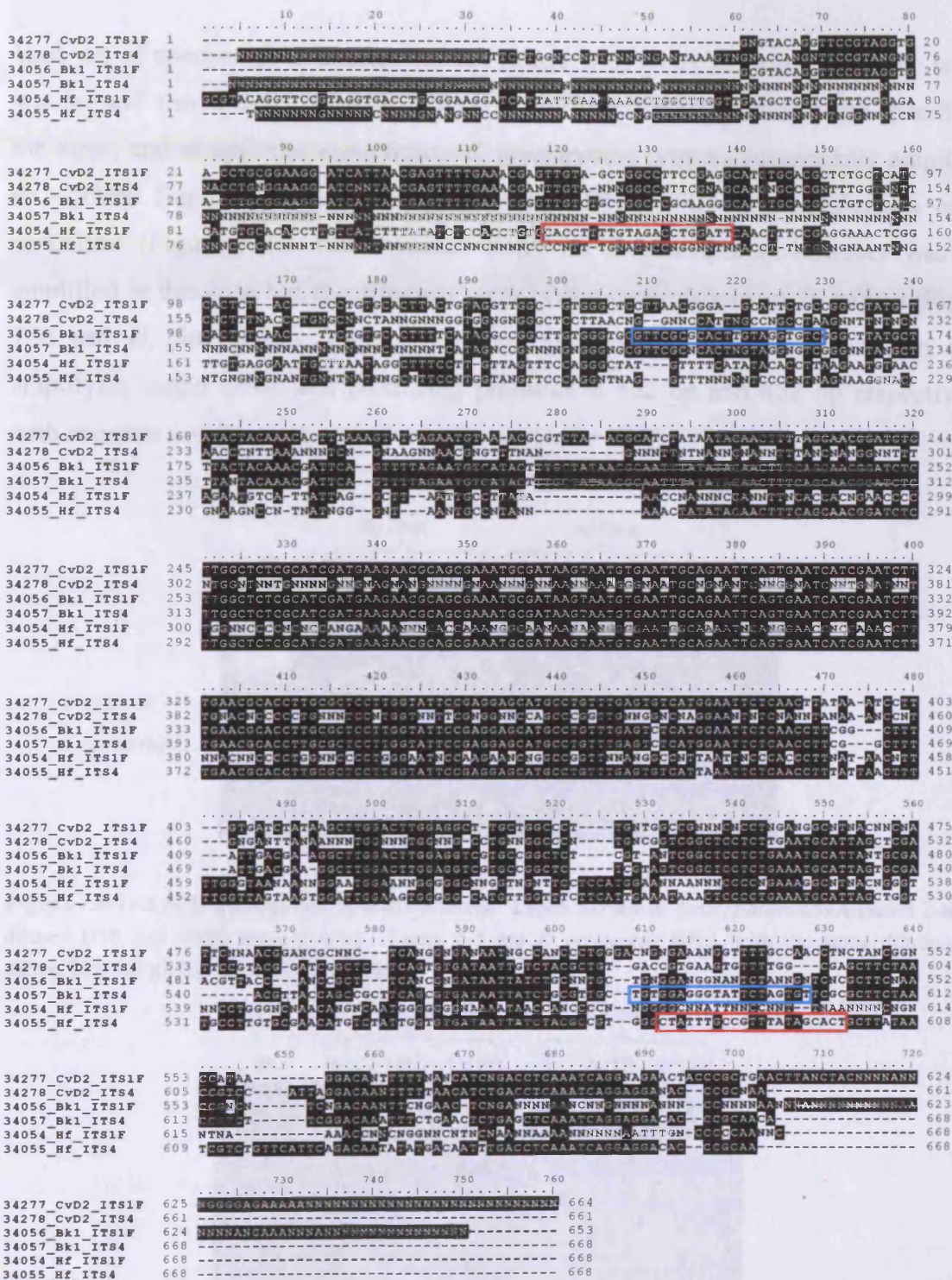
**Figure 7.6** *S. gausapatum* DNA amplified with ITS 1F/4 primers. Lanes 1-3 are *S. gausapatum* DNA with Lanes 2 and 3 diluted 1/10 and 1/100 respectively, Lane 4 is H<sub>2</sub>O negative control. M = 10  $\mu$ l 1kb ladder (Invitrogen) 10 ng  $\mu$ l<sup>-1</sup>.

### 7.3.5 ITS sequence alignments

The alignments of the sequenced ITS1F/4 fragments for *T. versicolor*, *B. adusta* and *H. fasciculare* (Figure 7.7) show some homology between species but also areas of variability from which species specific sequences can be found to design primers. The forward and reverse primers (Table 7.3) designed to be specific for *B. adusta* and *H. fasciculare* are marked on the alignment in red and blue respectively.

**Table 7.3** Species specific primers used to test extracted *T. versicolor* RNA for contamination by opposing species.

Primer	Primer sequence (5' to 3')	No. bases	Specific for:	Annealing temperature (°C)	No. of cycles	Product size
SgauF	GCGGGGGTCTCTTCGTTA	18	<i>S. gausapatum</i>	65-59 (0.2 steps)	30	520 bp
ITS4	TCCTCCGCTTATTGATATGC	20				
BkF	GTTCGCGCACTTGTAGGT	18	<i>B. adusta</i>	52	40	458 bp
BkR	ACACTAGAATACCCTCCACA	20				
HfF	CACCTTTTGTAGACCTGGATT	21	<i>H. fasciculare</i>	54	40	482 bp
HfR	AGTGCTATAAACGGCAAATAG	21				



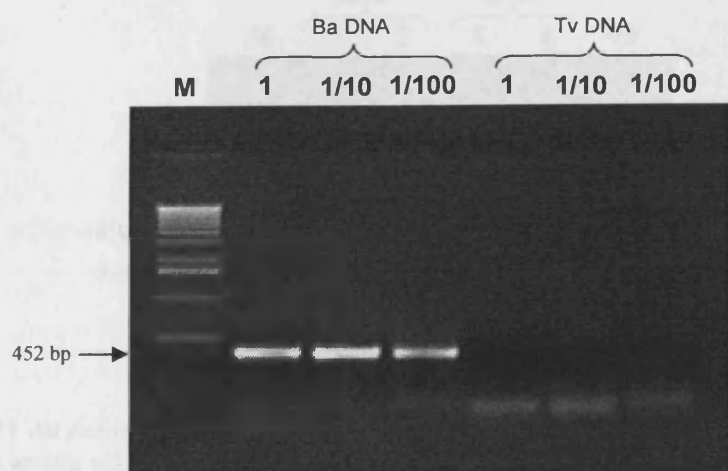
**Figure 7.7** Alignment of ITS sequences for *T. versicolor* (TvD2), *B. adusta* (Bk1), *H. fasciculare* (HfGTW2). Forward and reverse primers for *B. adusta* and *H. fasciculare* are highlighted in blue and red respectively.

### 7.3.6 Testing of species specific primers

Each set of species specific primers was tested with DNA extracted from the target species and also with *T. versicolor* DNA to confirm that the primers were specific to the target and to optimise conditions. *S. gausapatum* primers successfully amplified an ~500bp fragment for only *S. gausapatum* DNA with no amplification of *T. versicolor* (Figure 7.8). Concentrated DNA for *S. gausapatum* however was not amplified in this case but the dilutions were. All concentrations of *B. adusta* (Figure 7.9) and *H. fasciculare* (Figure 7.10) specific primers were successful in only amplifying target DNA and producing products at 452 bp and 482 bp respectively, with negative results when tested with *T. versicolor* DNA.

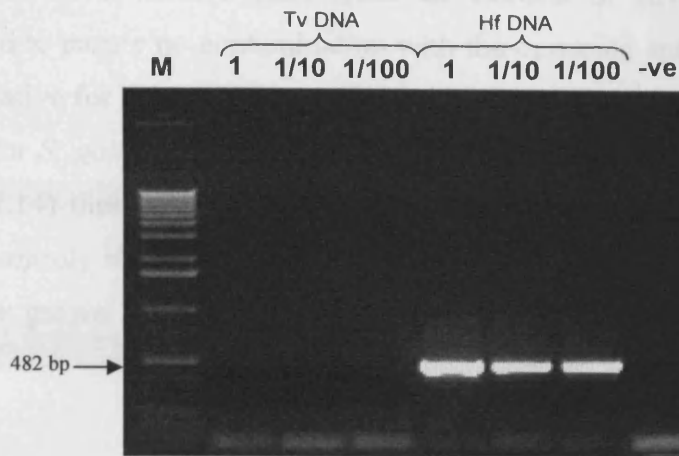


**Figure 7.8** Test of *S. gausapatum* specific primers. Lanes 1-3 are *S. gausapatum* DNA (lanes 2 and 3 diluted 1/10 and 1/100 respectively). Lanes 4-5 are *T. versicolor* DNA with the same dilutions as above. M = 10 µl 1 kb ladder (Invitrogen) 10 ng µl<sup>-1</sup>.



**Figure 7.9** Test of *B. adusta* specific primers. Lanes 1-3 are *B. adusta* DNA (lanes 2 and 3 diluted 1/10 and 1/100 respectively). Lanes 4-5 are *T. versicolor* DNA with the same dilutions as above. M = 10 µl 1 kb ladder (Invitrogen) 10 ng µl<sup>-1</sup>.

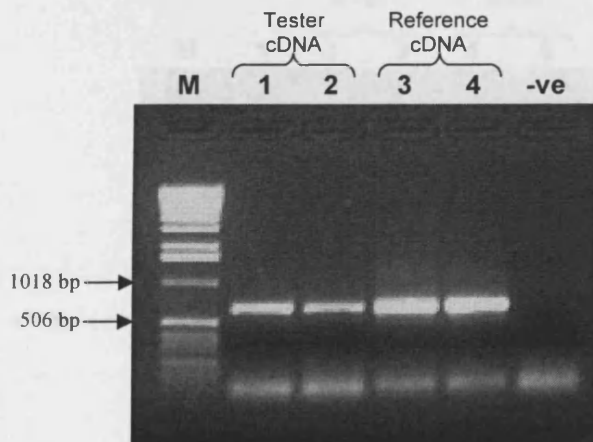




**Figure 7.10** Test of *H. fasciculare* specific primers. Lanes 1-3 are *T. versicolor* DNA (lanes 2 and 3 diluted 1/10 and 1/100 respectively). Lanes 4-5 are *H. fasciculare* DNA with the same dilutions as above. M = 10 µl 1kb ladder (Invitrogen) 10 ng µl<sup>-1</sup>.

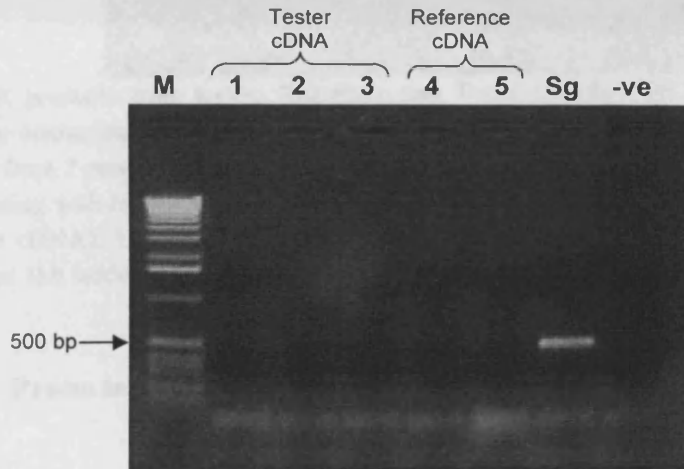
### 7.3.7 Analysis of cDNA with species specific primers

Testing of cDNA with the ITS1F/4 primer pair confirmed that cDNA synthesis was successful and produced products at approximately 600 bp (Figure 7.11). It is important to ensure that cDNA integrity is satisfactory as the tests with the species specific primers will produce no bands if there is no contamination thus it is vital to confirm that the negative result is due to a lack of contamination rather than a failed PCR.



**Figure 7.11** An example of the PCR products from testing Reference and Tester cDNAs with ITS1F/4 primers to ensure cDNA synthesis was successful. Lanes 1-4 are cDNA made from two sets of RNA extracted from biological replicates. Lanes 1 and 2 are from *T. versicolor* interacting with *B. adusta* (Tester cDNAs), Lanes 3 and 4 are from *T. versicolor* growing alone (Reference cDNAs). Lane 5 is H<sub>2</sub>O negative control. M = 10 µl 1kb ladder (Invitrogen) 10 ng µl<sup>-1</sup>.

Tester and driver cDNA made from all extracts of RNA were tested by PCR performed to ensure no contamination with the opposing species. All samples tested were negative for contamination when tested with the corresponding species specific primers for *S. gausapatum* (Figure 7.12), *B. adusta* (Figure 7.13) and *H. fasciculare* (Figure 7.14) thus confirming RNA samples were suitable for probe making. The driver (control) should not contain any contamination as this is derived from *T. versicolor* grown alone but samples were tested to act as a further set of negative controls.



**Figure 7.12** PCR products from testing Reference and Tester cDNAs with *S. gausapatum* specific primers to test for contamination with *S. gausapatum* in extracted RNA from *T. versicolor*, Lanes 2-4 are cDNA made from 2 sets of RNA extracted from biological replicates. Lanes 2 and 3 are from *T. versicolor* interacting with *S. gausapatum* (Tester cDNA), Lanes 4 and 5 are from *T. versicolor* growing alone (Reference cDNA), Lane 6 is *S. gausapatum* DNA positive control, Lane 7 is H<sub>2</sub>O negative control. M = 10  $\mu$ l 1kb ladder (Invitrogen) 10 ng  $\mu$ l<sup>-1</sup>.



**Figure 7.13** PCR products from testing Reference and Tester cDNAs with *B. adusta* specific primers to test for contamination with *B. adusta* in extracted RNA from *T. versicolor*. Lane 1 is *B. adusta* DNA positive control, Lanes 2-5 are cDNA made from 2 sets of RNA extracted from biological replicates. Lanes 2 and 3 are from *T. versicolor* interacting with *B. adusta* (Tester cDNA), Lanes 4 and 5 are from *T. versicolor* growing alone (Reference cDNA). Lane 6 is H<sub>2</sub>O negative control. M = 10  $\mu$ l 1kb ladder (Invitrogen) 10 ng  $\mu$ l<sup>-1</sup>.



**Figure 7.14** PCR products from testing Reference and Tester cDNAs with *H. fasciculare* specific primers to test for contamination with *H. fasciculare* in extracted RNA from *T. versicolor*. Lanes 1-4 are cDNA made from 2 sets of RNA extracted from biological replicates. Lanes 2 and 3 are from *T. versicolor* interacting with *H. fasciculare* (Tester cDNA), Lanes 4 and 5 are from *T. versicolor* growing alone (Reference cDNA), Lane 5 is *H. fasciculare* DNA positive control, Lane 6 is H<sub>2</sub>O negative control. M = 10 µl 1kb ladder (Invitrogen) 10 ng µl<sup>-1</sup>.

**7.3.8 Probe label assessment**

Labelled probes showed size distributions over approximately the same range for Cy3 and Cy5 labelled probes (Figure 7.15). Cy5 labelling of probes tended to be less efficient than with Cy3, which is probably due to the greater instability of the Cy5 dye. Gel pictures show well-labelled probes with no unincorporated dye which would appear as a spot beneath the main smear. Gel images were not used to estimate concentrations of incorporated dye, only to assess the integrity of the labelled probes.



**Figure 7.15** Scanned image of John gel for probe labelling assessment. Lanes 1 and 3 are the Cy5 labelled control probes, Lanes 2 and 4 are Cy3 labelled control probes. Image gain Cy3:50, Cy5: 55.

Table 7.4 shows some typical values when probe concentration and labelling efficiency was assessed using spectrophotometric readings. In general Cy5 labelling was less efficient than Cy3 labelling. Probes with a frequency of incorporation between 20-50 and total concentration of incorporated dye sufficient to probe each slide with 50 pmols of probe were considered useable for hybridisation.

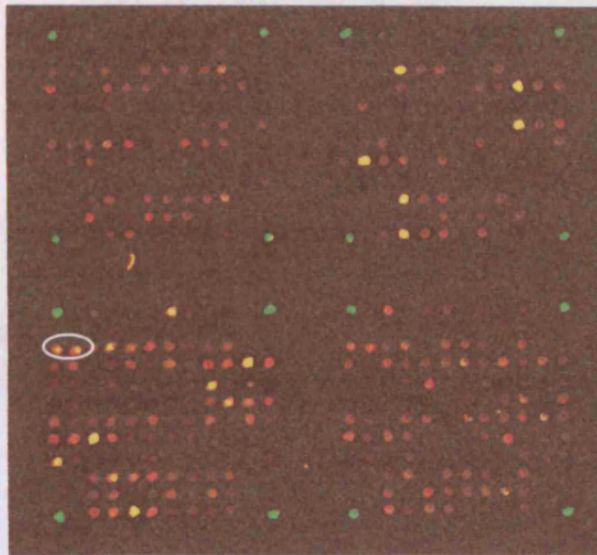
**Table 7.4** Typical values from assessment of probe labelling with spectrophotometer.

Sample	260	Cy3	Cy5	Labelled cDNA yield (ng)	Cy Dye incorporation (pmols)	FOI	Labelled cDNA conc. (pmol $\mu\text{l}^{-1}$ )
		550	650				
Control A	2.021	0.801	-	4112.73	293.7	23.17	5.3
Test A	1.136	-	0.869	2769.64	191.18	22.40	3.5
Control B	1.373	0.615	-	2794.06	225.50	26.19	4.1
Test B	1.360	-	0.704	2767.6	154.88	18.16	2.8
Control C	1.823	0.791	-	3709.8	290.03	25.37	5.3
Test C	1.166	-	0.642	2372.81	141.24	19.32	2.6
Control D	0.989	0.401	-	2012.61	147.03	23.71	2.7
Test D	1.362	-	0.695	2771.67	152.90	17.9	2.8

FOI= frequency of incorporation; Wavelengths 260, 550, 650 nm.

### 7.3.9 Microarray image scanning and spot finding

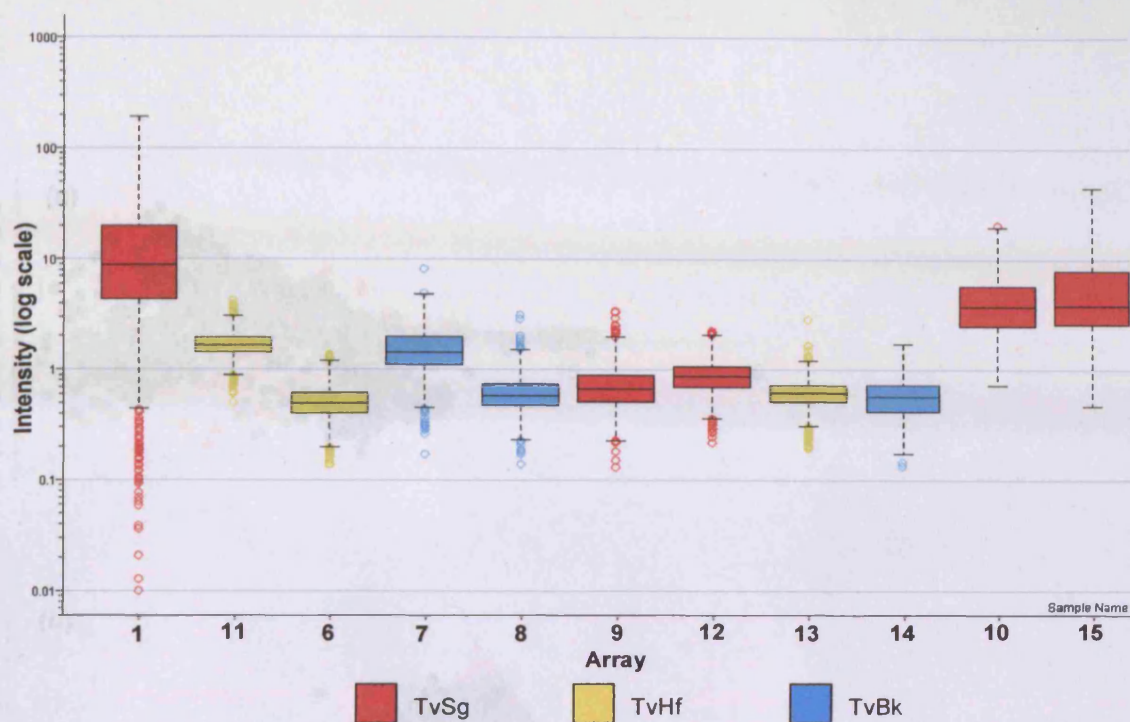
Microarray scanned images showed distinct spots and landmarks were clear (Figure 7.16). There was some fluorescence due to dust and/or wash buffer residue in a few cases. In general the parameters used for spot finding and flagging in Imagene were suitable and visual inspection of images required relatively few manual changes of flag allocations. There were some areas where high fluorescence within spots was clearly due to contamination from smears on the slide, and these were marked manually as poor spots.



**Figure 7.16** Composite scanned image of a microarray slide. Cy 3 (control) and Cy5 (test) channels are overlaid. Spots are: Landmarks (green), blanks (around corners), scorecard (circled), spotted clones (for map see Figure 7.2).

### 7.3.10 Assessment and normalisation of array data

Box plots of the data from the 11 slides hybridised showed that the distribution of data was similar for the majority of slides but that data for slides 1 and 15 (replicates for TvSg experiment) were heavily skewed and indicated poor arrays (Figure 7.17), thus these were removed from the dataset. MA plots of slides 1 and 15 (Figure 7.18) confirm that the slides were poor and should be excluded from further analysis.  $M$  is the average ratio and  $A$  is the signal intensity.



**Figure 7.17** Box plots of raw data for all replicate slides of all experiments. Arrays were testing gene expression during the interaction of *T. versicolor* with *S. gausapatum* (TvSg; red), *H. fasciculare* (TvHf; yellow) and *B. adusta* (TvBk; blue).

MA plots for raw data for all spots within the arrays show distinct groups of points for blanks, landmarks and scorecard (Figure 7.19, 7.20, 7.21). These points, in particular the landmarks which form a very distinct group, could potentially skew the data during further analysis and thus these data were removed. In general, the majority of data points for genes are at relatively low levels of expression with few at higher average expression. Gene points show that, in the experiment of *T. versicolor* vs *S. gausapatum* (Figure 7.19), the data for slide *a* have an increasing sloped trend, slide *c* are distributed around  $M=0$  and slide *e* are asymmetrically distributed around approximately  $M=3$ . The MA plots for *T. versicolor* vs *B. adusta* slides (Figure 7.20) are approximately symmetrically distributed but slides *a* and *e* are distributed below and above  $M=0$  respectively. The cluster of landmark spots for slide *a* are also more diffuse compared with other slides, which may indicate some variability within the slide. MA plots for *T. versicolor* vs *H. fasciculare* (Figure 7.21) show that slides *a* and *c* are both distributed below  $M=0$  with slide *a* with an upward trend. Slide *e* has an upward trend but centred above  $M=0$ .

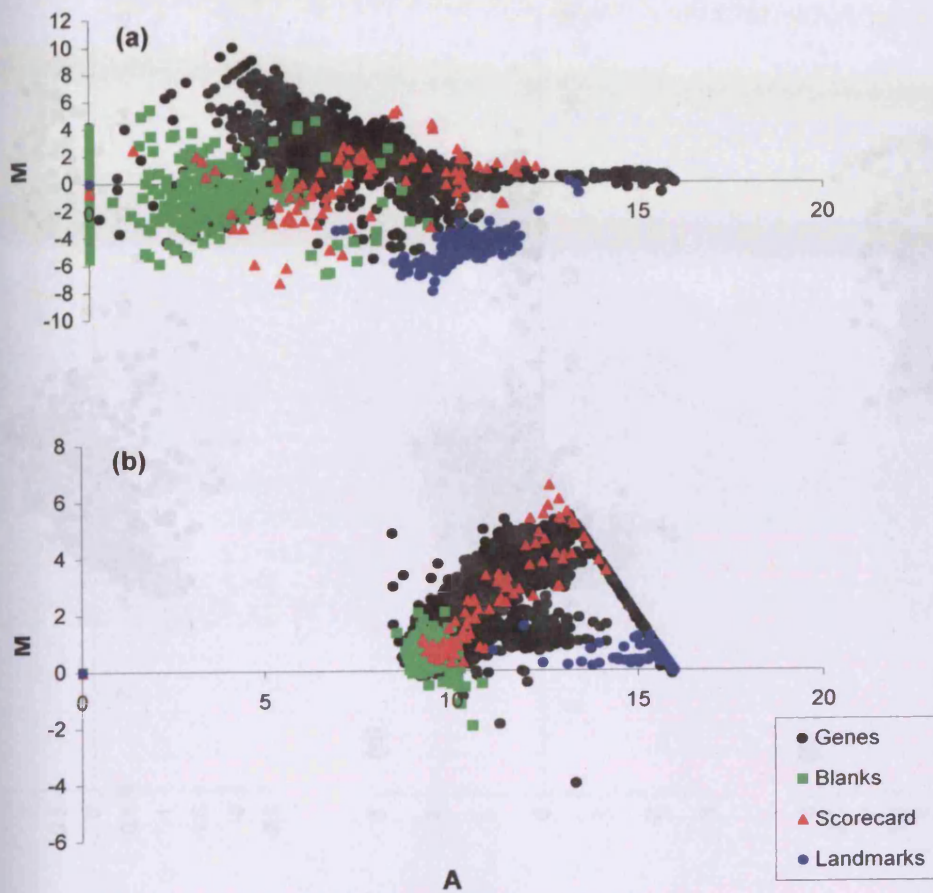
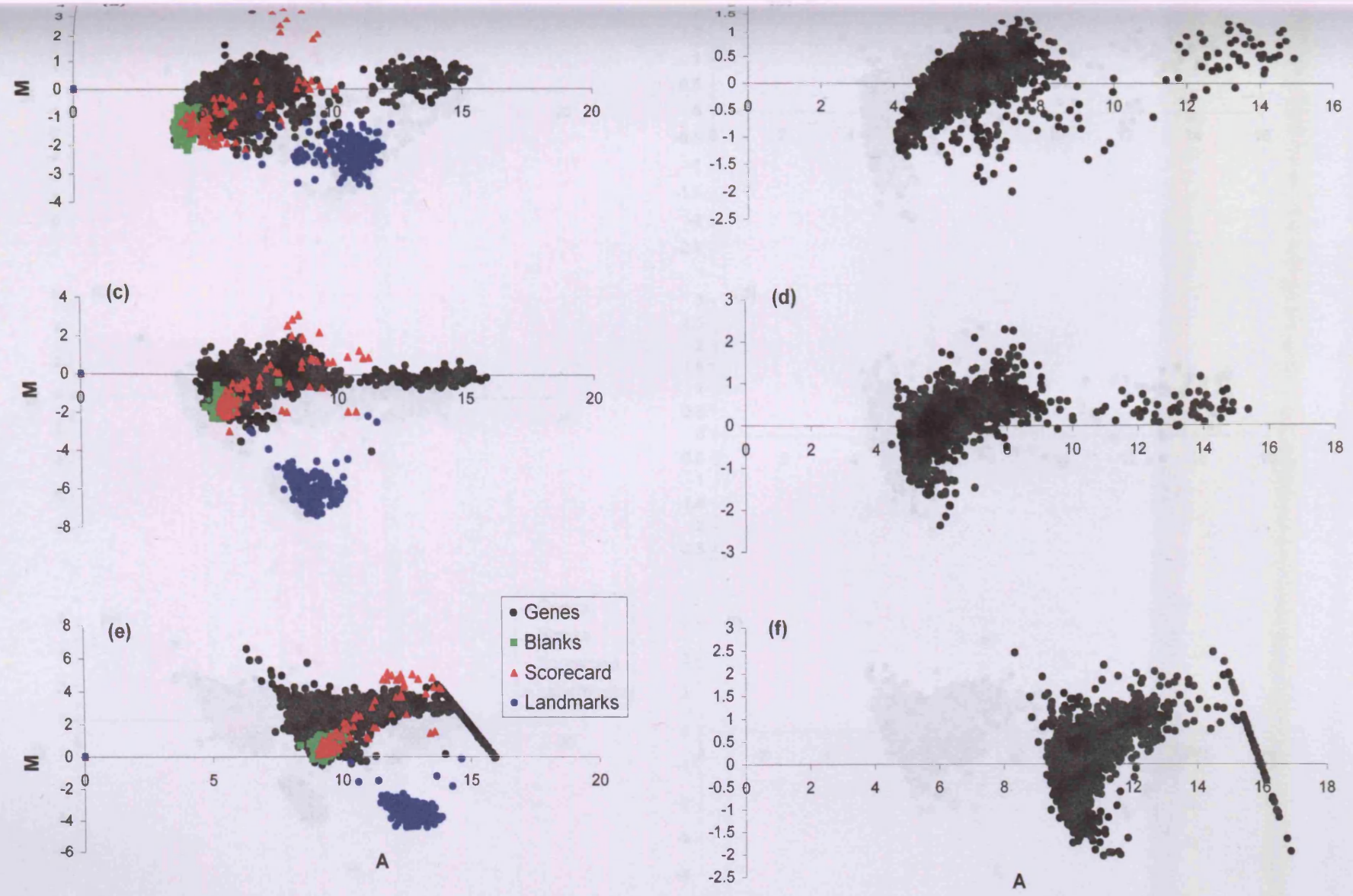
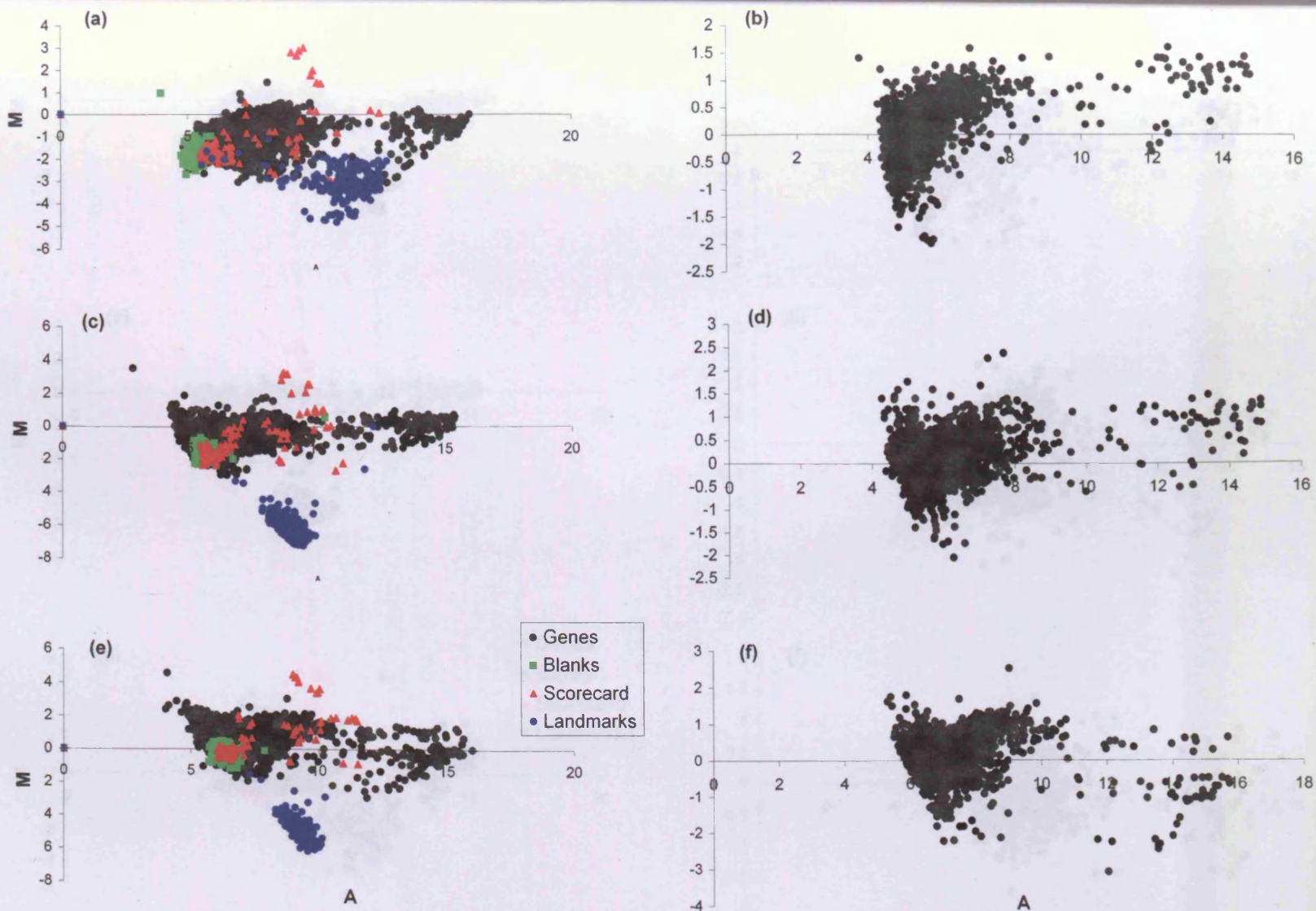


Figure 7.18 MA plots for microarray slides probed with RNA from *T. versicolor* interacting with *S. gausapatum* for raw data of (a) slides 1 and (b) slide 15 which were omitted from further analysis.  $M = \log_2(\text{Cy5}/\text{Cy3})$ ,  $A = 0.5(\log_2(\text{Cy3} * \text{Cy5}))$

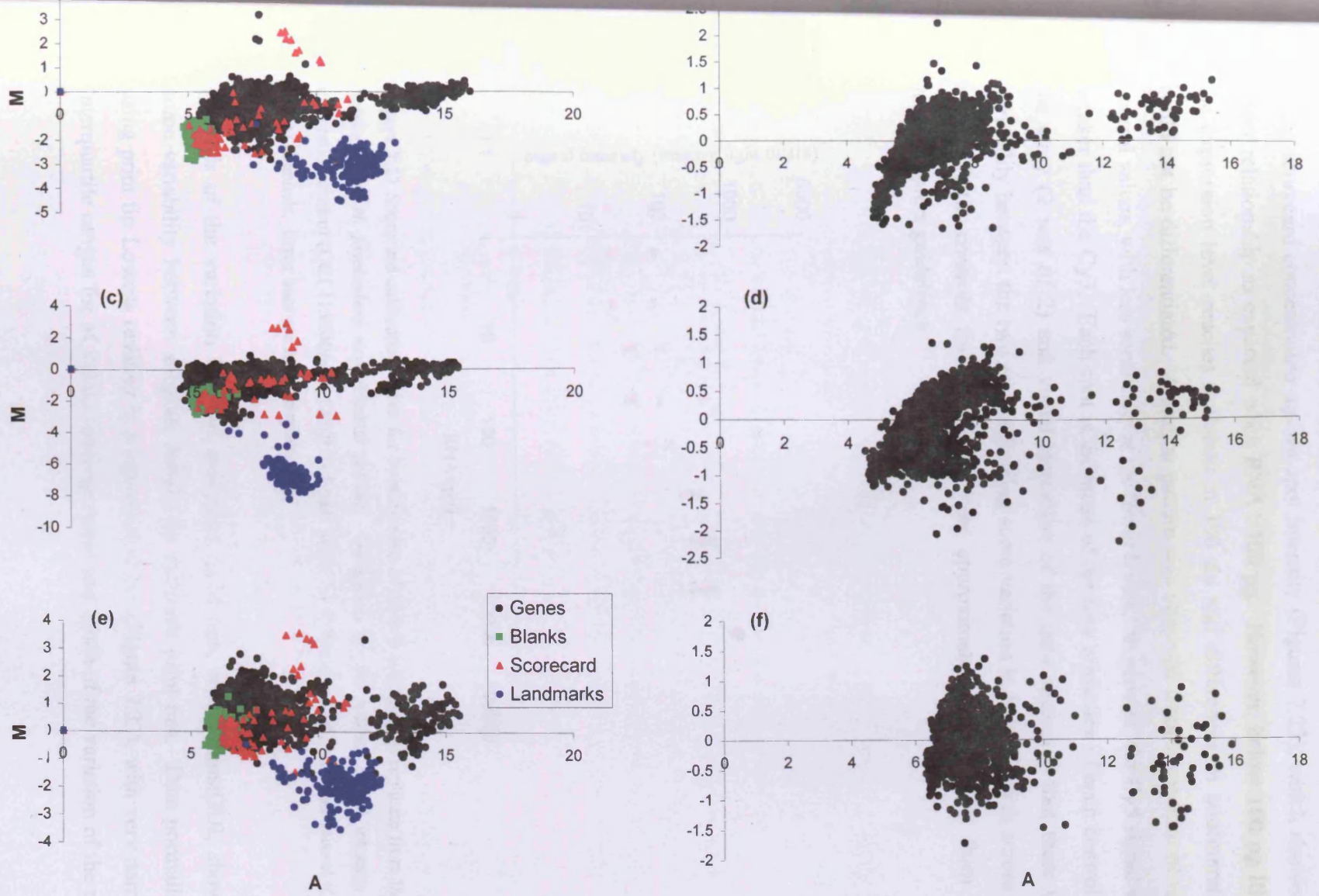


**Figure 7.19** MA plots for replicate microarray slides probed with RNA from *T. versicolor* interacting with *S. gausapatum* for raw data (a,c,e) and normalised data (b,d,f). Normalisations are Per Spot:divide by control channel, Per Chip: normalise to 50th percentile  $M=\log_2(Cy5/Cy3)$ ,  $A=0.5(\log_2(Cy3 * Cy5))$ . Slide12 (a&b), Slide9 (c&d), Slide10 (e&f)



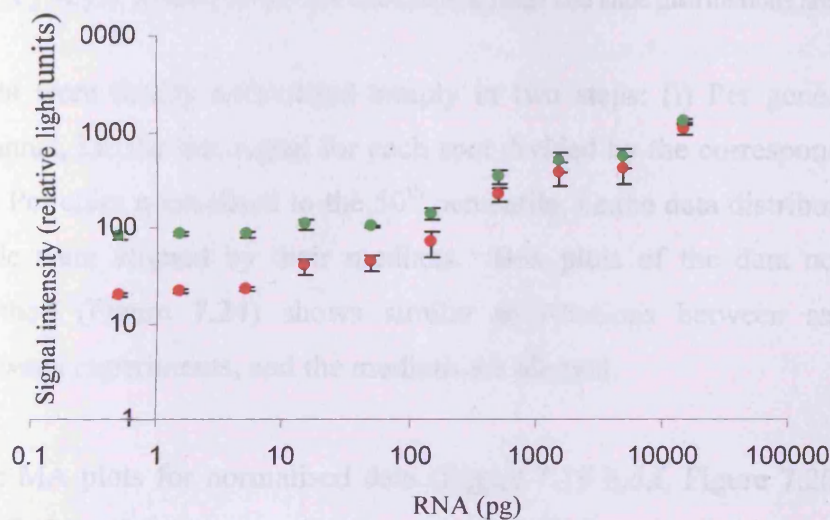


**Figure 7.20** MA plots for replicate microarray slides probed with RNA from *T. versicolor* interacting with *B. adusta* for raw data (a,c,e) and normalised data (b,d,f). Normalisations are Per Spot:divide by control channel, Per Chip: normalise to 50th percentile  $M = \log_2(\text{Cy}5/\text{Cy}3)$ ,  $A = 0.5(\log_2(\text{Cy}3 * \text{Cy}5))$ . Slide 14 (a&b), Slide 8 (c&d), Slide 9 (e&f).



**Figure 7.21** MA plots for replicate microarray slides probed with RNA from *T. versicolor* interacting with *H. fasciculare* for raw data (a,c,e) and normalised data (b,d,f). Normalisations are Per Spot:divide by control channel, Per Chip: normalise to 50th percentile  $M = \log_2(Cy5/Cy3)$ ,  $A = 0.5(\log_2(Cy3 * Cy5))$ . Slide 13 (a&b), Slide 6 (c&d), Slide 11 (e&f).

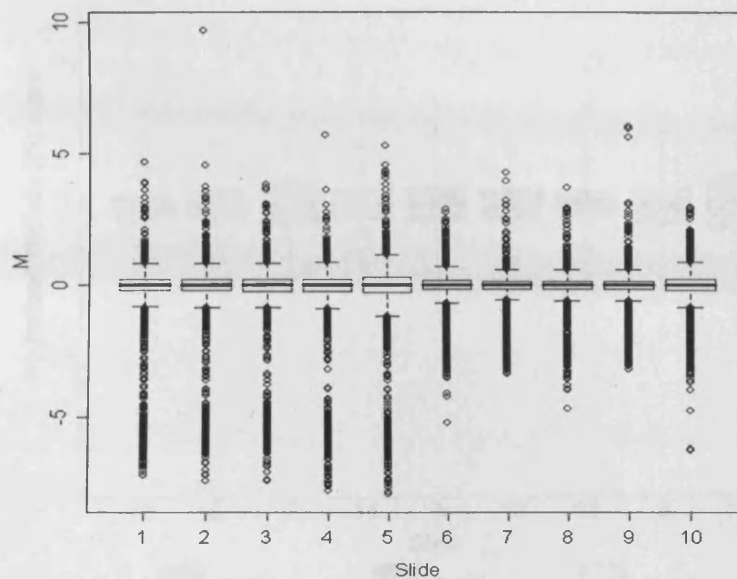
Some scorecard spots were clustered around the same signal intensity as the blank spots, indicating that some of the scorecard concentrations were below the level that could be detected and differentiated from empty spots. This was confirmed by plots of the scorecard concentration against spot intensity (Figures 7.22), which showed a linear relationship as expected when RNA >100 pg. However, below 100 pg RNA the expression level reaches a plateau at 100 rlu and differences in concentration could not be differentiated. A similar pattern was observed from inspection of ratio control values, with less sensitivity at the lower levels. In general, the Cy5 signal was weaker than the Cy3. Each spot is the mean of the four replicates of each control on the array (2 sets of 2) and visual inspection of the data suggested that there was variability between the two sets, indicating some variation in hybridisation across the slide. Ratio controls for each slide were approximately as expected from the manufacturers guidelines.



**Figure 7.22** Scorecard calibration curve for hybridisation of slide 6, a biological replicate from the *T. versicolor* vs *H. fasciculare* experimental pairing. Datapoints are the median signal intensity for calibration control (CC1 (15000pg) - CC10 (0.5 pg); Table 7.2 in the test (Cy5, red) and control (Cy3, green) channels. Error bars are  $\pm$  SE median.

Analysis of the variation between individual print tips, with LimmaGUI, showed some variability between subgrids printed by different print tips. Data normalised using print tip Lowess resulted in boxplots of slides (Figure 7.23), with very narrow interquartile ranges for M values (average ratio) and much of the variation of the raw

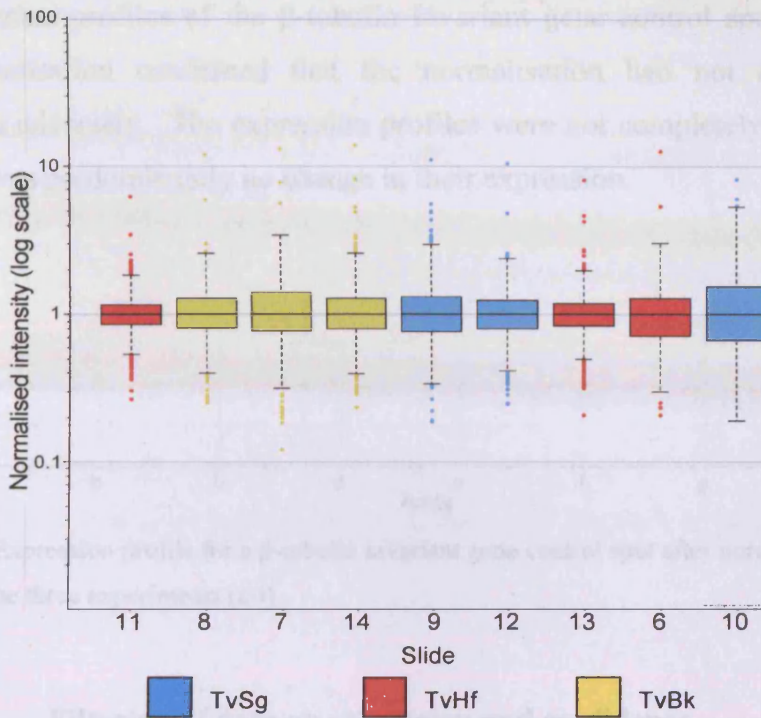
data was removed. Thus, data were not subjected to normalisation using print-tip Lowess.



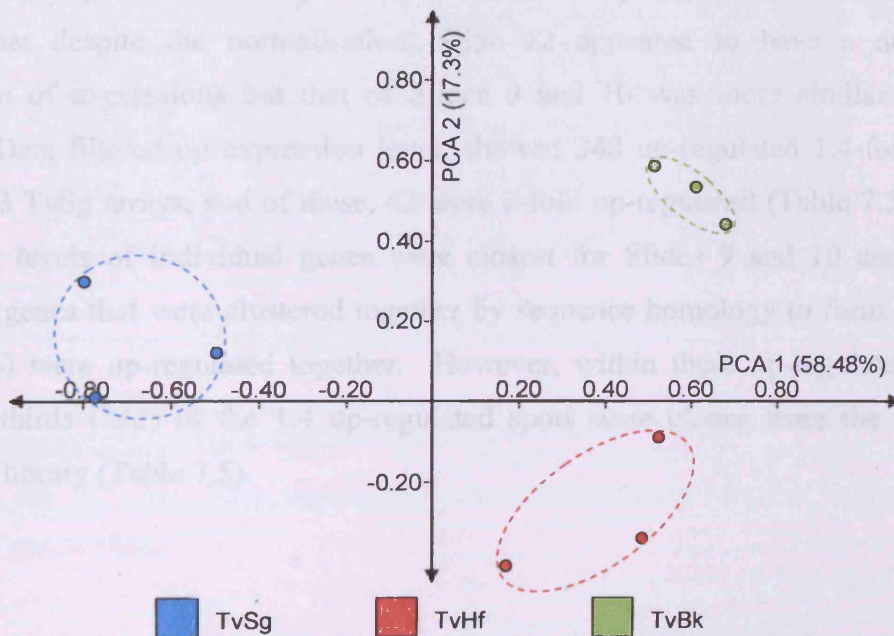
**Figure 7.23** Boxplots of data normalised with print-tip lowess.  $M$  is the log ratio intensity  $\log_2(\text{Cy5}/\text{Cy3})$ , boxes represent the interquartile range and slide distributions are aligned at the median.

Data were finally normalised simply in two steps: (i) Per gene: divide by control channel, i.e. the test signal for each spot divided by the corresponding control signal; (ii) Per chip: normalised to the 50<sup>th</sup> percentile, i.e. the data distributions for each array slide were aligned by their medians. Box plots of the data normalised with this method (Figure 7.24) shows similar distributions between samples within and between experiments, and the medians are aligned.

The MA plots for normalised data (Figure 7.19 b,d,f, Figure 7.20 b,d,f, Figure 7.21 b,d,f) show that the normalisation successfully brought the data to be centred around  $M=0$  in all cases. Statistical analysis of the three experimental data sets with 1-way ANOVA identified a set of 171 genes that were significantly different between experiments ( $p < 0.05$ ). When PCA was performed on these data the experimental groupings were distinct (Figure 7.25).

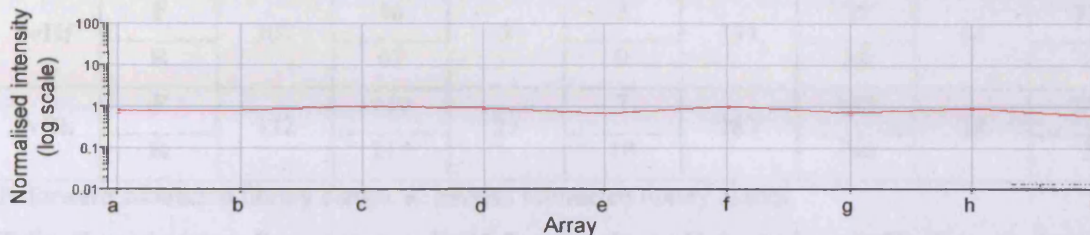


**Figure 7.24** Box plot of normalised data for all three experiments (3 biological replicate slides, per experiment): TvSg – *T. versicolor* vs *S. gausapatum* (blue); TvHf – *T. versicolor* vs *H. fasciculare* (red); TvBk – *T. versicolor* vs *B. adusta* (yellow). Normalisation: Per spot: divide by control channel; Per chip: normalise to the 50th percentile.



**Figure 7.25** PCA plot of normalised data for replicate slides for all experiments. Data was normalised (Per spot: divide by control channel; Per chip: normalise to the 50th percentile) and filtered with ANOVA p0.05 with no multiple sample correction. Experiments are *T. versicolor* vs *S. gausapatum* (TvSg, Blue), *T. versicolor* vs *H. fasciculare* (TvHf, red), *T. versicolor* vs *B. adusta* (TvBk, lime). Dashed lines are the

The expression profiles of the  $\beta$ -tubulin invariant gene control spots (Figure 7.26) after normalisation confirmed that the normalisation had not altered the data distribution adversely. The expression profiles were not completely flat but indicate that there was predominantly no change in their expression.



**Figure 7.26** Expression profile for a  $\beta$ -tubulin invariant gene control spot after normalisation, across all 9 arrays for the three experiments (a-i).

### 7.3.11 Filtering of data on expression and confidence

#### 7.3.11.1 *T. versicolor* vs *S. gausapatum*

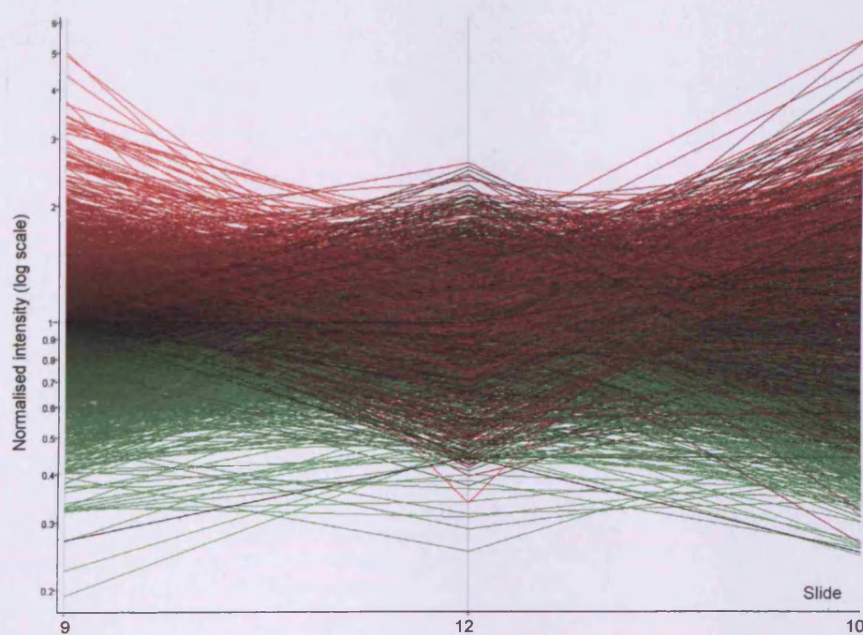
The expression profiles of all spots across all three replicate arrays (Figure 7.27) showed that despite the normalisation, Slide 12 appeared to have a narrower distribution of expressions but that of Slides 9 and 10 was more similar to one another. Data filtered on expression level, showed 348 up-regulated 1.4-fold in at least 2 of 3 TvSg arrays, and of these, 42 were 2-fold up-regulated (Table 7.5). The expression levels of individual genes were closest for Slides 9 and 10 and many individual genes that were clustered together by sequence homology to form contigs (Chapter 6) were up-regulated together. However, within these up-regulated gene lists, two thirds (232) of the 1.4 up-regulated spots were clones from the reverse subtracted library (Table 7.5).

**Table 7.5** Summary of the numbers of genes identified for each experimental pairing when filtered on expression level. Signal expression ratios (Cy5/Cy3; Test/Control) for each fold change were: 1.4 up,  $\geq 1.4$ ; 2 up,  $\geq 2.0$ ; 1.4 down,  $\leq 0.71$ ; 2 down,  $\leq 0.5$ .

Pairing		1.4 up		2 up		1.4 down		2 down	
TvSg	F	348	116	42	18	328	228	77	50
	R		232		24		100		27
TvHf	F	107	46	3	3	131	75	14	13
	R		61		0		56		1
TvBk	F	322	110	25	7	283	143	22	20
	R		212		18		140		2

F: forward subtracted library clones, R: reverse subtracted library clones

TvSg, *T. versicolor* vs *S. gausapatum*; TvHf, *T. versicolor* vs *H. fasciculare*; TvBk, *T. versicolor* vs *B. adusta*.



**Figure 7.27** Line graph showing the normalised expression profile of all *T. versicolor* spots for hybridisations with test probes for *T. versicolor* vs *S. gausapatum* across the three biological replicates, slides 9, 12 and 10. Line colour indicates expression level: Red, up-regulation; Green, down-regulation; Black, no change.

When data were filtered on confidence at various levels, the numbers of genes within lists were greatly reduced. The most stringent confidence filtering,  $p0.05$  with Benjamini and Hochberg, multiple sample correction (MSC B&H), reduced the number of significantly up-regulated genes with annotations (Table 7.6) to only 6. Filtering on less stringent criteria ( $p0.05$  no MSC and  $p0.1$  with MSC B&H) allowed

the majority of spots up-regulated to be considered significant results. Of the up-regulated genes 44 had functional annotations (Table 7.6). The largest group were for peroxidases, within which there were two sets of 4 spots from the same contigs, TVC00830 and TVC00429, which are both derived from large clusters (9 and 14 sequences in each contig respectively). In addition, there were 4 other genes representing peroxidases from other contigs. Proportionally high numbers of ribosomal genes were also up-regulated and other genes involved in protein synthesis (elongation factor, chaperone, tRNA transferase, splicing factor) and metabolism (fatty acid desaturase, glycogen debranching enzyme and aorsin protease). Spots which showed 2 fold up-regulation were two peroxidases, a chaperone protein, elongation factor, glycogen debranching enzyme, clathrin coat assembly protein, ribosomal proteins, plasma membrane associated protein phosphatase and a glycerol dehydrogenase.



**Table 7.6** List of genes, with significant annotation that were 1.4 fold up-regulated in at least 2 out of 3 microarray replicate slides, filtered on expression level, during the interaction *T. versicolor* vs *S. gausapatum*. P-values indicate the significance of differential expression when filtered on confidence, with and without multiple sample corrections (MSC) applied.

Tv_ssh ID	Contig ID	F/R	Seq#	Putative function	E value	mean ratio of all 3	Mean ratio upreg only	mean p value	2 fold up	p0.05 MSC	p0.05 no MSC 3/3	p0.05 no MSC	p0.1 MSC
Tv_sshR_07F06	TVC00655	R	3	1,3-beta-glucan synthase component bgs2	7.00E-15	1.42	1.70	0.03				x	x
Tv_sshR_02F03	TVC00655	R	3	1,3-beta-glucan synthase component bgs3	7.00E-15	1.59	1.95	0.03		x		x	x
Tv_sshR_06D05	TVC00914	R	1	40S ribosomal protein S4	1.00E-55	1.88	2.35	0.01	*		x	x	x
Tv_sshR_04G02	TVC00799	R	1	60S ribosomal protein L17	6.00E-12	1.57	1.71	0.02			x	x	x
Tv_sshR_03C02	TVC00695	R	2	60S ribosomal protein L38	5.00E-13	1.56	1.56	0.03			x	x	x
Tv_sshR_09B07	TVC01120	R	1	Acyl-CoA fatty acid desaturase	2.00E-24	1.38	1.60	0.07				x	x
Tv_sshR_04G05	TVC00801	R	1	Acyl-CoA fatty acid desaturase	1.00E-20	1.84	1.84	0.01			x	x	x
Tv_sshR_07G09	TVC01018	R	1	Aorsin precursor	1.00E-08	1.52	1.52	0.04				x	x
Tv_sshR_05C04	TVC00832	R	2	Catalase	4.00E-34	1.50	1.58	0.04				x	x
Tv_sshR_10B08	TVC01200	R	1	Clathrin coat assembly protein AP50	3.00E-28	2.00	2.43	0.14	*	x		x	x
Tv_sshR_08G03	TVC00014	R	29	DNA polymerase I, thermostable	1.00E-124	1.36	1.60	0.19				x	x
Tv_sshR_06C02	TVC00014	R	29	DNA polymerase I, thermostable	1.00E-124	2.59	3.47	0.06	*			x	x
Tv_sshR_09D11	TVC01145	R	1	Elongation factor 2	3.00E-23	1.74	2.11	0.33	*	x		x	x
Tv_sshR_01F03	TVC00574	R	9	Glycogen debranching enzyme	9.00E-15	1.59	1.59	0.04				x	x
Tv_sshR_01D07	TVC00574	R	9	Glycogen debranching enzyme	9.00E-15	3.17	4.34	0.12	*	x	x	x	x
Tv_sshR_02D02	TVC00638	R	2	GrpE protein homolog	2.00E-13	1.41	1.64	0.23				x	x
Tv_sshR_01B07	TVC00575	R	1	GTP-binding protein YPTC1	9.00E-19	1.46	1.76	0.18					
Tv_sshR_04B06	TVC00286	R	9	large subunit ribosomal RNA gene	2.00E-26	1.63	1.68	0.24					
Tv_sshR_01G03	TVC00286	R	9	large subunit ribosomal RNA gene	2.00E-26	1.68	1.92	0.04				x	
Tv_sshR_06G06	TVC00286	R	9	large subunit ribosomal RNA gene	2.00E-26	2.05	2.05	0.02	*		x	x	x
Tv_sshR_08C07	TVC01008	R	1	Low-affinity zinc transport protein ZRT2	1.00E-05	1.38	1.54	0.09				x	x
Tv_sshF_07H04	TVC00354	F	1	Oligomeric mitochondrial matrix chaperone	2.00E-04	2.09	2.09	0.01	*	x	x	x	x
Tv_sshR_08B03	TVC01039	R	2	Peroxidase	8.00E-06	1.54	1.68	0.07				x	
Tv_sshR_07C06	TVC00959	R	6	Peroxidase	2.00E-09	2.38	2.38	0.02	*		x	x	
Tv_sshR_07F03	TVC00830	R	9	Peroxidase	3.00E-05	1.26	1.44	0.24					
Tv_sshR_06D04	TVC00830	R	9	Peroxidase	3.00E-05	1.39	1.61	0.18		x		x	x
Tv_sshR_06F02	TVC00830	R	9	Peroxidase	3.00E-05	1.78	2.36	0.04	*			x	
Tv_sshR_05H09	TVC00830	R	9	Peroxidase	3.00E-05	1.87	1.78	0.17				x	x
Tv_sshR_04D01	TVC00760	R	1	Peroxidase	3.00E-06	1.49	1.72	0.31				x	
Tv_sshF_10B08	TVC00432	F	1	Peroxidase	2.00E-04	1.65	2.04	0.05				x	x
Tv_sshR_08B04	TVC00429	R	14	Peroxidase	4.00E-10	1.40	1.53	0.14				x	
Tv_sshR_01H09	TVC00429	R	14	Peroxidase	4.00E-10	1.48	1.71	0.34				x	x
Tv_sshF_10B06	TVC00429	F	14	Peroxidase	4.00E-10	1.60	1.78	0.11				x	
Tv_sshF_10B03	TVC00429	F	14	Peroxidase	4.00E-10	1.78	2.03	0.03			x	x	x
Tv_sshF_02C10	TVC00032	F	5	Plasma membrane associated protein phosphatase (stress response)	6.00E-05	1.97	2.41	0.15	*			x	x
Tv_sshR_06C04	TVC00902	R	1	Pre-mRNA processing splicing factor 8	3.00E-31	1.72	1.97	0.03				x	x

Tv_sshR_05C07	TVC00834	R	2	Probable small nuclear ribonucleoprotein Sm D3	6.00E-27	1.23	1.47	0.09				x	
Tv_sshR_01H01	TVC00603	R	3	Putative dioxygenase	2.00E-23	1.32	1.74	0.01			x	x	x
Tv_sshR_02D05	TVC00640	R	2	Putative NADP(+) coupled glycerol dehydrogenase	2.00E-04	1.33	1.63	0.02				x	x
Tv_sshR_09D02	TVC00640	R	2	Putative NADP(+) coupled glycerol dehydrogenase	2.00E-04	1.85	2.53	0.01	*		x	x	x
Tv_sshR_04D09	TVC00775	R	1	serine/threonine kinase receptor associated protein	5.00E-08	1.56	1.74	0.13				x	x
Tv_sshR_04D02	TVC00769	R	1	Synaptic glycoprotein SC2	7.00E-08	1.33	1.63	0.08					
Tv_sshR_03H08	TVC00740	R	1	Threonyl-tRNA synthetase	3.00E-24	1.45	1.52	0.05				x	x
Tv_sshF_02G10	TVC00071	F	3	<i>Trametes versicolor</i> mitochondrial small subunit ribosomal RNA	1.00E-133	1.65	1.78	0.01				x	x

An approximately equal number of spots (328) were 1.4-fold down-regulated (Table 7.4, Table 7.7), with 77 of those 2 fold down-regulated in at least 2 out of 3 arrays. Approximately 70% of these down-regulated spots were clones from the forward library. Again the most abundant group of genes down-regulated were peroxidases (10 spots), two of which were 2 fold down-regulated, and one was significant at the most stringent level of confidence filtering ( $p < 0.05$  with MSC B&H). All peroxidase spots were from different contigs and many were singletons. One gene, Tv\_sshR\_06D02, was from a contig (TVC00830), members of which were also up-regulated (Tables 7.6, 7.7). The next largest group of down-regulated spots was cytochrome c oxidase subunit 1s. Two spots representing HBS-1 like proteins and a single spot representing a putative actin, were all 2 fold down-regulated significantly at  $p < 0.05$  with no MSC.

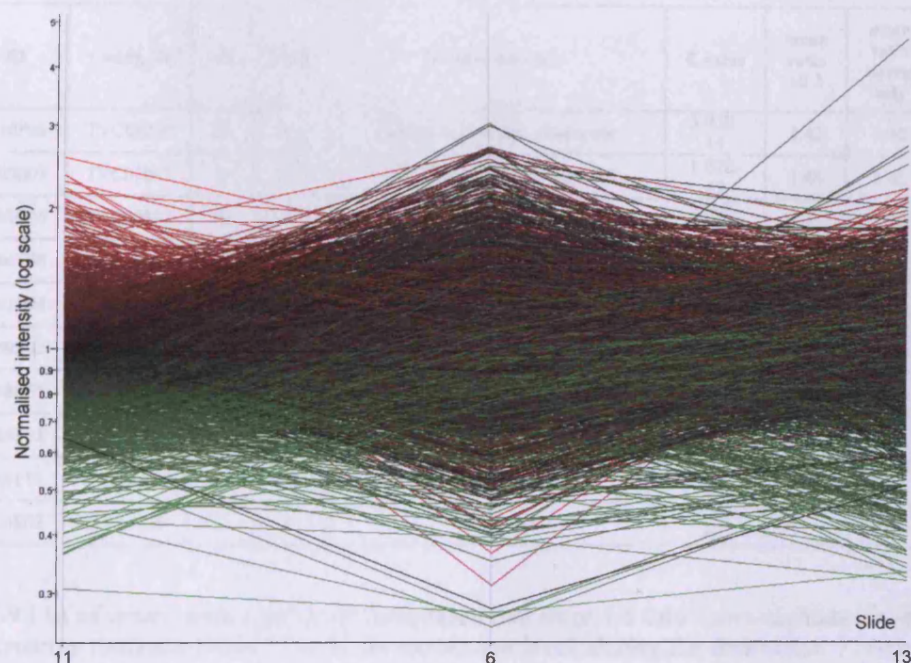
**Table 7.7** List of genes, with significant annotation that were 1.4 fold down-regulated in at least 2 out of 3 microarray replicate slides, filtered on expression level, during the interaction *T. versicolor* vs *S. gausapatum*. P-values indicate the significance of differential expression when filtered on confidence, with and without multiple sample corrections (MSC) applied.

Tv_ssh ID	Contig ID	F/R	Seq#	Putative function	E value	mean ratio all 3	mean down reg only	Fold change	mean p value	2 fold down	p0.05 MSC	p0.05 no MSC 3/3	p0.05 no MSC	p0.1 MSC
Tv_sshR_05E07	TVC00655	R	3	1,3-beta-glucan synthase component bgs2	7.00E-15	0.681	0.55	1.83	0.43					
Tv_sshR_03E01	TVC00712	R	1	60S ribosomal protein L19	3.00E-07	0.678	0.44	2.26	0.08	*				
Tv_sshR_10H12	TVC01230	R	2	Acyl-CoA fatty acid desaturase	3.00E-15	0.585	0.50	1.99	0.07					
Tv_sshF_03A01	TVC00047	F	3	Cytochrome c oxidase subunit I	1.00E-11	0.374	0.37	2.67	0.01	*				
Tv_sshF_06C07	TVC00101	F	4	Cytochrome c oxidase subunit I	2.00E-21	0.674	0.51	1.94	0.31		x		x	x
Tv_sshR_01E02	TVC00590	R	1	Cytochrome c oxidase subunit I	3.00E-16	0.745	0.68	1.48	0.26				x	x
Tv_sshR_04E02	TVC00743	R	2	Cytochrome c oxidase subunit I	8.00E-53	0.521	0.38	2.61	0.03	*				
Tv_sshR_04A01	TVC00743	R	2	Cytochrome c oxidase subunit I	8.00E-53	0.544	0.45	2.23	0.05	*				
Tv_sshF_02E08	TVC00047	F	3	Cytochrome c oxidase subunit I	1.00E-11	0.687	0.63	1.60	0.16					
Tv_sshF_03H07	TVC00144	F	3	Cytochrome c oxidase subunit I	2.00E-55	0.596	0.60	1.68	0.05				x	
Tv_sshR_03A09	TVC00101	R	4	Cytochrome c oxidase subunit I	2.00E-21	0.744	0.66	1.51	0.08				x	x
Tv_sshR_02E09	TVC00650	R	1	Cytochrome P450 51	1.00E-05	0.648	0.54	1.84	0.07					
Tv_sshR_01E03	TVC00574	R	9	Glycogen debranching enzyme	9.00E-15	0.632	0.44	2.25	0.32	*			x	x
Tv_sshF_07E12	TVC00333	F	2	HBS1-like protein	3.00E-07	0.514	0.41	2.45	0.06	*			x	x
Tv_sshF_10E12	TVC00333	F	2	HBS1-like protein	3.00E-07	0.550	0.46	2.16	0.02	*			x	
Tv_sshF_08E07	TVC00395	F	1	Hypothetical 95.4 kDa protein in SEC4-MSH4 intergenic region	3.00E-07	0.542	0.54	1.84	0.33		x		x	x
Tv_sshR_10C11	TVC01209	R	1	large subunit ribosomal RNA gene	5.00E-16	0.925	0.69	1.44	0.05				x	
Tv_sshF_10E02	TVC00455	F	1	Peroxidase	6.00E-08	0.553	0.45	2.20	0.01	*	x	x	x	x
Tv_sshR_08A01	TVC01031	R	1	Peroxidase	5.00E-10	0.660	0.49	2.04	0.50	*				
Tv_sshF_04G01	TVC00191	F	1	Peroxidase	9.00E-06	0.624	0.51	1.98	0.04				x	x
Tv_sshF_03E11	TVC00122	F	1	Peroxidase	5.00E-08	0.615	0.51	1.98	0.17				x	x
Tv_sshF_06A12	TVC00232	F	1	Peroxidase	3.00E-09	0.647	0.53	1.90	0.11				x	x
Tv_sshR_09E08	TVC01039	R	2	Peroxidase	8.00E-06	0.766	0.55	1.83	0.06				x	x
Tv_sshR_06D02	TVC00830	R	9	Peroxidase	3.00E-05	0.638	0.56	1.79	0.10				x	
Tv_sshF_10E05	TVC00458	F	1	Peroxidase	4.00E-04	0.570	0.57	1.75	0.03				x	
Tv_sshR_04A09	TVC00749	R	1	Peroxidase	7.00E-06	0.570	0.57	1.75	0.02				x	
Tv_sshR_10B11	TVC00678	R	2	Peroxidase	9.00E-04	0.902	0.66	1.52	0.05				x	
Tv_sshF_02H01	TVC00032	F	5	Plasma membrane associated protein phosphatase (stress response)	6.00E-05	0.630	0.51	1.97	0.11				x	
Tv_sshR_03A03	TVC00032	R	5	Plasma membrane associated protein phosphatase (stress response)	6.00E-05	0.883	0.56	1.77	0.09					
Tv_sshR_05D01	TVC00838	R	1	Probable reductase	9.00E-14	0.819	0.63	1.58	0.24					
Tv_sshF_11E12	TVC00534	F	1	Putative actin 9	7.00E-10	0.599	0.38	2.60	0.30	*			x	x
Tv_sshF_02B07	TVC00014	F	29	<i>Taq</i> polymerase 1	1.00E-124	0.585	0.43	2.34	0.32	*				
Tv_sshF_04E02	TVC00014	F	29	<i>Taq</i> polymerase 2	1.00E-124	0.623	0.56	1.79	0.04				x	x
Tv_sshF_03B12	TVC00014	F	29	<i>Taq</i> polymerase 3	1.00E-124	0.651	0.58	1.71	0.17					
Tv_sshF_10A07	TVC00014	F	29	<i>Taq</i> polymerase 4	1.00E-124	0.677	0.62	1.61	0.13					
Tv_sshF_04A07	TVC00014	F	29	<i>Taq</i> polymerase 5	1.00E-124	0.657	0.63	1.59	0.15					
Tv_sshF	TVC00014	F	29	<i>Taq</i> polymerase 6	1.00E-	0.828	0.66	1.52	0.07					

03A10					124									
Tv_sshR-06H01	TVC00948	R	I	Ubiquinol-cytochrome c reductase complex 14 kDa protein	8.00E-19	0.842	0.70	1.44	0.08					

### 7.3.11.2 *T. versicolor* vs *H. fasciculare*

The expression profiles of all spots for individual arrays within the *T. versicolor* vs *H. fasciculare* experiment showed that there was some variation between slides and that the majority of genes did not change in expression (Figure 7.28).



**Figure 7.28** Line graph showing the normalised expression profile of all Tv spots for hybridisations with test probes for *T. versicolor* vs *H. fasciculare* across the three biological replicates, slides 11, 6 and 13. Line colour indicates expression level: Red, up-regulation; Green, down-regulation; Black, no change.

One hundred and seven spots were 1.4-fold up-regulated and three of those 2-fold up-regulated in at least two out of three arrays (Table 7.5). These spots were divided almost equally between forward and reverse subtracted clones (46 forward and 61 reverse; Table 7.5). Only 10 of these spots had functional annotations (Table 7.8) and included 3 peroxidases, a low-affinity zinc transporter protein, a fatty acid desaturase, endonucleases, cytochrome c oxidase and an electron transfer protein. When filtered on confidence none of these spots were significant at the most stringent level ( $p < 0.05$  with MSC B&H), although some were significant at  $p < 0.05$  with no MSC.

One hundred and thirty one spots were 1.4 down-regulated and 14 2-fold down-regulated when filtered on expression level (Table 7.5). Sixteen had functional

annotations (Table 7.9) and included two peroxidases, a plasma membrane associated protein phosphatase, cytochrome c oxidase subunit 1 and a tumour necrosis factor. A glycerol dehydrogenase, a reductase and a cytochrome c oxidase were 2 fold up-regulated. Very few of these genes were significant when filtered on confidence.

**Table 7.8** List of genes, with significant annotation that were 1.4 fold up-regulated in at least 2 out of 3 microarray replicate slides, filtered on expression level, during the interaction *T. versicolor* vs *H. fasciculare*. P-values indicate the significance of differential expression when filtered on confidence, with and without multiple sample corrections (MSC) applied.

Tv_ssh ID	Contig ID	F/R	Seq#	Putative function	E value	mean ratio all 3	mean ratio upreg only	mean p value	p0.05 MSC	p0.05 no MSC 3/3	p0.05 no MSC	p0.1 MSC
Tv_sshR_10F06	TVC01230	R	2	Acyl-CoA fatty acid desaturase	3.00E-15	1.42	1.48	0.12				
Tv_sshR_08B07	TVC01047	R	1	Cytochrome c oxidase subunit 1	1.00E-49	1.44	1.65	0.27				
Tv_sshR_04G06	TVC00802	R	1	Electron transfer protein 1	2.00E-04	1.55	1.55	0.02			x	
Tv_sshR_06F08	TVC00936	R	1	GrpE protein homolog	4.00E-16	1.62	1.83	0.01		x	x	
Tv_sshR_01B04	TVC00573	R	2	Intron-encoded DNA endonuclease a14 precursor	3.00E-34	1.26	1.53	0.01		x	x	
Tv_sshR_09E02	TVC00573	R	2	Intron-encoded DNA endonuclease a14 precursor	3.00E-34	1.71	1.97	0.02		x	x	
Tv_sshR_08C07	TVC01008	R	1	Low-affinity zinc transport protein ZRT2	1.00E-05	1.54	1.64	0.04			x	
Tv_sshR_06F02	TVC00830	R	9	Peroxidase	3.00E-05	1.61	1.83	0.16				
Tv_sshR_09F11	TVC00429	R	14	Peroxidase	4.00E-10	1.43	1.54	0.39				
Tv_sshF_06E02	TVC00260	F	1	Peroxidase	2.00E-07	1.52	1.78	0.33				

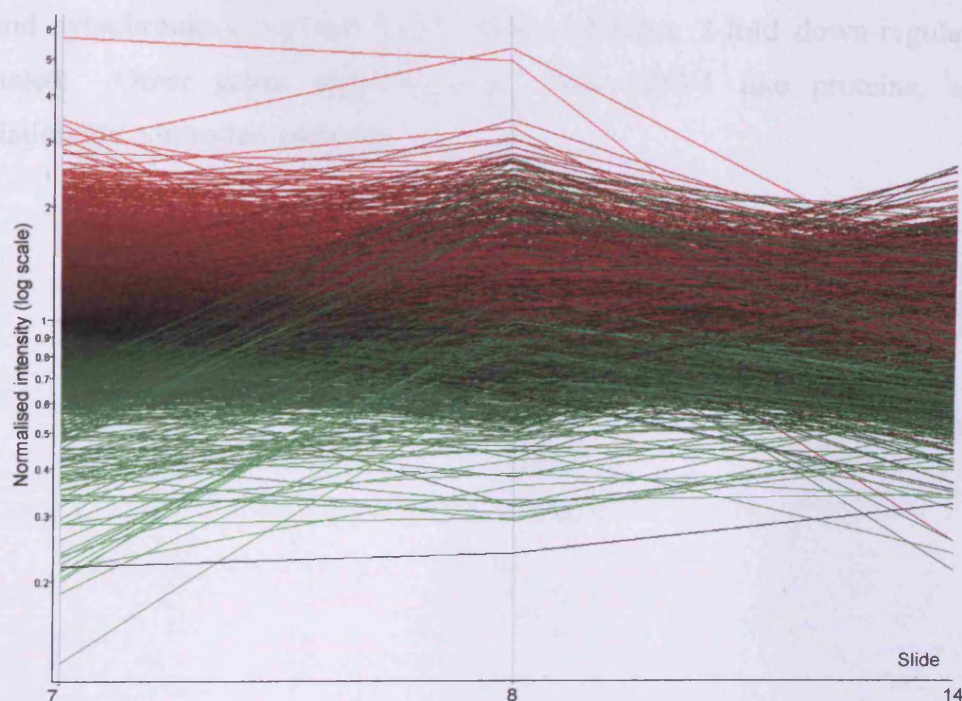
**Table 7.9** List of genes, with significant annotation that were 1.4 fold down-regulated in at least 2 out of 3 microarray replicate slides, filtered on expression level, during the interaction *T. versicolor* vs *H. fasciculare*. P-values indicate the significance of differential expression when filtered on confidence, with and without multiple sample corrections (MSC) applied.

Tv_ssh ID	Contig ID	F/R	Seq#	Putative function	E value	mean ratio all 3	mean ratio downreg only	mean p value	2 fold	p0.05 MSC	p0.05 no MSC 3/3	p0.05 no MSC	p0.1 MSC
Tv_sshR_10D01	TVC01211	R	1	30S ribosomal protein S2	2.00E-06	0.63	0.49	2.03				x	
Tv_sshR_01B09	TVC00577	R	1	Aminomethyltransferase	9.00E-08	1.22	0.49	2.04			x	x	
Tv_sshF_03A01	TVC00047	F	3	Cytochrome c oxidase subunit 1	1.00E-11	0.58	0.59	1.70	*				
Tv_sshF_02B07	TVC00014	F	29	DNA polymerase I, thermostable	1.00E-124	0.67	1.30	0.77					
Tv_sshF_08E07	TVC00395	F	1	Hypothetical 95.4 kDa protein in SEC4-MSH4 intergenic region	3.00E-07	0.74	0.57	1.74					
Tv_sshR_10D08	TVC01215	R	1	hypothetical protein CC1G_03111 [Coprinopsis cinerea okayama7#130]	1.00E-10	0.69	0.60	1.67					
Tv_sshR_06D09	TVC00917	R	1	Mitochondrial intermediate peptidase	5.00E-51	0.74	0.61	1.64					
Tv_sshR_06D02	TVC00830	R	9	Peroxidase	3.00E-05	0.73	0.55	1.80					
Tv_sshF_04G01	TVC00191	F	1	Peroxidase	9.00E-06	0.70	0.60	1.67					
Tv_sshF_02H01	TVC00032	F	5	Plasma membrane associated protein phosphatase (stress response)	6.00E-05	0.56	0.74	1.35					
Tv_sshR_02H01	TVC00670	R	2	predicted protein [Coprinopsis cinerea okayama7#130]	1.00E-06	1.01	0.68	1.47			x		
Tv_sshR_05H07	TVC00878	R	1	predicted protein [Coprinopsis cinerea okayama7#130]	3.00E-05	0.66	0.71	1.41			x		
Tv_sshR_09D02	TVC00640	R	2	Putative NADP(+) coupled glycerol dehydrogenase	2.00E-04	0.62	0.74	1.34	*				

Tv_sshR_05D01	TVC00838	R	1	Reductase	9.00E-14	0.57	0.70	1.43	*		x		
Tv_sshR_06C02	TVC00014	R	29	Taq polymerase 1	1.00E-124	0.94	0.71	1.40					
Tv_sshR_03H04	TVC00737	R	1	Tumor necrosis factor ligand superfamily member 6	0	0.60	0.76	1.32					

### 7.3.11.3 *T. versicolor* vs *B. adusta*

The three replicate arrays for this experiment showed the most consistency between arrays (Figure 7.29). The majority of genes did not show any differential expression (i.e. ratio approx. = 1) and there appeared to be a larger number of down-regulated genes than up-regulated.



**Figure 7.29** Line graph showing the normalised expression profile of all Tv spots for hybridisations with test probes for *T. versicolor* vs *B. adusta* across the three biological replicates, slides 7, 8 and 14. Line colour indicates expression level: Red, up-regulation; Green, down-regulation; Black, no change.

Spots filtered on expression level showed that 322 spots were 1.4-fold up-regulated, and 25 of these were 2-fold up-regulated in at least two out of three arrays (Table 7.5). Approximately two thirds of 1.4-fold up-regulated spots were clones from the reverse subtracted library. Thirty-six spots had functional annotations (Table 7.10) and the major group up-regulated were the peroxidases, 14 spots with a set of 5, and three of these spots from within single contigs (TVC00429 and TVC00830 respectively), all of which were significant at  $p < 0.05$  with no MSC. The other major groups were

cytochrome c oxidase subunit 1 and ribosomal proteins. Other genes included 1,3-beta-glucan synthase, catalase, clathrin coat assembly protein, high affinity zinc transport protein and glycogen debranching enzymes. The majority of annotated up-regulated spots were significant at  $p < 0.05$  with no MSC but more stringent filtering on confidence with  $p < 0.05$  with MSC B&H or  $p < 0.1$  MSC reduced the number of significant spots.

Spots that were 1.4-fold down-regulated (283) were distributed equally between forward and reverse libraries (Table 7.5), although 22 were 2-fold down-regulated and the majority of these (20) were from the forward library. Thirty-five of the spots had functional annotations (Table 7.11) and the most common groups were peroxidases (7) and cytochrome c oxidase 1 (7). None of those 2-fold down-regulated were annotated. Other genes down-regulated were HBS-1 like proteins, actin and translationally controlled proteins.

**Table 7.10** List of genes, with significant annotation that were 1.4 fold up-regulated in at least 2 out of 3 microarray replicate slides, filtered on expression level, during the interaction *T. versicolor* vs *B. adusta*. P-values indicate the significance of differential expression when filtered on confidence, with and without multiple sample corrections (MSC) applied.

Tv_ssh ID	Contig ID	F/R	Seq #	Putative function	E value	mean ratio	mean ratio upreg only	mean p value	2 fold	p0.05 MSC	p0.05 no MSC 3/3	p0.05 no MSC	p0.1 MSC
Tv_sshR_02F03	TVC00655	R	3	1,3-beta-glucan synthase component bgs2	7.00 E-15	2.01	2.43	0.01	*		x	x	x
Tv_sshR_07F06	TVC00655	R	3	1,3-beta-glucan synthase component bgs2	7.00 E-15	1.40	1.61	0.30					
Tv_sshR_04G02	TVC00799	R	1	60S ribosomal protein L17	6.00 E-12	1.47	1.65	0.07				x	
Tv_sshR_10E05	TVC00695	R	2	60S ribosomal protein L38	5.00 E-13	1.51	1.81	0.14					
Tv_sshR_09B10	TVC01123	R	1	60S ribosomal protein L39	1.00 E-18	1.46	1.66	0.08				x	
Tv_sshR_04G05	TVC00801	R	1	Acyl-CoA desaturase	1.00 E-20	1.63	1.77	0.03			x	x	
Tv_sshR_06A02	TVC00884	R	1	Catalase	7.00 E-13	1.60	1.60	0.05				x	
Tv_sshR_10B08	TVC01200	R	1	Clathrin coat assembly protein AP50	3.00 E-28	1.72	1.94	0.05				x	x
Tv_sshF_10E11	TVC00144	F	3	Cytochrome c oxidase subunit 1	2.00 E-55	1.74	2.00	0.08					
Tv_sshR_08B07	TVC01047	R	1	Cytochrome c oxidase subunit 1	1.00 E-49	1.48	1.55	0.03			x	x	
Tv_sshR_10A04	TVC01187	R	1	Cytochrome c oxidase subunit 1	3.00 E-11	1.44	1.61	0.12					
Tv_sshR_03B07	TVC00689	R	5	Cytochrome c oxidase subunit 1	1.00 E-31	1.76	2.01	0.06					
Tv_sshR_06C02	TVC00014	R	29	DNA polymerase I, thermostable	1.00 E-124	2.17	2.89	0.02	*			x	x
Tv_sshR_01F03	TVC00574	R	9	Glycogen debranching enzyme	9.00 E-15	1.72	1.72	0.03				x	
Tv_sshR_02F09	TVC00574	R	9	Glycogen debranching enzyme	9.00 E-15	2.02	2.02	0.02			x	x	
Tv_sshR_06F08	TVC00936	R	1	GrpE protein homolog	4.00 E-16	1.30	1.44	0.33				x	x
Tv_sshR_08E06	TVC01073	R	1	High-affinity zinc transport protein ZRT1	8.00 E-18	1.59	1.77	0.08					
Tv_sshR_09A07	TVC01110	R	1	Hypothetical 107.7 kDa protein in TSP3-IPP2 intergenic region	7.00 E-12	1.50	1.50	0.07					
Tv_sshR_01B04	TVC00573	R	2	Intron-encoded DNA endonuclease al4 precursor	3.00 E-34	1.69	1.83	0.05				x	
Tv_sshF_07F06	TVC00337	F	1	Peroxidase	3.00 E-07	1.49	1.63	0.01				x	
Tv_sshF_10B06	TVC00429	F	14	Peroxidase	4.00 E-10	1.89	1.89	0.02			x	x	
Tv_sshR_02B03	TVC00429	R	14	Peroxidase	4.00 E-10	1.57	1.82	0.10				x	
Tv_sshF_10B03	TVC00429	F	14	Peroxidase	4.00 E-10	1.83	1.83	0.01			x	x	x
Tv_sshR_06F03	TVC00429	R	14	Peroxidase	4.00 E-10	1.74	1.74	0.02			x	x	x
Tv_sshR_08B04	TVC00429	R	14	Peroxidase	4.00 E-10	1.60	1.79	0.09				x	
Tv_sshF_10B08	TVC00432	F	1	Peroxidase	2.00 E-04	1.68	1.97	0.11				x	
Tv_sshR_07F03	TVC00830	R	9	Peroxidase	3.00 E-05	1.48	1.69	0.26				x	
Tv_sshR_06F02	TVC00830	R	9	Peroxidase	3.00 E-05	2.02	2.02	0.01	*		x	x	x
Tv_sshR_06B09	TVC00830	R	9	Peroxidase	3.00 E-05	1.54	1.69	0.10				x	
Tv_sshR_07C06	TVC00959	R	6	Peroxidase	2.00 E-09	1.80	1.80	0.02				x	x
Tv_sshR_09B03	TVC00982	R	3	Peroxidase	2.00 E-11	1.45	1.71	0.17					
Tv_sshR_07F01	TVC01000	R	1	Peroxidase	6.00 E-07	1.66	1.93	0.04				x	
Tv_sshR_08B03	TVC01039	R	2	Peroxidase	8.00 E-06	1.61	1.75	0.03				x	x
Tv_sshR_01A05	TVC00567	R	1	Phosphoglucomutase	4.00 E-11	1.45	1.68	0.31				x	x
Tv_sshF_02C10	TVC00032	F	5	Plasma membrane associated protein phosphatase	6.00 E-05	1.51	1.65	0.03				x	
Tv_sshR_06C04	TVC00902	R	1	Pre-mRNA processing splicing factor 8	3.00 E-31	1.57	1.83	0.04				x	



**Table 7.11** List of genes, with significant annotation that were 1.4 fold down-regulated in at least 2 out of 3 microarray replicate slides, filtered on expression level, during the interaction *T. versicolor* vs *B. adusta*. P-values indicate the significance of differential expression when filtered on confidence, with and without multiple sample corrections (MSC) applied.

Tv_ssh ID	Contig ID	F/R	Seq #	Putative function	E value	mean ratio	mean ratio downreg only	fold down	mean p value	p0.05 MSC	p0.05 no MSC 3/3	p0.05 no MSC	p0.1 MSC
Tv_sshR_05E07	TVC00655	R	3	1,3-beta-glucan synthase component bgs2	7.00E-15	0.84	0.68	1.47	0.11			x	x
Tv_sshR_10D01	TVC01211	R	1	30S ribosomal protein S2	2.00E-06	0.69	0.67	1.49	0.02		x	x	
Tv_sshR_03E01	TVC00712	R	1	60S ribosomal protein L19	3.00E-07	0.86	0.62	1.60	0.03			x	x
Tv_sshR_10H12	TVC01230	R	2	Acyl-CoA desaturase	3.00E-15	0.67	0.62	1.62	0.04				
Tv_sshR_06H08	TVC00832	R	2	Catalase	4.00E-34	0.68	0.60	1.67	0.02		x		x
Tv_sshR_06H06	TVC00951	R	1	Cell division control protein 3	2.00E-10	0.68	0.64	1.55	0.05			x	
Tv_sshF_03A01	TVC00047	F	3	Cytochrome c oxidase subunit 1	1.00E-11	0.62	0.49	2.02	0.18				
Tv_sshR_10H11	TVC00144	R	3	Cytochrome c oxidase subunit 1	2.00E-55	0.65	0.49	2.04	0.07				
Tv_sshF_03H07	TVC00144	F	3	Cytochrome c oxidase subunit 1	2.00E-55	0.60	0.60	1.65	0.07			x	
Tv_sshR_03H09	TVC00689	R	5	Cytochrome c oxidase subunit 1	1.00E-31	0.72	0.62	1.62	0.29				
Tv_sshF_06C07	TVC00101	F	4	Cytochrome c oxidase subunit 1	2.00E-21	0.83	0.62	1.60	0.03			x	
Tv_sshF_03F09	TVC00014	F	29	DNA polymerase I, thermostable	1.00E-124	0.74	0.65	1.54	0.12				
Tv_sshF_02D10	TVC00014	F	29	DNA polymerase I, thermostable	1.00E-124	0.69	0.66	1.52	0.06				
Tv_sshF_08H06	TVC00014	F	29	DNA polymerase I, thermostable	1.00E-124	0.78	0.67	1.48	0.03				
Tv_sshR_09D11	TVC01145	R	1	Elongation factor 2	3.00E-23	0.66	0.55	1.83	0.31				
Tv_sshR_01D02	TVC00574	R	9	Glycogen debranching enzyme	9.00E-15	0.68	0.41	2.42	0.25				
Tv_sshF_07E12	TVC00333	F	2	HBS1-like protein	3.00E-07	0.51	0.38	2.62	0.15				
Tv_sshF_10E12	TVC00333	F	2	HBS1-like protein	3.00E-07	0.72	0.62	1.61	0.14				
Tv_sshR_04A01	TVC00743	R	2	intronic ORF at intron 6 of cox1	8.00E-53	0.76	0.60	1.66	0.69				
Tv_sshR_04E02	TVC00743	R	2	intronic ORF at intron 6 of cox1	8.00E-53	0.79	0.61	1.65	0.18			x	x
Tv_sshR_01D04	TVC00587	R	1	large subunit ribosomal RNA gene	4.00E-12	0.65	0.65	1.54	0.16				
Tv_sshR_08A01	TVC01031	R	1	Peroxidase	5.00E-10	0.86	0.61	1.63	0.07			x	x
Tv_sshF_06A12	TVC00232	F	1	Peroxidase	3.00E-09	0.80	0.63	1.60	0.07			x	
Tv_sshR_06D02	TVC00830	R	9	Peroxidase	3.00E-05	0.63	0.63	1.59	0.02			x	
Tv_sshR_06D04	TVC00830	R	9	Peroxidase	3.00E-05	0.69	0.63	1.58	0.10				
Tv_sshF_10E02	TVC00455	F	1	Peroxidase	6.00E-08	0.72	0.64	1.57	0.03		x	x	
Tv_sshR_10B11	TVC00678	R	2	Peroxidase	9.00E-04	0.80	0.67	1.49	0.16			x	
Tv_sshR_01H06	TVC00429	R	14	Peroxidase	4.00E-10	0.72	0.69	1.46	0.34				
Tv_sshF_05H01	TVC00032	F	5	Plasma membrane associated protein phosphatase	6.00E-05	0.73	0.63	1.58	0.18				
Tv_sshR_05D04	TVC00841	R	1	Probable ornithine aminotransferase	4.00E-05	0.68	0.61	1.64	0.09			x	
Tv_sshF_11E12	TVC00534	F	1	Putative actin 9	7.00E-10	0.72	0.55	1.83	0.20				
Tv_sshR_04D02	TVC00769	R	1	Synaptic glycoprotein SC2	7.00E-08	0.79	0.63	1.58	0.25				
Tv_sshR_03H08	TVC00740	R	1	Threonyl-tRNA synthetase, cytoplasmic	3.00E-24	0.67	0.61	1.63	0.14			x	
Tv_sshF_05H06	TVC00224	F	2	Translationally controlled tumor protein (TCTP)	1.00E-10	0.72	0.65	1.54	0.03			x	
Tv_sshR_06H01	TVC00948	R	1	Ubiquinol-cytochrome c reductase complex 14 kDa protein	8.00E-19	0.75	0.60	1.68	0.07			x	

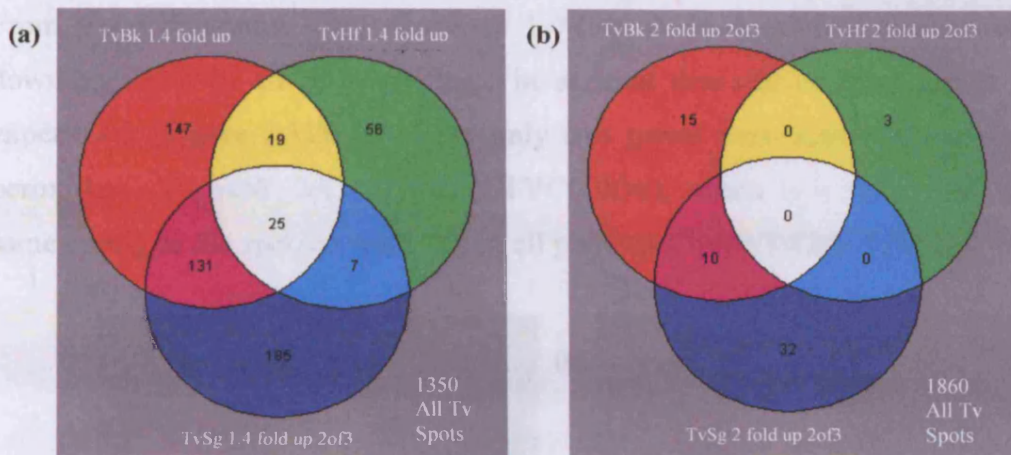
#### 7.3.11.4 *Comparison of experimental pairings*

Simple comparison between the gene lists generated for each experimental pairing revealed several common genes that appeared to be up-regulated during interactions. Although there were several common peroxidase sequences up-regulated, in particular contigs TVC00830 and TVC00429 tended to be present in the list of up-regulated genes for each pairing. Contig TVC00191 and some members of TVC00830 were also common to the down-regulated peroxidase sequences in the different pairings.

A contig encoding a 1,3-beta-glucan synthase gene was differentially expressed. Within the contig encoding this enzyme, which was derived from 3 clone sequences, two of these sequences (R7F6, R2F3) were up-regulated in both TvSg and TvBk and the third clone sequence (R5E7) was down-regulated in both.

Genes that were up-regulated in all pairings include zinc transport proteins, acyl-CoA fatty acid desaturases, cytochrome oxidase, ribosomal proteins, glycogen debranching enzymes and 1,3-glucan synthase.

Venn diagrams showed the number of spots whose expression was up or down in the separate experiments. There were 25 spots 1.4-fold up-regulated in all three experimental pairings (TvSg, TvBk, TvHf; Figure 7.30 a), but none were 2-fold up-regulated (Figure 7.30 b). Only one of the 25 up-regulated genes had a functional annotation, which was a peroxidase (Tv\_sshR\_06F02, contig TVC00830) with a mean ratio of 1.81. There were more genes shared between TvSg and TvBk (131, 1.4-fold up; 10 2-fold up) than was shared with TvHf by either (19 with TvBk and 7 with TvSg, 1.4-fold up; 0 for both, 2-fold up) (Figure 7.30 a, b). The similarities in the types of genes expressed were not as apparent in these interpretations as manual inspections above, since Venn diagrams only picked out individual clones that were up or down-regulated in all, rather than groups types of genes and contigs.



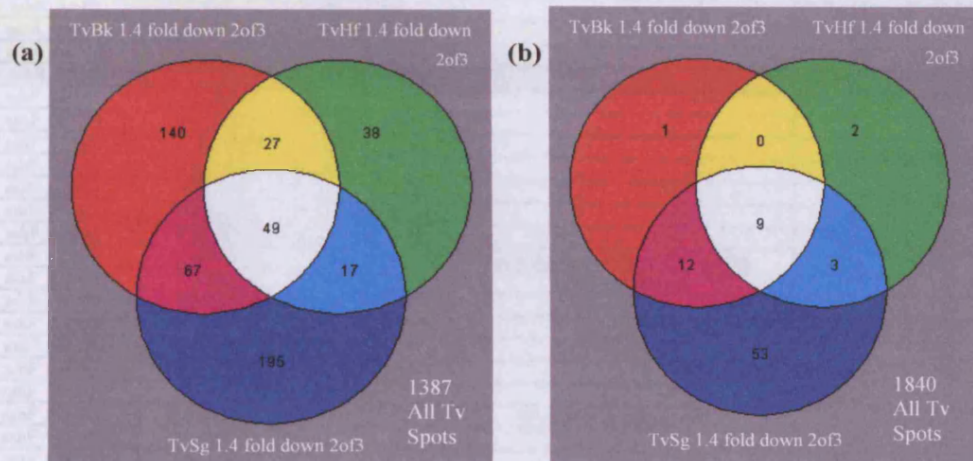
**Figure 7.30** Venn diagrams showing up-regulated genes for all three experiments. Genes were filtered on expression level (a) 1.4 fold change (b) 2 fold change.

**Table 7.12** Genes with 1.4 fold up-regulated expression levels in all experimental pairings of *T. versicolor* i.e. with *S. gausapatum*, *H. fasciculare* and *B. adusta*, in at least 2 out of 3 replicate microarrays.

Tv_ssh ID	Contig ID	F/R	Seq#	Putative function	mean ratio	mean p value
Tv_sshF_09C04	-	F	-	-	1.57	0.158
Tv_sshR_04B09	-	R	-	-	1.81	0.070
Tv_sshR_7C11	-	R	-	-	1.74	0.167
Tv_sshR_1F11	-	R	-	-	1.67	0.090
Tv_sshR_7C10	-	R	-	-	1.61	0.091
Tv_sshR_8B12	-	R	-	-	1.61	0.021
Tv_sshR_04C04	-	R	-	-	1.55	0.077
Tv_sshF_05B03	TVC00015	F	3	-	1.66	0.043
Tv_sshF_04G12	TVC00079	F	8	<i>T. versicolor</i> EST	1.83	0.042
Tv_sshF_10A03	TVC00203	F	6	-	1.73	0.028
Tv_sshF_11F07	TVC00300	F	3	-	1.65	0.131
Tv_sshF_08G09	TVC00408	F	1	<i>T. versicolor</i> EST	1.72	0.038
Tv_sshF_10G12	TVC00484	F	1	<i>T. versicolor</i> EST	1.83	0.042
Tv_sshR_02B08	TVC00625	R	1	-	1.69	0.040
Tv_sshR_03F02	TVC00703	R	2	hypothetical protein	1.52	0.056
Tv_sshR_10F08	TVC00748	R	8	-	1.64	0.275
Tv_sshR_04B05	TVC00748	R	8	-	1.62	0.074
Tv_sshR_06B06	TVC00762	R	2	-	1.56	0.034
Tv_sshR_08F04	TVC00807	R	11	-	1.67	0.060
Tv_sshR_06F02	TVC00830	R	9	Peroxidase	1.87	0.017
Tv_sshR_06F05	TVC00933	R	2	-	1.58	0.087
Tv_sshR_06F07	TVC00935	R	1	-	1.63	0.066
Tv_sshR_07F02	TVC01001	R	1	hypothetical protein	1.50	0.104
Tv_sshR_07F07	TVC01004	R	1	-	1.71	0.036
Tv_sshR_09A01	TVC01106	R	1	-	1.73	0.035

Manual inspection of gene lists for each experiment showed that there were several genes down-regulated in all pairings. A peroxidase (TVC00830), cytochrome c oxidase (TVC00047) and a plasma membrane associated protein phosphatase (TVC00032) were both represented in lists of down-regulated genes in all pairings. TvSg and TvBk shared more down-regulated genes including peroxidases (TVC00232, TVC01031, TVC00455, TVC00678) and HBS-1 like proteins (TVC00333).

From Venn diagrams, 49 genes were 1.4-fold down-regulated, and 9 were 2-fold down-regulated in all three pairings, in at least two out of three arrays for each experiment (Figure 7.31). Of these only two genes were annotated and included a peroxidase (Tv\_sshR\_06D02, contig TVC00830), which is a spot from within the same contig as the spot up-regulated in all pairings (Table 7.13).



**Figure 7.31** Venn diagrams showing down-regulated genes for all three experiments. Genes were filtered on expression level (a) 1.4 fold change (b) 2 fold change.

**Table 7.13** Genes with 1.4 fold down-regulated expression levels in all experimental pairings of *T. versicolor* i.e. with *S. gausapatum*, *H. fasciculare* and *B. adusta* in at least 2 out of 3 replicate microarrays. Genes with 2 fold down-regulation are indicated with asterisks.

Tv_ssh ID	Contig ID	F/R	Seq#	Putative function	mean ratio	fold down	mean p value	2 fold down on venn
Tv_sshF_03D11	-	F	-	-	0.37	2.68	0.05	*
Tv_sshF_03D05	-	F	-	-	0.42	2.36	0.07	
Tv_sshF_03A03	-	F	-	-	0.44	2.29	0.05	*
Tv_sshF_03D12	-	F	-	-	0.60	1.66	0.03	
Tv_sshF_03C09	-	F	-	-	0.62	1.61	0.12	
Tv_sshR_5A12	-	R	-	-	0.62	1.62	0.09	
Tv_sshR_06E01	-	R	-	-	0.65	1.53	0.04	
Tv_sshR_10D10	-	R	-	-	0.70	1.43	0.19	
Tv_sshR_7E12	-	R	-	-	0.86	1.16	0.10	
Tv_sshF_02A01	TVC00001	F	3	-	0.51	1.94	0.14	
Tv_sshF_02A03	TVC00003	F	2	-	0.55	1.82	0.03	
Tv_sshF_02A05	TVC00005	F	3	-	0.50	2.00	0.07	
Tv_sshF_02A07	TVC00007	F	2	-	0.50	2.01	0.04	
Tv_sshF_02A11	TVC00011	F	3	-	0.47	2.12	0.09	*
Tv_sshF_06D01	TVC00011	F	3	-	0.60	1.67	0.01	
Tv_sshF_02B01	TVC00013	F	2	-	0.54	1.86	0.02	
Tv_sshF_02B03	TVC00015	F	3	<i>Antrodia cinnamomea</i> cDNA clone	0.51	1.96	0.17	
Tv_sshF_02D05	TVC00017	F	27	predicted protein	0.51	1.95	0.04	
Tv_sshF_02C01	TVC00023	F	2	-	0.54	1.84	0.08	
Tv_sshF_02D03	TVC00025	F	4	-	0.49	2.05	0.14	
Tv_sshF_02C03	TVC00025	F	4	-	0.51	1.97	0.03	
Tv_sshF_02C07	TVC00029	F	6	-	0.51	1.95	0.04	
Tv_sshF_02D01	TVC00035	F	2	-	0.33	2.99	0.05	*
Tv_sshF_02D07	TVC00039	F	9	<i>T. versicolor</i> cDNA clone	0.42	2.37	0.02	
Tv_sshF_02D09	TVC00041	F	4	-	0.38	2.64	0.02	*
Tv_sshF_02D11	TVC00042	F	3	-	0.35	2.84	0.03	
Tv_sshF_05D12	TVC00043	F	4	-	0.72	1.40	0.10	
Tv_sshF_03A01	TVC00047	F	3	Cytochrome c oxidase subunit 1	0.53	1.90	0.12	
Tv_sshF_03A05	TVC00083	F	1	-	0.55	1.81	0.09	
Tv_sshF_03A07	TVC00085	F	1	-	0.45	2.23	0.04	
Tv_sshF_03A09	TVC00087	F	4	-	0.49	2.05	0.14	
Tv_sshF_03D09	TVC00087	F	4	-	0.49	2.04	0.03	
Tv_sshF_03A11	TVC00088	F	1	-	0.41	2.43	0.01	*
Tv_sshF_03B05	TVC00093	F	4	-	0.50	1.99	0.02	
Tv_sshF_03B07	TVC00095	F	1	-	0.41	2.42	0.04	*
Tv_sshF_03B09	TVC00097	F	1	-	0.44	2.28	0.02	
Tv_sshF_03B11	TVC00098	F	1	-	0.40	2.50	0.03	
Tv_sshF_03C01	TVC00099	F	1	-	0.59	1.70	0.05	
Tv_sshF_03C03	TVC00100	F	3	-	0.58	1.71	0.08	
Tv_sshF_03C05	TVC00102	F	2	<i>Phanerochaete chrysosporium</i> , whole genome shotgun sequence	0.63	1.59	0.08	
Tv_sshF_03C11	TVC00106	F	1	-	0.47	2.11	0.03	
Tv_sshF_03D01	TVC00108	F	5	<i>T. versicolor</i> cDNA clone	0.48	2.08	0.04	*
Tv_sshF_03D03	TVC00110	F	1	-	0.41	2.45	0.02	*
Tv_sshR_01E01	TVC00286	R	9	large ribosomal subunit	0.82	1.22	0.24	
Tv_sshF_11D01	TVC00518	F	1	<i>T. versicolor</i> cDNA clone	0.63	1.60	0.16	
Tv_sshR_09D01	TVC00807	R	11	<i>Pleurotus ostreatus</i> cDNA clone	0.72	1.39	0.14	
Tv_sshR_06D02	TVC00830	R	9	Peroxidase	0.66	1.51	0.15	
Tv_sshR_09E12	TVC00924	R	4	-	0.85	1.18	0.04	
Tv_sshR_10D11	TVC01104	R	1	-	0.70	1.44	0.17	

## 7.4 Discussion

### 7.4.1 Technical aspects of microarray analysis

Identification of genes differentially expressed during interactions is part of the process of understanding the molecular pathways and biological processes taking place during interspecific interactions between *T. versicolor* and its competitors. The analysis of the cDNA microarray data showed that there are distinct sets of genes that are up and down-regulated during interactions, and that several are common to interactions involving *T. versicolor* regardless of the opponent. However, further verification of individual clones would be required to compare relative levels between pairings.

The process of microarray analysis is very convoluted and there is potential for variation between samples at every stage. Therefore, every effort was made to reduce this variation. At the initial mycelial harvest stage mycelium was taken from many replicate plates to provide sufficient material. Variation could arise between each individual plates due to subtle differences in gaseous regime and humidity. However, harvesting from many replicate plates would have averaged any individual plate bias that might exist. The biological replication was very important and the processing of each of these samples separately, simultaneously provides technical replication. A drawback of the mycelium harvest method was that mycelium had to be harvested from a zone that was not directly in contact with the opposing mycelium but was as close as possible. This was necessary as the expression profile of *T. versicolor* alone was desired for comparison of the changes taking place when paired against different competitors. If there was contamination with mycelium from the competitor it would not be possible to differentiate between which genes were up or down-regulated in *T. versicolor* or the competitor, without further analysis. There was no detectable contamination of RNA extracts with competitor species when tested with the species specific primers. Although there could have potentially been minute amounts of competitor mycelium in the RNA extracted, that it was not detected by PCR implies that if there was a small amount of contamination, then its effect on the overall profile of transcripts would be minimal. The damage during harvesting could also potentially

result in altered gene expression in response to the wounding of mycelium. However, the harvesting of mycelium must be destructive, and it was carried out as quickly as possible to minimise the potential for this effect and it is assumed that both tester and driver samples were affected equally. Although experimental variation was consciously kept to a minimum, and normalisation aims to remove systematic bias, there is potential for variation throughout the process; such as RNA handling, extraction and purification efficiency could have improved with over time with experience, efficiency of probe labelling (although this is measured and equal concentrations hybridised), subtle differences in the temperature of hybridisation chambers, unequal hybridisation of the different dye labelled probes. In addition, ideally one of the arrays would have been probed with the RNA used to construct the SSH library which would have allowed direct verification of the expression of the library. However, this was not possible as there was insufficient RNA left following library construction.

Data analysis is one of the major challenges of microarray experiments. The use of Imogene for initial spot finding and flagging of spots was useful to remove poor spots. Empty spots were not removed in this case as the nature of the SSH libraries means that empty spots may not necessarily indicate a failed hybridisation but it may indicate a massive down-regulation of a particular gene or an absence of it in a particular condition. The normalisation of the data is potentially one of the most difficult tasks during data analysis as this affects the comparability of arrays and no single normalisation method fits all data. For these experiments where SSH libraries were used, it was expected that the majority of genes would be up or down-regulated as the subtracted cDNA libraries were enriched for differentially expressed genes. Therefore the global and print-tip Lowess normalisation methods were inappropriate as they assume that the expression will not change for the majority of spots. This was evident particularly in the print-tip Lowess test normalisation of the data where the box plots for each array became very narrow and almost all of the variation in the data had been removed. Thus, it seemed that this method overcorrected for systematic variation and would have resulted in a loss of biological information. The invariant  $\beta$ -tubulin genes were not used for normalisation of the data despite their flat expression profiles because they were not evenly distributed across the slide and would not have sufficiently accounted for spatial bias. Perhaps ideally several other different

invariant genes should have been spotted as well, to allow comparisons between them, and to check for consistency. The generally weaker signal for Cy5 labelled spots for the scorecard was probably due to the greater instability of the Cy5 dye as compared with Cy3. It is more susceptible to degradation when exposed during hybridisation, washing and laser scanning. However, this effect was generally at the lower concentrations of RNA which were below the lower limit of detection and this discrepancy was unlikely to have had an impact on the higher intensity ratios.

Although it was expected that some biological differences would be found between the gene expression of *T. versicolor* when paired against the different competitors, it is likely that there is significant overlap and that these differences are subtle. Hence, when trying to separate groups using principal component analysis it would be expected to find overlap between groups. Genes filtered with ANOVA enabled complete distinction between the different pairings, which confirmed that the normalisation method used was sufficient to separate the differences between the groups. It was perhaps surprising that there were large numbers of genes from the forward library down-regulated in the interaction between *T. versicolor* and *S. gausapatum* arrays, and genes from the reverse library that were up-regulated. However, it is unlikely that the SSH process was 100% efficient.

That more up or down-regulated genes were detected for the pairings of *T. versicolor* with *S. gausapatum* and *B. adusta*, than with *H. fasciculare*, is most likely a product of a better reproducibility of the *S. gausapatum* and *B. adusta* arrays. The *T. versicolor* vs *H. fasciculare* arrays appear, from inspection of line graphs, to be relatively variable. Consequently, during filtering, genes that were genuinely up-regulated but not consistently between arrays would be eliminated from the analysis. Similarly, two of the arrays for *T. versicolor* vs *S. gausapatum* appeared to be in agreement for the majority of up and down-regulated genes, while the third did not. It would be beneficial for all of these experiments to have more biological replicates to produce more consistent results.

Ideally statistical fold change would be used for filtering genes using a multiple sample correction to avoid the risk of type I and type II errors (i.e. false positives and negatives). However, it is important to remember that the data produced from these



arrays was intended to produce focussed lists of genes that are likely to be differentially expressed, supported by some evidence of differential gene expression. Thus, to maximise the number of potential candidates for future study a combination of filtering methods seems optimal. Filtering on fold change can provide initially larger lists which highlight broad processes that may be involved, such as the oxidative stress response genes. Subsequently, more stringent filtering with statistical analyses, can be used to choose candidate genes for verification of differential expression and further detailed and quantitative study. In particular, for those clones with no functional annotation, but with consistent up or down-regulation in all experiments, more stringent filtering on confidence would be advisable before extensive time and resources are spent investigating their expression further. Furthermore, during interactions only very subtle changes in gene expression may be required to cause morphological changes and contribute to determining their outcome. At these early stages of analysis over stringent filtering methods could result in some of these transcripts being missed.

#### 7.4.2 Gene lists

The gene lists generated from the microarray expression data allowed the identification of some of the processes active during the different interactions. However, the interpretation of these gene lists is limited by the annotation of the sequences within them. While there are some groups of enzyme and processes that appear to be active during interactions at a molecular level there are clearly many other genes as yet to be identified which are being differentially regulated and are potentially important during interactions. Interestingly, there were more genes shared by the interaction between *T. versicolor* and *S. gausapatum* and *B. adusta*, than with the interaction with *H. fasciculare*. *S. gausapatum* and *B. adusta* are replaced by and deadlock with *T. versicolor*, respectively and *H. fasciculare* replaces *T. versicolor*. Perhaps different genes are required against species with less combative abilities.

There are different types of peroxidases known to be active within white-rot fungi including the lignin peroxidases (LiP) and manganese peroxidases (MnP), and these are produced as several isozymes which are encoded by families of structurally

related genes (Collins *et al.*, 1999). That peroxidases were both up and down-regulated in all pairings may indicate the presence of different peroxidases acting in different situations (Kersten & Cullen, 2007). Peroxidases are involved in lignin decomposition by many white-rot fungi, including *T. versicolor* (Collins *et al.*, 1999) and also in dealing with an oxidative environment which may be present during interactions (White & Boddy, 1992; Score *et al.*, 1997). It has been suggested that during interactions fungi concentrate their energy into combat rather than nutrient metabolism and that mycelium at the interaction zone is non-assimilative (Boddy, 2000). If this were the case then perhaps the expression of genes encoding peroxidases that are produced during constitutive growth for the decomposition of lignin are down-regulated in mycelium in the interaction zone of interacting fungi. Similarly there may be peroxidases that are predominantly involved in dealing with oxidative stress environments. When paraquat is applied to cultures of *T. versicolor* to produce oxidative stress, intracellular MnP increases while extracellular MnP activity is inhibited (Jaszek *et al.*, 2006). The production of peroxidase is observed during some interspecific interactions (Griffith *et al.*, 1994), as is the production of H<sub>2</sub>O<sub>2</sub> (Silar, 2005) and in some cases this is localised around the interaction zone between interacting mycelium of opposing species (Score *et al.*, 1997). Thus the putative peroxidases that were up-regulated in all pairings, in particular contigs TVC00830 and TVC00429, may be enzymes which are specifically required for detoxification of the environment during interactions, including peroxide produced by the fungus itself or by the competitor. Indeed, both competitors may be producing peroxide in response to the others' presence and this would be interesting to investigate for each species in isolation. There were some contigs encoding putative peroxidases containing genes that showed different expression patterns, with one gene from within the contig up-regulated and another down-regulated in the same pairing. This could arise if these gene sequences are sufficiently similar to cluster together but actually encode very similar, yet distinct, isozymes that have differences in expression that became apparent during the microarray analysis. Contigs encoding peroxidases with similar expression profiles may be different peroxidases expressed in parallel or gene sequences from the same peroxidases that were unable to cluster together.

Catalase is an enzyme that catalyses the degradation of H<sub>2</sub>O<sub>2</sub> to water and oxygen and is similar to peroxidase in that it is also involved in dealing with oxidative stress.

Catalase was also up-regulated in the interactions between *T. versicolor* and *S. gausapatum* (TVC00832) and *T. versicolor* vs *B. adusta* (TVC00884). However, another gene from within the contig up-regulated in the interaction with *S. gausapatum* (TVC00832) was found to be down-regulated in the interaction with *B. adusta*. The two contigs up-regulated may represent different isozymes or they may represent sequences from the same gene that were unable to cluster together, something that could be investigated with closer manual inspection of individual clone sequences. Catalase is produced in response to oxidative stress, especially in pathogens subjected to the oxidative burst produced by plants (Zhang *et al.*, 2004) and is produced by *T. versicolor* in the presence of paraquat, which creates an oxidatively stressful environment (Jaszek *et al.*, 2006). Catalase is encoded by the *katG* gene in *E. coli* (Kim *et al.*, 2007) and the gene CTT1 in yeast (Mager & Moradas Ferreira, 1993), which are both expressed in response to oxidative stress. It is likely, therefore, that it is also produced during an oxidative burst during interactions and in response to wounding (Splivallo *et al.*, 2007). That it appears to be down-regulated in the interaction with *B. adusta* may be erroneous or it may be a result of the control tissue responding more dramatically to harvest damage than the interacting mycelium which, while they are both producing catalase, would manifest as a negative expression ratio and down-regulation.

An interesting gene that consistently appeared in the gene lists filtered on expression level was the GrpE protein homolog (contig TVC00638 in TvSg, TVC00936 in TvHf and TvBk). In *E. coli* GrpE forms part of a protein chaperone machinery consisting of DnaK and DnaJ, which is responsible for responding to protein damage following temperature changes or exposure to chemicals. It prevents protein aggregation by promoting protein degradation (Kim *et al.*, 2007; Winter *et al.*, 2005). Oxidative stress can cause post translational protein modification such as carbonylation, oxidation of side chains, loss of structure and aggregation (Berlett & Stadtman, 1997). This oxidative stress is often accompanied by expression of molecular chaperones and proteases (VanBogelen *et al.*, 1997), which degrade damaged proteins. Furthermore, Kim *et al.* (2007) showed that GrpE protein is a stress response gene specifically expressed following protein damage caused by exposure to polycyclic aromatic hydrocarbons, known to cause protein damage, in *E. coli*. Its expression can be used to diagnose the type of damage that is taking place within cells (Kim *et al.*, 2007).

Mge1 protein is the budding yeast homolog to GrpE and performs a similar function as a co-chaperone protein expressed following DNA damage (Trabold *et al.*, 2005). Thus, the increased expression of a gene homologous to GrpE, by *T. versicolor* during interactions with competitors, is perhaps required to deal with the oxidative environment produced during the interaction. It may also be in response to exposure to volatile and diffusible chemicals that may be produced by either fungal competitor.

Zinc is an essential micronutrient for all organisms, although too much can be toxic. It is unable to enter cells passively through the lipid bilayer of the plasma membrane and thus specific membrane transporter proteins are required for cellular uptake (Gaither & Eide, 2001). There are 7 transmembrane zinc transporters in *Neurospora crassa* (Kiranmayi & Mohan, 2006) and transporters are also found in mycorrhizal fungi, which aid zinc uptake by their symbiotic hosts (González-Guerrero *et al.*, 2005). Zinc transporters, Zrt1 (high affinity) and Zrt2 (low affinity), in *S. cerevisiae* are both induced by zinc limitation (Zhao & Eide, 1996 *a,b*). Zinc transporter proteins were up-regulated in all pairings, and were similar to Zrt1 and Zrt2. These may have been expressed in response to a deficiency of zinc in the malt agar growth medium. However, if this was the only factor affecting the expression of the zinc transporters up-regulation during interactions would not be expected, as both test and control samples were grown on the same medium. Therefore, there must be some effect of the interaction on the expression of zinc transporter proteins. Perhaps the presence of competitor mycelium within the interaction zone depleted any zinc available more quickly, and induced a greater expression of genes for zinc uptake. In *Aspergillus fumigatus*, ZrfA and ZrfB are structural homologs to Zrt1 and Zrt2 in yeast, and similarly expression of the genes encoding them is increased in low zinc environments (Vicente-franqueira *et al.*, 2005). However, there is also increased expression in acidic conditions (Vicente-franqueira *et al.*, 2005) and it would be interesting to see if there is altered pH in the interaction zone, which may play a role in inducing increased zinc transporter activity. Alternatively, these zinc transporter proteins in *T. versicolor* may have different functions and may be regulated by different factors, as yet unknown.

1,3-beta-glucan synthase is involved in the production and maintenance of fungal cell walls. Some genes within the contig encoding this enzyme were up-regulated, while

one was down-regulated. This could be due to similar sequences having clustered together, which actually encode subtly different enzymes. An increase in expression of enzymes involved in cell wall production would be expected at the interaction zone, as this is the site of production of large barrages of aerial mycelium by *T. versicolor*. However, down-regulation might be expected further behind the interaction zone, where mycelium during interactions tends to be more sparse. It is perhaps possible that normal vegetative mycelial growth and aerial mycelium production are controlled by different but related enzymes. Some mycelium from behind the interaction zone was collected during harvest, and perhaps it is here that there was down-regulation of a 1,3-beta-glucan synthase gene, while closer to the zone where mycelial barrages were being produced there may have been up-regulation of another 1,3-beta glucan synthase gene.

Genes involved in metabolism, such as the glycogen debranching enzyme and fatty acid synthase, also appeared to have representatives that are both up and down-regulated, again possibly indicating that there are different but related enzymes, controlling similar functions, that are differentially expressed. Although these metabolic genes might be considered 'housekeeping' genes perhaps this is not an accurate description as metabolism and respiration are just as labile with respect to gene expression in response to different environments and treatments.

The array data have successfully identified a number of candidates for future study. The expression profiles of genes can now be confirmed in the future using either semi-quantitative RT-PCR for looking at relative changes of genes or quantitative PCR can be used for more detailed quantitative analysis of their expression. This can be used to verify their expression in the three experiments here but also to examine their expression in different regions of the interacting mycelium, against more competitors, and also at different timepoints throughout the interaction. If the complete genome sequence for *T. versicolor* was available in the future this would also facilitate the identification of some of the other genes that are clearly differentially expressed during interactions and shed even more light on interactions.

## 8. Synthesis

This is one of the first studies to look at the molecular basis of interspecific interactions between saprotrophic basidiomycetes at the molecular level. Previously studies have focussed on predominantly qualitative differences between interactions with respect to the species involved, the environmental conditions and the overall outcomes. Very little is known about the molecular and chemical processes that underlie these changes, and where there has been study in these areas it has mainly been regarding pathogenic and mycorrhizal fungi (Carpenter *et al.*, 2005; Küster *et al.*, 2007).

The initial investigation of interactions on agar (Chapter 3) showed that *T. versicolor* is capable of producing a number of outcomes depending on the species with which it is interacting, ranging from total replacement by a competitor, to totally replacing a competitor. During these interactions there are characteristic changes in morphology, such as the production of barrages of aerial mycelium at the interaction front. Morphological changes are induced in competitors simultaneously. This is often preceded by significant inhibition of mycelial growth in the presence of other mycelium, whether that is self mycelium or a competitor. Inhibition is more pronounced in the presence of a competitor (Chapter 3, Section 3.3.2.3), and varies depending on which species it is competing with.

The detection of volatile compounds produced specifically during an interaction (Chapter 4) shows that interactions trigger the production of secondary metabolites and there is recognition of non-self mycelium. It may be that it is these volatile compounds that enable fungi to sense the presence of a competitor prior to contact, as well as diffusible chemicals not studied here, and that the combination of the volatiles are to some extent species specific. The majority of volatile compounds that were detected were aromatic hydrocarbons (Chapter 4, Section 4.3.7) such as benzoic acid based compounds and sesquiterpenoid compounds, which have known roles in the ecology of fungi for the attraction and repulsion of invertebrates (Fäldt *et al.*, 1999; Schiestl *et al.*, 2006; Stadler & Sterner, 2006), have antifungal activity (Wu *et al.*, 2005) and can be involved in the modulation of fungal morphology (Calistru *et al.*,

1997) and development (Chitarra *et al.*, 2005). Exposure of fungi to VOCs is known to alter protein synthesis (Humphris *et al.*, 2002; Wheatley, 2002; Myung *et al.*, 2007), affect gene expression (Kim *et al.*, 2007) and to induce DNA and protein damage, cytoplasmic degradation and vacuolation within mycelium (Zucchi *et al.*, 2005). The type of damage that is occurring within cells can be detected by studying the expression of certain genes, which can act as markers for various types of damage, e.g. DNA and protein damage and oxidative stress (Kim *et al.*, 2007). Although the exact nature of the damage taking place during the interaction between *T. versicolor* and *S. gausapatum* has not been studied here, there is evidence of growth inhibition and evidence that these fungi are producing and being exposed to potentially damaging volatile compounds. This supports the hypothesis that a set of volatile compounds were produced during the interaction between *T. versicolor* and *S. gausapatum*. Furthermore, the detection of genes associated with protein and DNA damage, such as the GrpE and heat shock proteins, during this interaction suggests that this sort of damage is taking place. Perhaps, other marker genes could be used to investigate further the nature of mycelial damage taking place during interactions. The microarray data (Chapter 7) revealed a number of 'stress' genes, that perform these functions, such as the GrpE gene, chaperones, catalases and peroxidases, were upregulated and may well be expressed, at least in part, as a consequence of exposure to these volatile compounds. However, despite the fact that sesquiterpenes were detected during the interaction (Chapter 4), no sesquiterpene synthase genes were identified by sequencing analysis (Chapter 6), although they have been identified in various plant and fungal species (Zook *et al.*, 1996; Yoshioka *et al.*, 1999; Greenhagen *et al.*, 2006). These may of course be present within the sets of genes that have not been annotated. In the future, the volatile compounds detected could be investigated further and more conclusively identified using standards. The effects of pure extracts of individual compounds on mycelial growth, development and with invertebrate associations could be studied. The compounds that play key roles in mediating morphological changes and differential gene expression, and the nature of mycelial damage could be characterised. Furthermore, if compounds could be identified further, then the biosynthetic pathways of these compounds could be used to identify other candidate genes and enzymes to investigate, with respect to their effects on interactions. Also further analysis of the sequence data by extending the cDNA length using RACE may identify VOC related genes in the cDNA libraries.

These could then be expressed *in vitro* and their enzyme activity in relation to specific substrates could be investigated.

It was not possible from these experiments to distinguish which species was producing which volatile compound. Although *T. versicolor* was expressing genes that imply that it is dealing with oxidative stress and cellular damage (Chapter 6 & 7) it is unclear whether this is a result of a defence mechanism or an offensive attack, if indeed there is a distinction to be made. It may be that *T. versicolor* is defending itself against volatiles and toxic compounds produced by the competitor or it may be mounting an offensive attack on a competitor where it produces the toxic compounds and an oxidative environment itself, and is using these systems to protect itself from the hostile environment it has created. Exactly what makes one species a better competitor than another is not clear and it may be the ability of one species to produce toxic or inhibitory compounds that gives it the competitive edge or it may be its ability to degrade them, although it seems likely to be a combination of both. The ability of individual species to degrade compounds and the effect they have on each species in isolation, could be studied.

There were three experiments within the microarray analysis (Chapter 7), comparing gene expression of *T. versicolor* during interactions, with three different competitors, which result in different outcomes. This was designed to determine if there were any common genes or processes common to interactions in general, and whether there is a correlation between those genes and the outcomes of the interactions. Sets of genes were identified that were common to all interactions of *T. versicolor* and its opponents, which supported the original hypothesis that there may be common genes and mechanisms active during interactions.

During interactions an oxidative environment can be produced (Silar, 2005; Glass & Dementhon, 2006) especially in the interaction zone (Tsujiyama & Minami, 2005). Mycelium can also be sparse behind the interaction zone, and it has been suggested that metabolism of nutrients is variable during interactions (Boddy, 2000). *T. versicolor* is a white-rot fungus and is capable of degrading lignin, for which it uses phenoloxidising enzymes such as peroxidases and laccases (Baldrian, 2004), and are often localised to the interaction zone during confrontations (Tsujiyama & Minami,



2005). A proportionally large number of peroxidases were detected from the SSH library (Chapter 6, Section 6.6.3) and several of these genes were up or down regulated during the interaction (Chapter 7, Section 7.3), implying that there may be several isozymes active during the interaction. Some may be those used by the fungus for the decomposition of lignin. Mycelium was more sparse in areas other than the interaction zone during agar interactions and the downregulation of a set of peroxidases during the interaction may corroborate the theory that nutrient acquisition is reduced in the interaction zone and surrounding area. In contrast, the peroxidases that were upregulated (Chapter 7, Section 7.3) may be isozymes that are mobilised to deal with an oxidative environment resulting from the interaction between competing species. Similarly, peroxidases are able to decompose hydrocarbons (Scheel *et al.*, 2000; Prenafeta-Boldú *et al.*, 2006) and there was some evidence that *T. versicolor* was degrading hydrocarbons emitted by the Reacsyn vessel (Chapter 4, Section 4.4.2). Perhaps these peroxidases were also involved in this process. If these specific peroxidases could be isolated and further characterised, together with sesquiterpene biosynthesis related genes, then perhaps the processes involved when a reduction in a particular volatile was observed could be elucidated. Currently, it is not clear whether reductions in particular compounds are due to increased degradation or to suppressed production. It would also be interesting to follow this work up, initially with relatively simple enzyme assays from different areas and over time, with interactions between *T. versicolor* and *S. gausapatum*. This could then be extended further with proteomic studies of enzyme and protein synthesis during interactions, which could also be coupled to the microarray work.

SSH (Chapter 5 & 6) and cDNA microarray technology (Chapter 7) was used to address the issue of the molecular basis of interspecific interactions. As a method the SSH is a useful tool for identifying a set of differentially expressed genes, which can then be further screened for study. In this respect this has been successful as sets of genes have been identified which can be the starting point for more in depth study of interactions. However, the lack of annotation for these libraries is a limitation when trying to elucidate the main processes occurring during interactions. The short length of fragments produced by the *RsaI* digestion (Chapter 5, Section 5.2.4) is partly responsible for this. The clustering analysis of SSH sequences (Chapter 6, Section 6.3.2) did serve to elongate some of the sequences, which enabled more annotations

of genes than would have been possible from the clone sequences alone. However, the short sequences produced during the SSH procedure (Chapter 5) rely on partial digestion in order for sequences from the same cDNAs to cluster together, and a conventional EST library would perhaps have yielded more clusters and longer sequences. However, this approach may have identified a higher proportion of housekeeping genes and represented only those that were highly abundant. In contrast, the SSH library does appear to have identified many unique sequences and potentially some of the rarer transcripts from the interaction. The relative lack of basidiomycete sequence information and annotation was also a limiting factor in this study. In the future, if the full genome sequence of *T. versicolor* were available it would be invaluable for studies of this nature. SSH clone sequences could be aligned directly with the genome and full length gene sequences could be found and used in homology searches, which would significantly improve the chances of finding a function for these genes.

Genes which are largely up or down regulated have been identified and the next step is to verify the expression of these genes using semi-quantitative PCR or qPCR. It may also be the case that some of the important processes that are taking place during interactions, are modulated by relatively small changes in gene expression, and these may not have been detected in the microarray analysis, but may have been detected in the SSH libraries. Consequently, in the future it would be interesting to study a set of genes selected from both the microarray analysis and SSH libraries. For example, genes with known function and strong up or down regulation, some genes which have significant up or down regulation but with no annotation, and some genes which have clustered together within the SSH libraries in significant numbers, and are therefore likely to have a role in interactions for further study.

To allow comparisons to be made between replicates, it was necessary to carry out these studies in controlled environments, to keep external influences on gene expression constant. However, the environment that saprotrophic basidiomycetes naturally occupy is much more complex and heterogeneous. It would be interesting to take some of the genes identified and study their temporal and spatial expression in the same systems used here, but also in conditions closer to their natural environments. Based on the confirmation of the involvement of these genes in

interactions, and their characterisation, it would be interesting to see if the outcomes of interactions could be manipulated and altered through fungal transformation, and to study the effects on interactions if these genes could be mutagenised or silenced using RNAi.

---

## 9. References

- Aaronson JS, Eckman B, Blevins RA, *et al.* (1996) Toward the development of a gene index to the human genome: an assessment of the nature of high-throughput EST sequence data. *Genome Research* **6**, 829-845.
- Abanda-Nkpwatt D, Krimm U, Coiner HA, Schreiber L, Schwab W (2006) Plant volatiles can minimize the growth suppression of epiphytic bacteria by the phytopathogenic fungus *Botrytis cinerea* in co-culture experiments. *Environmental and Experimental Botany* **56**, 108-119.
- Abraham WR (2001) Bioactive sesquiterpenes produced by fungi: Are they useful for humans as well? *Current Medicinal Chemistry* **8**, 583-606.
- Adomas A, Eklund M, Johansson M, Asiegbu FO (2006) Identification and analysis of differentially expressed cDNAs during nonself-competitive interaction between *Phlebiopsis gigantea* and *Heterobasidion parviporum*. *FEMS Microbiology Ecology* **57**, 26-39.
- Aggarwal KK, Khanuja SPS, Ahmad A, *et al.* (2002) Antimicrobial activity profiles of the two enantiomers of limonene and carvone isolated from the oils of *Mentha spicata* and *Anethum sowa*. *Flavour and Fragrance Journal* **17**, 59-63.
- Akiyama K, Matsuzaki K-i, Hayashi H (2005) Plant sesquiterpenes induce hyphal branching in arbuscular mycorrhizal fungi. *Nature* **435**, 824-827.
- Allmér J, Vasiliauskas R, Ihrmark K, Stenlid J, Dahlberg A (2006) Wood-inhabiting fungal communities in woody debris of Norway spruce (*Picea abies* (L.) Karst.), as reflected by sporocarps, mycelial isolations and T-RFLP identification. *FEMS Microbiology Ecology* **55**, 57-67.
- Almeida FBDR, Cerqueira FM, Silva RDN, Ulhoa CJ, Lima AL (2007) Mycoparasitism studies of *Trichoderma harzianum* strains against *Rhizoctonia solani*: Evaluation of coiling and hydrolytic enzyme production. *Biotechnology Letters* **29**, 1189-1193.

- Altschul SF, Gish W, Miller W, Myers EW, Lipman DJ (1990) Basic local alignment search tool. *Journal of Molecular Biology* **215**, 403-410.
- Amey RC, Mills PR, Bailey A, Foster GD (2003) Investigating the role of a *Verticillium fungicola*  $\beta$ -1,6-glucanase during infection of *Agaricus bisporus* using targeted gene disruption. *Fungal Genetics and Biology* **39**, 264-275.
- Arroyo FT, Moreno J, Daza P, Boianova L, Romero F (2007) Antifungal activity of strawberry fruit volatile compounds against *Colletotrichum acutatum*. *Journal of Agricultural and Food Chemistry* **55**, 5701-5707.
- Baborová P, Möder M, Baldrian P, Cajthamlová K, Cajthami T (2006) Purification of a new manganese peroxidase of the white-rot fungus *Irpex lacteus*, and degradation of polycyclic aromatic hydrocarbons by the enzyme. *Research in Microbiology* **157**, 248-253.
- Baldrian P (2004) Increase of laccase activity during interspecific interactions of white-rot fungi. *FEMS Microbiology Ecology* **50**, 245-253.
- Baldrian P (2006) Fungal laccases - occurrence and properties. *FEMS Microbiology Reviews* **30**, 215-242.
- Baldwin IT, Halitschke R, Paschold A, von Dahl CC, Preston CA (2006) Volatile signaling in plant-plant interactions: "Talking Trees" in the Genomics Era. *Science* **311**, 812-815.
- Ball C, Brazma A (2006) MGED Standards: work in progress. *OMICS A Journal of Integrative Biology* **10**, 138-144.
- Belmain SR, Simmonds MSJ, Blaney WM (2002) Influence of odor from wood-decaying fungi on host selection behavior of deathwatch beetle, *Xestobium rufovillosum*. *Journal of Chemical Ecology* **28**, 741-754.
- Benson DA, Karsch-Mizrachi I, Lipman DJ, Ostell J, Wheeler DL (2007) GenBank. *Nucleic Acids Research* **35**, D21-25.

- 
- Berlett BS, Stadtman ER (1997) Protein oxidation in aging, disease, and oxidative stress. *Journal of Biological Chemistry* **272**, 20313-20316.
- Beyer K, Jiménez SJ, Randall TA, *et al.* (2002) Characterization of *Phytophthora infestans* genes regulated during the interaction with potato. *Molecular Plant Pathology* **3**, 473-485.
- Boddy L (1993) Saprotrophic cord-forming fungi: warfare strategies and other ecological aspects. *Mycological Research* **97**, 641-655.
- Boddy L (1999) Saprotrophic cord-forming fungi: meeting the challenge of heterogeneous environments. *Mycologia* **91**, 13-32.
- Boddy L (2000) Interspecific combative interactions between wood-decaying basidiomycetes. *FEMS Microbiology Ecology* **31**, 185-194.
- Boddy L (2001) Fungal community ecology and wood decomposition processes in angiosperms: from standing tree to complete decay of coarse woody debris. *Ecological Bulletin* **49**, 43-56.
- Boddy L, Gibbon OM, Grundy MA (1985) Ecology of *Daldinia concentrica*: effect of abiotic variables on mycelial extension and interspecific interactions. *Transactions of the British Mycological Society* **85**, 201-211.
- Boddy L, Rayner ADM (1983)*a* Ecological roles of basidiomycetes forming decay communities in attached oak branches. *New Phytologist* **93**, 77-88.
- Boddy L, Rayner ADM (1983)*b* Mycelial interactions, morphogenesis and ecology of *Phlebia radiata* and *P. rufa* from oak. *Transactions of the British Mycological Society* **80**, 437-448.
- Boguski MS, Lowe TM, Tolstoshev CM (1993) dbEST--database for "expressed sequence tags". *Nature Genetics* **4**, 332-333.

- Borg-Karlson A-K, O. Englund F, Unelius CR (1994) Dimethyl oligosulphides, major volatiles released from *Sauromatum guttatum* and *Phallus impudicus*. *Phytochemistry* **35**, 321-323.
- Boswell GP, Jacobs H, Ritz K, Gadd GM, Davidson FA (2007) The development of fungal networks in complex environments. *Bulletin of Mathematical Biology* **69**, 605-634.
- Bottone EJ, Nagarsheth N, Chiu K (1998) Evidence of self-inhibition by filamentous fungi accounts for unidirectional hyphal growth in colonies. *Canadian Journal of Botany* **44**, 390-393.
- Bradley DJ, Kjellbom P, Lamb CJ (1992) Elicitor- and wound-induced oxidative cross-linking of a proline-rich plant cell wall protein: A novel, rapid defense response. *Cell* **70**, 21-30.
- Brazma A, Hingamp P, Quackenbush J, *et al.* (2001) Minimum information about a microarray experiment (MIAME) toward standards for microarray data. *Nature Genetics* **29**, 365-371.
- Breakspear A, Momany M (2007) The first fifty microarray studies in filamentous fungi. *Microbiology* **153**, 7-15.
- Brenner S, Johnson M, Bridgham J, *et al.* (2000) Gene expression analysis by massively parallel signature sequencing (MPSS) on microbead arrays. *Nat Biotech* **18**, 630-634.
- Bridge P, Spooner B (2001) Soil fungi: diversity and detection. *Plant and Soil* **232**, 147-154.
- Broeker K, Bernard F, Moerschbacher BM (2006) An EST library from *Puccinia graminis* f. sp. *tritici* reveals genes potentially involved in fungal differentiation. *FEMS Microbiology Letters* **256**, 273-281.
- Bruce A, Austin WJ, King B (1984) Control of growth of *Lentinus lepideus* by volatiles from *Trichoderma*. *Transactions of the British Mycological Society* **82**, 423-428.

- Bruce A, Kundzewicz A, Wheatley R (1996) Influence of culture age on the volatile organic compounds produced by *Trichoderma aureoviride* and associated inhibitory effects on selected wood decay fungi. *Material und Organismen* **30**.
- Bruce A, Stewart D, Verrall S, Wheatley RE (2003) Effect of volatiles from bacteria and yeast on the growth and pigmentation of sapstain fungi. *International Biodeterioration and Biodegradation* **51**, 101-108.
- Bruce A, Verrall S, Hackett CA, Wheatley RE (2004) Identification of volatile organic compounds (VOCS) from bacteria and yeast causing growth inhibition of sapstain fungi. *Holzforschung* **58**, 193-198.
- Bruce A, Wheatley RE, Humphris SN, Hackett C, Florence MEJ (2000) Production of Volatile Organic Compounds by *Trichoderma* in media containing different amino acids and their effect on selected wood decay fungi. *Holzforschung* **54**, 481-486.
- Bruno G, Sparapano L (2006) Effects of three esca-associated fungi on *Vitis vinifera* L.: III. Enzymes produced by the pathogens and their role in fungus-to-plant or in fungus-to-fungus interactions. *Physiological and Molecular Plant Pathology* **69**, 182-194.
- Bülow N, König WA (2000) The role of germacrene D as a precursor in sesquiterpene biosynthesis: investigations of acid catalyzed, photochemically and thermally induced rearrangements. *Phytochemistry* **55**, 141-168.
- Burke DI, Woodward K, Setterquist RA, Kawasaki ES (2001) Comparative examination of probe labeling methods for microarray hybridization. *Minerva Biotec* **13**, 301-306.
- Buzzini P, Romano S, Turchetti B, *et al.* (2005) Production of volatile organic sulfur compounds (VOSCs) by basidiomycetous yeasts. *FEMS Yeast Research* **5**, 379-385.
- Calistru C, McLean M, Berjak P (1997) *In vitro* studies on the potential for biological control of *Aspergillus flavus* and *Fusarium moniliforme* by *Trichoderma* species. *Mycopathologia* **137**, 115-124.



- Calonje M, Novaes-Ledieu M, Bernardo D, Ahrazem O, Garcia Mendoza C (2000) Chemical components and their locations in the *Verticillium fungicola* cell wall. *Canadian Journal of Botany* **46**, 101-109.
- Cao W, Epstein C, Liu H, *et al.* (2004) Comparing gene discovery from Affymetrix GeneChip microarrays and Clontech PCR-select cDNA subtraction: a case study. *BMC Genomics* **5**, 26.
- Cappellazzo G, Lanfranco L, Bonfante P (2007) A limiting source of organic nitrogen induces specific transcriptional responses in the extraradical structures of the endomycorrhizal fungus *Glomus intraradices*. *Current Genetics* **51**, 59-70.
- Carpenter MA, Stewart A, Ridgway HJ (2005) Identification of novel *Trichoderma hamatum* genes expressed during mycoparasitism using subtractive hybridisation. *FEMS Microbiology Letters* **251**, 105-112.
- Carr-Schmid A, Pfund C, Craig EA, Kinzy TG (2002) Novel G-Protein complex whose requirement is linked to the translational status of the cell. *Molecular Cell Biology* **22**, 2564-2574.
- Cary JW, Wright M, Bhatnagar D, Lee R, Chu FS (1996) Molecular characterization of an *Aspergillus parasiticus* dehydrogenase gene, norA, located on the aflatoxin biosynthesis gene cluster. *Applied and Environmental Microbiology* **62**, 360-366.
- Chen Y, Dougherty ER, Bittner ML (1997) Ratio-based decisions and the quantitative analysis of cDNA microarray images. *Journal of Biomedical Optics* **2**, 364-374.
- Chenchik A, Zhu YY, Diatchenko L, *et al.* (1998) Generation and use of high-quality cDNA from small amounts of total RNA by SMART PCR. . In: *Gene Cloning and Analysis by RT-PCR*, pp. 305-319. BioTechniques Books, MA.
- Cheng XY, Xu RM, Xie BY (2005) The role of chemical communication in the infection and spread of pine wood nematodes (*Bursaphelenchus xylophilus*). *Acta Ecologica Sinica* **25**, 339-345.

- 
- Chi Y, Hatakka A, Majjala P (2007) Can co-culturing of two white-rot fungi increase lignin degradation and the production of lignin-degrading enzymes? *International Biodeterioration & Biodegradation* **59**, 32-39.
- Chitarra GS, Abee T, Rombouts FM, Dijksterhuis J (2005) 1-Octen-3-ol inhibits conidia germination of *Penicillium paneum* despite of mild effects on membrane permeability, respiration, intracellular pH, and changes the protein composition. *FEMS Microbiology Ecology* **54**, 67-75.
- Collins PJ, O'Brien MM, Dobson ADW (1999) Cloning and characterization of a cDNA encoding a novel extracellular peroxidase from *Trametes versicolor*. *Applied and Environmental Microbiology* **65**, 1343-1347.
- Combet E, Henderson J, Eastwood DC, Burton KS (2006) Eight-carbon volatiles in mushrooms and fungi: Properties, analysis, and biosynthesis. *Mycoscience* **47**, 317-326.
- Conesa A, Gotz S, Garcia-Gomez JM, *et al.* (2005) Blast2GO: a universal tool for annotation, visualization and analysis in functional genomics research. *Bioinformatics* **21**, 3674-3676.
- Cox KD, Scherm H (2006) Interaction dynamics between saprobic lignicolous fungi and *Armillaria* in controlled environments: Exploring the potential for competitive exclusion of *Armillaria* on peach. *Biological Control* **37**, 291-300.
- Cramer RA, Lawrence CB (2003) Cloning of a gene encoding an Alt a 1 isoallergen differentially expressed by the necrotrophic fungus *Alternaria brassicicola* during *Arabidopsis* infection. *Applied and Environmental Microbiology* **69**, 2361-2364.
- Curtis H, Noll U, Störmann J, Slusarenko AJ (2004) Broad-spectrum activity of the volatile phytoanticipin allicin in extracts of garlic (*Allium sativum* L.) against plant pathogenic bacteria, fungi and oomycetes. *Physiological and Molecular Plant Pathology* **65**, 79-89.

- Daisy BH, Strobel GA, Castillo U, *et al.* (2002) Naphthalene, an insect repellent, is produced by *Muscodor vitigenus*, a novel endophytic fungus. *Microbiology* **148**, 3737-3741.
- De Boer W, Wagenaar A-M, Klein Gunnewiek PJA, van Veen JA (2007) *In vitro* suppression of fungi caused by combinations of apparently non-antagonistic soil bacteria. *FEMS Microbiology Ecology* **59**, 177-185.
- De Fatima Alpendurada M (2000) Solid-phase microextraction: a promising technique for sample preparation in environmental analysis. *Journal of Chromatography A* **889**, 3-14.
- De Lacy Costello BPJ, Evans P, Ewen RJ, *et al.* (2001) Gas chromatography-mass spectrometry analyses of volatile organic compounds from potato tubers inoculated with *Phytophthora infestans* or *Fusarium coeruleum*. *Plant Pathology* **50**, 489-496.
- Delgado N, Hung CY, Tarcha E, Gardner MJ, Cole GT (2004) Profiling gene expression in *Coccidioides posadasii*. *Medical Mycology* **42**, 59-71.
- Delneri D, Gardner DCJ, Oliver SG (1999) Analysis of the seven-member AAD gene set demonstrates that genetic redundancy in yeast may be more apparent than real. *Genetics* **153**, 1591-1600.
- Demir G (2004) Degradation of toluene and benzene by *Trametes versicolor*. *Journal of Environmental Biology* **25**, 19-25.
- Demyttenaere JCR, Morina RM, De Kimpe N, Sandra P (2004) Use of headspace solid-phase microextraction and headspace sorptive extraction for the detection of the volatile metabolites produced by toxigenic *Fusarium* species. *Journal of Chromatography A* **1027**, 147-154.
- Diatchenko L, Lau Y-FC, Campbell AP, *et al.* (1996) Suppression subtractive hybridisation: A method for generating differentially regulated or tissue-specific cDNA probes and libraries. *Proceedings of the National Academy of Science USA* **93**, 6025-6030.

- Dogra N, Breuil C (2004) Suppressive subtractive hybridization and differential screening identified genes differentially expressed in yeast and mycelial forms of *Ophiostoma piceae*. *FEMS Microbiology Letters* **238**, 175-181.
- Doma MK, Parker R (2006) Endonucleolytic cleavage of eukaryotic mRNAs with stalls in translation elongation. *Nature* **440**, 561-564.
- Donnelly DP, Boddy L (2001) Mycelial dynamics during interactions between *Stropharia caerulea* and other cord-forming saprotrophic basidiomycetes. *New Phytologist* **151**, 691-704.
- Dowson CG, Rayner ADM, Boddy L (1988) The form and outcome of mycelial interactions involving cord-forming decomposer basidiomycetes in homogenous and heterogeneous environments. *New Phytologist* **109**, 423-432.
- Dubey SC, Suresh M (2006) Randomly amplified polymorphic DNA markers for *Trichoderma species* and antagonism against *Fusarium oxysporum* f. sp. *ciceris* causing chickpea wilt. *Journal of Phytopathology* **154**, 663-669.
- Dudoit S, Yang TH, Callow M, Speed T (2002) Statistical methods for identifying differentially expressed genes in replicated cDNA microarray experiments. *Statistica Sinica* **12**, 111-139.
- Ehrlich KC, Chang P-K, Yu J, Cotty PJ (2004) Aflatoxin biosynthesis cluster gene *cypA* is required for G aflatoxin formation. *Applied and Environmental Microbiology* **70**, 6518-6524.
- Evans CS, Dutton MV, GuillPn F, Veness RG (1994) Enzymes and small molecular agents involved with lignocellulose degradation. *FEMS Microbiology Reviews* **13**, 235-240.
- Ewen RJ, Jones PRH, Ratcliffe NM, Spencer-Phillips PTN (2004) Identification by gas chromatography-mass spectrometry of the volatile organic compounds emitted from the wood-rotting fungi *Serpula lacrymans* and *Coniophora puteana*, and from *Pinus sylvestris* timber. *Mycological Research* **108**, 806-814.

- Ewing B, Green P (1998) Basecalling of automated sequencer traces using phred. II. Error probabilities. *Genome Research* **8**, 186-194.
- Fäldt J, Jonsell M, Nordlander G, Borg-Karlson AK (1999) Volatiles of bracket fungi *Fomitopsis pinicola* and *Fomes fomentarius* and their functions as insect attractants. *Journal of Chemical Ecology* **25**, 567-590.
- Florianowicz T (2000) Inhibition of growth and sporulation of *Pencillium expansum* by extracts of selected basidiomycetes. *Acta Societatis Botanicorum Poloniae*. **69**, 263-267.
- Frenzel A, Manthey K, Perlick AM, *et al.* (2005) Combined transcriptome profiling reveals a novel family of arbuscular mycorrhizal-specific *Medicago truncatula* lectin genes. *Molecular Plant-Microbe Interactions* **18**, 771-782.
- Gaither LA, Eide D (2001) Eukaryotic zinc transporters and their regulation. *BioMetals* **14**, 251-270.
- Garcia Mendoza C (2005) The *Verticillium fungicola* mycoparasitism on the *Agaricus bisporus* fruit bodies: The *Verticillium* disease or 'dry bubble' of mushrooms *Anales de la Real Academia Nacional de Farmacia* **71**, 571-586.
- Georg RdC, Gomes SL (2007) Comparative expression analysis of members of the Hsp70 family in the chytridiomycete *Blastocladiella emersonii*. *Gene* **386**, 24-34.
- Glass NL, Dementhon K (2006) Non-self recognition and programmed cell death in filamentous fungi. *Current Opinion in Microbiology* **9**, 553-558.
- Glass NL, Jacobson DJ, Shiu PKT (2000) The genetics of hyphal fusion and vegetative incompatibility in filamentous ascomycete fungi. *Annual Review of Genetics* **34**, 165-186.
- Gonzalez-Guerrero M, Azcon-Aguilar C, Mooney M, *et al.* (2005) Characterization of a *Glomus intraradices* gene encoding a putative Zn transporter of the cation diffusion facilitator family. *Fungal Genetics and Biology* **42**, 130-140.

- Greenhagen BT, O'Maille PE, Noel JP, Chappell J (2006) Identifying and manipulating structural determinates linking catalytic specificities in terpene synthases. *Proceedings of the National Academy of Science USA* **103**, 9826-9831.
- Griffith GS, Boddy L (1991)*a* Fungal decomposition of attached angiosperm twigs. III. Effect of water potential and temperature on fungal growth, survival and decay of wood. *New Phytologist* **117**, 259-269.
- Griffith GS, Boddy L (1991)*b* Fungal decomposition of attached angiosperm twigs. II. Moisture relations of twigs of ash (*Fraxinus excelsior* L.). *New Phytologist* **117**, 251-257.
- Griffith GS, Boddy L (1991)*c* Fungal decomposition of attached angiosperm twigs. IV. Effect of water potential on interactions between fungi on agar and in wood. *New Phytologist* **117**, 633-641.
- Griffith GS, Rayner ADM (1994) Interspecific interactions, mycelial morphogenesis and extracellular metabolite production in *Phlebia radiata* (Aphylophorales). *Nova Hedwigia* **59**, 331-344.
- Griffith GS, Rayner ADM, Wildman HG (1994) Extracellular metabolites and mycelial morphogenesis of *Hypholoma fasciculare* and *Phlebia radiata* (Hymenomycetes). *Nova Hedwigia* **59**, 311-329.
- Guillen F, Evans CS (1994) Anisaldehyde and veratraldehyde acting as redox cycling agents for H<sub>2</sub>O<sub>2</sub> production by *Pleurotus eryngii*. *Applied and Environmental Microbiology* **60**, 2811-2817.
- Gutierrez A, Caramelo L, Prieto A, Martinez MJ, Martinez AT (1994) Anisaldehyde production and aryl-alcohol oxidase and dehydrogenase activities in ligninolytic fungi of the genus *Pleurotus*. *Applied and Environmental Microbiology* **60**, 1783-1788.
- Hakola H, Tarvainen V, Bäck J, *et al.* (2005) Seasonal variation of mono- and sesquiterpene emission rates of Scots pine. *Biogeosciences Discussions* **2**, 1697-1717.

- 
- Hall TA (1999) BioEdit: a user friendly biological sequence alignment editor and analysis program for Windows 95/98/NT. *Nucleic Acids Symposium Series* **41**, 95-98.
- Hamilton-Kemp TR, McCracken Jr CT, Loughrin JH, Andersen RA, Hildebrand DF (1992) Effects of some natural volatile compounds on the pathogenic fungi *Alternaria alternata* and *Botrytis cinerea*. *Journal of Chemical Ecology* **18**, 1083-1091.
- Hättenschwiler S, Tiunov AV, Scheu S (2005) Biodiversity and litter decomposition in terrestrial ecosystems. *Annual Review of Ecology, Evolution, and Systematics* **36**, 191-218.
- Hatvani N, Kredics L, Antal Z, Mecs I (2002) Changes in activity of extracellular enzymes in dual cultures of *Lentinula edodes* and mycoparasitic *Trichoderma* strains. *Journal of Appl Microbiology* **92**, 415-423.
- Hawksworth DL (2001) The magnitude of fungal diversity: the 1.5 million species estimate revisited. *Mycological Research* **105**, 1422-1432.
- Hawksworth DL, Kirk PM, Sutton BC, Pegler DN (1995) Ainsworth and Bisby's Dictionary of the Fungi (8th Ed.), p. 616. CAB International, Wallingford, United Kingdom.
- Hegde P, Qi R, Abernathy K, *et al.* (2000) A concise guide to cDNA microarray analysis. *BioTechniques* **29**, 548-562.
- Heilmann-Clausen J, Boddy L (2005) Inhibition and stimulation effects in communities of wood decay fungi: Exudates from colonized wood influence growth by other species. *Microbial Ecology* **49**, 399-406.
- Hibbett DS, Binder M, Bischoff JF, *et al.* (2007) A higher-level phylogenetic classification of the Fungi. *Mycological Research* **111**, 509-547.
- Holm S (1979) A simple sequentially rejective multiple test procedure. *Scandinavian Journal of Statistics* **6**.

- Holmer L, Renvall P, Stenlid J (1997) Selective replacement between species of wood-rotting basidiomycetes, a laboratory study. *Mycological Research* **101**, 714-720.
- Holmer L, Stenlid J (1993) The importance of inoculum size for the competitive ability of wood decomposing fungi. *FEMS Microbiology Ecology* **12**, 169-176.
- Holmer L, Stenlid J (1997) Competitive hierarchies of wood decomposing basidiomycetes in artificial systems based on variable inoculum sizes. *OIKOS* **79**, 77-84.
- Hosono K, Sasaki T, Minoshima S, Shimizu N (2004) Identification and characterisation of a novel gene family YPEL in a wide spectrum of eukaryotic species. *Gene* **340**, 31-43.
- Huang J, Schmelz EA, Alborn H, Engelberth J, Tumlinson JH (2005) Phytohormones mediate volatile emissions during the interaction of compatible and incompatible pathogens: The role of ethylene in *Pseudomonas syringae* infected tobacco. *Journal of Chemical Ecology* **31**, 439-459.
- Hubank M, Schatz DG (1994) Identifying differences in mRNA expression by representational difference analysis of cDNA. *Nucleic Acids Research* **22**, 5640-5648.
- Humphris SN, Bruce A, Buultjens E, Wheatley RE (2002) The effects of volatile microbial secondary metabolites on protein synthesis in *Serpula lacrymans*. *FEMS Microbiology Letters* **210**, 215-219.
- Hynes J, Muller C, Jones TH, Boddy L (2007) Changes in volatile production during the course of fungal mycelial interactions between *Hypholoma fasciculare* and *Resinicium bicolor*. *Journal of Chemical Ecology* **33**, 43-57.
- Iakovlev A, Olson A, Elfstrand M, Stenlid J (2004) Differential gene expression during interactions between *Heterobasidion annosum* and *Physisporinus sanguinolentus*. *FEMS Microbiology Letters* **241**, 79-85.
- Iakovlev A, Stenlid J (2000) Spatiotemporal patterns of laccase activity in interacting mycelia of wood-decaying basidiomycete fungi. *Microbial Ecology* **39**, 236-245.



- Ikediegwu FEO (1976) The interface in hyphal interference by *Peniophora gigantea* against *Heterobasidion annosum*. *Transactions of the British Mycological Society* **66**, 291-296.
- Irie T, Matsumura H, Terauchi R, Saitoh H (2003) Serial Analysis of Gene Expression (SAGE) of *Magnaporthe grisea*: Genes involved in appressorium formation. *Molecular Genetics and Genomics* **270**, 181-189.
- James TY, Kauff F, Schoch CL, *et al.* (2006) Reconstructing the early evolution of Fungi using a six-gene phylogeny. *Nature* **443**, 818-822.
- Jaszek M, Grzywnowicz K, Malarczyk E, Leonowicz A (2006) Enhanced extracellular laccase activity as a part of the response system of white rot fungi: *Trametes versicolor* and *Abortiporus biennis* to paraquat-caused oxidative stress conditions. *Pesticide Biochemistry and Physiology* **85**, 147-154.
- Jelen HH (2002) Volatile sesquiterpene hydrocarbons characteristic for *Penicillium roqueforti* strains producing PR toxin. *Journal of Agricultural and Food Chemistry* **50**, 6569-6574.
- Jelen HH (2003) Use of solid phase microextraction (SPME) for profiling fungal volatile metabolites. *Letters in Applied Microbiology* **36**, 263-267.
- Kahlos K, Kiviranta JLJ, Hiltunen RVK (1994) Volatile constituents of wild and in vitro cultivated *Gloeophyllum odoratum*. *Phytochemistry* **36**, 917-922.
- Kai M, Effmert U, Berg G, Piechulla B (2007) Volatiles of bacterial antagonists inhibit mycelial growth of the plant pathogen *Rhizoctonia solani*. *Archives of Microbiology* **187**, 351-360.
- Kaiser R (2006) Flowers and fungi use scents to mimic each other. *Science* **311**, 806-807.
- Kamada F, Abe S, Hiratsuka N, Wariishi H, Tanaka H (2002) Mineralization of aromatic compounds by brown-rot basidiomycetes-mechanisms involved in initial attack on the aromatic ring. *Microbiology* **148**, 1939-1946.

- Karlsson M, Stenlid J, Olson A (2005) Identification of a superoxide dismutase gene from the conifer pathogen *Heterobasidion annosum*. *Physiological and Molecular Plant Pathology* **66**, 99-107.
- Keddy PA (1989) *Competition* Chapman & Hall, New York.
- Kennedy N, Clipson N (2003) Fingerprinting the fungal community. *Mycologist* **17**, 158-164.
- Kennedy PG, Bergemann SE, Hortal S, Bruns TD (2007) Determining the outcome of field-based competition between two *Rhizopogon* species using real-time PCR. *Molecular Ecology* **16**, 881-890.
- Kersten P, Cullen D (2007) Extracellular oxidative systems of the lignin-degrading Basidiomycete *Phanerochaete chrysosporium*. *Fungal Genetics and Biology* **44**, 77-87.
- Kexiang G, Xiaoguang L, Yonghong L, Tianbo Z, Shuliang W (2002) Potential of *Trichoderma harzianum* and *T. atroviride* to control *Botryosphaeria berengeriana* f. sp. *piricola*, the cause of apple ring rot. *Journal of Phytopathology* **150**, 271-276.
- Kim MIS, Huh EJ, Kim HK, Moon KW (1998) Degradation of polycyclic aromatic hydrocarbons by selected white-rot fungi and the influence of lignin peroxidase. *Journal of Microbiology and Biotechnology* **8**, 129-133.
- Kim YS, Min J, Hong HN, *et al.* (2007) Gene expression analysis and classification of mode of toxicity of polycyclic aromatic hydrocarbons (PAHs) in *Escherichia coli*. *Chemosphere* **66**, 1243-1248.
- Kiranmayi P, Mohan PM (2006) Metal transportome of *Neurospora crassa*. *In Silico Biology* **6**, 169-180.
- Kishimoto K, Matsui K, Ozawa R, Takabayashi J (2007) Volatile 1-octen-3-ol induces a defensive response in *Arabidopsis thaliana*. *Journal of General Plant Pathology* **73**, 35-37.

- 
- Knudsen JT, Tollsten L, Bergstrom LG (1993) Floral scents--a checklist of volatile compounds isolated by head-space techniques. *Phytochemistry* **33**, 253-280.
- Korpi A, Kasanen JP, Alarie Y, Kosma VM, Pasanen AL (1999) Sensory irritating potency of some microbial volatile organic compounds (MVOCs) and a mixture of five MVOCs. *Archives of Environmental Health* **54**, 347-352.
- Krause K, Kothe E (2006) Use of RNA fingerprinting to identify fungal genes specifically expressed during ectomycorrhizal interaction. *Journal of Basic Microbiology* **46**, 387-399.
- Kulikova T, Akhtar R, Aldebert P, *et al.* (2006) EMBL Nucleotide Sequence Database in 2006. *Nucleic Acids Research Database issue*, D1-D5.
- Küster H, Becker A, Firnhaber C, *et al.* (2007) Development of bioinformatic tools to support EST-sequencing, in silico- and microarray-based transcriptome profiling in mycorrhizal symbioses. *Phytochemistry* **68**, 19-32.
- Lee PD, Sladek R, Greenwood CMT, Hudson TJ (2002) Control genes and variability: Absence of ubiquitous reference transcripts in diverse mammalian expression studies. *Genome Research* **12**, 292-297.
- Leonowicz A, Matuszewska A, Luterek J, *et al.* (1999) Biodegradation of lignin by white rot fungi. *Fungal Genetics and Biology* **27**, 175-185.
- Li GH, Li L, Duan M, Zhang KQ (2006) The chemical constituents of the fungus *Stereum* sp. *Chemistry and Biodiversity* **3**, 210-216.
- Liang P, Pardee AB (1992) Differential display of eukaryotic messenger RNA by means of the polymerase chain reaction. *Science* **257**, 967-971.
- Lin H, Phelan PL (1992) Comparison of volatiles from beetle-transmitted *Ceratocystis fagacearum* and four non-insect-dependent fungi. *Journal of Chemical Ecology* **18**, 1623-1632.

- Lindahl BD, Finlay RD (2006) Activities of chitinolytic enzymes during primary and secondary colonization of wood by basidiomycetous fungi. *New Phytologist* **169**, 389-397.
- Lindquist S (1992) Heat-shock proteins and stress tolerance in microorganisms. *Current Opinion in Genetics & Development* **2**, 748-755.
- Lisitsyn N, Lisitsyn N, Wigler M (1993) Cloning the differences between two complex genomes. *Science* **259**, 946-951.
- Liu Y, Sun W, Zhang K, *et al.* (2007) Identification of genes differentially expressed in human primary lung squamous cell carcinoma. *Lung Cancer* **56**, 307-317.
- Liu Z-M, Kolattukudy PE (1998) Identification of a gene product induced by hard-surface contact of *Colletotrichum gloeosporioides* conidia as a ubiquitin-conjugating enzyme by yeast complementation. *Journal of Bacteriology* **180**, 3592-3597.
- Lockwood JL (1992) Exploitation competition. In: *The Fungal Community: Its organisation and role in the ecosystem* (eds. Carroll GC, Wicklow DT), pp. 265-274. Marcel Dekker, New York.
- Lu JP, Liu TB, Lin FC (2005) Identification of mature appressorium-enriched transcripts in *Magnaporthe grisea*, the rice blast fungus, using suppression subtractive hybridization. *FEMS Microbiology Letters* **245**, 131-137.
- Luis P, Kellner H, Zimdars B, *et al.* (2005) Patchiness and spatial distribution of laccase genes of ectomycorrhizal, saprotrophic, and unknown basidiomycetes in the upper horizons of a mixed forest cambisol. *Microbial Ecology* **50**, 570-579.
- Mackie AE, Wheatley RE (1999) Effects and incidence of volatile organic compound interactions between soil bacterial and fungal isolates. *Soil Biology and Biochemistry* **31**, 375-385.

- Madura K, Prakash S, Prakash L (1990) Expression of the *Saccharomyces cerevisiae* DNA repair gene RAD6 that encodes a ubiquitin conjugating enzyme, increases in response to DNA damage and in meiosis but remains constant during the mitotic cell cycle. *Nucleic Acids Research* **18**, 771-778.
- Maga JA (1981) Mushroom flavor. *Journal of Agricultural and Food Chemistry* **29**, 1-4.
- Mager WH, Moradas Ferreira P (1993) Stress response of yeast. *Biochemical Journal* **290**, 1-13.
- Manduchi E, Scearce LM, Brestelli JE, *et al.* (2002) Comparison of different labeling methods for two-channel high-density microarray experiments. *Physiological Genomics* **10**, 169-179.
- Martínez AS, Fernández-Arhex V, Corley JC (2006) Chemical information from the fungus *Amylostereum areolatum* and host-foraging behaviour in the parasitoid *Ibalia leucospoides*. *Physiological Entomology* **31**, 336-340.
- Martínez AT (2002) Molecular biology and structure-function of lignin-degrading heme peroxidases. *Enzyme and Microbial Technology* **30**, 425-444.
- Matsumura H, Ito A, Saitoh H, *et al.* (2005) SuperSAGE. *Cellular Microbiology* **7**, 11-18.
- McAfee BJ, Taylor A (1999) A review of the volatile metabolites of fungi found on wood substrates. *Natural Toxins* **7**, 283-303.
- McErlean C, Marchant R, Banat IM (2006) An evaluation of soil colonisation potential of selected fungi and their production of ligninolytic enzymes for use in soil bioremediation applications. *Antonie van Leeuwenhoek, International Journal of General and Molecular Microbiology* **90**, 147-158.
- Mendgen K, Wirsel SGR, Jux A, Hoffmann J, Boland W (2006) Volatiles modulate the development of plant pathogenic rust fungi. *Planta* **224**, 1353-1361.

- Micali CO, Smith ML (2003) On the independence of barrage formation and heterokaryon incompatibility in *Neurospora crassa*. *Fungal Genetics and Biology* **38**, 209-219.
- Mitchell JI, Zuccaro A (2006) Sequences, the environment and fungi. *Mycologist* **20**, 62-74.
- Monteiro MC, De Carvalho MEA (1998) Pulp bleaching using laccase from *Trametes versicolor* under high temperature and alkaline conditions. *Applied Biochemistry and Biotechnology - Part A Enzyme Engineering and Biotechnology* **70-72**, 983.
- Morales P, Thurston CF (2003) Efficient isolation of genes differentially expressed on cellulose by suppression subtractive hybridization in *Agaricus bisporus*. *Mycological Research* **107**, 401-407.
- Mozuraitis R, Strandén M, Ramirez MI, Borg-Karlson AK, Mustaparta H (2002) (-)-Germacrene D increases attraction and oviposition by the tobacco budworm moth *Heliothis virescens*. *Chem. Senses* **27**, 505-509.
- Muheim A, Leisola MSA, Schoemaker HE (1990) Aryl-alcohol oxidase and lignin peroxidase from the white-rot fungus *Bjerkandera adusta*. *Journal of Biotechnology* **13**, 159-167.
- Muheim A, Waldner R, Sanglard D, *et al.* (1991) Purification and properties of an aryl-alcohol dehydrogenase from the white-rot fungus *Phanerochaete chrysosporium*. *European Journal of Biochemistry* **195**, 369-375.
- Mukherjee M, Mukherjee PK, Kale SP (2007) cAMP signalling is involved in growth, germination, mycoparasitism and secondary metabolism in *Trichoderma virens*. *Microbiology* **153**, 1734-1742.
- Myung K, Hamilton-Kemp TR, Archbold DD (2007) Interaction with and effects on the profile of proteins of *Botrytis cinerea* by C6 aldehydes. *Journal of Agriculture and Food Chemistry*. **55**, 2182-2188.
- Nagaraj SH, Gasser RB, Ranganathan S (2007) A hitchhiker's guide to expressed sequence tag (EST) analysis. *Briefings in Bioinformatics* **8**, 6-21.

- 
- Neilson L, Andalibi A, Kang D, *et al.* (2000) Molecular phenotype of the human oocyte by PCR-SAGE. *Genomics* **63**, 13-24.
- Nilsson T, Larsen TO, Montanarella L, Madsen JO (1996) Application of head-space solid-phase microextraction for the analysis of volatile metabolites emitted by *Penicillium* species. *Journal of Microbiological Methods* **25**, 245-255.
- Novotny C, Svobodova K, Erbanova P, *et al.* (2004) Ligninolytic fungi in bioremediation: Extracellular enzyme production and degradation rate. *Soil Biology and Biochemistry* **36**, 1545-1551.
- Nugent KG, Choffe K, Saville BJ (2004) Gene expression during *Ustilago maydis* diploid filamentous growth: EST library creation and analyses. *Fungal Genetics and Biology* **41**.
- Ohkumah M, Maeda Y, Johjima T, Kudo T (2001) Lignin degradation and roles of white rot fungi: Study on an efficient symbiotic system in fungus-growing termites and its application to bioremediation. *Ecomolecular Science Research* **42**, 39-42.
- Ouziad F, Hildebrandt U, Schmelzer E, Bothe H (2005) Differential gene expressions in arbuscular mycorrhizal-colonized tomato grown under heavy metal stress. *Journal of Plant Physiology* **162**, 634-649.
- Owens EM, Reddy CA, Grethlein HE (1994) Outcome of interspecific interactions among brown-rot and white-rot wood decay fungi. *FEMS Microbiology Ecology* **14**, 19-24.
- Parkinson J, Anthony A, Wasmuth J, *et al.* (2004) PartiGene--constructing partial genomes. *Bioinformatics* **20**, 1398-1404.
- Parkinson J, Guiliano D, Blaxter M (2002) Making sense of EST sequences by CLOBBing them. *BMC Bioinformatics* **3**, 31.
- Pearce MH (1990) In vitro interactions between *Armillaria luteobubalina* and other wood decay fungi. *Mycological Research* **94**, 753-761.

- 
- Penn SG, Rank DR, Hanzel DK, Barker DL (2000) Mining the human genome using microarrays of open reading frames. *Nature Genetics* **26**, 315-318.
- Peters DG, Kassam AB, Yonas H, *et al.* (1999) Comprehensive transcript analysis in small quantities of mRNA by SAGE-lite. *Nucleic Acids Research* **27**.
- Pichersky E, Noel JP, Dudareva N (2006) Biosynthesis of plant volatiles: Nature's diversity and ingenuity. *Science* **311**, 808-811.
- Pines J, Lindon C (2005) Proteolysis: anytime, any place, anywhere? *Nature Cell Biology* **7**, 731-735.
- Prakash L (1989) The structure and function of RAD6 and RAD18 DNA repair genes of *Saccharomyces cerevisiae*. *Genome* **31**, 597-600.
- Prenafeta-Boldú FX, Summerbell R, Sybren De Hoog G (2006) Fungi growing on aromatic hydrocarbons: Biotechnology's unexpected encounter with biohazard? *FEMS Microbiology Reviews* **30**, 109-130.
- Prosser I, Altug IG, Phillips AL, *et al.* (2004) Enantiospecific (+)- and (-)-germacrene D synthases, cloned from goldenrod, reveal a functionally active variant of the universal isoprenoid-biosynthesis aspartate-rich motif. *Archives of Biochemistry and Biophysics* **432**, 136-144.
- Qi B, Moe W, Kinney K (2002) Biodegradation of volatile organic compounds by five fungal species. *Applied Microbiology and Biotechnology* **58**, 684-689.
- Quackenbush J (2002) Microarray data normalization and transformation. *Nature Genetics* **32**, 496-501.
- Raguso RA, Roy BA (1998) 'Floral' scent production by *Puccinia* rust fungi that mimic flowers. *Molecular Ecology* **7**, 1127-1136.



- Ramin AA, Braun PG, Prange RK, DeLong JM (2005) *In vitro* effects of *Muscodor albus* and three volatile components on growth of selected postharvest microorganisms. *HortScience* **40**, 2109-2114.
- Rayner ADM, Boddy L (1988) Fungal communities in the decay of wood. *Advances in Microbial Ecology* **10**, 115-166.
- Rayner ADM, Griffith GS, Wildman HG (1994) Induction of metabolic and morphogenetic changes during mycelial interactions among species of higher fungi. *Biochemical Society Transactions* **22**, 389-394.
- Rayner ADM, Turton MN (1982) Mycelial interactions and population structure in the genus *Stereum*: *S. rugosum*, *S. sanguinolentum* and *S. rameale*. *Transactions of the British Mycological Society* **78**, 483-493.
- Rayner ADM, Webber JF (1986) Interspecific mycelial interactions - an overview. In: *The ecology and physiology of the fungal mycelium*. British Mycological Society (eds. Jennings DH, Rayner ADM), pp. 383-417. Cambridge University Press.
- Rayner T, Rocca-Serra P, Spellman P, *et al.* (2006) A simple spreadsheet-based, MIAME-supportive format for microarray data: MAGE-TAB. *BMC Bioinformatics* **7**, 489.
- Reina M, Orihuela JC, Gonzalez-Coloma A, *et al.* (2004) Four illudane sesquiterpenes from *Coprinopsis episcopalis*. *Phytochemistry* **65**, 381-385.
- Reiser J, Muheim A, Hardegger M, Frank G, Fiechter A (1994) Aryl-alcohol dehydrogenase from the white-rot fungus *Phanerochaete chrysosporium*. Gene cloning, sequence analysis, expression, and purification of the recombinant enzyme. *Journal of Biological Chemistry* **269**, 28152-28159.
- Reithner B, Brunner K, Schuhmacher R, *et al.* (2005) The G protein  $\alpha$ -subunit Tga1 of *Trichoderma atroviride* is involved in chitinase formation and differential production of antifungal metabolites. *Fungal Genetics and Biology* **42**, 749-760.

- Reynolds P, Koken MH, Hoeijmakers JH, Prakash S, Prakash L (1990) The *rhp6+* gene of *Schizosaccharomyces pombe*: a structural and functional homolog of the RAD6 gene from the distantly related yeast *Saccharomyces cerevisiae*. *The EMBO Journal* **9**, 1423-1430.
- Rinnerthaler M, Jarolim S, Heeren G, *et al.* (2006) MMI1 (YKL056c, TMA19), the yeast orthologue of the translationally controlled tumor protein (TCTP) has apoptotic functions and interacts with both microtubules and mitochondria. *Biochimica et Biophysica Acta (BBA) - Bioenergetics* **1757**, 631-638.
- Romaní AM, Fischer H, Mille-Lindblom C, Tranvik LJ (2006) Interactions of bacteria and fungi on decomposing litter: differential extracellular enzyme activities. *Ecology* **87**, 2559-2569.
- Rösecke J, Pietsch M, König WA (2000) Volatile constituents of wood-rotting basidiomycetes. *Phytochemistry* **54**, 747-750.
- Røstelién T, Borg-Karlson AK, Fäldt J, Jacobsson U, Mustaparta H (2000) The plant sesquiterpene Germacrene D specifically activates a major type of antennal receptor neuron of the tobacco budworm moth *Heliothis virescens*. *Chemical Senses* **25**, 141-148.
- Roxström-Lindquist K, Faye I (2001) The *Drosophila* gene Yippee reveals a novel family of putative zinc binding proteins highly conserved among eukaryotes. *Insect Molecular Biology* **10**, 77-86.
- Roy G, Laflamme G, Bussières G, Dessureault M (2003) Field tests on biological control of *Heterobasidion annosum* by *Phaeothea dimorphospora* in comparison with *Phlebiopsis gigantea*. *Forest Pathology* **33**, 127-140.
- Ryan D, Leukes W, Burton S (2007) Improving the bioremediation of phenolic wastewaters by *Trametes versicolor*. *Bioresource Technology* **98**, 579-587.
- Saha S, Sparks AB, Rago C, *et al.* (2002) Using the transcriptome to annotate the genome. *Nature Biotechnology* **20**, 508-512.

- Said S, Neves FM, Griffiths AJF (2004) Cinnamic acid inhibits the growth of the fungus *Neurospora crassa*, but is eliminated as acetophenone. *International Biodeterioration and Biodegradation* **54**, 1-6.
- Sarkanen S, Razal RA, Piccariello T, Yamamoto E, Lewis NG (1991) Lignin peroxidase: Toward a clarification of its role *in vivo*. *Journal of Biological Chemistry* **266**, 3636-3643.
- Savoie J-M, Mata G, Mamoun M (2001) Variability in brown line formation and extracellular laccase production during interactions between white-rot basidiomycetes and *Trichoderma harzianum* biotype Th2. *Mycologia* **93**, 243-248.
- Schade F, Legge RL, Thompson JE (2001) Fragrance volatiles of developing and senescing carnation flowers. *Phytochemistry* **56**, 703-710.
- Scheel T, Hofer M, Ludwig S, Holker U (2000) Differential expression of manganese peroxidase and laccase in white-rot fungi in the presence of manganese or aromatic compounds. *Applied Microbiology and Biotechnology* **54**, 686-691.
- Schiestl FP, Steinebrunner F, Schulz C, *et al.* (2006) Evolution of 'pollinator'-attracting signals in fungi. *Biology Letters* **2**, 401-404.
- Schlosser D, Grey R, Fritsche W (1997) Patterns of ligninolytic enzymes in *Trametes versicolor*. Distribution of extra- and intracellular enzyme activities during cultivation on glucose, wheat straw and beech wood. *Applied Microbiology and Biotechnology* **47**, 412-418.
- Schoeman MW, Webber JF, Dickinson DJ (1996) The effect of diffusible metabolites of *Trichoderma harzianum* on *in vitro* interactions between basidiomycete isolates at two different temperature regimes. *Mycological Research* **100**, 1454-1458.
- Schrey SD, Schellhammer M, Ecke M, Hampp R, Tarkka MT (2005) Mycorrhiza helper bacterium *Streptomyces* AcH 505 induces differential gene expression in the ectomycorrhizal fungus *Amanita muscaria*. *New Phytologist* **168**, 205-216.

- Score AJ, Palfreyman JW, White NA (1997) Extracellular phenoloxidase and peroxidase enzyme production during interspecific fungal interactions. *International Biodeterioration & Biodegradation* **39**, 225-233.
- Scotter JM, Langford VS, Wilson PF, McEwan MJ, Chambers ST (2005) Real-time detection of common microbial volatile organic compounds from medically important fungi by Selected Ion Flow Tube-Mass Spectrometry (SIFT-MS). *Journal of Microbiological Methods* **63**, 127-134.
- Sellam A, Dongo A, Guillemette T, Hudhomme P, Simoneau P (2007) Transcriptional responses to exposure to the brassicaceous defence metabolites camalexin and allyl-isothiocyanate in the necrotrophic fungus *Alternaria brassicicola*. *Molecular Plant Pathology* **8**, 195-208.
- Shearer CA (1995) Fungal competition. *Canadian Journal of Botany* **73**, S1259-S1264.
- Shuen SK, Buswell JA (1992) Effect of lignin derived phenols and their methylated derivatives on the growth of *Lentinus* spp. *Letters in Applied Microbiology* **15**, 12-14.
- Silar P (2005) Peroxide accumulation and cell death in filamentous fungi induced by contact with a contestant. *Mycological Research* **109**, 137-149.
- Silver N, Best S, Jiang J, Thein S (2006) Selection of housekeeping genes for gene expression studies in human reticulocytes using real-time PCR. *BMC Molecular Biology* **7**, 33.
- Skinner W, Keon J, Hargreaves J (2001) Gene information for fungal plant pathogens from expressed sequences. *Current Opinion in Microbiology* **4**, 381-386.
- Šnajdr J, Baldrian P (2006) Production of lignocellulose-degrading enzymes and changes in soil bacterial communities during the growth of *Pleurotus ostreatus* in soil with different carbon content. *Folia Microbiologica* **51**, 579-590.
- Sonenshine DE (1985) Pheromones and other semiochemicals of the acari. *Annual Review of Entomology* **30**, 1-28.

- Soundy P, Wheeler C, Latham H (2001) Preparing highly fluorescent, evenly labelled probes for microarray hybridisation using the amino allyl methods with CyScribe Post- Labelling Kit. *Life Science News* **9**, 1-3.
- Splivallo R, Novero M, Berteà CM, Bossi S, Bonfante P (2007) Truffle volatiles inhibit growth and induce an oxidative burst in *Arabidopsis thaliana*. *New Phytologist* **175**, 417-424.
- Stadler M, Sterner O (1998) Production of bioactive secondary metabolites in the fruit bodies of macrofungi as a response to injury. *Phytochemistry* **49**, 1013-1019.
- Stahl PD, Parkin TB (1996) Microbial production of volatile organic compounds in soil microcosms. *Soil Science Society of America Journal* **60**, 821-828.
- Staszczak M (2002) Proteasomal degradation pathways in *Trametes versicolor* and *Phlebia radiata*. *Enzyme and Microbial Technology* **30**, 537-541.
- Stein J, Liang P (2002) Differential display technology: A general guide. *Cellular and Molecular Life Sciences* **59**, 1235-1240.
- Steiner S, Erdmann D, Steidle JLM, Ruther J (2007) Host habitat assessment by a parasitoid using fungal volatiles. *Frontiers in Zoology* **4**, 3.
- Sterky F, Regan S, Karlsson J, *et al.* (1998) Gene discovery in the wood-forming tissues of poplar: Analysis of 5,692 expressed sequence tags. *Proceedings of the National Academy of Sciences* **95**, 13330-13335.
- Stoeckert C, Parkinson H (2003) The MGED ontology: a framework for describing functional genomics experiments. *Comparative and Functional Genomics* **4**, 127-132.
- Sunesson A, Vaes W, Nilsson C, *et al.* (1995) Identification of volatile metabolites from five fungal species cultivated on two media. *Applied Environmental Microbiology* **61**, 2911-2918.

- Taylor JW, Berbee ML (2006) Dating divergences in the Fungal Tree of Life: review and new analyses. *Mycologia* **98**, 838-849.
- Thain D, Tannenbaum T, Livny M (2005) Distributed computing in practice: The Condor Experience. *Concurrency and Computation: Practice and Experience* **17**, 323-356.
- Thelen J, Harbinson J, Jansen R, *et al.* (2005) The sesquiterpene  $\alpha$ -copaene is induced in tomato leaves infected by *Botrytis cinerea*. *Journal of Plant Interactions* **1**, 163-170.
- Thellin O, Zorzi W, Lakaye B, *et al.* (1999) Housekeeping genes as internal standards: use and limits. *Journal of Biotechnology* **75**, 291-295.
- Thomas SW, Glaring MA, Rasmussen SW, Kinane JT, Oliver RP (2002) Transcript profiling in the barley mildew pathogen *Blumeria graminis* by serial analysis of gene expression (SAGE). *Molecular Plant-Microbe Interactions* **15**, 847-856.
- Thompson JD, Higgins DG, Gibson TJ (1994) CLUSTAL W: improving the sensitivity of progressive multiple sequence alignment through sequence weighting position-specific gap penalties and weight matrix choice. *Nucleic Acids Research* **22**, 4673-4680.
- Toljander YK, Lindahl BD, Holmer L, Högborg NOS (2006) Environmental fluctuations facilitate species co-existence and increase decomposition in communities of wood decay fungi. *Oecologia* **148**, 625-631.
- Tordoff GM, Boddy L, Jones TH (2006) Grazing by *Folsomia candida* (Collembola) differentially affects mycelial morphology of the cord-forming basidiomycetes *Hypholoma fasciculare*, *Phanerochaete velutina* and *Resinicium bicolor*. *Mycological Research* **110**, 335-345.
- Tortella GR, Diez MC, Durán N (2005) Fungal diversity and use in decomposition of environmental pollutants. *Critical Reviews in Microbiology* **31**, 197-212.

- Trabold PA, Weinberger M, Feng L, Burhans WC (2005) Activation of budding yeast replication origins and suppression of lethal DNA damage effects on origin function by ectopic expression of the co-chaperone protein Mge1. *Journal of Biological Chemistry* **280**, 12413-12421.
- Tsujiyama SI, Minami M (2005) Production of phenol-oxidising enzymes in the interaction between white-rot fungi. *Mycoscience* **46**, 268-271.
- Tunc S, Chollet E, Chalier P, Preziosi-Belloy L, Gontard N (2007) Combined effect of volatile antimicrobial agents on the growth of *Penicillium notatum*. *International Journal of Food Microbiology* **113**, 263-270.
- Valaskova V, Baldrian P (2006) Degradation of cellulose and hemicelluloses by the brown rot fungus *Piptoporus betulinus* - production of extracellular enzymes and characterization of the major cellulases. *Microbiology* **152**, 3613-3622.
- VanBogelen RA, Kelley PM, Neidhardt FC (1987) Differential induction of heat shock, SOS, and oxidation stress regulons and accumulation of nucleotides in *Escherichia coli*. *Journal of Bacteriology* **169**, 26-32.
- Velculescu VE, Zhang L, Vogelstein B, Kinzler KW (1995) Serial analysis of gene expression. *Science* **270**, 484-487.
- Vicente-franqueira R, Moreno MA, Leal F, Calera JA (2005) The zrfA and zrfB genes of *Aspergillus fumigatus* encode the zinc transporter proteins of a zinc uptake system induced in an acid, zinc-depleted environment. *Eukaryotic Cell* **4**, 837-848.
- Vilain C, Libert F, Venet D, Costagliola S, Vassart G (2003) Small amplified RNA-SAGE: an alternative approach to study transcriptome from limiting amount of mRNA. *Nucleic Acids Research* **31**, e24-e24.
- Virlon B, Cheval L, Buhler J-M, *et al.* (1999) Serial microanalysis of renal transcriptomes. *Proceedings of the National Academy of Science USA* **96**, 15286-15291.

- Wady L, Parkinson D-R, Pawliszyn J (2005) Methyl benzoate as a marker for the detection of mold in indoor building materials. *Journal of Separation Science* **28**, 2517-2525.
- Wald P, Crockatt M, Gray V, Boddy L (2004)a Growth and interspecific interactions of the rare oak polypore *Piptoporus quercinus*. *Mycological Research* **2**, 189-197.
- Wald P, Pitkänen S, Boddy L (2004)b Interspecific interactions between the rare tooth fungi *Creolophus cirrhatus*, *Hericium erinaceus* and *H. coralloides* and other wood decay species in agar and wood. *Mycological Research* **108**, 1447-1457.
- Walter M, Boyd-Wilson K, Boul L, *et al.* (2005) Field-scale bioremediation of pentachlorophenol by *Trametes versicolor*. *International Biodeterioration and Biodegradation* **56**, 51-57.
- Wardle DA, Parkinson D, Waller JE (1993) Interspecific competitive interactions between pairs of fungal species in natural substrates. *Oecologia* **94**.
- Welford SM, Gregg J, Chen E, *et al.* (1998) Detection of differentially expressed genes in primary tumor tissues using representational differences analysis coupled to microarray hybridization. *Nucleic Acids Research* **26**, 3059-3065.
- Wells JM, Boddy L (2002) Interspecific carbon exchange and cost of interactions between basidiomycete mycelia in soil and wood. *Functional Ecology* **16**, 153-161.
- Wessels JGH (1992) Gene expression during fruiting in *Schizophyllum commune*. *Mycological Research* **96**, 609-620.
- Wettenhall JM, Smyth GK (2004) limmaGUI: A graphical user interface for linear modeling of microarray data. *Bioinformatics* **20**, 3705-3706.
- Wheatley R, Hackett C, Bruce A, Kundzewicz A (1997) Effect of substrate composition on production of volatile organic compounds from *Trichoderma* spp. inhibitory to wood decay fungi. *International Biodeterioration & Biodegradation* **39**, 199-205.



- Wheatley RE (2002) The consequences of volatile organic compound mediated bacterial and fungal interactions. *Antonie van Leeuwenhoek* **81**, 357-364.
- Whetzel PL, Parkinson H, Causton HC, *et al.* (2006) The MGED Ontology: a resource for semantics-based description of microarray experiments. *Bioinformatics* **22**, 866-873.
- White GJ, Traquair JA (2006) Necrotrophic mycoparasitism of *Botrytis cinerea* by cellulolytic and ligninocellulolytic Basidiomycetes. *Canadian Journal of Botany* **52**, 508-518.
- White NA, Boddy L (1992)*a* Differential extracellular enzyme production in colonies of *Coriolus versicolor*, *Phlebia radiata* and *Phlebia rufa*: effect of gaseous regime. *Journal of General Microbiology* **138**, 2589-2598.
- White NA, Boddy L (1992)*b* Extracellular enzyme localization during interspecific fungal interactions. *FEMS Microbiology Letters* **98**, 75-80.
- White NA, Sturrock C, Ritz K, *et al.* (1998) Interspecific fungal interactions in spatially heterogenous systems. *FEMS Microbiology Ecology* **27**, 21-32.
- Wiens JA, Cates RG, Rotenberry JT, *et al.* (1991) Arthropod dynamics on sagebrush (*Artemisia tridentata*) - effects of plant chemistry and avian predation. *Ecological Monographs* **61**, 299-321.
- Winter J, Linke K, Jatzek A, Jakob U (2005) Severe oxidative stress causes inactivation of DnaK and activation of the redox-regulated chaperone Hsp33. *Molecular Cell* **17**, 381-392.
- Woods CM, Woodward S, Pinard MA, Redfern DB (2006) Colonization of Sitka spruce stumps by decay-causing hymenomycetes in paired inoculations. *Mycological Research* **110**, 854-868.
- Woodward S, Boddy L (2008) Interactions between saprotrophic fungi. In: *Ecology of Saprotrophic Basidiomycetes* (eds. Boddy L, Frankland JC, van West P), pp. 123-139. Elsevier, Amsterdam.

- Wu S, Krings U, Zorn H, Berger RG (2005) Volatile compounds from the fruiting bodies of beefsteak fungus *Fistulina hepatica* (Schaeffer: Fr.) Fr. *Food Chemistry* **92**, 221-226.
- Yoo N-H, Kim J-P, Yun B-S, *et al.* (2006) Hirsutenols D, E and F, new sesquiterpenes from the culture broth of *Stereum hirsutum*. *Journal of Antibiotics* **59**, 110-113.
- Yoshioka H, Yamada N, Doke N (1999) cDNA cloning of sesquiterpene cyclase and squalene synthase, and expression of the genes in potato tuber infected with *Phytophthora infestans*. *Plant and Cell Physiology* **40**, 993-998.
- Yu J, Chang PK, Cary JW, *et al.* (1995) Comparative mapping of aflatoxin pathway gene clusters in *Aspergillus parasiticus* and *Aspergillus flavus*. *Applied and Environmental Microbiology* **61**, 2365-2371.
- Zamponi L, Michelozzi M, Capretti P (2006) Effects of four monoterpenes on the growth in vitro of some *Heterobasidion* spp. and two *Leptographium* species. *Journal of Plant Diseases and Protection* **113**, 164-167.
- Zhang Z, Henderson C, Gurr SJ (2004) *Blumeria graminis* secretes an extracellular catalase during infection of barley: potential role in suppression of host defence. *Molecular Plant Pathology* **5**, 537-547.
- Zhao H, Eide D (1996)*a* The yeast ZRT1 gene encodes the zinc transporter protein of a high-affinity uptake system induced by zinc limitation. *Proceedings of the National Academy of Science USA* **93**, 2454-2458.
- Zhao H, Eide D (1996)*b* The ZRT2 Gene encodes the low affinity zinc transporter in *Saccharomyces cerevisiae*. *J. Biol. Chem.* **271**, 23203-23210.
- Zook M, Hohn T, Bonnen A, Tsuji J, Hammerschmidt R (1996) Characterization of novel sesquiterpenoid biosynthesis in tobacco expressing a fungal sesquiterpene synthase. *Plant Physiology* **112**, 311-318.
- Zou CS, Mo MH, Gu YQ, Zhou JP, Zhang KQ (2007) Possible contributions of volatile-producing bacteria to soil fungistasis. *Soil Biology and Biochemistry* **39**, 2371-2379.

Zucchi TD, Zucchi FD, Poli P, de Melo IS, Zucchi TMAD (2005) A short-term test adapted to detect the genotoxic effects of environmental volatile pollutants (benzene fumes) using the filamentous fungus *Aspergillus nidulans*. *Journal of Environmental Monitoring* 7, 598-602.

## **Appendix 1**

### **A1.1 The basis of Gas Chromatography-Mass Spectrometry**

#### **A1.1.1 Analysis of volatiles**

Once VOCs from a sample have been collected they are desorbed, separated and identified by gas chromatography-mass spectrometry (GC-MS). The basis of GC-MS analysis is that a mixture of compounds is injected into the gas chromatograph and vapourised. If SPME is used the fibre is inserted into a port and the compounds are desorbed at a high temperature, determined by the type of fibre used (e.g. 220°C when using PDMS). The mixture of gases then travels onto the GC column where the compounds are separated as they interact with the column. The compounds travel along the column at different speeds determined by their molecular weight, structure and polarity, thus they separate and enter the mass spectrometer once the end of the column is reached. The mass spectrometer itself consists of an ion source, a filter and a detection system.

#### **A1.1.2 Ionisation with MS**

There are various different methods of ionisation which have different suitability depending on the application, compounds to be analysed and sample type. They include electron ionisation (EI), chemical ionisation (CI), electrospray (ESI), fast atom bombardment (FAB) and matrix assisted laser desorption (MALDI) which can detect masses in that range of 1000 Daltons (for EI) to 500,000 Daltons (for MALDI).

Electron impact ionisation is used in this study. It is appropriate for relatively small analytes up to 1000 Daltons and can provide structural information. An ionisation source produces electrons, which are accelerated towards another electrode called the ion trap. The gas molecules exiting the GC column travel into this electron beam and are bombarded by the electrons, which may impart enough energy to cause fragmentation and ionisation of the compound. This method usually produces singly charged ions. The energy of the electrons determines the degree of fragmentation of

the compound. A relatively low energy electron will only remove a single electron from the compound and no fragmentation will occur. This produces what is termed the “molecular ion” and the corresponding peak in the mass spectrum gives the molecular weight of the analyte. Instability in this molecular ion or higher energy electrons will produce a greater degree of fragmentation resulting in smaller fragments, thus mass spectra are usually made up of a number of peaks each representing a different fragment.

### **A1.1.3 Detection with MS**

Ions are accelerated into the mass spectrometer for analysis while negatively charged ions and uncharged molecules are pumped away. There are a number of mass analysers available such as a quadrupole, sector, time-of-flight (TOF) and ion cyclotron resonance (ICR) which in general increase in resolution respectively. A quadrupole mass analyser was used in this project (Figure 4.1). This consists of four metal rods - two pairs being oppositely charged - which control the path of the ions between the rods according to their mass/charge ( $m/z$ ) ratio. Different voltages across the quadrupole allow ions with different  $m/z$  ratios to reach the detector. Thus, the voltage can be constant to allow only a particular ion through to the detector, or a range of ions can be scanned by varying the voltage. Electron ionisation produces singly charged ions making the charge constant at one, thus it is the mass which determines an ion's path. A detector produces a signal when an ion strikes it. This, together with information about the quadrupole voltages, the  $m/z$  and abundance of each ion and its elution time, is recorded as it leaves the GC column. A chromatogram is produced, showing each peak as it comes off the column. From these the mass spectra, detected at the retention time that coincides with a compound peak, can be analysed.

## A1.3 Chromatograms

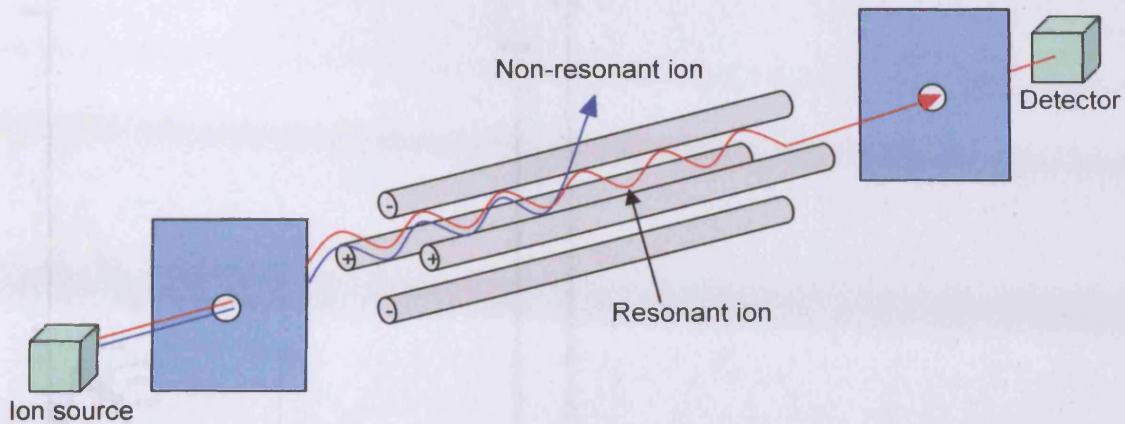


Figure A1.1 Schematic of a quadrupole mass filter

#### A1.1.4 Analysis of mass spectra

Spectra are compared to library databases of mass spectra to make putative identifications and spectra are visually inspected for distinctive patterns of fragment peaks which are characteristic of certain molecular groups or isotopes. Integration of chromatogram peaks gives the area under peak which can be equated to the relative abundance of each compound however this must be treated with caution as discussed earlier because many factors can affect how much compound is adsorbed hence relative peaks heights may not reflect the true composition of the sample.

Figure A1.3 Chromatogram for the analysis of a sample

A1.2 Chromatograms

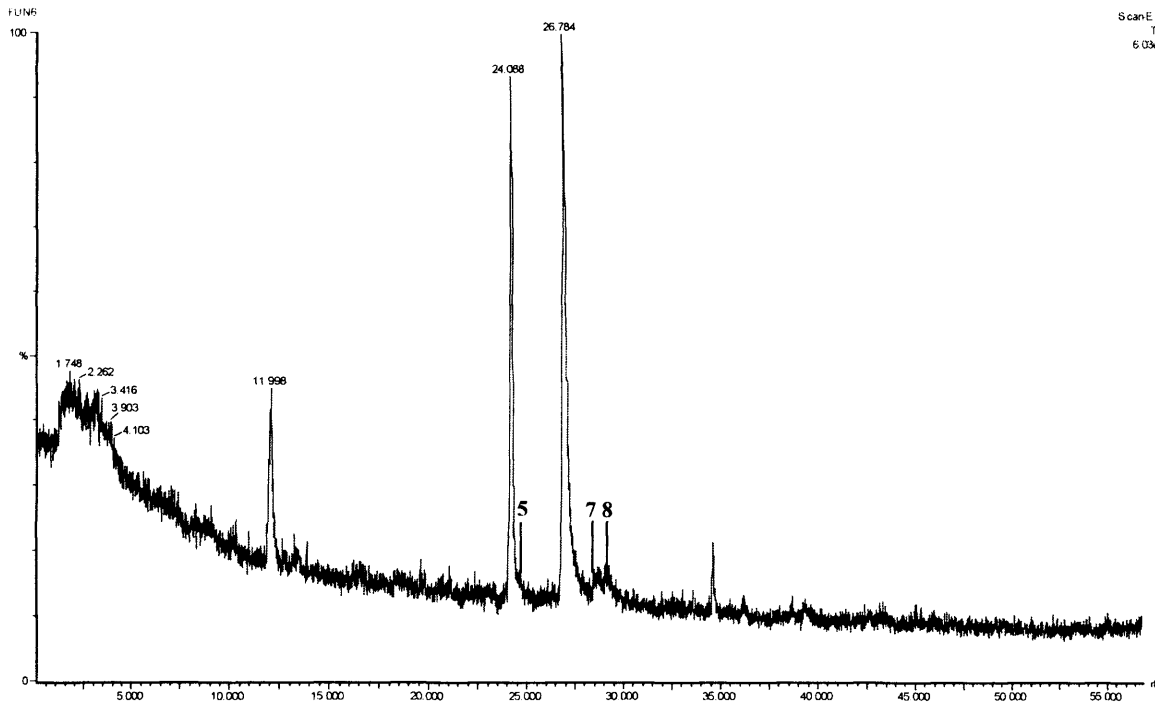


Figure A1.2 Chromatogram for TvSg day 1

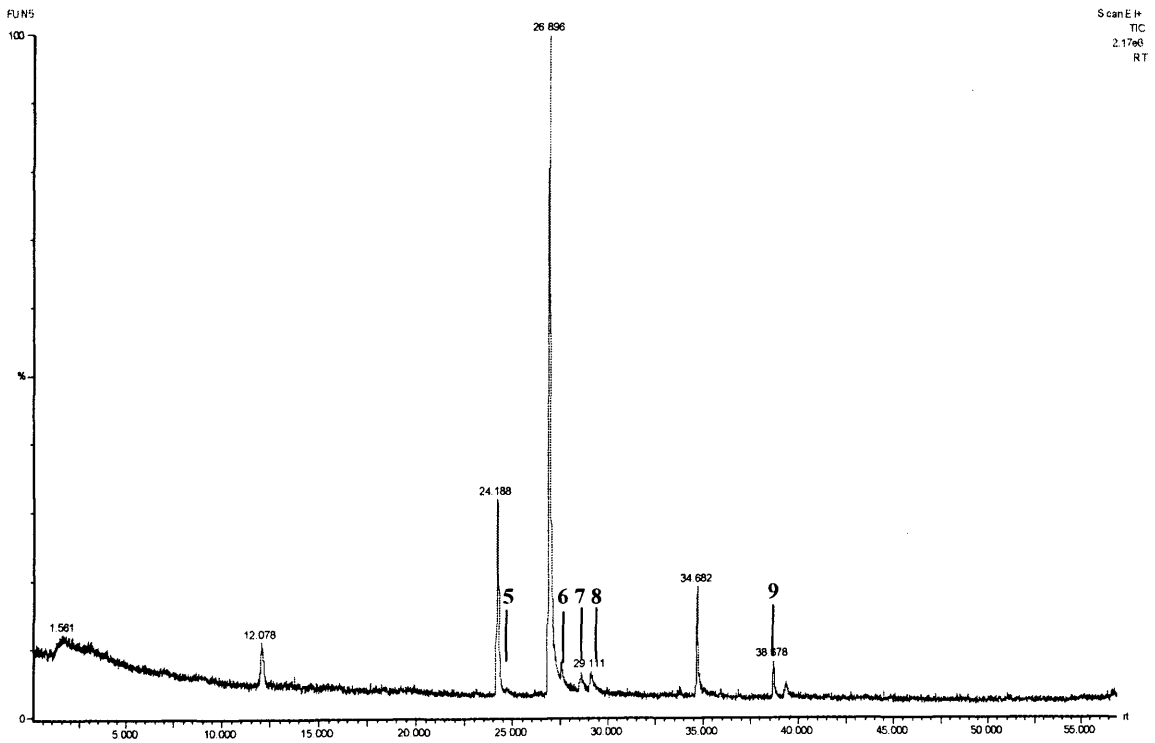


Figure A1.3 Chromatogram for SgSg, day 1.

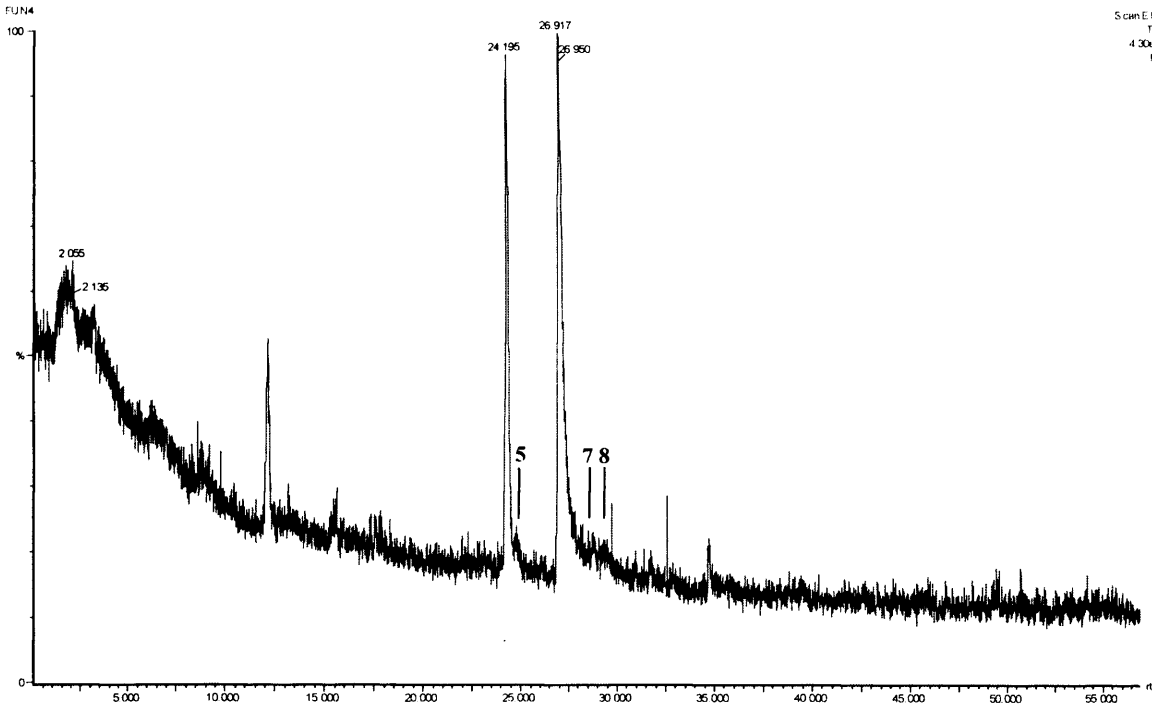


Figure A1.4 Chromatogram for TvTv, day 1.

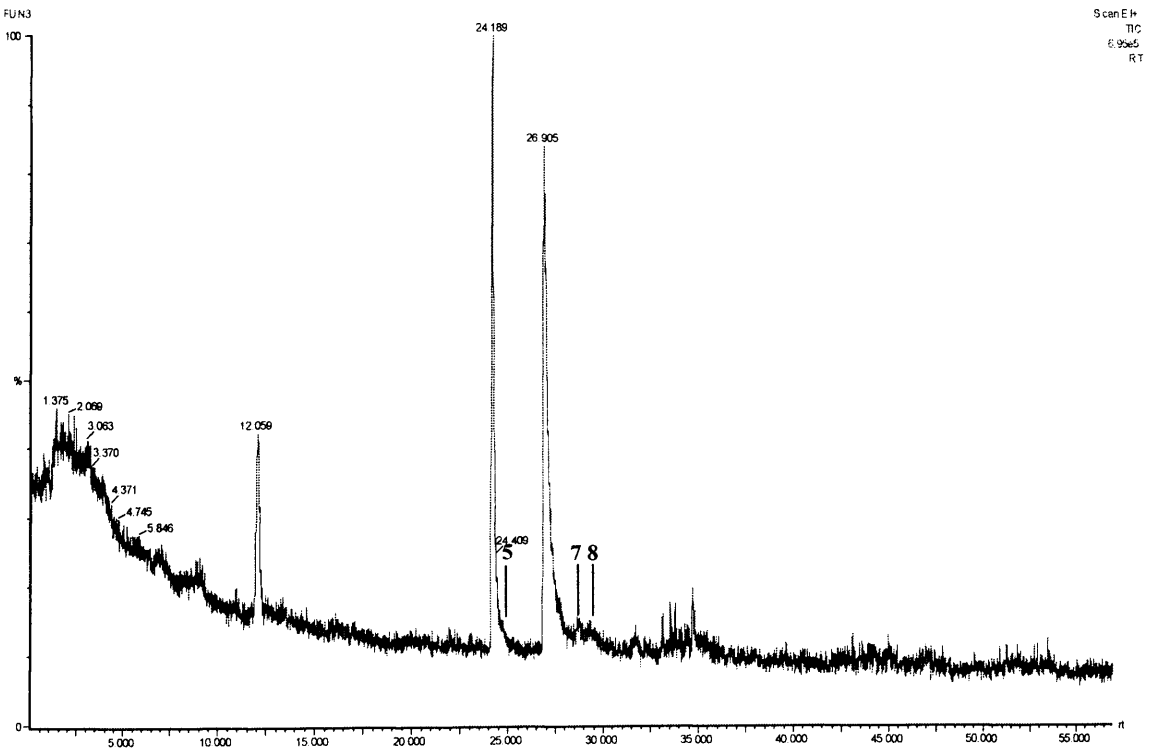


Figure A1.5 Chromatogram for Sg alone, day 1.



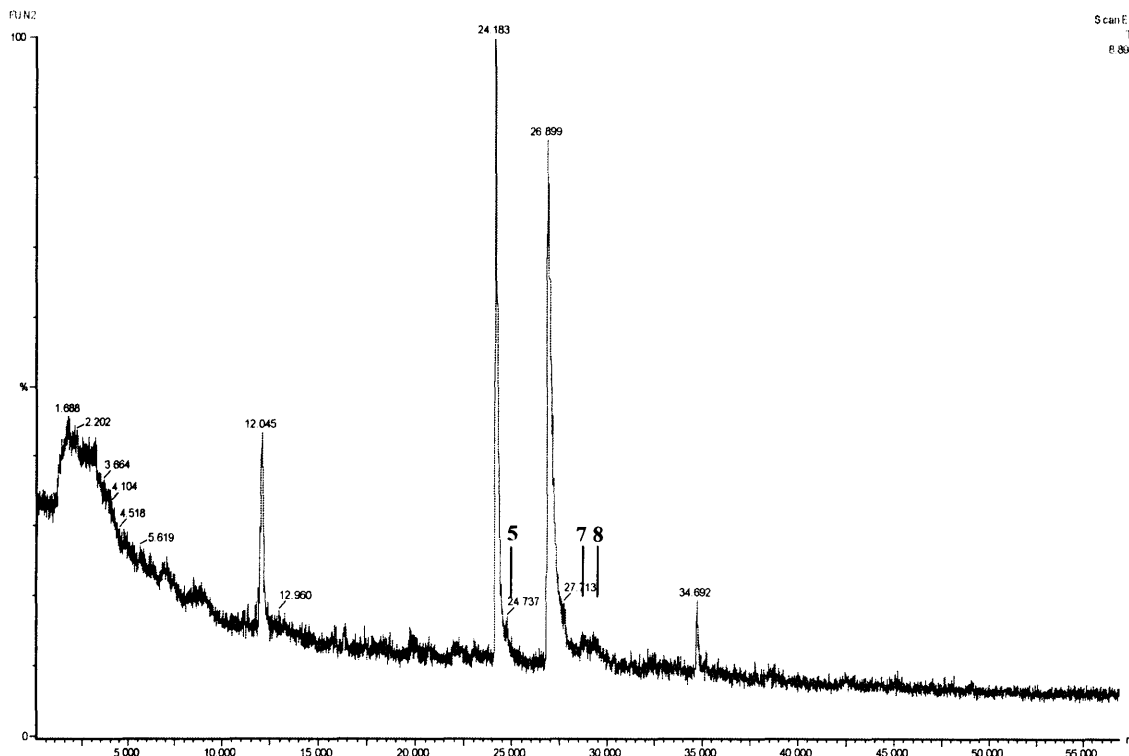


Figure A1.6 Chromatogram for Tv alone, day 1.

### A1.3 Volatile peak spectra

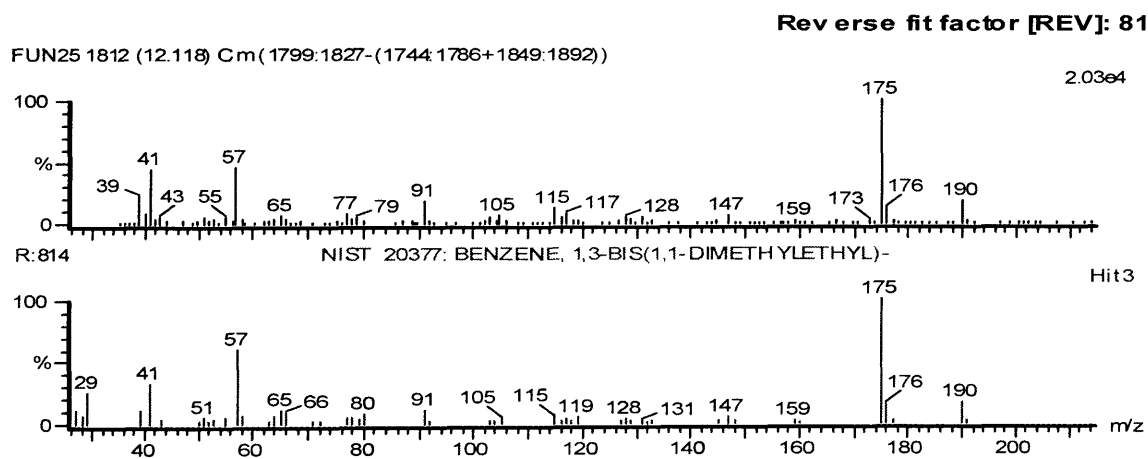


Figure A1.7 Spectra for peak 1 (top) and 1,3-bis(1,1-dimethylethyl) benzene (bottom).

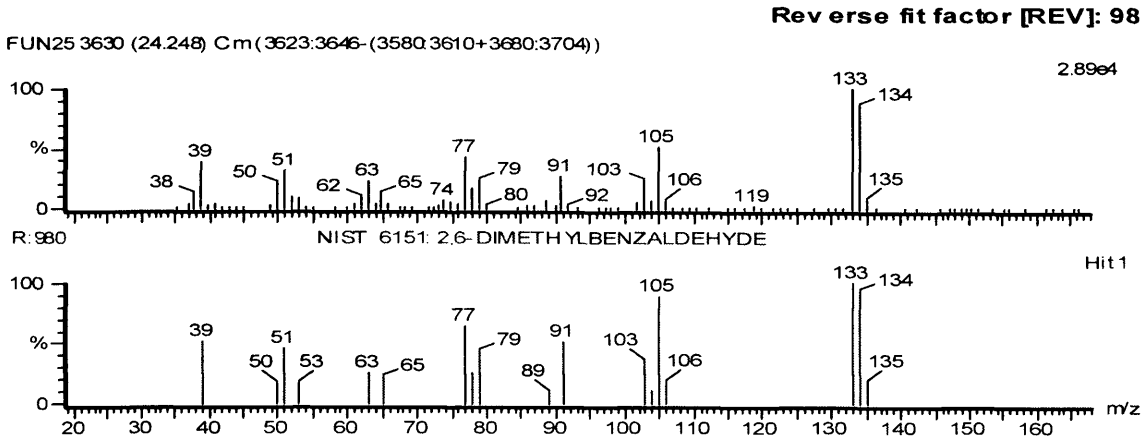


Figure A1.8 Spectra for peak 2 (top) and 2,6-dimethylbenzaldehyde (bottom)

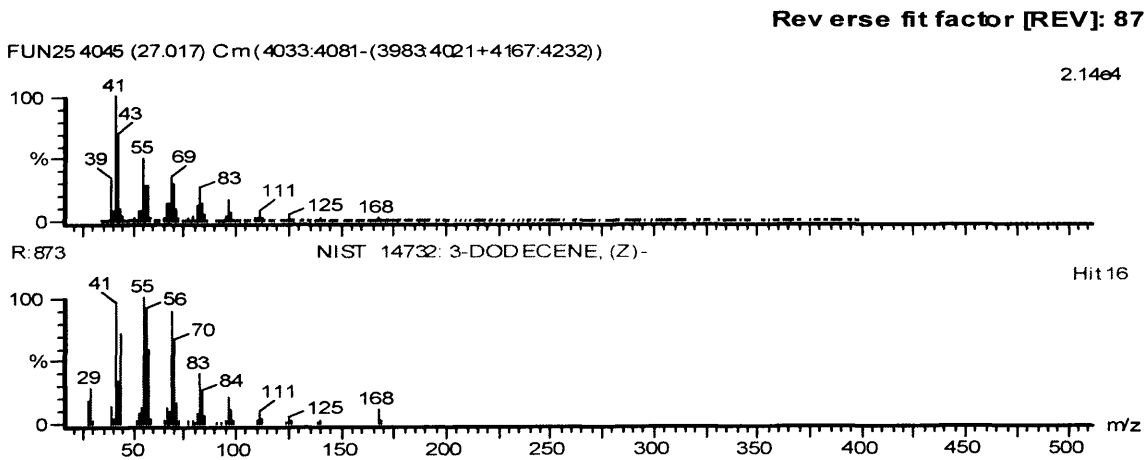


Figure A1.9 Spectra for peak 3 (top) and Z-3-dodecene (bottom)

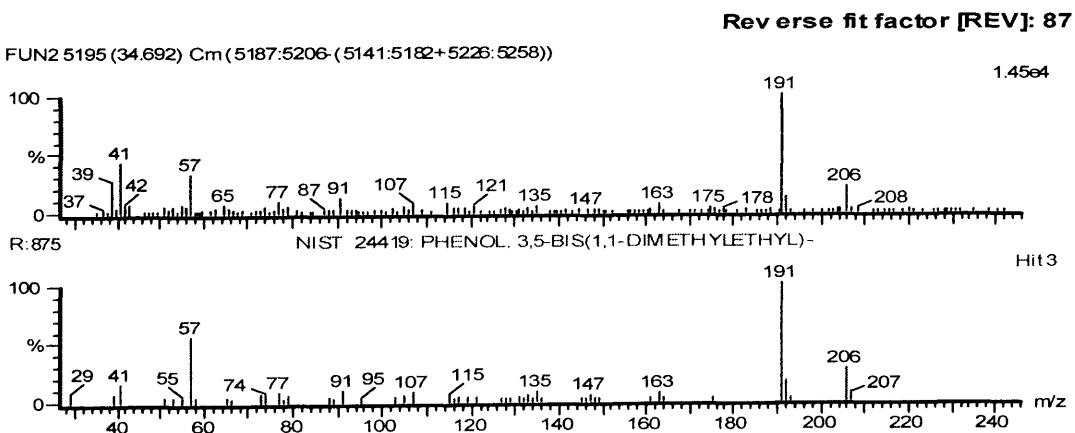


Figure A1.10 Spectra for peak 4 (top) and 3,5-bis(1,1-dimethylethyl) phenol (bottom)

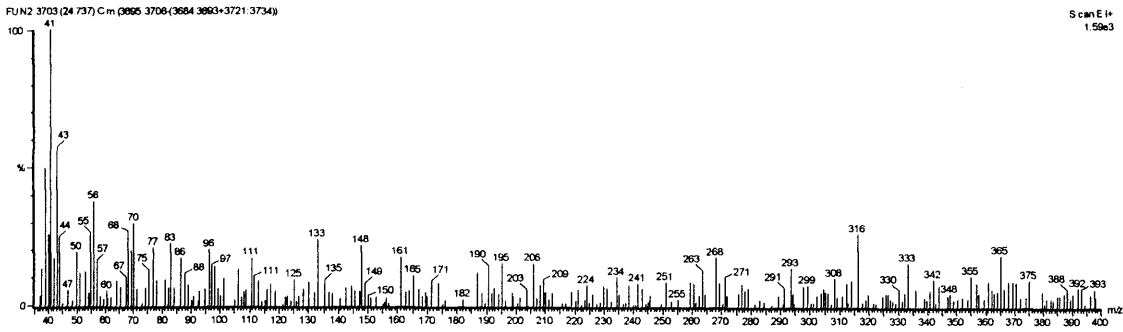
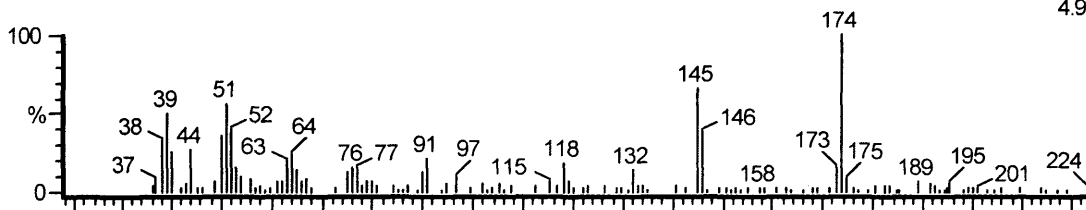


Figure A1.11 Spectrum for peak 5

Reverse fit factor [REV]: 73

FUN5 4123 (27.537) Cm(4116:4127-(4102:4113+4139:4147))

4.93e3



R: 731 NIST 16166: BENZENE, 1,3-DIISOCYANATOMETHYL-

Hit 3

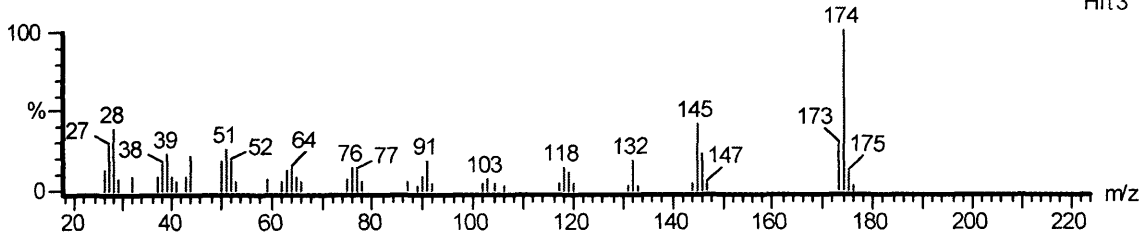


Figure A1.12 Spectra for peak 6 (top) and 1,3-diisocyanatomethyl-benzene (bottom)

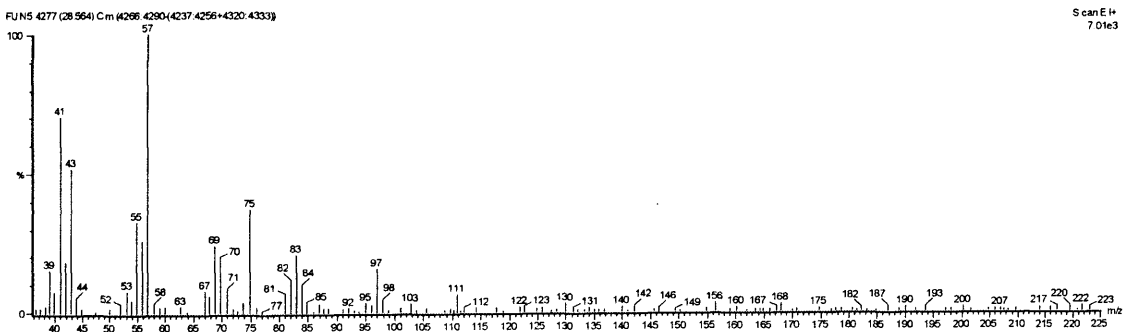


Figure A1.13 Spectrum for peak 7. Note the decreasing size of peaks, which indicates the fragmentation of a hydrocarbon chain.

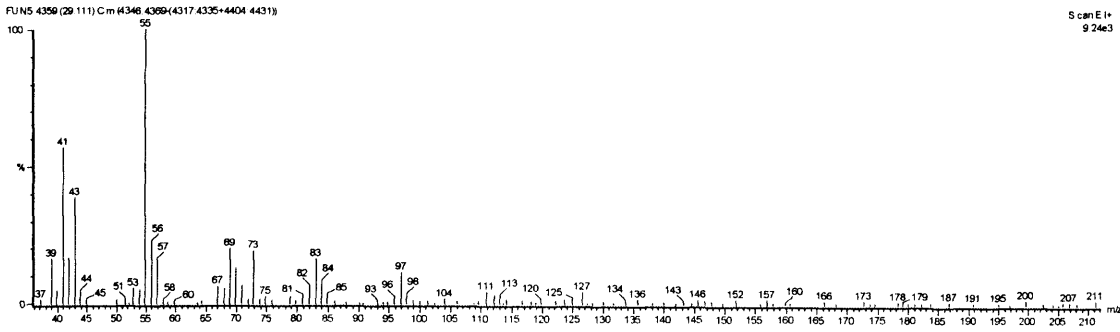


Figure A1.14 Spectrum for peak 8

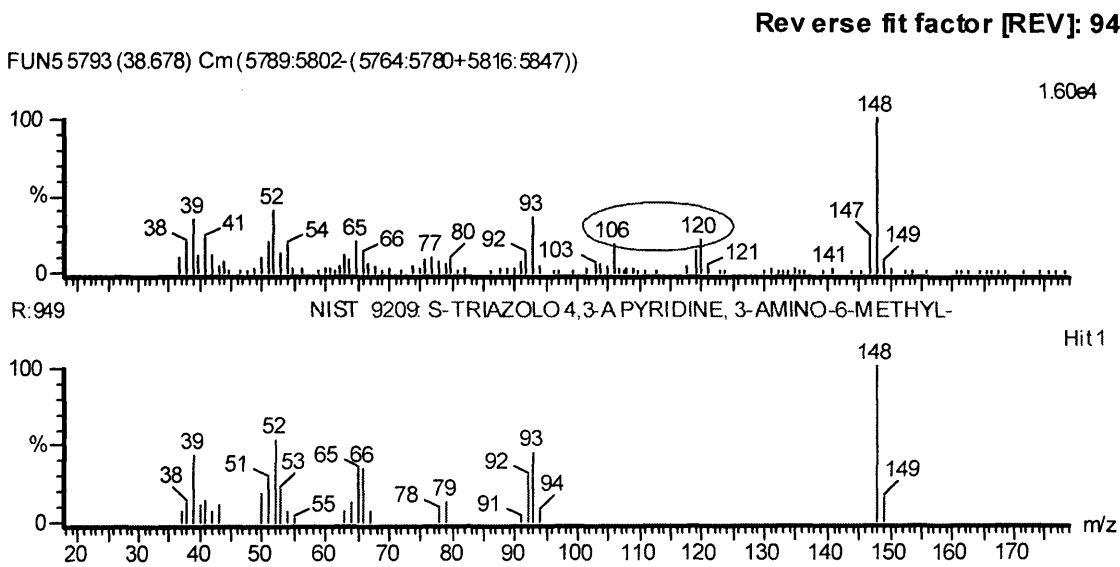


Figure A1.15 Spectra for peak 9 (top) and S-triazolo 4,3-apyridine,3-amino-6-methyl (bottom). Note the common peaks at  $m/z$  52, 66, 93 and 148 but the absence of 106 and 120 in peak 9 (top). This indicates that peak 9 may have a similar structure to S-triazolo 4,3-apyridine,3-amino-6-methyl but they are not a perfect match.

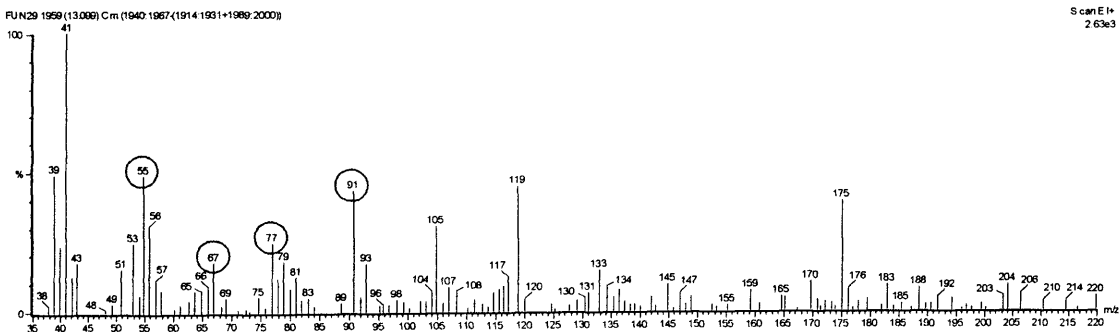
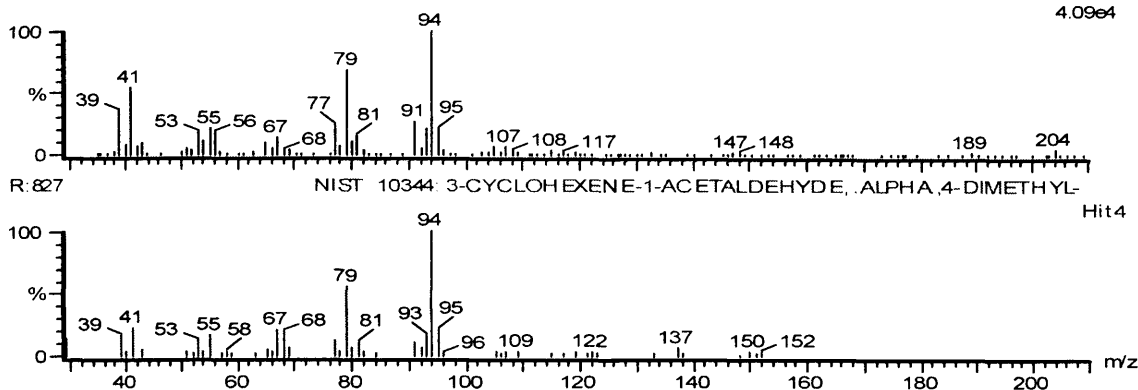


Figure A1.16 Spectrum for peak 10. Note peaks at  $m/z$  55, 67, 77 and 91, which indicate the presence of a benzene ring.

Reverse fit factor [REV]: 82

FUN69 2037 (13.620) Cm(2022:2052-(1976:1997+2098:2123))

4.09e4

Figure A1.17 Spectra for peak 11 (top) and  $\alpha$ -4-dimethyl-3-cyclohexene-1-acetaldehyde (bottom)

Reverse fit factor [REV]: 71

FUN69 2234 (14.934) Cm(2234:2264-(2187:2215+2306:2331))

1.49e4

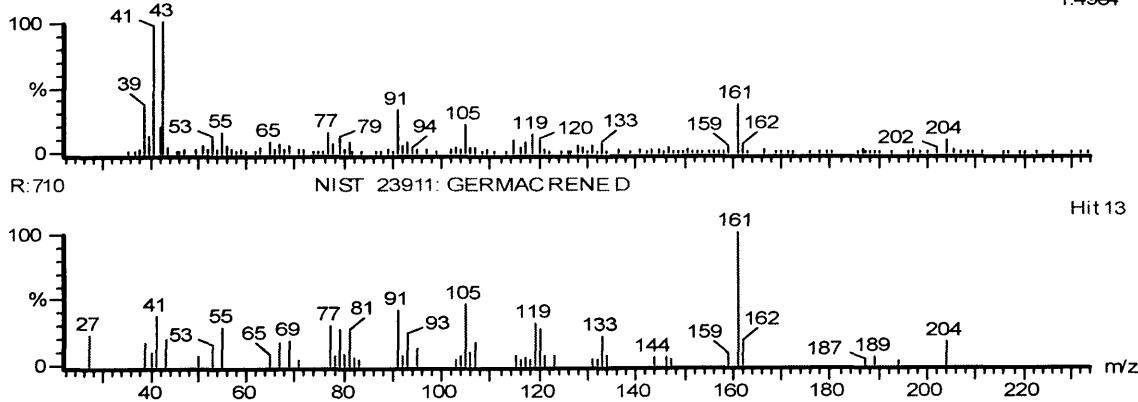


Figure A1.18 Spectra for peak 12 (top) and germacrene D (bottom). Note the similar m/z peaks present between spectra.

Reverse fit factor [REV]: 87

FUN68 2476 (16.548) Cm(2468:2488-(2437:2457+2519:2535))

8.28e3

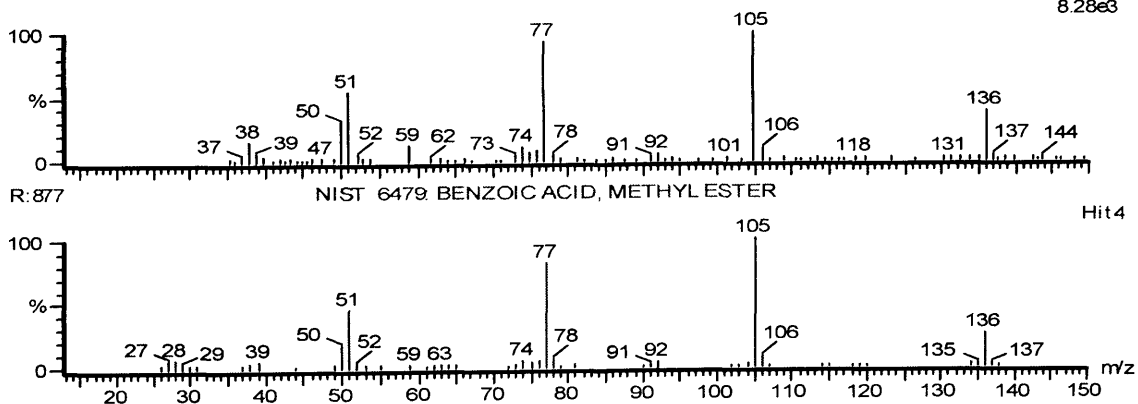


Figure A1.19 Spectra for peak 13 (top) and benzoic acid, methyl ester (bottom)

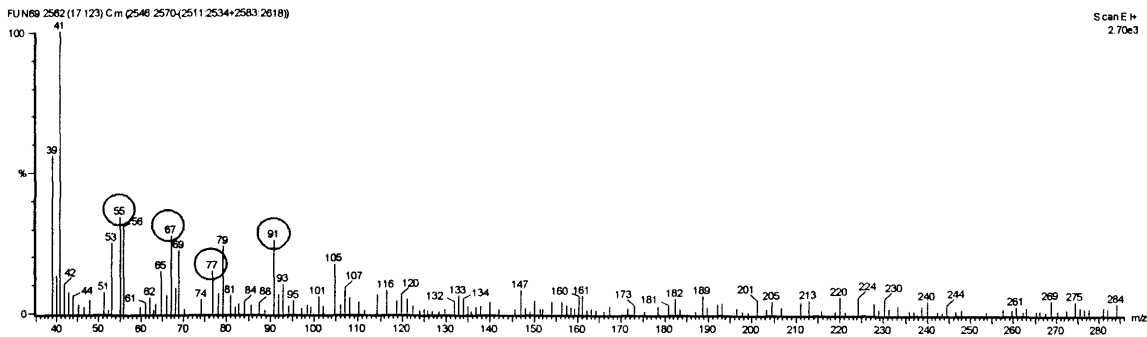


Figure A1.20 Spectrum for peak 14. Note peaks at  $m/z$  55, 67, 77 and 91, which indicate the presence of a benzene ring.

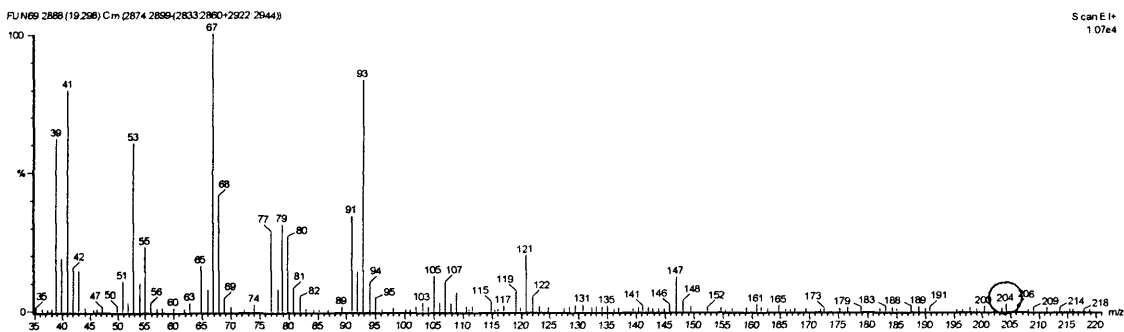


Figure A1.21 Spectrum for peak 15. Note the  $m/z$  maximum at 204 which indicates the compound is a sesquiterpene.

Reverse fit factor [REV]: 77

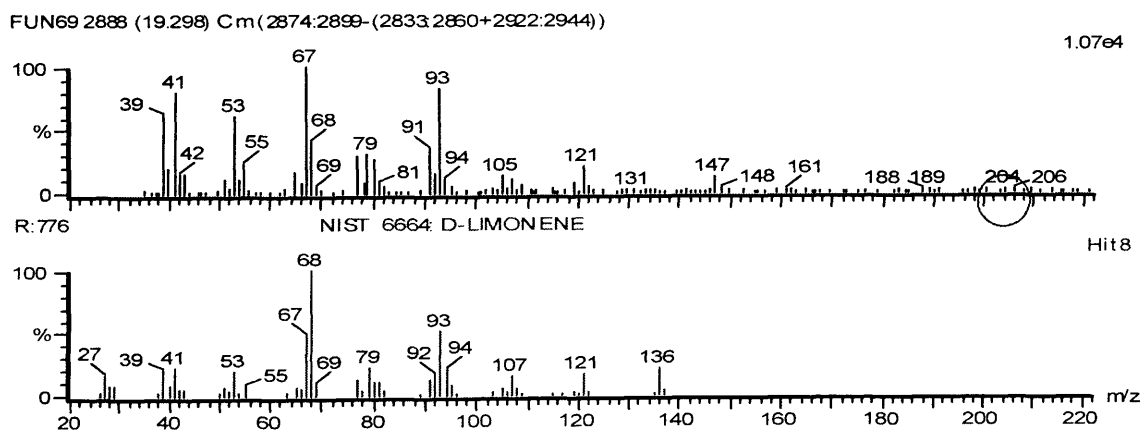
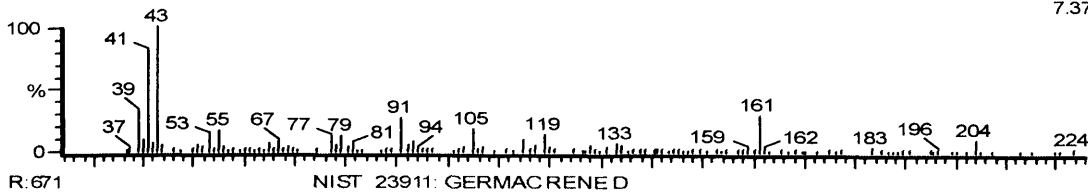


Figure A1.22 Spectra for peak 15 (top) and D-limonene (bottom). Note that although peak 15 has an  $m/z$  maximum of 204 there are many peaks in common between the two spectra indicating possible similar structures.

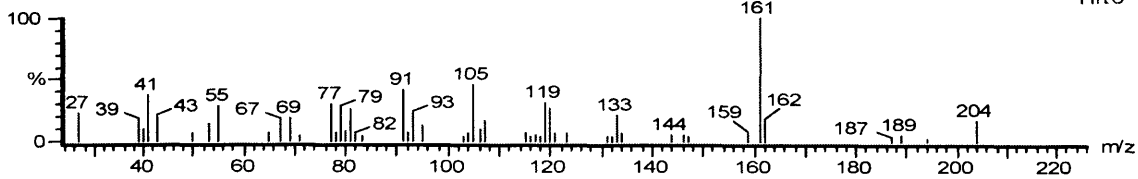
## Reverse fit factor [REV]: 67

FUN69 3059 (20.439) Cm(3052:3079-(3018:3038+3096:3124))

7.37e3



Hit 6

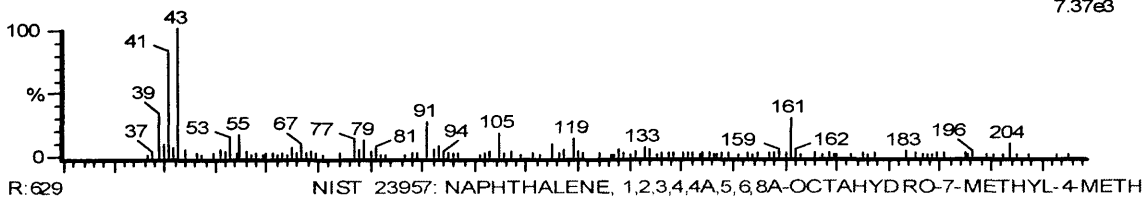


**Figure A1.23** Spectra for peak 16 (top) and germacrene D (bottom). Note the  $m/z$  maximum of 204 for peak 16, which indicates it is a sesquiterpene and the similar pattern of peaks between spectra suggesting that peak 16 could be germacrene D or a very closely related compound or isomer.

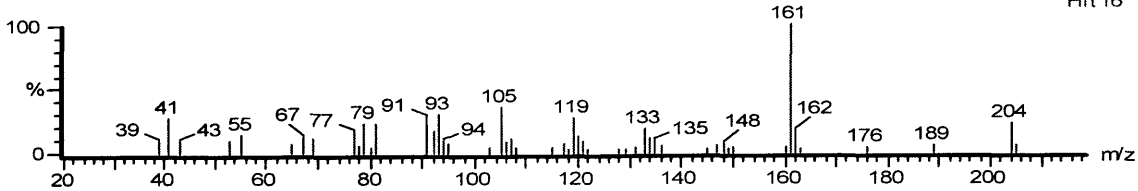
## Reverse fit factor [REV]: 62

FUN69 3059 (20.439) Cm(3052:3079-(3018:3038+3096:3124))

7.37e3



Hit 16

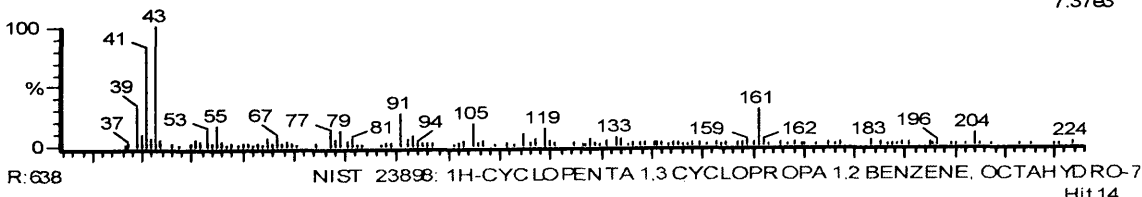


**Figure A1.24** Spectra for peak 16 (top) and  $\zeta$ -cadineine (bottom).

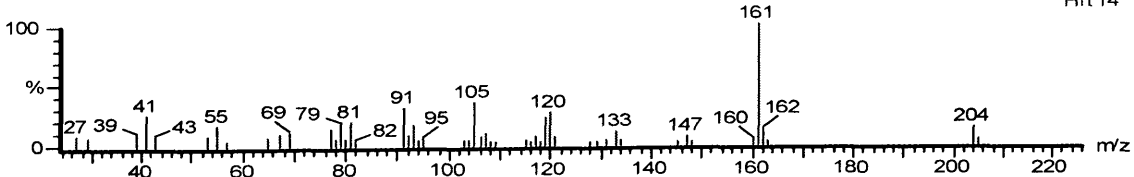
## Reverse fit factor [REV]: 63

FUN69 3059 (20.439) Cm(3052:3079-(3018:3038+3096:3124))

7.37e3



Hit 14



**Figure A1.25** Spectra for peak 16 (top) and 1H-cyclopenta-1,3-cyclopropa-1,2-benzene,octahydro-7-methyl-3- (bottom)

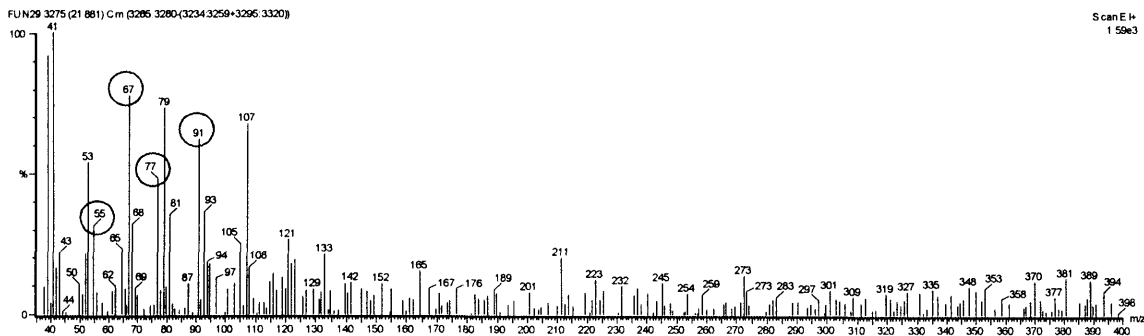


Figure A1.26 Spectrum for peak 17

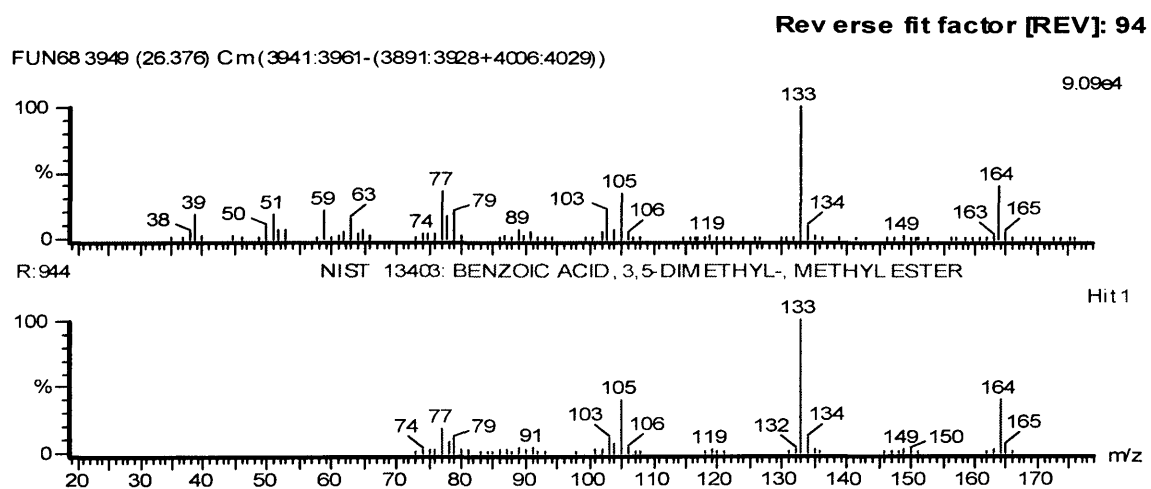


Figure A1.27 Spectra for peak 18 (top) and methyl 3,5-dimethyl benzoate (bottom)

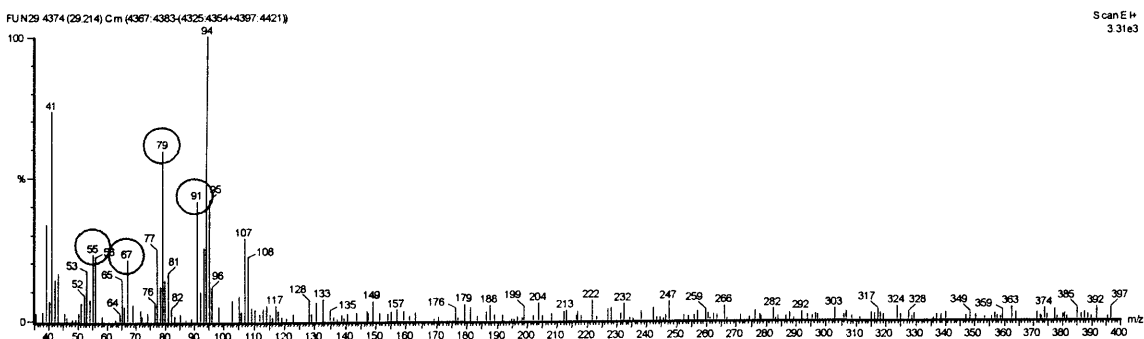


Figure A1.28 Spectrum for peak 19. Note peaks at 55, 67, 79 and 91, which indicate the presence of a benzene ring in the compound.



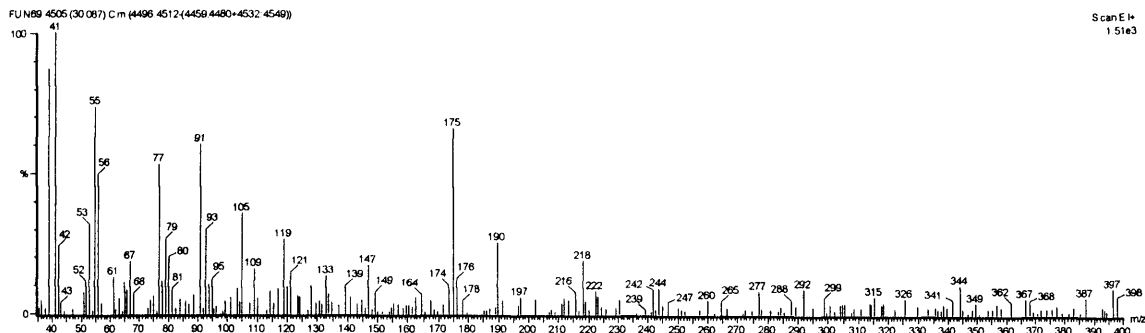


Figure A1.29 Spectrum for peak 20

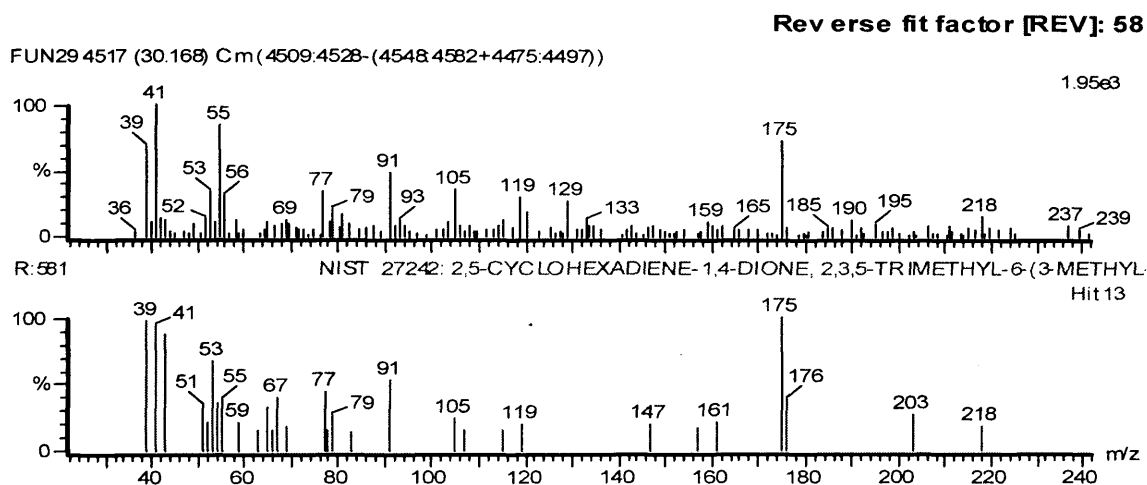


Figure A1.30 Spectra for peak 20 (top) and 2,5-cyclohexadiene-1,4-dione,2,3,5-trimethyl-6-(3-methyl-2-butenyl) (bottom)

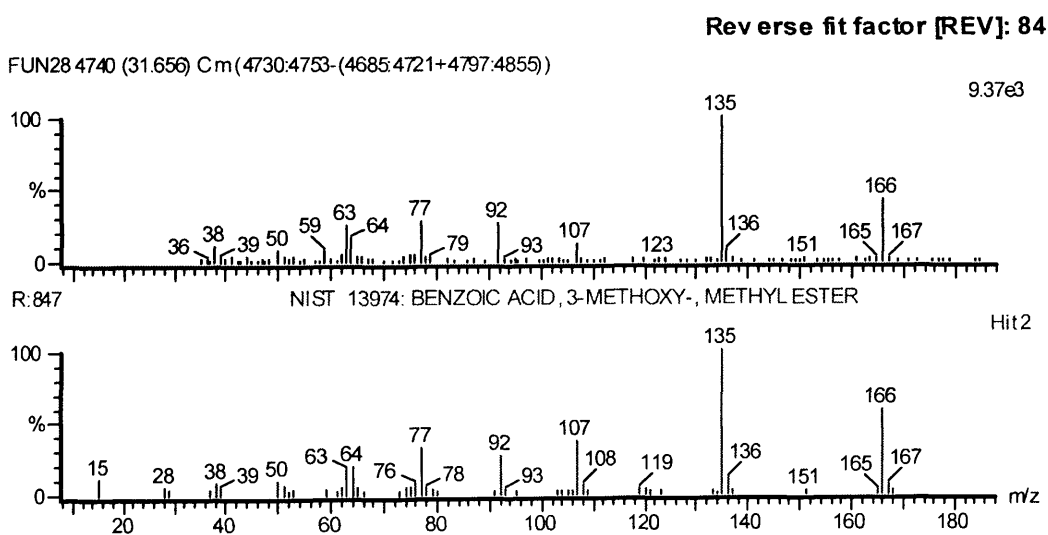


Figure A1.31 Spectra for peak 21 (top) and benzoic acid, 3-methoxy-,methyl ester (syn. m-anisic acid methyl ester) (bottom)

